COMPLETE ENGINEERING DESIGN REPORT-2020

Team IIT Roorkee Motorsports
IIT Roorkee

Formula Green 2020

Contents

I List of Abbreviations

NC: Normally Closed
NO: Normally Open
AMS/BMS: Accumulator/Battery Management System
HVD: High Voltage Disconnect
AIR: Accumulator Isolation Relay
IMD: Insulation Monitoring Device
TSMS: Tractive System Master Switch
BOTS: Brake Over Travel Switch
BSPD: Brake System Plausibility Device
BLDC: Brushless DC
TSAL: Tractive System Active Light
TSMP: Tractive System Measuring Point
SPDT: Single-Pole Double-Throw switch
RTDS: Ready-to-Drive Sound
GLVMS: Ground Low Voltage Master Switch

1. System Overview

The car runs on DC electric power supplied by a battery consisting of 128 Melasta High Power Lithium Polymer cells (15 Ah) connected in series. It powers an Emrax made Permanent Magnet Synchronous Motor. The output from this motor is fed to a mechanical differential. The motors are controlled by a Bamocar PG D3 700-400 motor controller. To monitor the cells, a self-designed Accumulator Monitoring System is used. All the components are appropriately rated for such use.

For LV system 7 Melasta cells have been used in series. The system consists of 24V, 12V, 5V and 3.3 V control voltages. These voltages have been created using Low DropOut Regulators (LDOs) and Buck Converters of appropriate ratings.

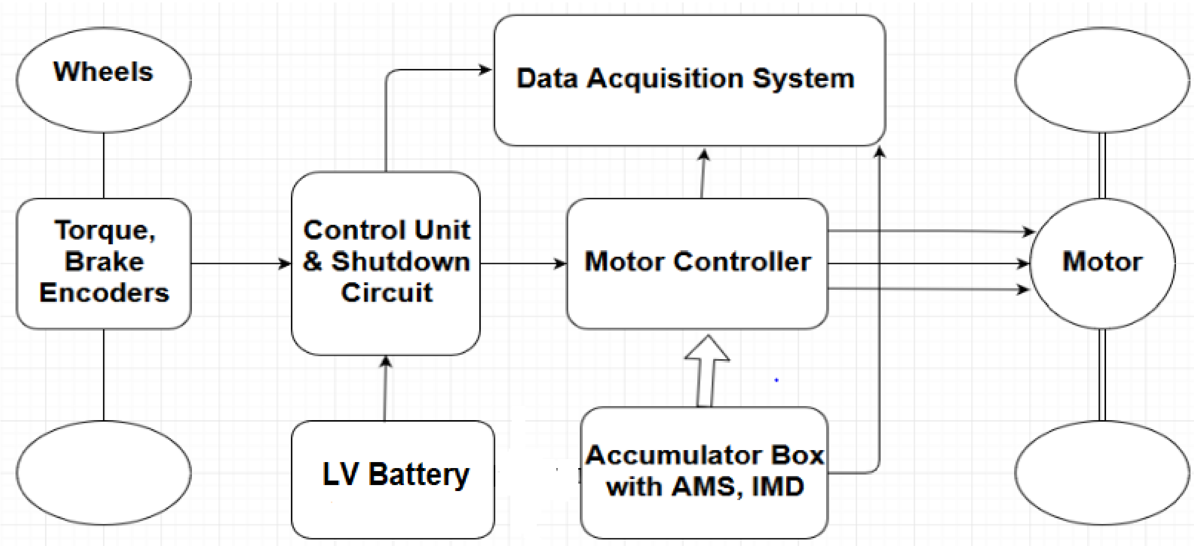

Fig.1: System Overview

Maximum Tractive-system voltage:	537.8VDC
Nominal Tractive-system voltage:	473.6VDC
Control-system voltage:	24VDC, 15VDC, 12VDC, 5VDC, 3.3VDC
Accumulator configuration:	128S1P
Total Accumulator capacity:	15 Ah
Motor type:	Permanent Magnet Synchronous Motor
Number of Motors:	1
Maximum combined Motor Power in kW	80

Table 1.1 General parameters

2. Electrical Systems

2.1 Shutdown Circuit

2.1.1 Description/concept

The safety circuit comprises several switches/relays lined in series with the 24V supply which powers the AIRs and HVD. When any of the switches/relays are open, the power supply to the connectors is cut off and the discharge circuit is activated. Thus, the accumulator is isolated from the motor controller and the TS is de-energized.

The GLVMS powers the BMS, BSPD, and IMD relay, and when all other shutdown buttons and switches are in their normal positions, it activates the pre-charge circuit and thus the TS is connected to the accumulator. When any of the shutdown buttons and/or the tractive system control switch is opened, the TS is de-energized. These switches are the push-rotate type which opens when pushed and the inertia switch and BOTS.

The brake over travel switch (BOTS) is activated in the event of brake failure. The switch is push-rotate type, which opens when pushed.

The motor controller that we are currently using consists of an **FRG/RUN(Enable)** signal which becomes activated only when the shutdown circuit gives no error.

The shutdown buttons, the BOTS, the TSMS and all interlocks are mechanically actuated switches and the power circuit has no control over it. The functioning of each switch can be shown by manually pressing or rotating the mechanical switch while for BSPD, BMS and IMD error signals are non-programmable and electrically hardwired and may be generated manually to showcase the error.

The method for each is as follows:

BMS: The error is generated manually by opening any maintenance plug of the accumulator.

BSPD: The current and pressure sensor signal is sent manually (which otherwise is generated in case of error) to test the BSPD.

IMD: The error is generated by adding a test resistor between TSMP -ve and LVMP -ve points.

HVD Interlock: Error can be demonstrated by simply opening the HVD which results in the opening of the pilot contact of the HVD and thus cuts supply to the AIRs.

.

. **Part**	**Function**
LVMS and TSMS	Normally Open
Brake over travel switch (BOTS)	Normally Closed
Shutdown buttons (SDB)	Normally Closed

Tractive System Control Switch	Normally Closed
Insulation Monitoring Device (IMD)	Normally Open
Battery Management System (BMS)	Normally Open
Inertia Switch	Normally Closed
Interlocks	Closed when circuits are connected
Brake System Plausibility Device	Normally Open

Table 2.1 List of switches in the shutdown circuit

2.1.2 Wiring / additional circuitry:-

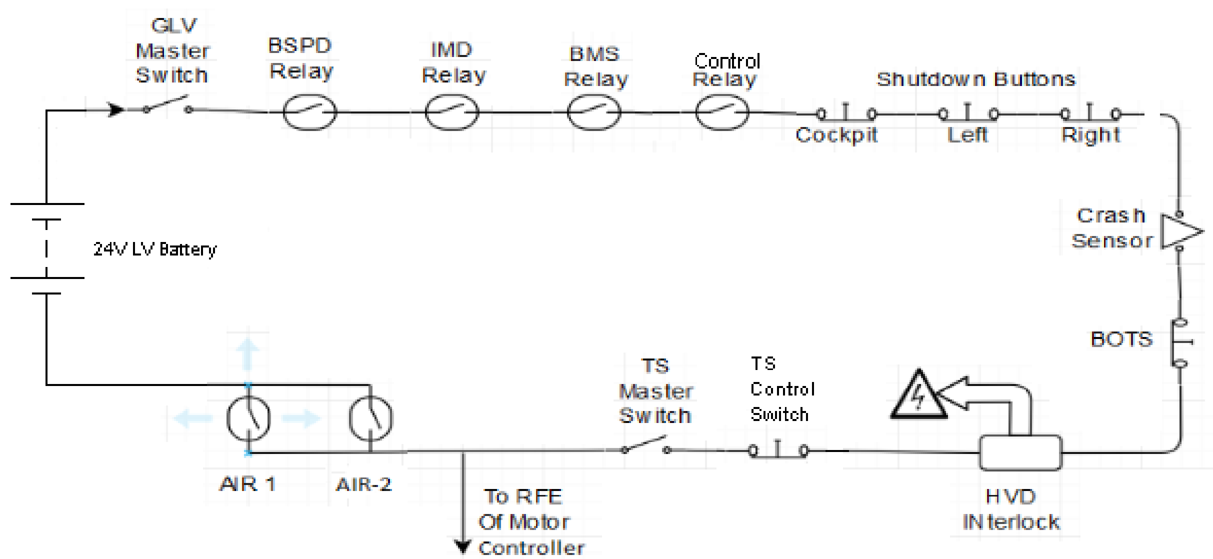

Fig.2: Power Shutdown Circuit

Total Number of AIRs:	2
Control Current per AIR:	0.5A
Additional parts consumption within the shutdown circuit:	2A
Total current:	3A
The cross-sectional area of the wiring used:	0.205 mm^2

Table 2.2 Wiring – Shutdown circuit

2.1.3 Position in car

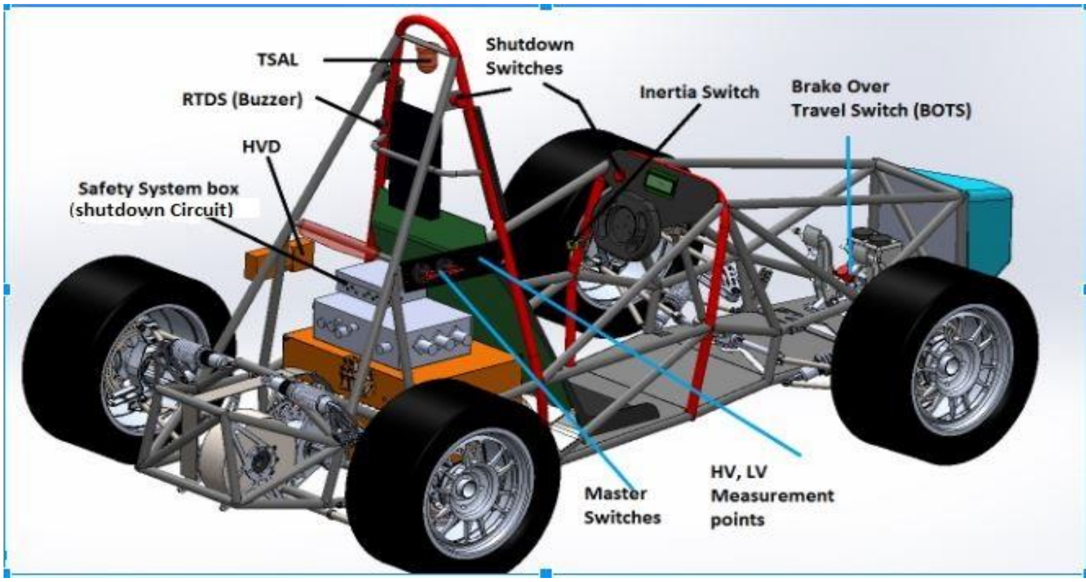

Fig.3: Power shutdown Circuit Overview (CAD Rendering)

2.1.4 Master Switches:-

The Master Switches are rotary switches having inbuilt lockout capability so LVMS & TSMS will not activate accidentally. As shown in the CAD rendering of the Master switches, TSMS is in the right position with orange background and triangle with the black lightning bolt on a yellow background sticker and marked TS adjacent to it. The GLVMS is left switch on the right position with the red background and a red spark in a white-edged blue triangle sticker adjacent to it with GLVS imprinted on the background. The diameter of each master switch as shown in the figure is 50mm.

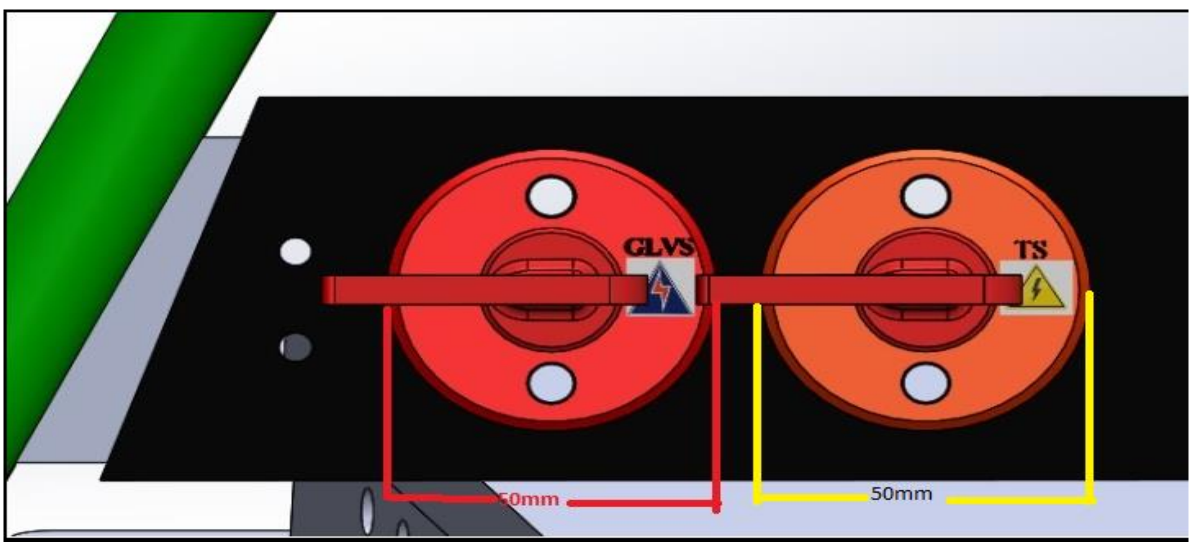

Fig 4:- Master Switches

2.1.5 Shutdown Switches

There are 3 Shutdown Buttons in the car: 1 in the cockpit (right), the other 2 at either side behind the driver accessible to any outsider. These switches are push-pull and are a part of the (series) shutdown circuit as shown in the diagram. Anyone of these switches can open the shutdown circuit, thus disconnecting the motor controller and accumulator as shown in Fig 1. The diameter of each shutdown button is 40mm.

One more switch on the cockpit (left) is dedicated to allowing the driver to control TS from within the cockpit itself, which is the last switch before TSMS in the path.

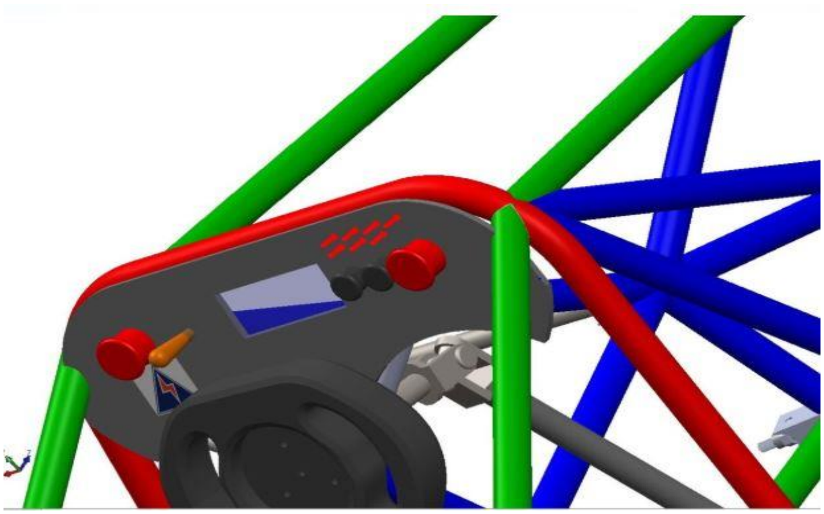

Fig 5:- Position Of Shutdown Buttons

2.2 IMD

2.2.1 Description (type, operation parameters)

Bender A-ISOMETER iso-F1 IR155-3204 is used as an IMD for our vehicle. It monitors the insulation resistance between TS Ground and LV Ground (reference earth: vehicle mass/chassis ground). If the insulation resistance falls below 269KΩ (500Ω/Volt) or if there is an error in the accumulator ground, electronic ground, and the chassis ground; it shuts off the relay in the shutdown system, thereby disabling AIRs and HVD.

Supply voltage range:	10 to 36VDC
Supply voltage	24 VDC
Environmental temperature range:	-40 to 105°C
Self-test interval:	Always at startup, then every 5 minutes
High voltage range:	0 - 1000 VDC

Set response value:	269kΩ (500Ω/Volt, 537.6V for our system)
Max. operation current:	150mA
Approximate time to shut down at 50% of the response value:	< the 20s

Table 2.3 Parameters of the IMD

2.2.2 Wiring/cables/connectors/

The following diagram shows the connections of IMD: consisting accumulator terminal connections (XLA +ve and XLA -ve), supply voltage, reference earth (chassis ground) and accumulator ground (chassis ground separate line). OKHS is the output signal of IMD which is fed to control the relay in the shutdown circuit through the IMD latch.

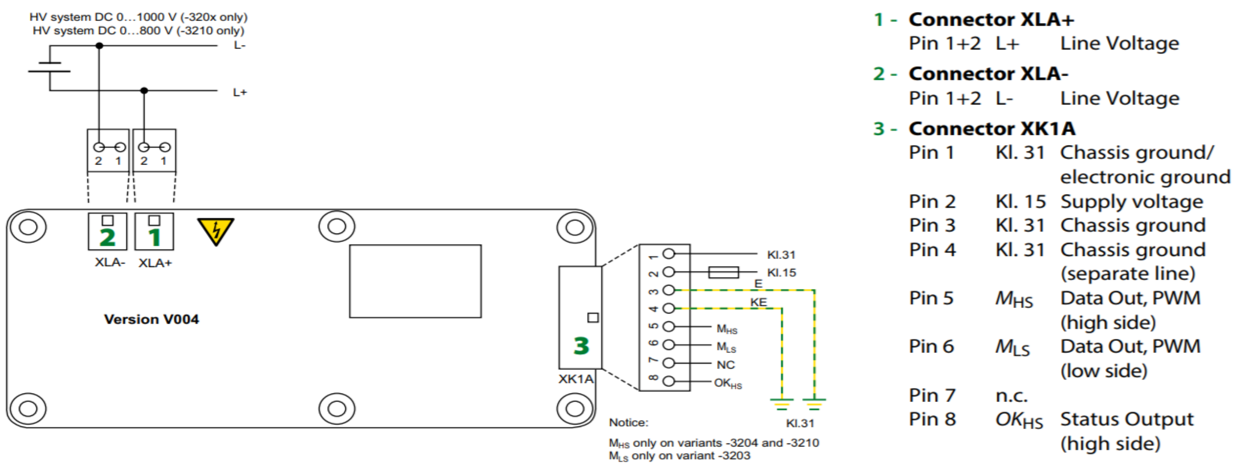

Fig.6: IMD Connections

2.2.3 Position in car

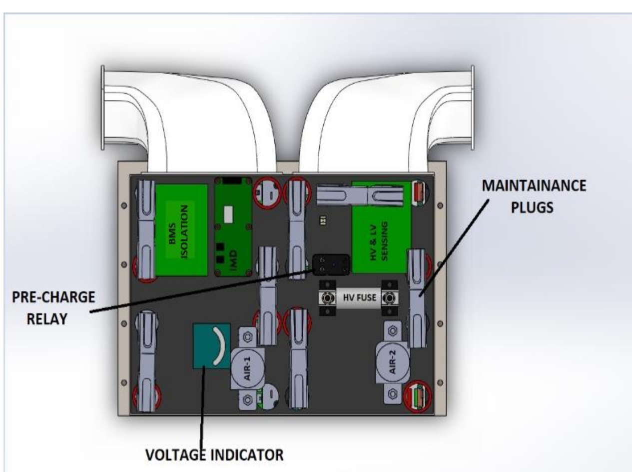

Fig 7: IMD location in the Battery Box

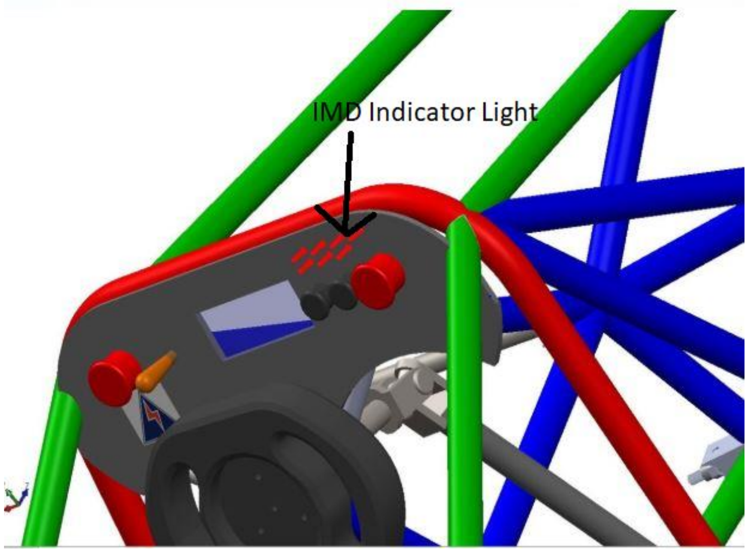

Fig 8: IMD indicator light on the dashboard

2.3 Inertia Switch

2.3.1 Description (type, operation parameters)

The inertia switch used is Sensata Technologies 360° Resettable Crash Sensor. It switches off the shutdown circuit upon vehicle impact, hence disconnecting the accumulator and motor controller in post-crash situations. The device triggers due to an impact load which decelerates the vehicle at between 6g and 11g depending on the duration of the deceleration.

Fig.9: Inertia Switch

Inertia Switch type:	Sensata 360° Resettable Crash Sensor
Supply voltage range:	10 - 36VDC
Supply voltage:	24VDC
Environmental temperature range:	-40 - 105°C
Max. operation current:	10A
Trigger characteristics:	6g for 50ms / 11g for 15ms

Table 2.4 Parameters of the Inertia Switch

2.3.2 Wiring/cables/connectors/

In normal operation, the switch remains closed (NC terminal is connected), thereby powering the shutdown circuit. In case of crash conditions, the switch becomes open (NO terminal is connected) and thus, power supply to HV contactors is broken leading to the shutdown of the HV system, and hence, isolation of accumulator and motor controller.

The inertia switch is mounted just below the dashboard on the right side. Its circuitry comes before the shutdown buttons and BOTS. The circuit is completed by means of series connectors.

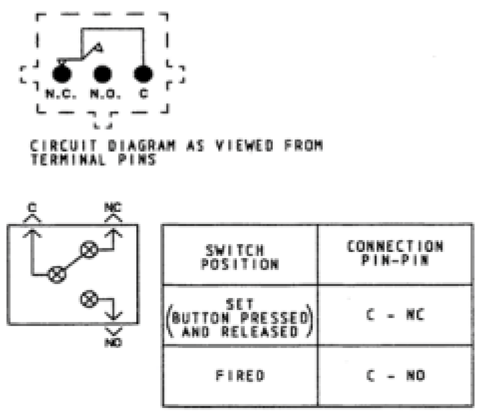

Fig.10: Inertia Switch Connection Diagram

2.3.3 Position in car

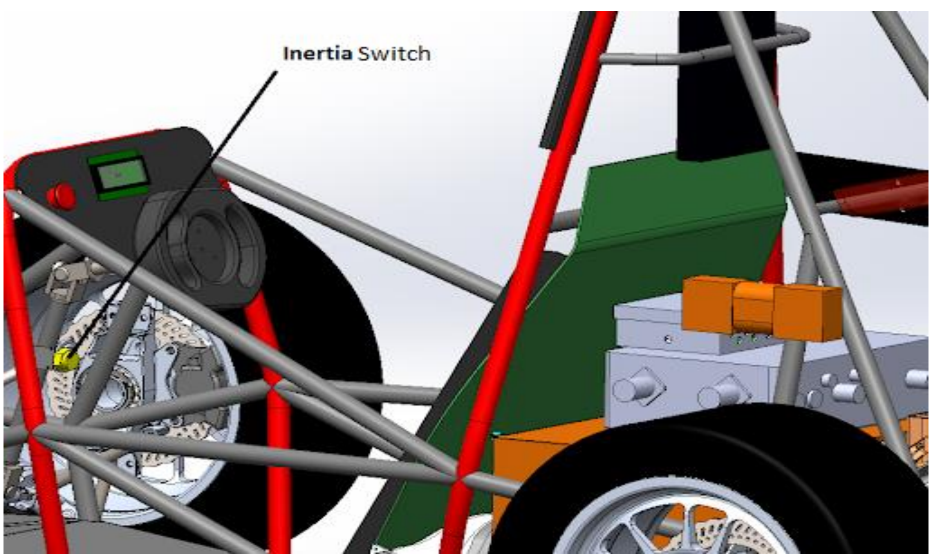

Fig.11: Inertia Switch Mounting on Vehicle.

As shown in figure inertia switch is clamped to chassis by means of nut and bolts thus making it rigidly attached. By unscrewing the bolts the inertia switch may be demounted to test its functionality

2.4 Brake System Plausibility Device

2.4.1 Description/additional circuitry

Brake plausibility device opens the power supply to the TS connectors in case of detection of plausibility. It takes brake pedal position and TS current sensor value as input and generates a signal to open the relay if:-

- Brake pedal position > Hard braking limit **AND**
- TS Current sensor output > Calibrated equivalent of 10 Amps.

Current limit – 10 Amps is decided by taking 5KW power flow detection into account. Since the nominal voltage of the battery is 470V, the current value (satisfying 5kW limit) = 5000/470 ~ 10 Amps.

Brake fluid pressure sensor used:	M304210000601KPG
Torque encoder used:	UNILIN - TEQ50
DC Current measurement used:	HK200T03
Supply voltages:	3.3V
Maximum supply currents:	20mA
Operating temperature:	-20 - 180 °C
Output used to control AIRs:	Open a relay

Table 2.5 Parameters of the Brake System Plausibility Device

2.4.2 Wiring/Cables/Connectors:-

Fig.12: BSPD Wiring Diagram

In the shown figure, we have 2 comparator stages comparing:
1.) HV current signal (with a threshold corresponding to 10A) and
2.) Brake pedal pressure sensor (which detects the hard braking).

We have used 2 comparators to detect the short circuit of sensor signal wires with supply lines. Their outputs are logically NORed giving low output if HV current and brake pedal cross their threshold and when a short circuit error is detected. Further, an RC circuit is connected to NOR's output giving a delay of 500ms for persistence. This signal will go to PRESET of D flip flop.

The BSPD has a multivibrator to provide a low-level signal to an active low CLEAR pin of D flip flop just after the GLVMS is switched ON for about 1 sec. This feature ensures power cycling the GLVMS will reset the BSPD latch.

As shown in the shutdown circuit, BSPD is just preceded by GLVMS. So, GLVMS directly supplies power to the BSPD.

BSPD have the following inputs:-

24V Direct:- From GLVMS
3.3V :- Using buck converter on BSPD PCB, with 24V Direct as input supply.
15V :- Used as supply for Hall Sensor.
Pressure sensor Output- From Brake pedal pressure sensor.

Hall Sensor Signal:- From TS Hall Sensor corresponding to current drawn for 5KW power.

GND:- -ve terminal of LV accumulator.

BSPD has the following outputs:-

BSPD Relay :- A signal connecting 24V input and IMD relay in series.

BSPD LED:- A signal to the dashboard which will switch ON led corresponding to an error in BSPD.

All these signals are connected using phoenix connectors and cables

2.4.3 Position in car/mechanical fastening/mechanical connection

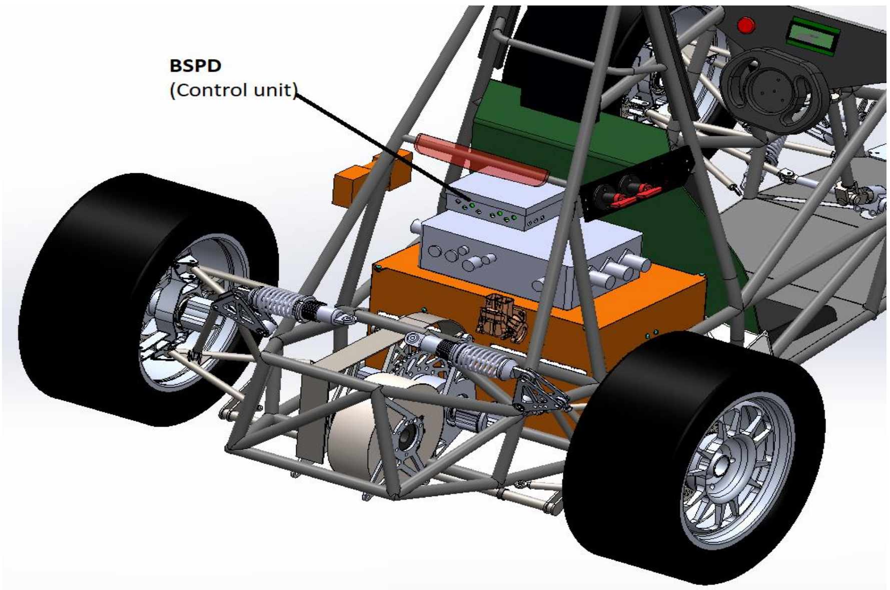

Fig.13: BSPD Position in Vehicle

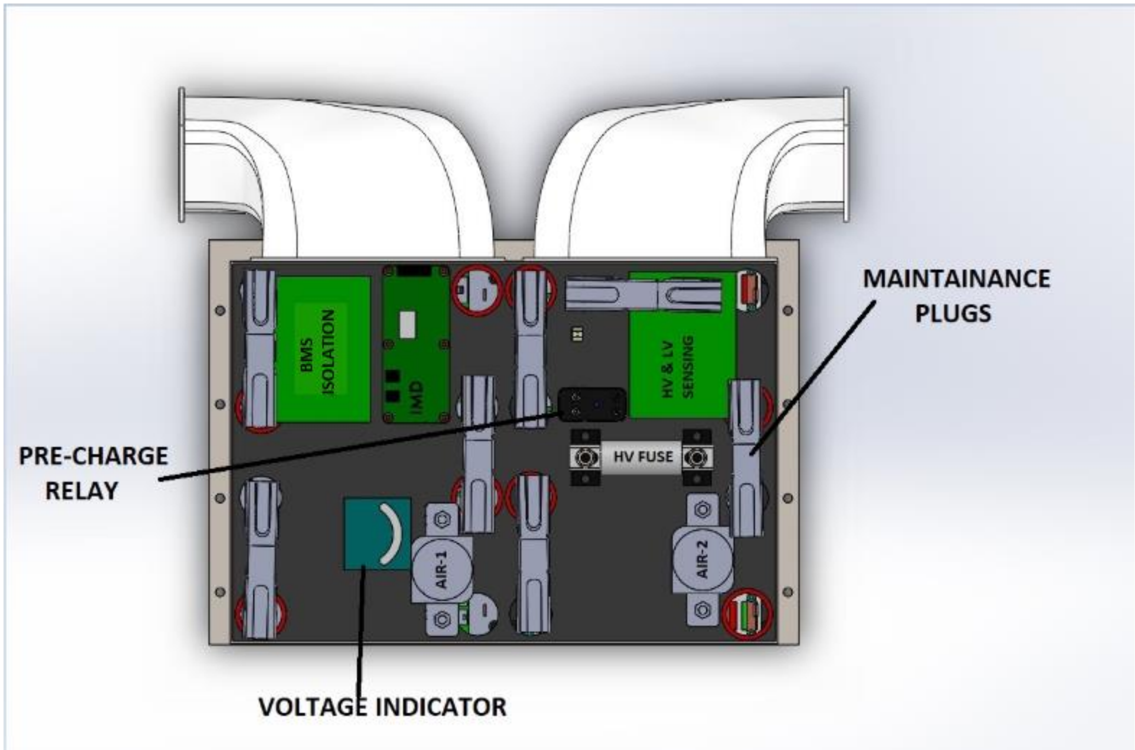

Fig 14:- CAD Rendering of HV & LV Sensing PCB in Accumulator (Battery Box)

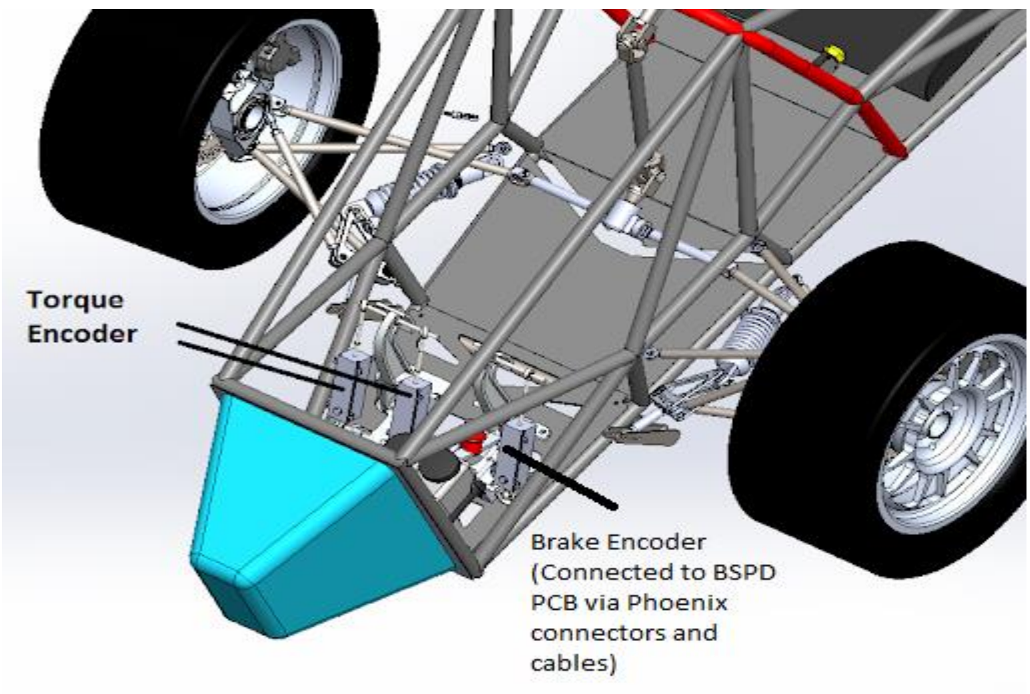

Fig 15:- CAD rendering of Brake Encoder (Back to List of Figures)

2.4.4 Testing Method:-

To test the BSPD, we will input a test signal of 3.3V to both brake signal and current sensor connectors. The 3.3V input corresponds to hard braking and 10A for the current sensor. This will result in disabling the shutdown circuit by opening the BSPD relay and switching OFF corresponding LED. As mentioned earlier, only power cycling the GLVMS will re-trigger the mono shot which will, in turn, reset the latch.

2.5 Reset / Latching for IMD and BMS

2.5.1 Description/circuitry

The circuit takes IMD & BMS output as input at the PRESET pin of D flip-flop. Whenever an error is detected by the IMD or BMS, PRESET (being active low) goes low resulting in disabling the shutdown circuit. An LED connected to these output turns ON indicating an error.

Both IMD and BMS will switch OFF their respective relay in the shutdown circuit, hence isolating the accumulator and motor controller. It will remain disconnected until it is manually reset using reset buttons provided with the PCB. It can be reset while GLVMS is switched ON.

2.5.2 Wiring/cables/connectors

Both IMD and BMS latches are in shutdown circuit PCB. Since IMD and BMS are contained in the accumulator box, their signals are connected with the accumulator box using rated phoenix connectors.

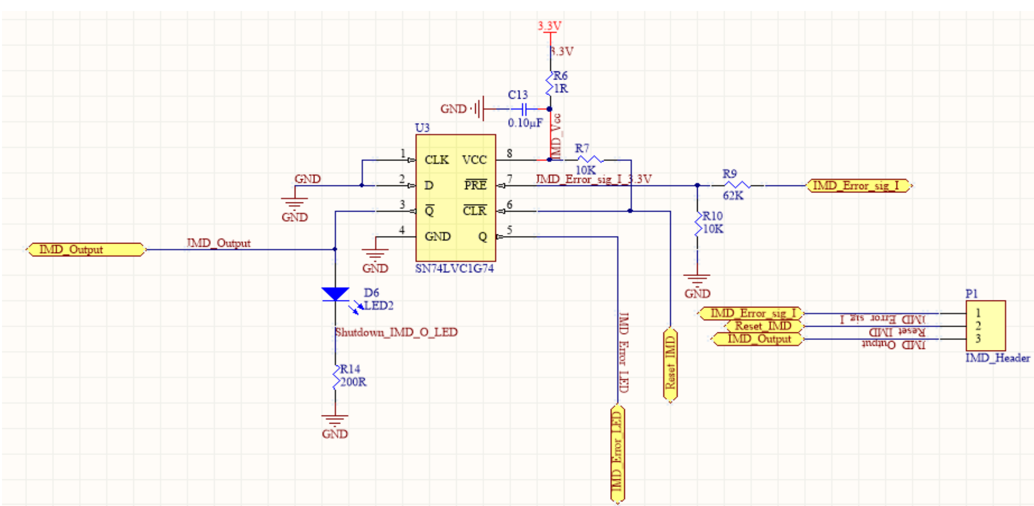

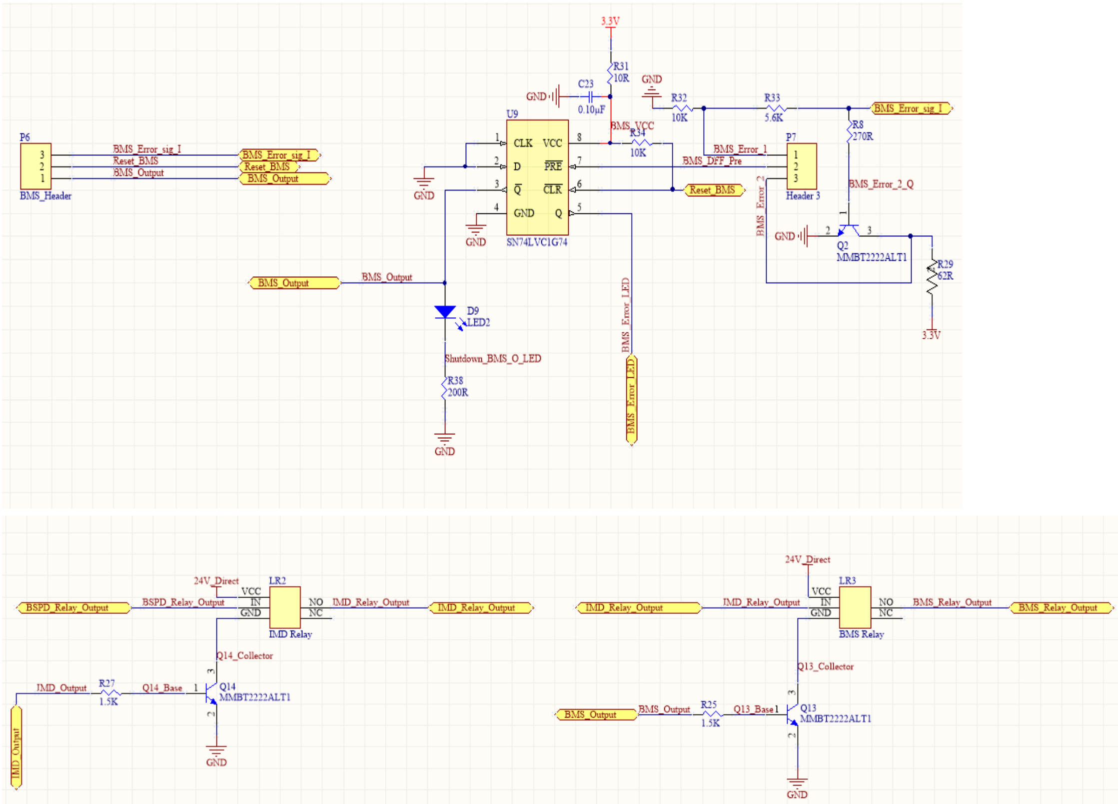

Fig.16: IMD/BMS Latch Wiring Diagram

2.5.3 Position in Car

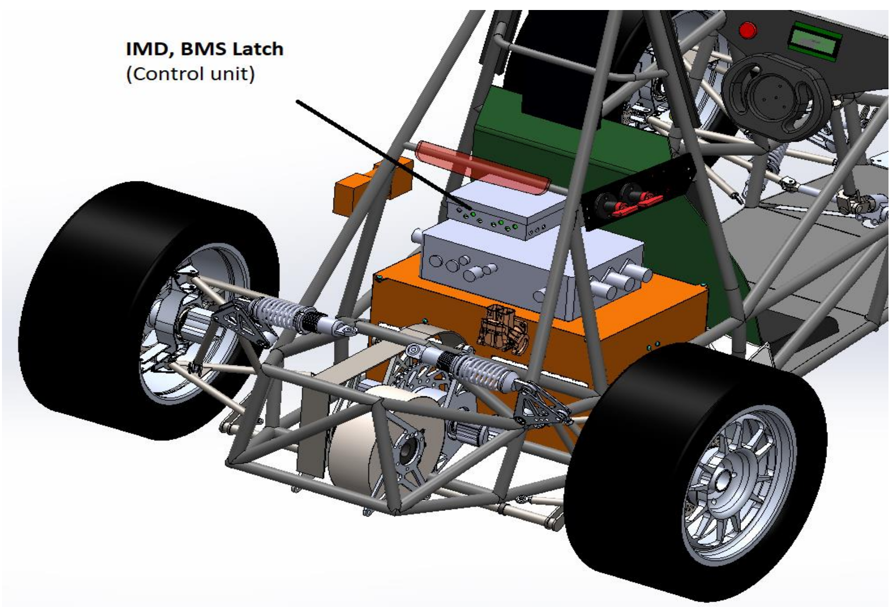

Fig.17: IMD/BMS Latch Position in Vehicle(Back to List of Figures)

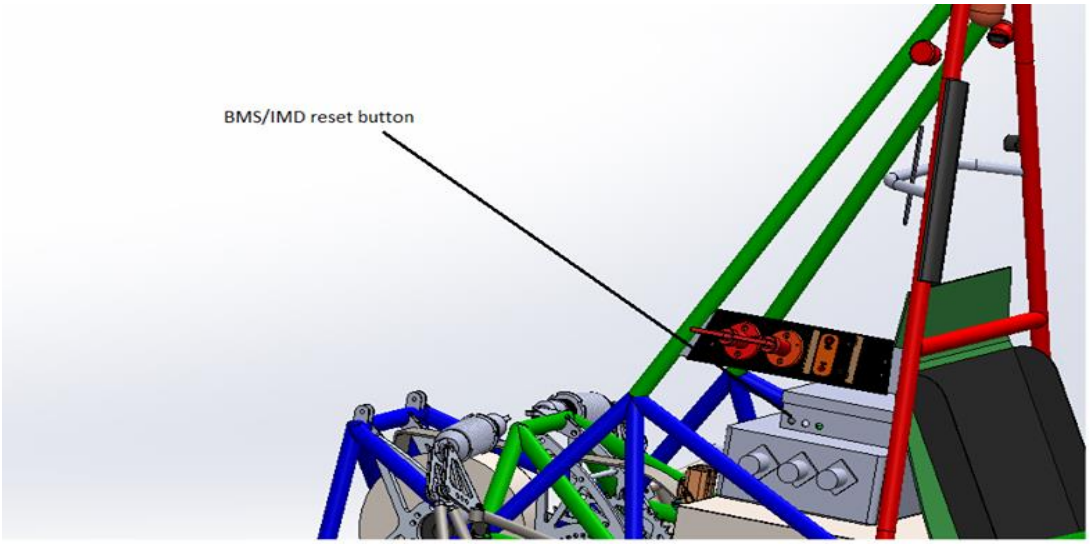

Fig 18: Position of IMD, BMS reset button (Back to List of Figures)

2.6 Shutdown System Interlocks

2.6.1 Description/circuitry

The interlock circuit is a series of normally closed switches, electrically connected in series with all other shutdown switches and hardwired electronic switches (IMD, BMS, BSPD). It is directly succeeded by TSMS as shown in Fig 2. If HVD is detached accidentally while TS is active then it automatically opens the shutdown circuit. This results in deactivating the AIRs resulting in the isolation of the accumulator and motor controller. It also activates the discharge circuit to de-energise TS.

2.6.2 Wiring/cables/connectors

2.6.3 Position in car

Fig: Shutdown Switches Interlocks Position in Vehicle (Refer to Fig.40)

2.7 Tractive System Active Light

2.7.1 Description/circuitry

The TSAL is switched ON when the voltage across the motor controller exceeds 60 VDC or the Precharge relay or AIR is on. Isolation between TS voltage level across the motor controller and LV system of TSAL is achieved using an optocoupler. The output of the motor controller's +ve terminal is compared with a potentiometer signal corresponding to 60VDC and then, an astable square wave of 4Hz is produced.

As per rule book, after GLVMS is switched ON, a green TSAL will illuminate until TSMS is switched ON. After TSMS is switched ON and/or TS voltage is above 60VDC, the green TSAL will switch OFF and red TSAL will start blinking with 4Hz frequency.

Supply voltage:	24VDC
Max. operational current:	60mA
Limiting resistor	1.5 kOhm
Lamp type	LED
No. of LED	12 (each for red / green light)
Power consumption:	5.76 W
Brightness	113 Lumen (approx)
Frequency:	4Hz
Size (length x height x width):	25.5mm Radius , 3cm Height

Table 2.6 Parameters of the TSAL

Calculations:-

Assuming all LEDs are present at the centre
No. of LEDs per color of light (Red/Green) = 12
Luminous Intensity per LED = 1.5 candela(Cd)
1 Cd gives 12.57 lumens for a solid angle of 4π. So,6.285 lumens for solid angle of 2π
Total Lumens=12*6.285*1.5=113.13 lumens

2.7.2 Wiring/cables/connector

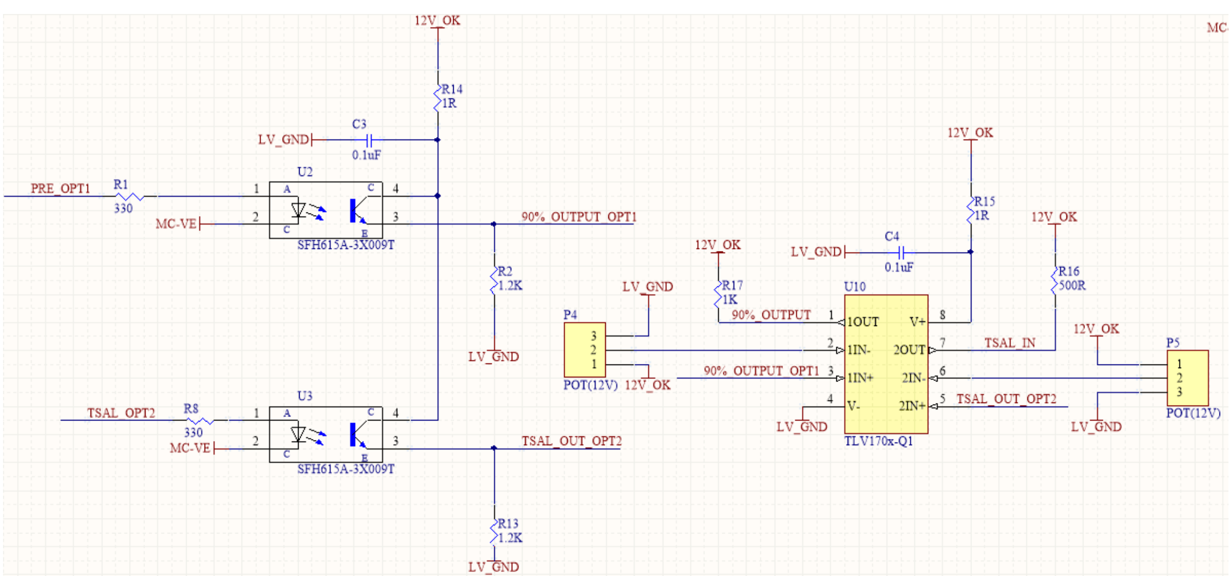

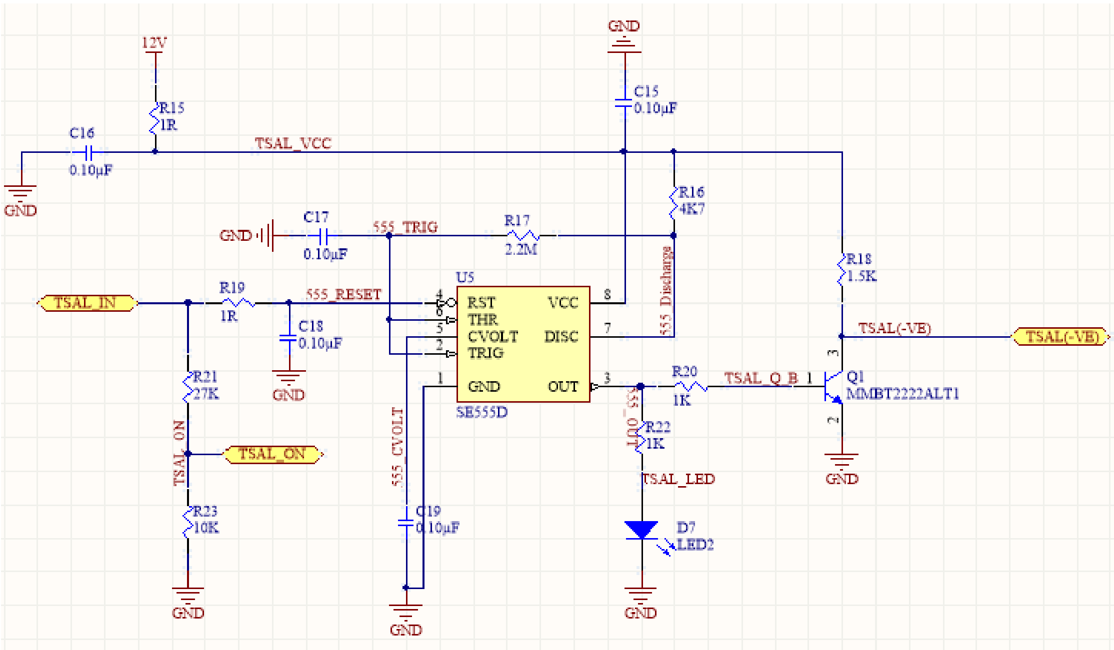

Fig.19: TSAL Connection Diagram for red led

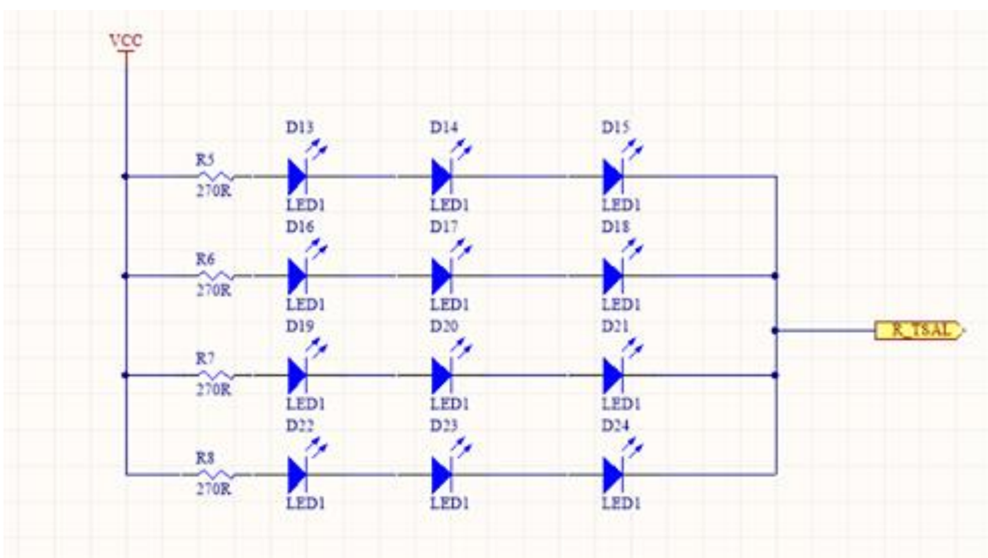

Fig 20: Array of Red LEDs

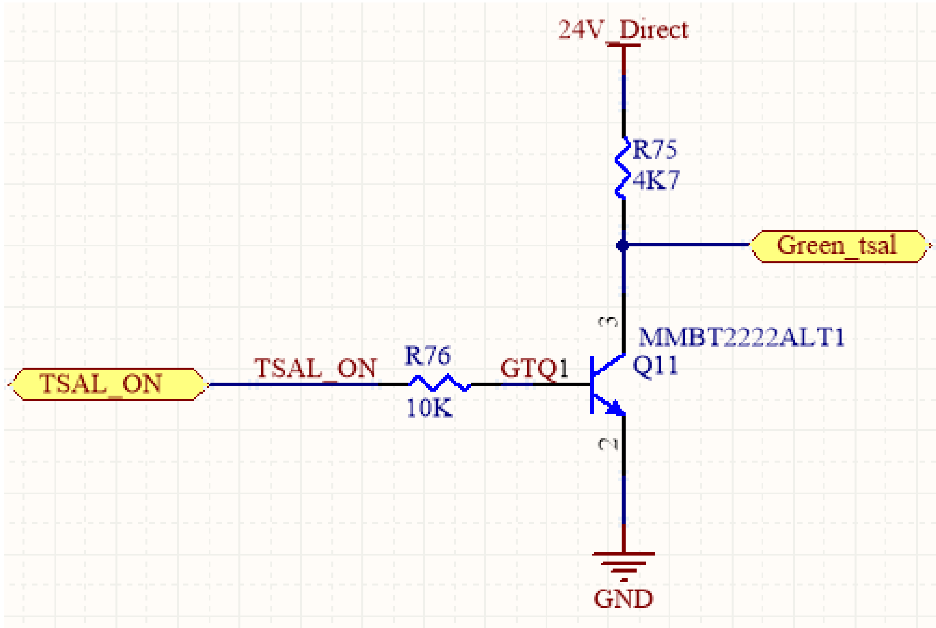

Fig 21.: TSAL Green LED circuit

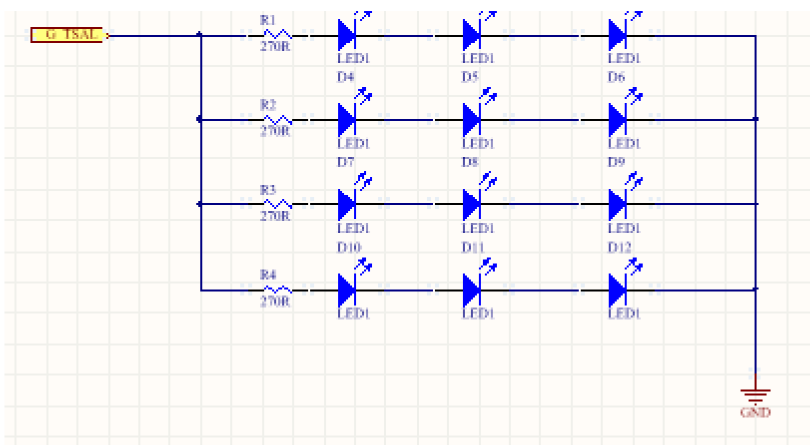

Fig 22:- Array of Green LEDs

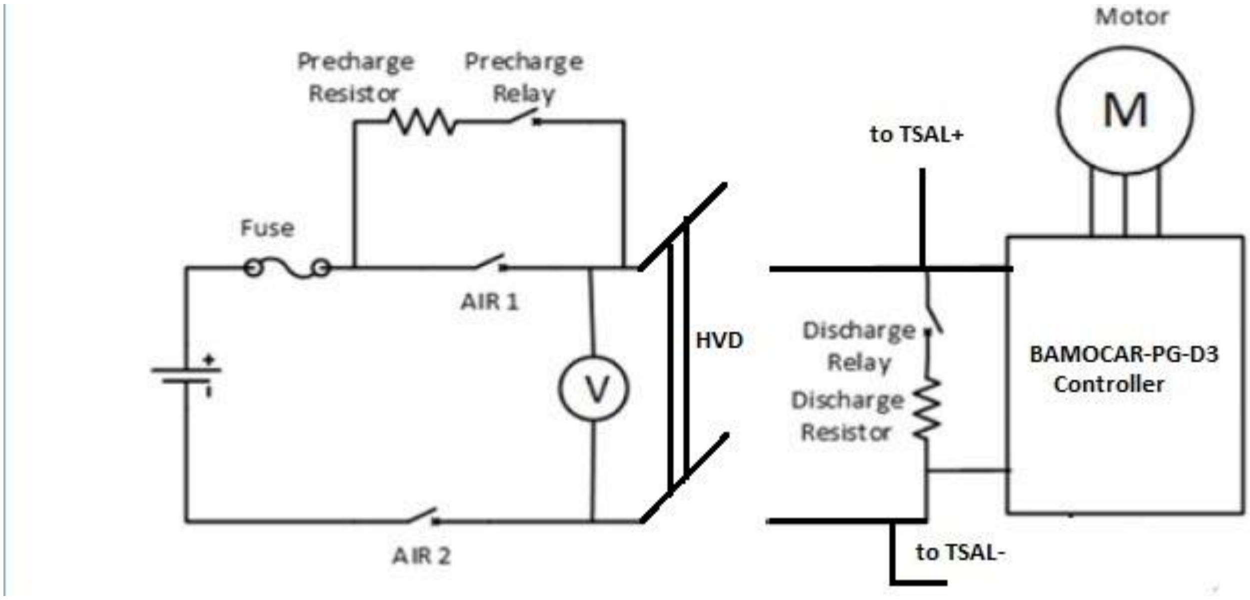

Fig 23: TSAL triggered by High Voltage and after AIR-1 is switched ON.

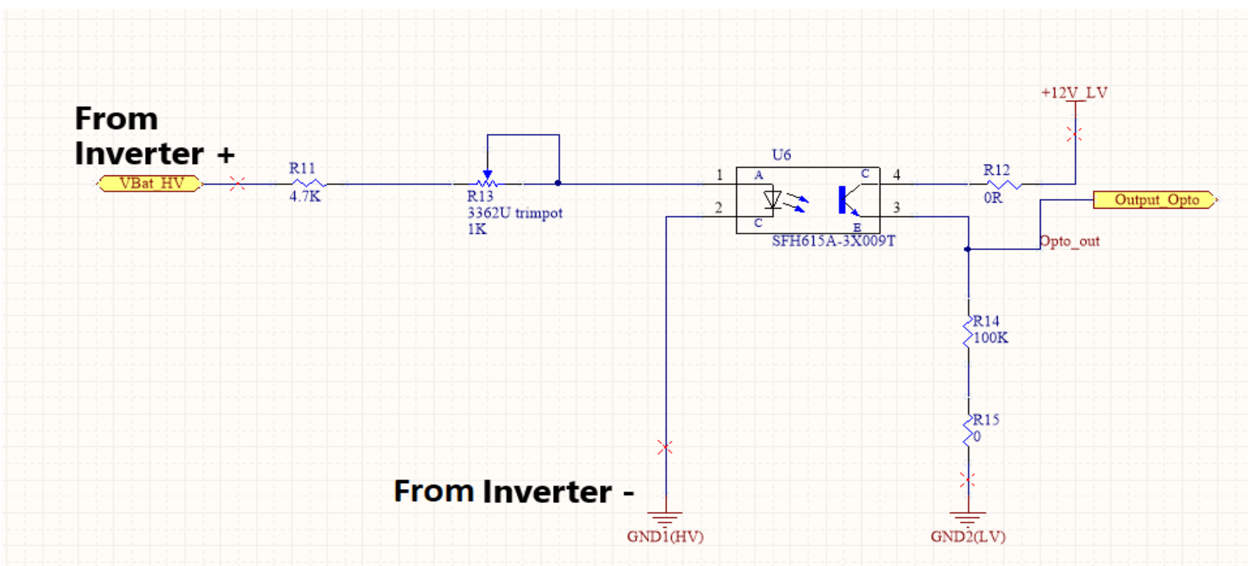

Fig 24:- Isolation provided by Optocoupler

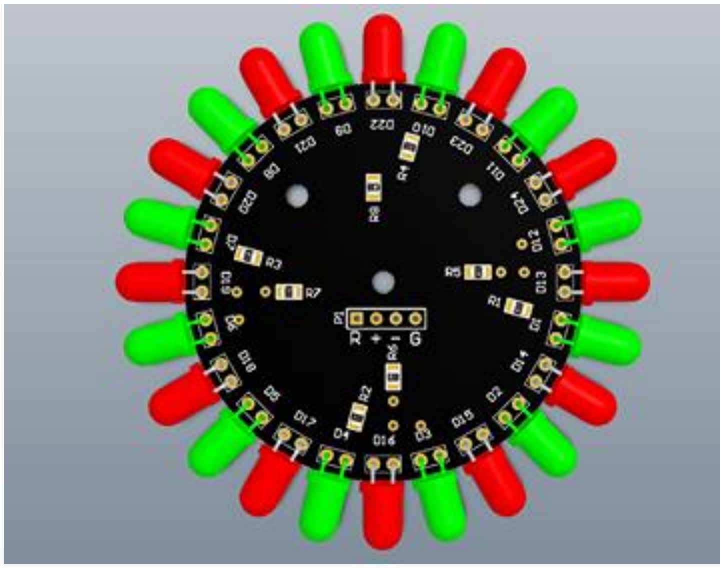

Fig 25:- PCB showing Green and Red TSAL.

When the accumulator is disconnected from the vehicle, a dummy connector will be used in place of the HV disconnect. The accumulator box can't be connected to the car until this dummy connector is in place.

2.7.3 Position in car

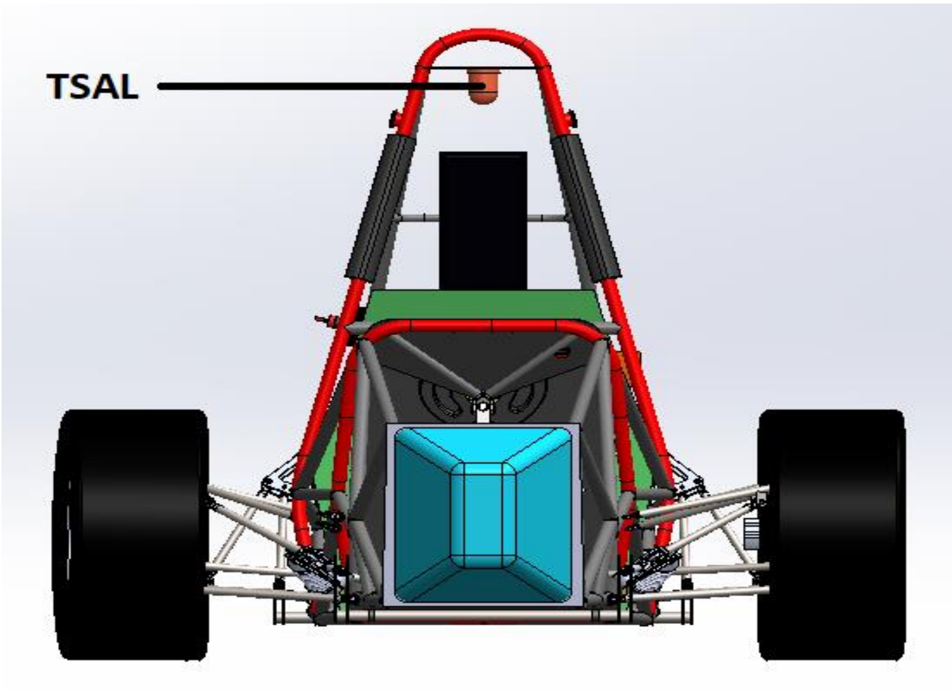

Fig.8: Fig.26: TSAL mounting on Vehicle (Back to List of Figures)

2.8 Measurement points

2.8.1 Description

There are 4 measurement points, 2 each for LV and HV. The points are used to check the voltage levels of respective systems. The measurement points are placed on the same panel as the master switches, near the main hoop of the vehicle. It is easily accessible from outside without any obstruction. TSMPs are protected with an insulated coating and can be opened without any tool. TSMPs are connected to the positive and negative motor controller/inverter supply through a 15k ohm resistor.

The TSMPs are marked "TS+" and "TS-" and are mounted on orange background in an electrically isolated casing. The resistors used are of adequate power ratings.

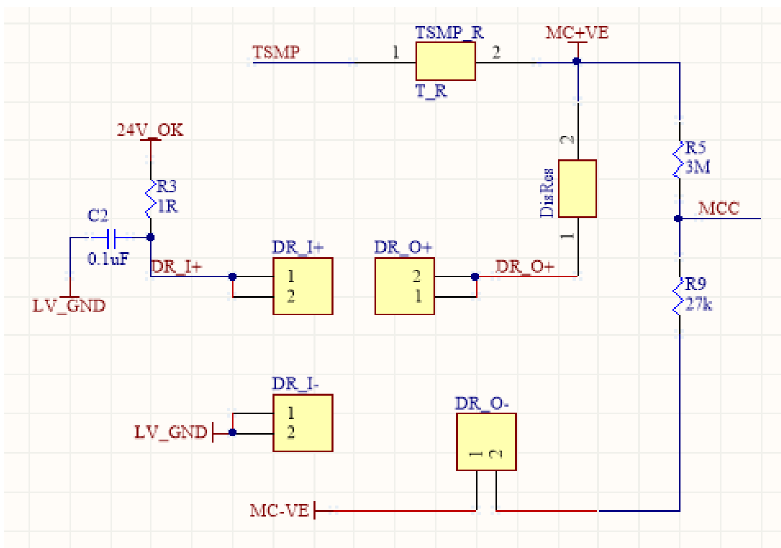

Fig 27:- Discharge Circuitry

2.8.2 Wiring, connectors, cables

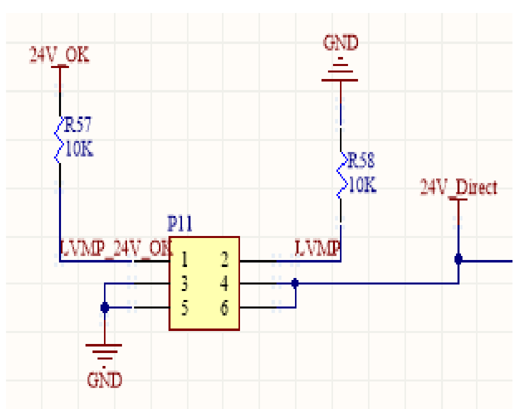

Fig 28: LVMP schematic

2.8.3 Position in car

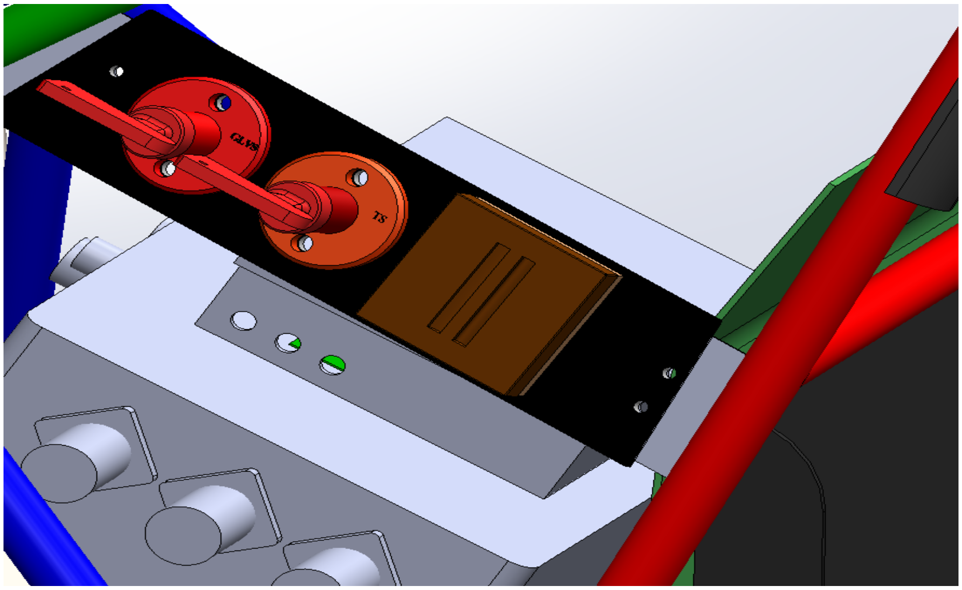

Fig.29: PSMP Position in Vehicle in non-conductive housing

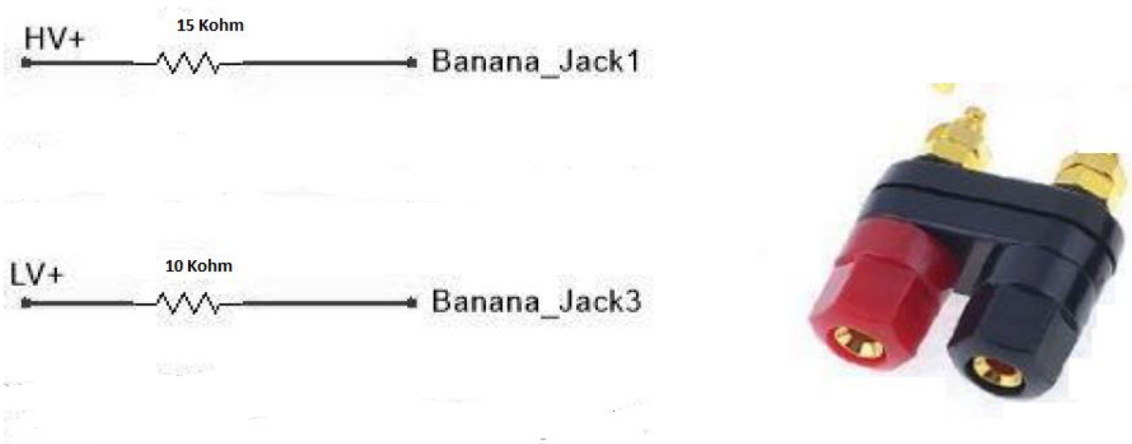

Fig.30:- PSMP Connection

The housing is made up of PLA (Polylactide). It is an interface locking mechanism that is locked up by interface between the two parts and it can be opened by directly opening the above part of the housing.

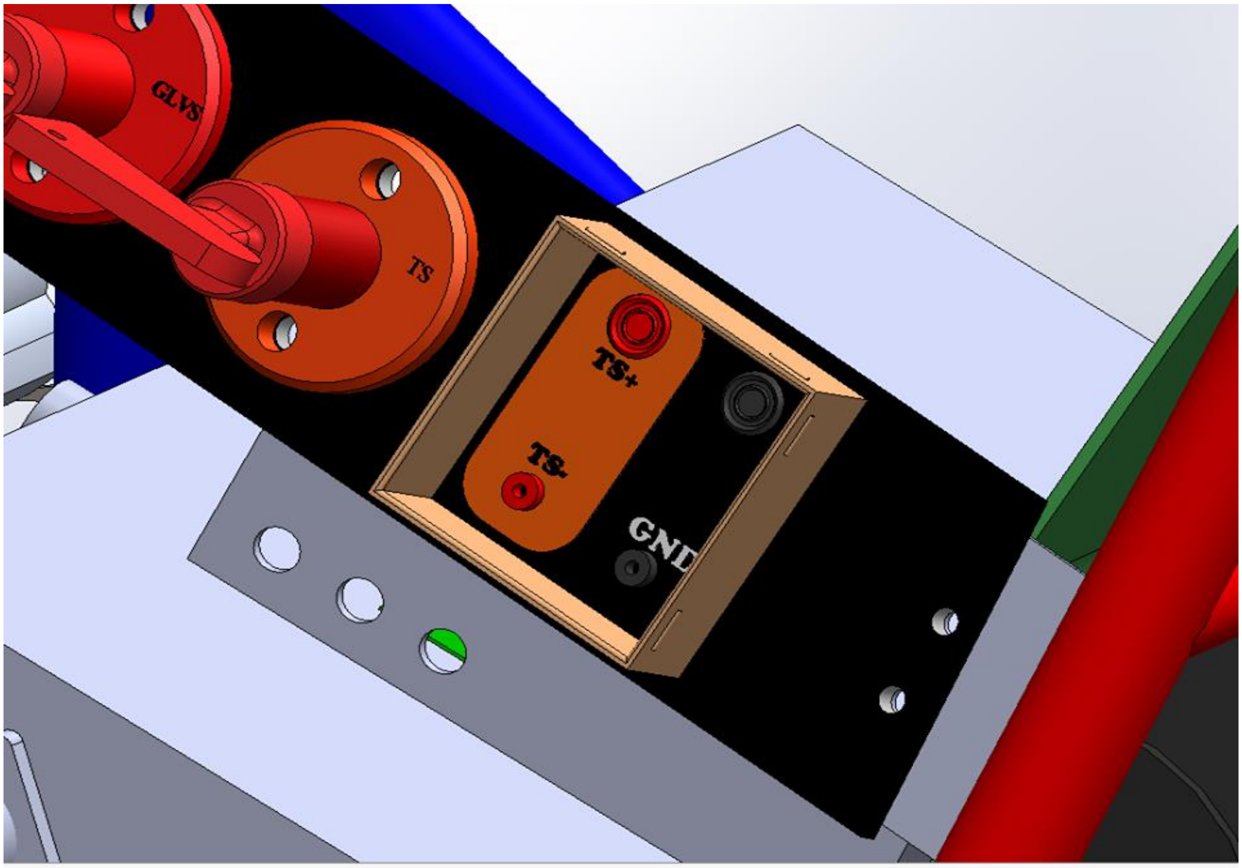

Fig 31:- Exact position of HV-LV measurement points

2.9 Pre-Charge Circuit

2.9.1 Description

Pre-charge Circuit is able to pre-charge the intermediate circuit to at least 95% of the current accumulator voltage before closing the AIR. When we initially connect the battery to the load with capacitive input, there is an inrush of current as the load capacitance is charged up to the battery voltage. With large batteries (with a low source resistance) and powerful loads (with large capacitors across the input), the inrush current can easily reach 1000 A.

A pre-charge circuit limits that inrush current, without limiting the operating current. A pre-charge circuit between the accumulator and its load is must because:

The load having input capacitors would be damaged by the inrush current. The main fuse would blow if it carries the inrush current. The contactors, if present, would be damaged by the inrush current. The battery cells would be damaged as they are not rated for the inrush current.

2.9.2 Wiring, cables, current calculations, connectors

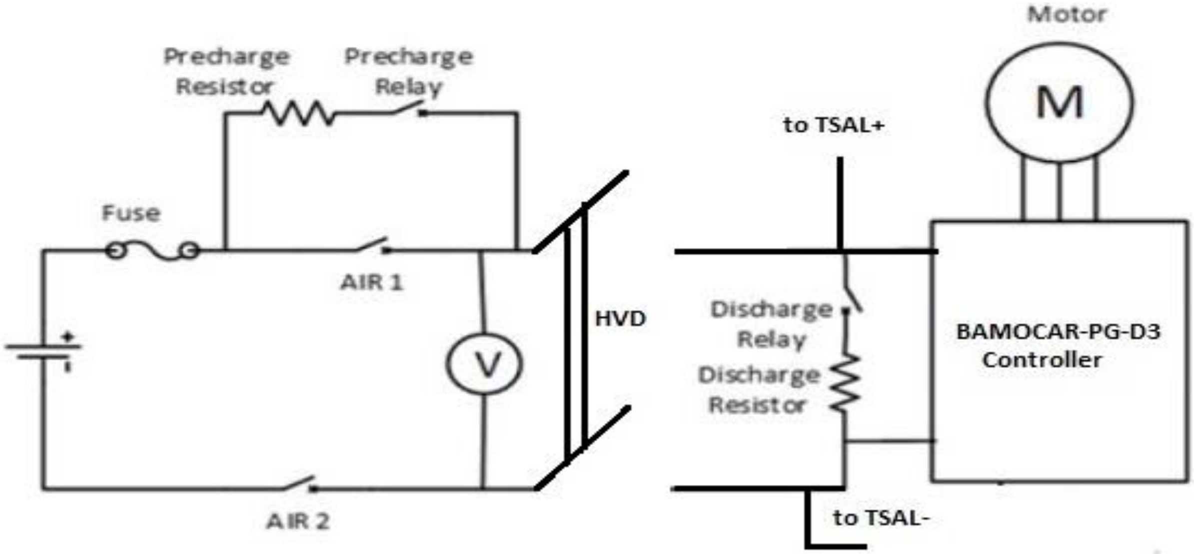

Fig 32:- Precharge Circuitry with Precharge Relay and Resistor

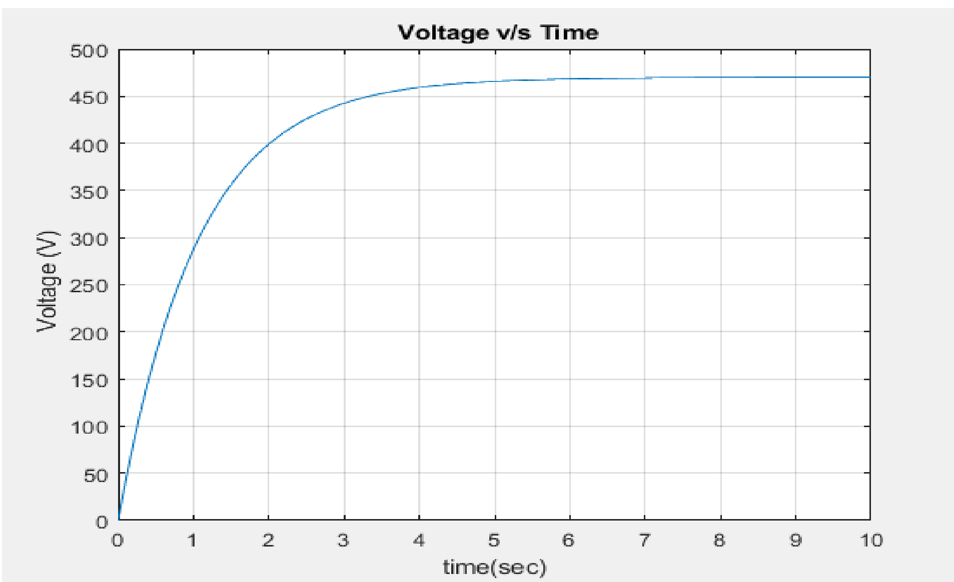

Fig 33:- Voltage analysis of Precharge Circuit

Formula:- V= 470*(1-exp(-t/(3300*320*10^-6)))

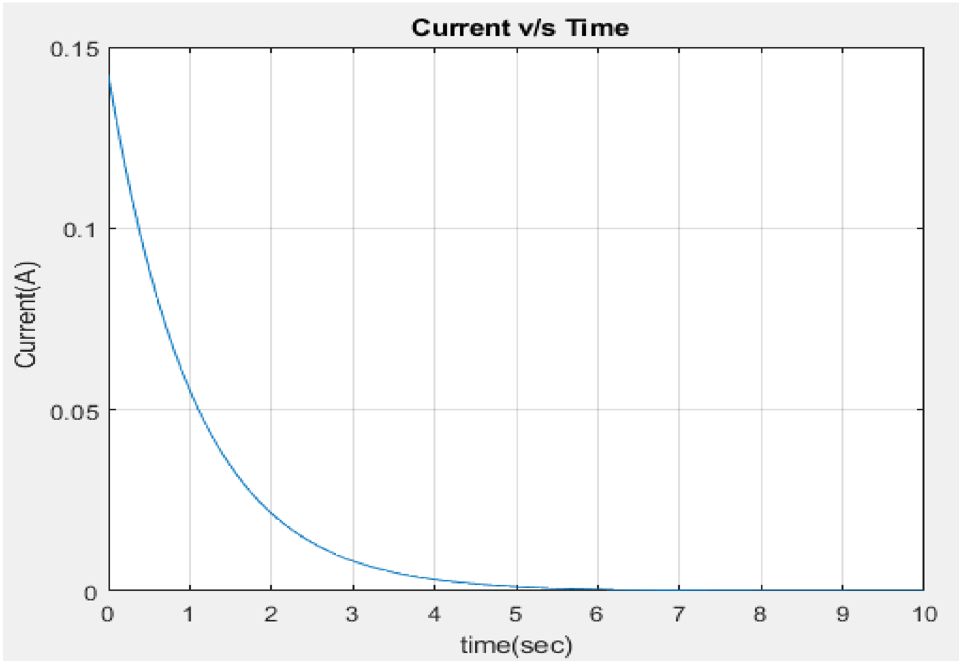

Fig 34:- Current analysis of Precharge Circuit

Formula:- I = (470/3300)*exp(-t/(3300*320*10^-6))

Resistor Type:	Ohmite
Resistance:	3.3 KΩ
Continuous power rating:	10 W
Overload power rating:	100W for 5 sec
Voltage rating:	500V
The cross-sectional area of the wire used:	0.5189 mm²

Table 2.7 General data of the pre-charge resistor

Relay Type:	MiniTACTOR P125CDA
Contact arrangement:	Form X
Continuous DC current:	30A
Voltage rating	1200VDC
The cross-sectional area of the wire used:	8 mm²

Table 2.8 General data of the pre-charge relay

2.9.3 Position in car

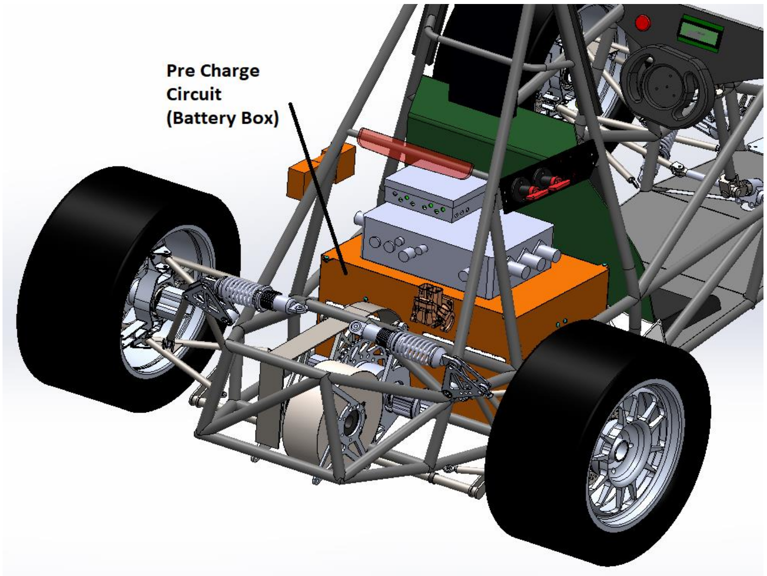

Fig.35: Pre-Charge Circuit Position in Vehicle

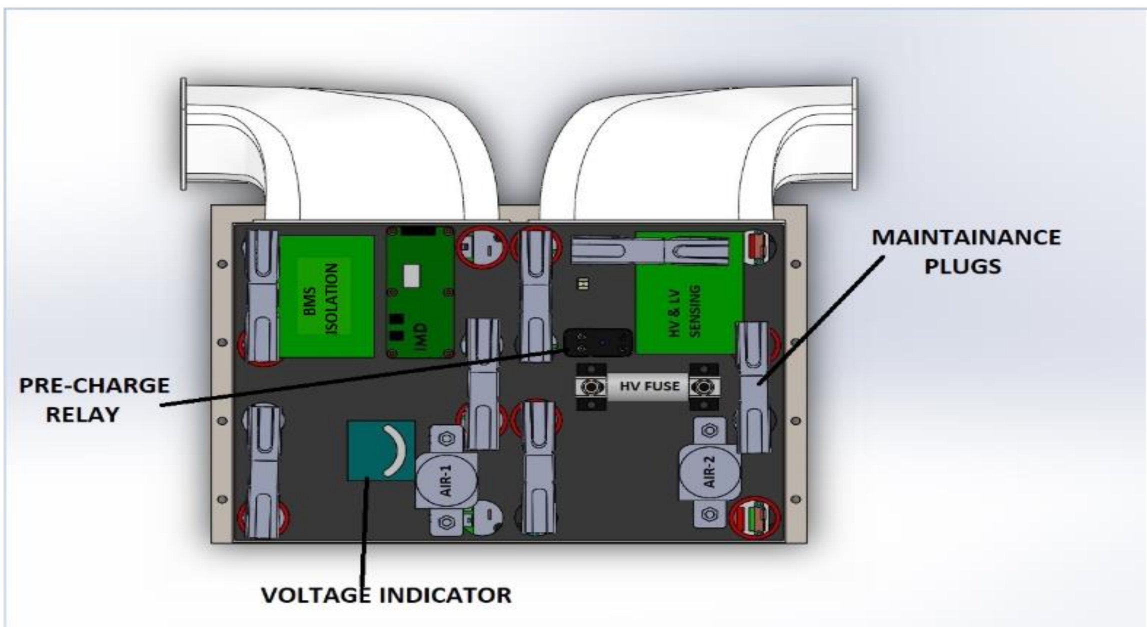

Fig 36: Precharge Relay location in Accumulator

2.10 Discharge circuitry

2.10.1 Description

When the safety circuit is activated, the power supply to contactors is broken and the HV system is isolated. But the load capacitance may be still charged to high voltage levels. The discharge circuit discharges the load capacitance so that the power system is de-energized. The discharge circuit used consists of:

A discharge resistor, to limit the discharge current and to activate the discharge circuit.

2.10.2 Wiring, cables, current calculations, connectors

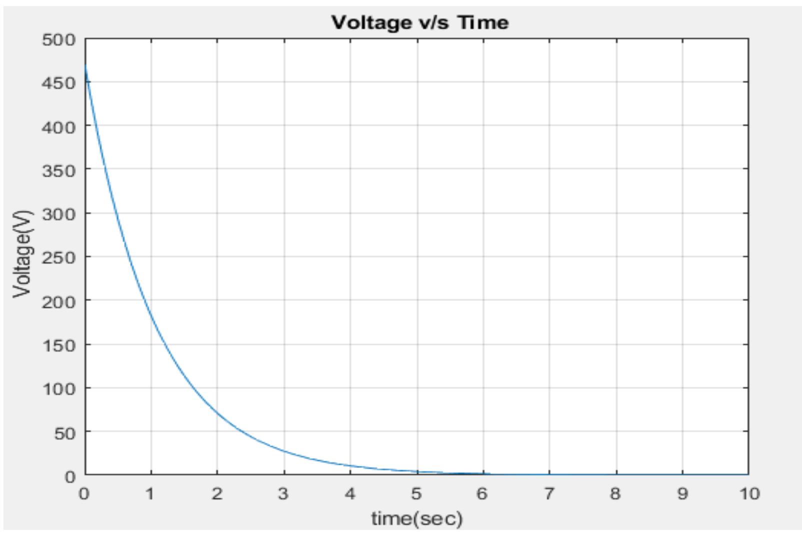

Fig 37: Voltage Characteristics of Discharge Circuit

MC formula :- V = 470*exp(-t/(3300*320*(10^(-6)))

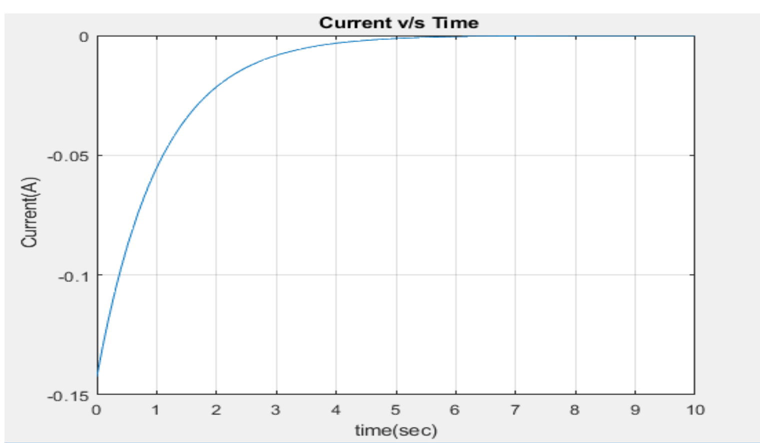

Fig 38: Current Characteristics of Discharge Circuit

Formula: I = -470*exp(-t/(3300*320*(10^(-6)))/3300

Resistor Type:	Ohmite
Resistance:	3.3kΩ
Continuous power rating:	10W
Overload power rating:	100W for 5 sec
Voltage rating:	500V
Maximum expected current:	1.25A
Average current:	0.625A
The cross-sectional area of the wire used:	0.5189 mm^2

Table 2.9 General data of the discharge circuit

2.10.3 Position in car

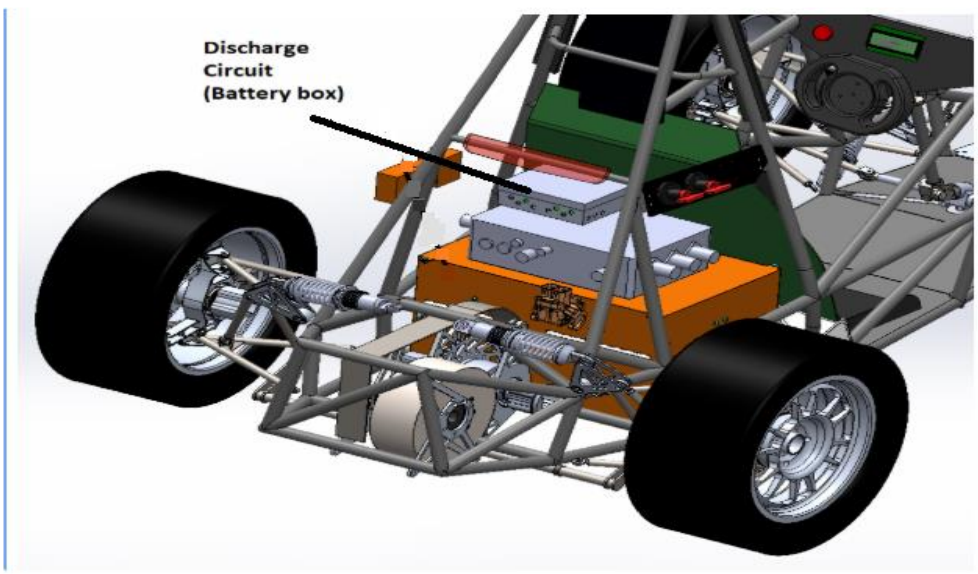

Fig.39: Discharge Circuit position in vehicle

2.11 HV Disconnect (HVD)

2.11.1 Description

The HVD used in the power system is the Rosenberger HVR200 PowerPole Connector. Since this connector does not require tools to get opened, it features an auxiliary contact which ensures the opening of the main contactors if the auxiliary contact is opened. The pilot contacts provided in the HVD will disable the shutdown circuit.

2.11.2 Wiring, cables, current calculations, connectors

The HV disconnect is placed between the contactors and Motor Controller input. It disconnects both positive and negative phase wires between the accumulator and motor controller

2.11.3 Position in car

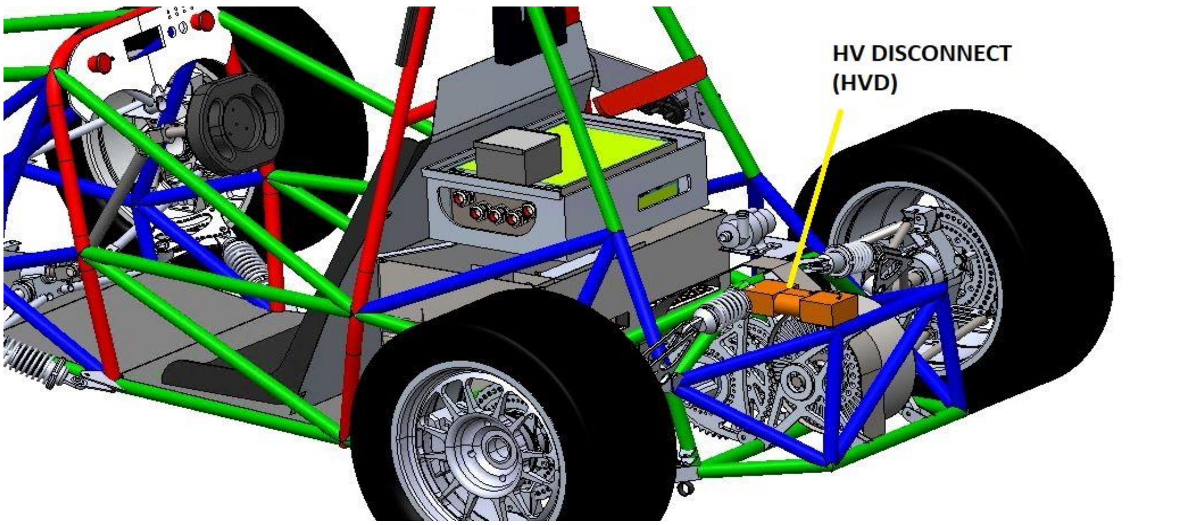

Fig.40: Position of HVD in Vehicle

2.12 Ready-To-Drive-Sound (RTDS)

2.12.1 Description

The car has to make a characteristic sound, once, when it is ready to drive. The car is ready to drive as soon as the motor will respond to the input of the torque encoder. The car will make a beep sound for 3 seconds. This sound is produced only when the power is provided to a buzzer which in turn, is only done when TS is active without any errors and the brake pedal is actuated for the first time (after which it takes 5 more seconds delay before activating the Motor Controller Run).

2.12.2 Wiring, cables, current calculations, connectors

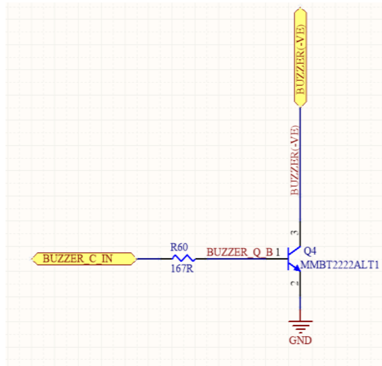

Fig.41: RTDS Circuit Diagram

BUZZER_C_IN signal from the microcontroller will get high, the transistor will get on. The buzzer will get potential GND and will produce sound.

2.12.3 Position in car

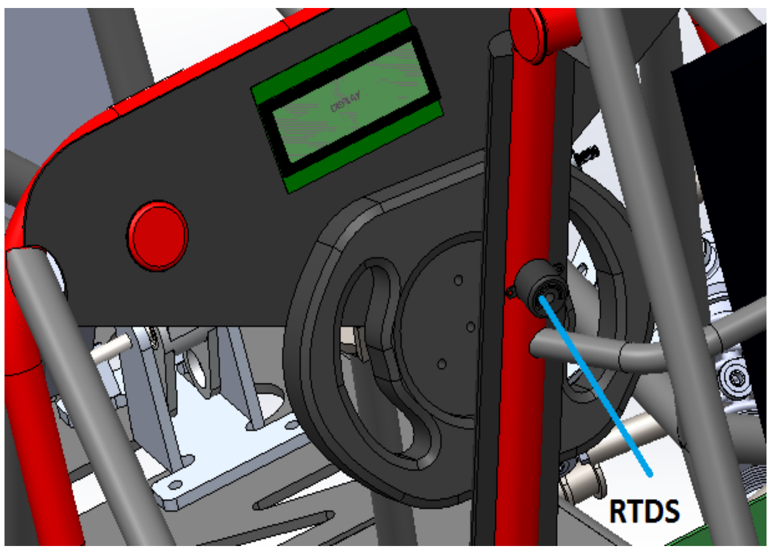

Fig.42: RTDS Position in Vehicle

2.13 Accumulator

2.13.1 Accumulator pack 1

2.13.1.1 Overview/description/parameters

The power system consists of two accumulator packs. Accumulator pack 1 is used for powering HV components of the vehicle. The cells are placed in a single steel box. The accumulator consists of 112 Melasta High Power LiP cells (15Ah). The entire accumulator pack is divided into 7 stacks (each stack voltage less than 120VDC) and each module consists of 16 cells. The cells are identical and based on

Lithium Yttrium chemistry. The accumulator is equipped with an AMS. Important parameters are listed below:

Maximum Voltage:	470.4VDC
Nominal Voltage:	414.4.6VDC
Minimum Voltage:	336VDC
Peak discharge current:	225A for 1s
Maximum continuous discharge current:	150A
Maximum continuous charging current:	15A
Total numbers of cells:	112
Cell configuration:	112S1P
Total Capacity:	15 Ah
Number of cell stacks < 120VDC	7

Table 3.1 Main accumulator parameters

The accumulator container is built with 1mm steel. To avoid any conductive penetration Laxen sheet is introduced between the container and the battery pack as well as between each separate module of the battery pack.

Refer to Fig23 for Circuit diagram of HV connections

The image shows Accumulator container and its components, viz, AIRs, BMS, BMS isolation and IMD. It clearly depicts that GLVS is not included in the container.

As depicted in Fig 43, the battery pack is divided into 7 modules each containing 16 cells to ensure that EV 6.3.2 is satisfied. The maintenance plug has a housing made of PC UL94 V-0 ensuring non-conduction. The length of cable wire chosen is such that it is impossible to connect a segment to other than that intended.

The Laxen Sheet is used between each segment as well as between the segment and conductor thus ensuring there is no electrical contact possible.

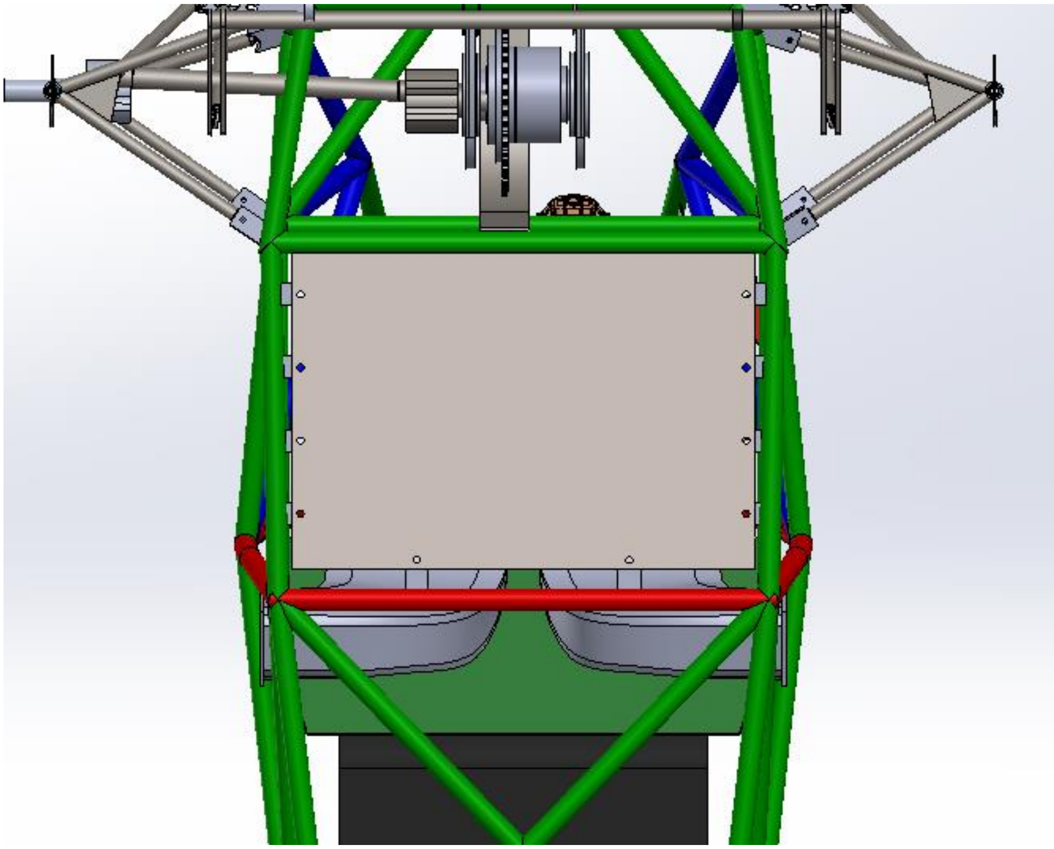

Fig66:- Comparison between dimensions of Battery Box and Bottom View of Vehicle

The figure shows that the dimensions of the battery box are clearly smaller than that of the bottom part of the vehicle. It is easy to remove the accumulator container from the bottom of the vehicle when required.

2.13.1.2 Cell description

Important parameters of cell used in the accumulator:

Cell Manufacturer and Type:	Melasta Polymer Li-Ion Battery
Cell nominal capacity:	15 Ah
Maximum Voltage:	4.2 V
Nominal Voltage:	3.7V
Minimum Voltage (0% SoC):	3V
Peak charging current:	30A for 1s
Maximum continuous discharge current:	150A
Maximum continuous charging current:	15A
Maximum Cell Temperature (discharging):	60°C
Maximum Cell Temperature (charging):	45°C

Cell chemistry:	Polymer Li-Ion

Table 3.2 Main cell specification

2.13.1.3 Cell configuration

Accumulator consists of 112 Melasta Polymer Li-Ion Battery cells connected in series. Cells are connected using copper bars. This 112S1P configuration has been distributed in 7 segments to ensure that the energy content of each segment should not be greater than 6MJ.

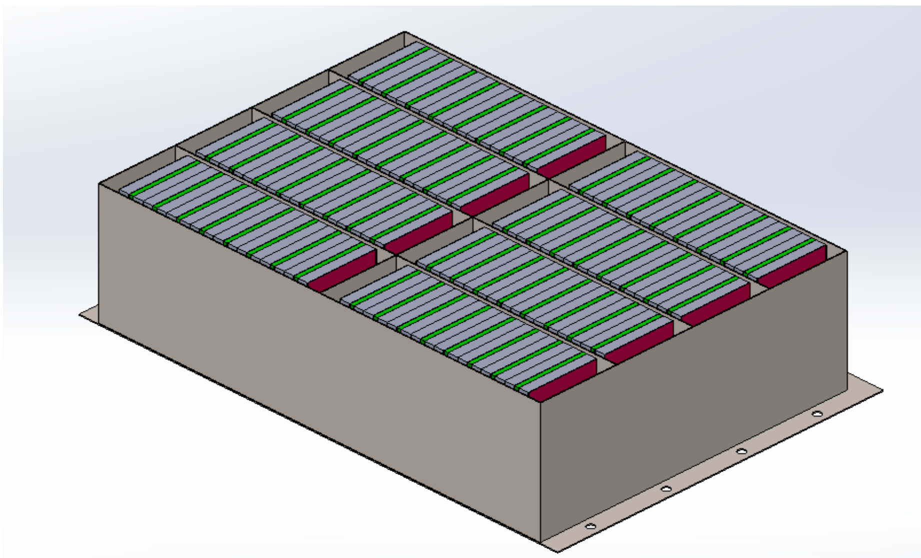

Fig.43: Accumulator Cell Configuration and CAD Rendering

2.13.1.4 Cell temperature monitoring

The BMS measures the temperature of 56 cells (50% of total cells). The BMS has thermistors connected to cell/s of each segment of the battery pack and hence monitor the temperature of cells. In the event that the temperature of any of the connected cells exceeds 60-degree celsius, the BMS will trip a relay connected in series in the shutdown circuit.

2.13.1.5 Accumulator Insulation Relays

The accumulator insulation relays used are GX14 350+ Amp 12-800 VDC Contactor. The accumulator insulation relays are placed inside the battery box. The coil voltage of the relay is 24V and it is connected to the shutdown circuit output.

Fig 36 shows the 2 mechanical AIRs which are normally open in the battery box.
Fig23 depicts the AIRs open both poles of the accumulators

Relay Type:	GX14 350+ Amp 12-800 Vdc Contactor
Contact arrangement:	SPST
Continuous DC current rating:	350A
Overload DC current rating:	750A for 10s
Maximum operation voltage:	800VDC

Nominal coil voltage:	24VDC
Normal Load switching: Maximum Load switching	Make and break up to 300A 10 times at 1000A

Table 3.3 Basic AIR data

2.13.1.6 Fusing

HV Fuse:

The fuse used for HV protection is L70QS175 LITTELFUSE.

Fuse type:	Round Body Bolted Type HF type fuse
Continuous current rating:	175A
Rated operating voltage	700VDC
Type of fuse:	High speed Body: Melamine Caps: Copper Alloy (Silver Plated)
I^2t rating:	16100A^2s at 700VDC
Interrupt Current (maximum current at which the fuse can interrupt the current)	50000A

Table 3.4 HV fuse data

Continuous RMS Current of Motor Controller:	200A
Peak Current of Motor Controller	400A
HV Fuse L70QS175 Ampere Rating	175A

Table 3.5: Components protected by HV fuse

2.13.1.7 Battery Management System

We are using **BQ76PL455A** as the cell voltage monitor. A maximum of 16 cells and a minimum of 6 cells can be monitored using this IC. A **14-bit ADC** is also present which provides sufficient accuracy in the voltage measurement on all measuring ports and auxiliary inputs utilized for temperature monitoring of 50% cells in each stack.

The BMS is used to monitor the voltage of all the cells continuously and use it to signal all kinds of faults such as over-voltage, under-voltage, over-temperature, open or short circuit. A special part of BMS is the HV sensing unit (PCB) which senses TS voltage and current in real-time to provide for necessary calculations like SOC, power, over-current, etc. All this data can be communicated to the main (shutdown circuit) PCB via CAN and can also be seen on the serial monitor of a laptop.

The voltage is sensed by the IC by VSENSE points. The software enables us to set a threshold for batteries here we have set the upper limit and lower limit as 4.2V and 3.0V respectively. The maximum permissible temperature during charging is 45º C and during discharge is 60º C. The software allows to set temperature threshold (which we get using thermistor). Whenever any of the conditions are violated the BMS error signal goes low (which is normally high i.e., in case of no error). Each thermistor wire connected to BMS contains a crimp that is bolted to the negative terminal of a cell and the positive terminal is connected to the auxiliary input points of the BMS, thus continuously measuring the temperature of the cell. The HV Sensing PCB which is a part of AMS is used to measure TS current.

Any communication between two BMS modules will be through a twisted pair wire cable coming out of the two connectors shown on the bottom right of the CAD. They are properly decoupled for any parasitic noise and the outer cable will be shielded for shorting protection and to prevent any unwanted touching with battery terminals.

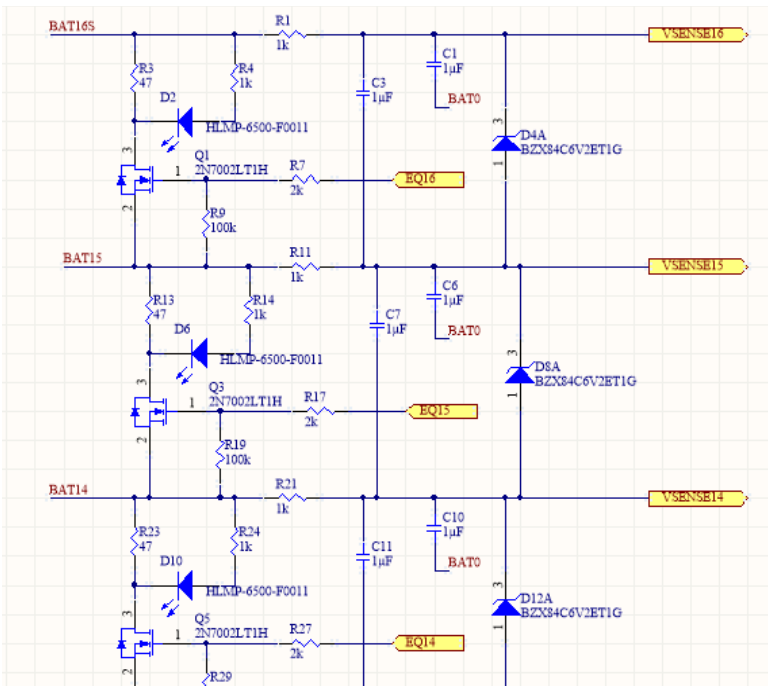

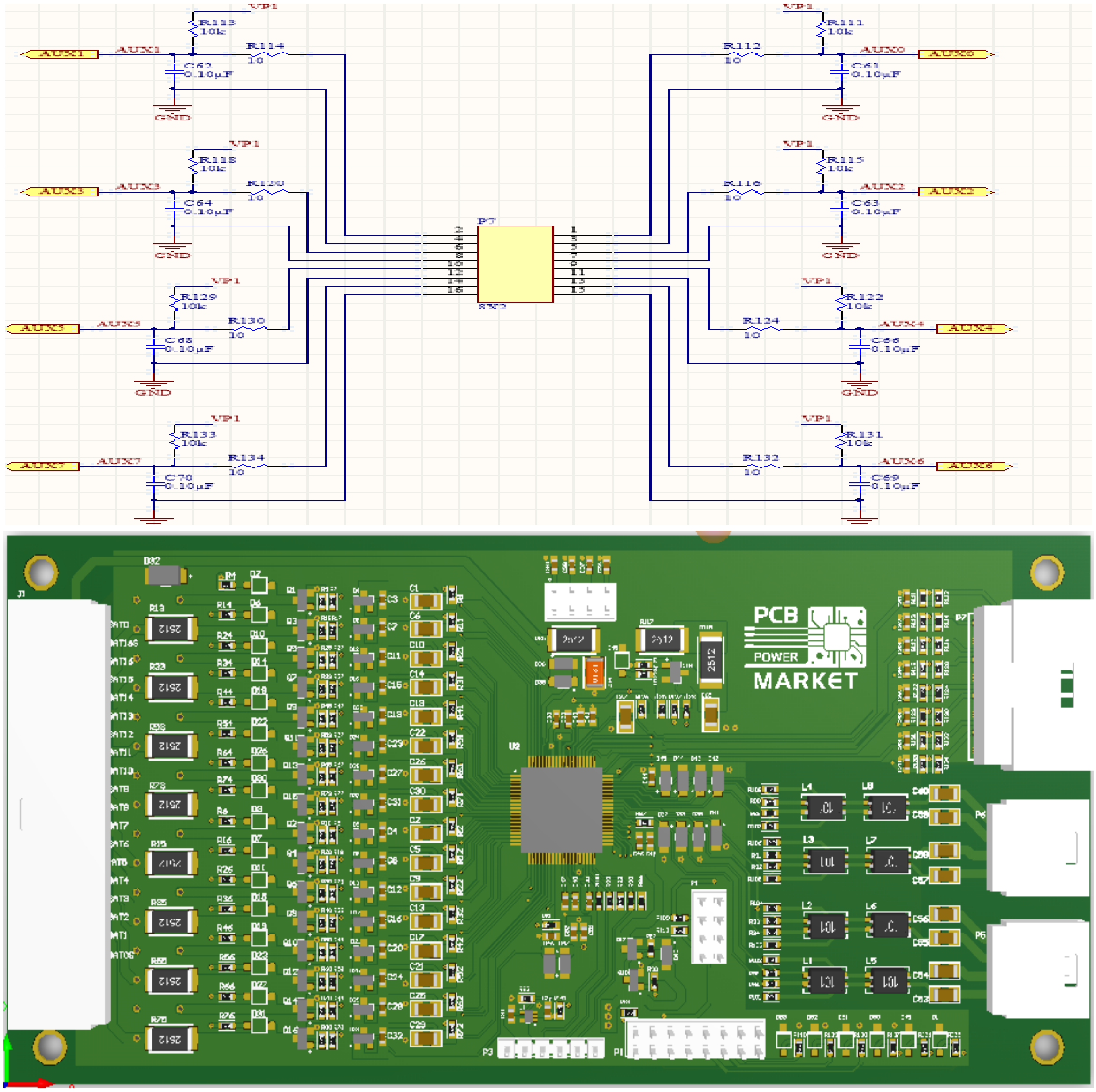

Fig 44 :- BMS Single Module (CAD)

2.13.1.8 Accumulator Indicator

An analog voltmeter has been used to measure the voltage on the motor controller side of the main contactors. It will be mounted on top of the battery box. The voltage present on the motor controller side of the AIRs would be indicated by the voltmeter.

Accumulator container contains a voltage indicator with a red led and will glow whenever TS voltage is greater than 60 VDC. The voltage indicator is mounted on the top of the accumulator container and is visible on the top of the container. The indicator is hard-wired electronics directly supplied by TS, it always gives TS voltage even if the accumulator is removed from the car or even if it is disconnected from the GLV system.

For Wiring, refer to Wiring diagram of Precharge Circuitry with Precharge Relay and Resistor

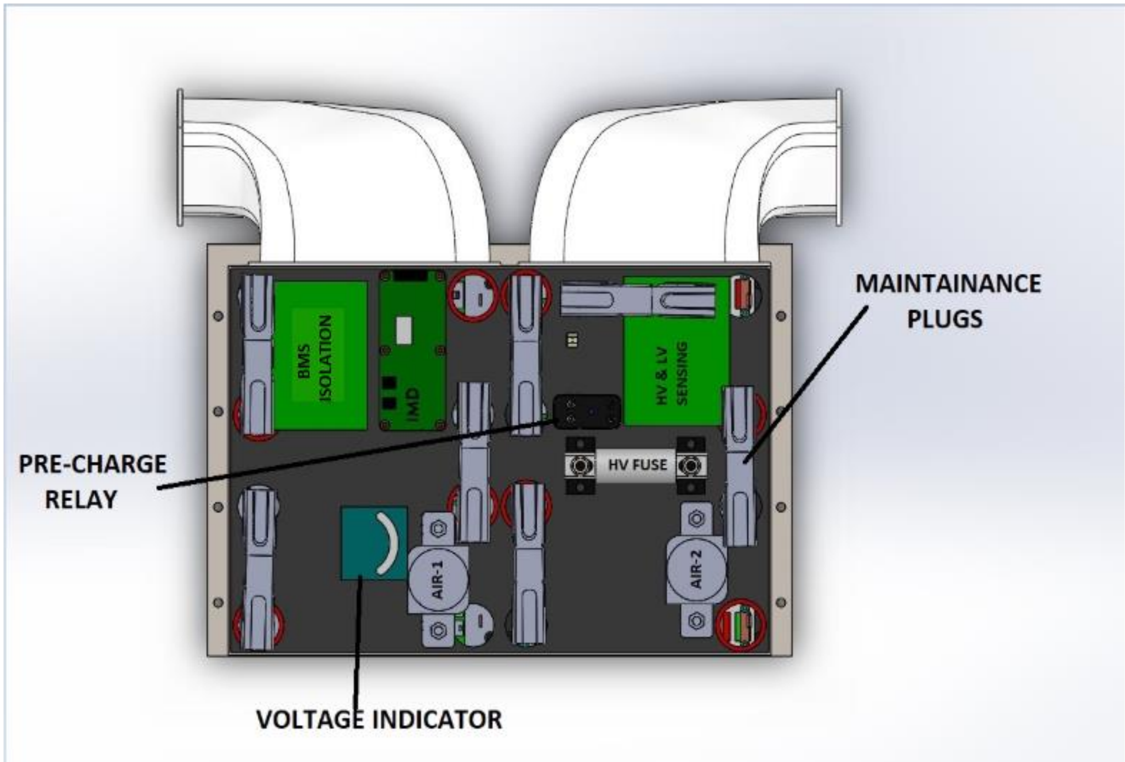

Fig 63: Position of Voltage Indicator in the Accumulator container.

2.13.1.9 Wiring, cables, current calculations, connectors

25 sq. mm Coroplast cables have been used for connections of the accumulator with the motor controller. Anderson Power's DS-PP180 is being used as maintenance plugs. The plug can be easily mated and unmated. The cells are connected using copper strips. The strips are placed between the cell rabs and bolted. The specifications of the wire used are as given in the table.

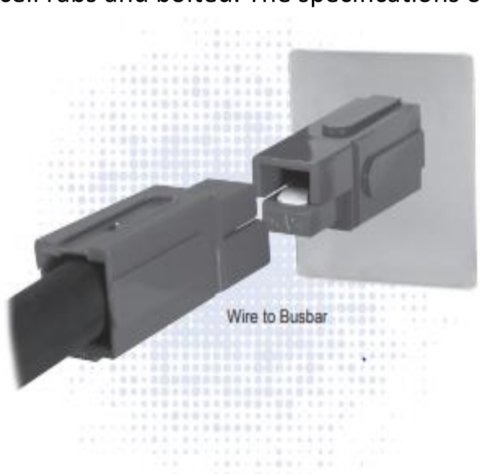

Fig 67 : Maintenance Plug

Model/ Part no:	DS_PP180
Ampacity:	350A
Voltage rating:	600V

Table 3.11: Maintenance plug data

Wire type	Coroplast Cables
Continuous current rating:	150A
Cross-sectional area	25mm²
Maximum operating voltage:	1000VDC
Operating Temperature range:	-40°C to 180°C
The wire connects the following components:	Accumulator and Motor-controller

Table 3.12: Wire data of HV wires 25 sq. mm

2.13.1.10 Charging / Chargers

The charging circuit will be placed outside the car to follow the rule that accumulators must be removed from the car for charging. Charger supplies 5-6A constant current with self- adjusting the voltage. The charging circuit includes IMD and BMS which will be capable to switch OFF the charger in case of any insulation failure or if any cell reaches beyond its operating range.

The TS charging wires are orange and during charging the BMS is ON. Whenever a fault is detected the charging circuit shuts down to prevent any further damage.
IMD is used separately and placed inside the battery box and is ON during charging as well. A red indicator light in the cockpit labeled as “IMD” and “BMS” turns on whenever a fault is detected due to it.

As the charger is purchased from the market, a shutdown circuit is designed for fault detection. It includes a Charger Emergency Shutdown Button. It is a push rotate button which will disable charger when pushed. It also has a Reset button. If the shutdown circuit is opened due to error, it won’t enable the charging system until it is manually reset.

Charger type:	General electronics charger
Maximum charging power:	0.96kW
Maximum charging voltage:	96V
Maximum charging current:	10A
Interface with accumulator	Proprietary, serial communication
Input voltage:	230 VAC
Maximum Input current:	5A

Table 3.13: General Charger data

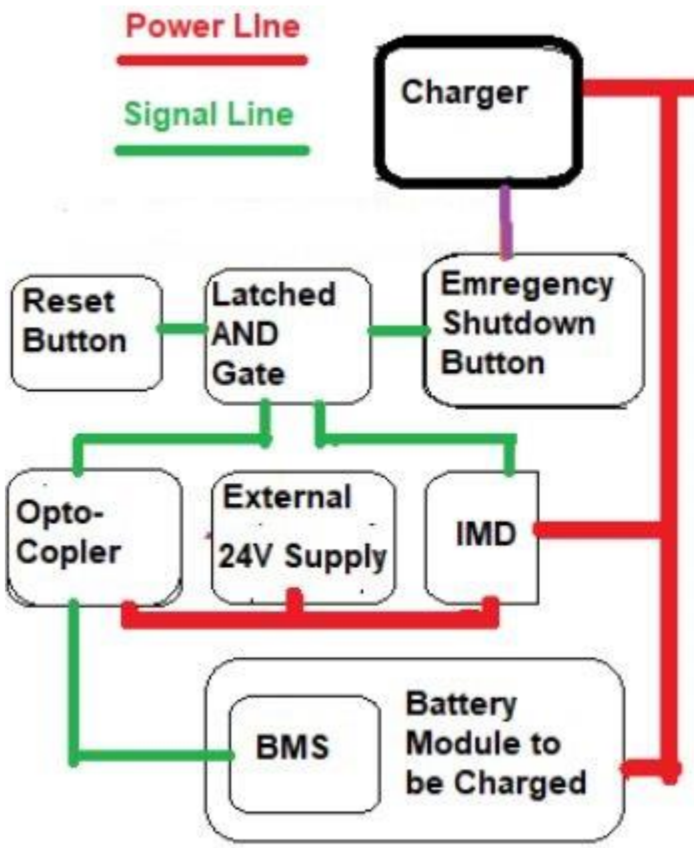

Fig65: Shutdown Circuit Of Charger

2.13.1.11 Mechanical Configuration/materials

The 112 cells are separated into 7 segments. Each segment is enclosed in a steel case to allow heat conduction. All segments are connected in series. The top of the case is covered using a transparent sheet of Lexan. The cell terminals are bolted to copper bars. A layer of Lexan separates these terminals from AIRs. The maintenance plugs and fuse are mounted on the same sheet. The connections between them are via copper plates, bus bars, and wires. The material used for the container is mild steel 4130.

Fig 69:CAD Rendering of cells in the battery box with transparent Lexan sheet on top

2.13.1.12 Position in car

The accumulator is attached in the rear part of the vehicle.

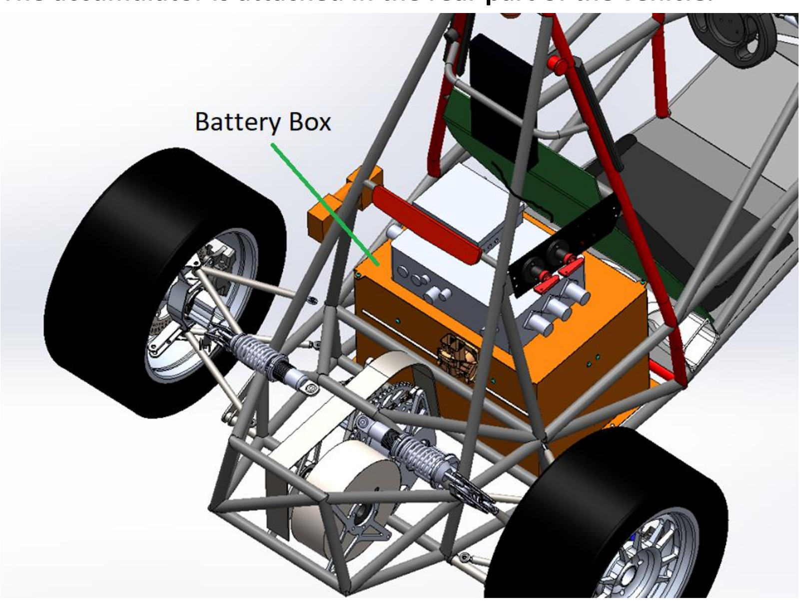

Fig.45: Accumulator Position in Vehicle

2.13.2 Accumulator pack 2

2.13.2.1 Overview/description/parameters

The accumulator pack 2 is used to power low voltage components of the vehicle. The cells are placed in a single steel box. The accumulator consists of 7 Melasta High Power LiP cells (15Ah). The entire accumulator pack consists of only one stack (each stack voltage less than 120VDC). The cells are identical and based on Lithium Yttrium chemistry. The accumulator is equipped with an AMS. Important parameters are listed below:

Maximum Voltage:	29.4VDC
Nominal Voltage:	25.9VDC
Minimum Voltage:	21VDC
Peak discharge current:	225A for 1s
Maximum continuous discharge current:	150A
Maximum continuous charging current:	15A
Total numbers of cells:	7
Cell configuration:	7S1P
Total Capacity:	15 Ah
Number of cell stacks < 120VDC	1

Table 3.1 Main accumulator parameters

The accumulator container is built with 1mm steel. To avoid any conductive penetration Laxen sheet is introduced between the container and the battery pack.

2.13.2.2 Cell description

Important parameters of cell used in the accumulator:

Cell Manufacturer and Type:	Melasta Polymer Li-Ion Battery
Cell nominal capacity:	15 Ah
Maximum Voltage:	4.2 V
Nominal Voltage:	3.7V
Minimum Voltage (0% SoC):	3V
Peak charging current:	30A for 1s
Maximum continuous discharge current:	150A
Maximum continuous charging current:	15A
Maximum Cell Temperature (discharging):	60°C
Maximum Cell Temperature (charging):	45°C
Cell chemistry:	Polymer Li-Ion

Table 3.2 Main cell specification

2.13.2.3 Cell configuration

Accumulator consists of 7 Melasta Polymer Li-Ion Battery cells connected in series. Cells are connected using copper bars. This 7S1P configuration consists of 7 cells connected in series and the energy content of the battery pack does not exceed 6MJ.

2.13.2.4 Cell temperature monitoring

The BMS measures the temperature of 4 cells (more than 50% of total cells). The BMS has thermistors connected to cell/s of each segment of the battery pack and hence monitor the temperature of cells. In the event that the temperature of any of the connected cells exceeds 60-degree celsius, the BMS will trip a relay connected in series in the shutdown circuit.

2.13.2.5 Accumulator Insulation Relays

The accumulator insulation relays used are GX14 350+ Amp 12-800 VDC Contactor. The accumulator insulation relays are placed inside the battery box. The coil voltage of the relay is 24V and it is connected to the shutdown circuit output.
Fig 36 shows the 2 mechanical AIRs which are normally open in the battery box.
Fig 23 depicts the AIRs open both poles of the accumulators

Relay Type:	GX14 350+ Amp 12-800 Vdc Contactor
Contact arrangement:	SPST
Continuous DC current rating:	350A
Overload DC current rating:	750A for 10s
Maximum operation voltage:	800VDC
Nominal coil voltage:	24VDC
Normal Load switching: Maximum Load switching	Make and break up to 300A 10 times at 1000A

Table 3.3 Basic AIR data

2.13.2.6 Fusing

LV Fuses:

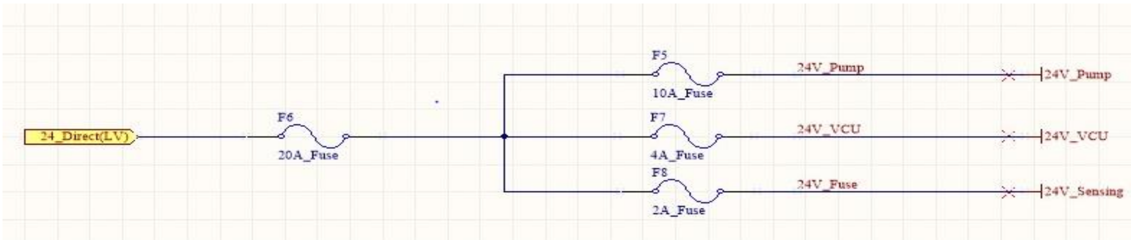

Fig 68: Schematic of LV fuses

Fuse type:	Surface mount slow blow fuse C1S-series 1206 PCB footprint
Continuous current rating:	2A
Rated operating voltage	63VDC
I^2t rating:	$0.26A^2s$
Interrupt Current (maximum current at which the fuse can interrupt the current)	50A

Table 3.6: 2A LV fuse data

Fuse type:	Surface mount slow blow fuse MFU-series 0805 PCB footprint
Continuous current rating:	4A
Rated operating voltage	32VDC
I^2t rating:	$0.0403A^2s$
Interrupt Current (maximum current at which the fuse can interrupt the current)	50A

Table 3.7: 4A LV fuse data

Fuse type:	Surface mount slow blow fuse 0679L-series 2410 PCB footprint
Continuous current rating:	10A
Rated operating voltage	125VDC
I^2t rating:	$25.7A^2s$
Interrupt Current (maximum current at which the fuse can interrupt the current)	300A

Table 3.8: 10A LV fuse data

Fuse type:	Surface mounted fuse SF-2410FxxxW series 2410 PCB footprint
Continuous current rating:	20A
Maximum operating voltage	65VDC
I^2t rating:	$126.2A^2s$
Interrupt Current (maximum current at which the fuse can interrupt the current)	100A @65VDC

Table 3.9: 20A LV fuse data

Radiator Pump Current Rating	2.5A
Radiator Fans Current Rating	2*2.8A = 5.6A
Accumulator Cooling Fan Rating	2*0.5A = 1A
Current drawn by Microcontroller	2*500mA = 1A
Current drawn by Isolation Relay and Latches	2A
Auxiliary Current is drawn by Motor Controller	2A

Table 3.10: Components protected by LV fuse

2.13.2.7 Position in the car-

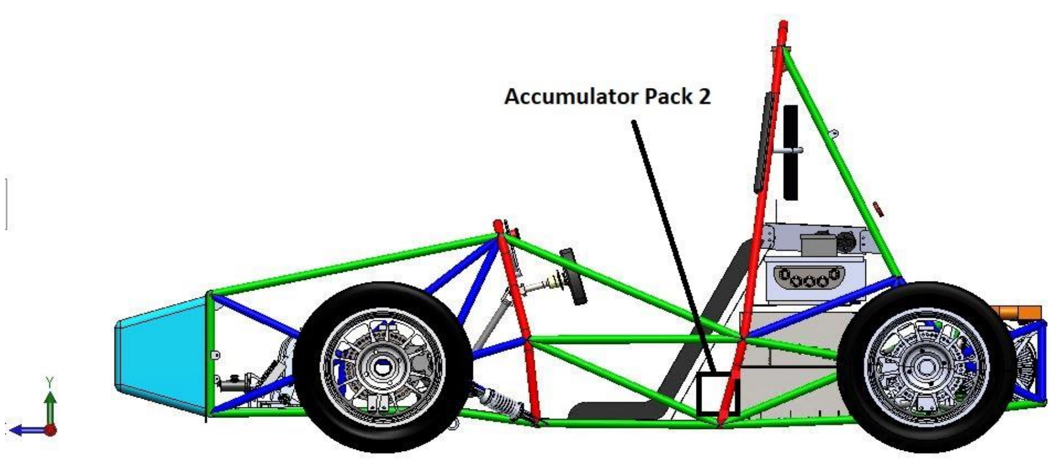

Fig.75 - Position of Accumulator Pack 2(Back to List of Figures)

2.13.2.8 Battery Management System

We are using **BQ76PL455A** as the cell voltage monitor. A maximum of 16 cells and a minimum of 6 cells can be monitored using this IC. A **14-bit ADC** is also present which provides sufficient accuracy in the voltage measurement on all measuring ports and auxiliary inputs utilized for temperature monitoring of 50% cells in each stack.
The BMS is used to monitor the voltage of all the cells continuously and use it to signal all kinds of faults such as over-voltage, under-voltage, over-temperature, open or short circuit. A special part of BMS is the HV sensing unit (PCB) which senses TS voltage and current in real-time to provide for necessary calculations like SOC, power, over-current, etc. All this data can be communicated to the main (shutdown circuit) PCB via CAN and can also be seen on the serial monitor of a laptop.
The voltage is sensed by the IC by VSENSE points. The software enables us to set a threshold for batteries here we have set the upper limit and lower limit as 4.2V and 3.0V respectively. The maximum permissible temperature during charging is 45º C and during discharge is 60º C. The software allows to set temperature threshold (which we get using thermistor). Whenever any of the conditions are violated the BMS error signal goes low (which is normally high i.e., in case of no error).
Each thermistor wire connected to BMS contains a crimp that is bolted to the negative terminal of a cell and the positive terminal is connected to the auxiliary input points of the BMS, thus continuously measuring the temperature of the cell. The HV Sensing PCB which is a part of AMS is used to measure TS current.
Any communication between two BMS modules will be through a twisted pair wire cable coming out of the two connectors shown on the bottom right of the CAD. They are properly decoupled for any parasitic noise and the outer cable will be shielded for shorting protection and to prevent any unwanted touching with battery terminals.

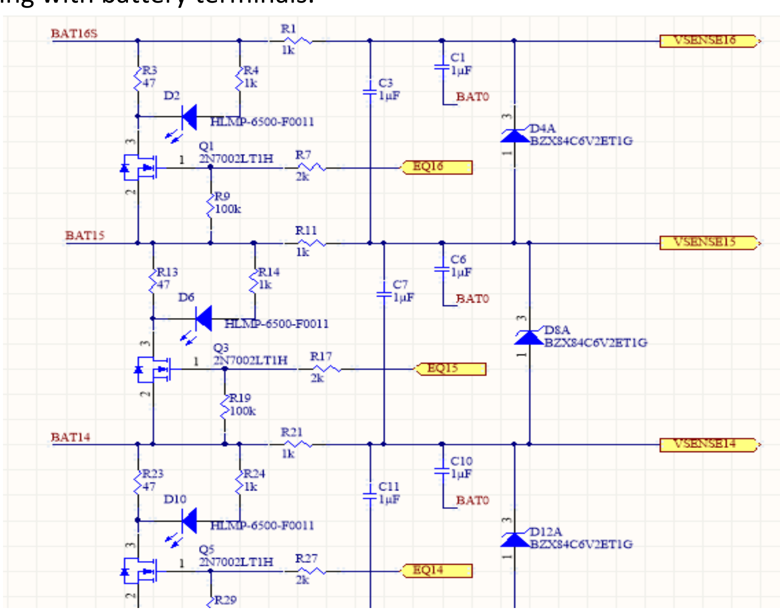

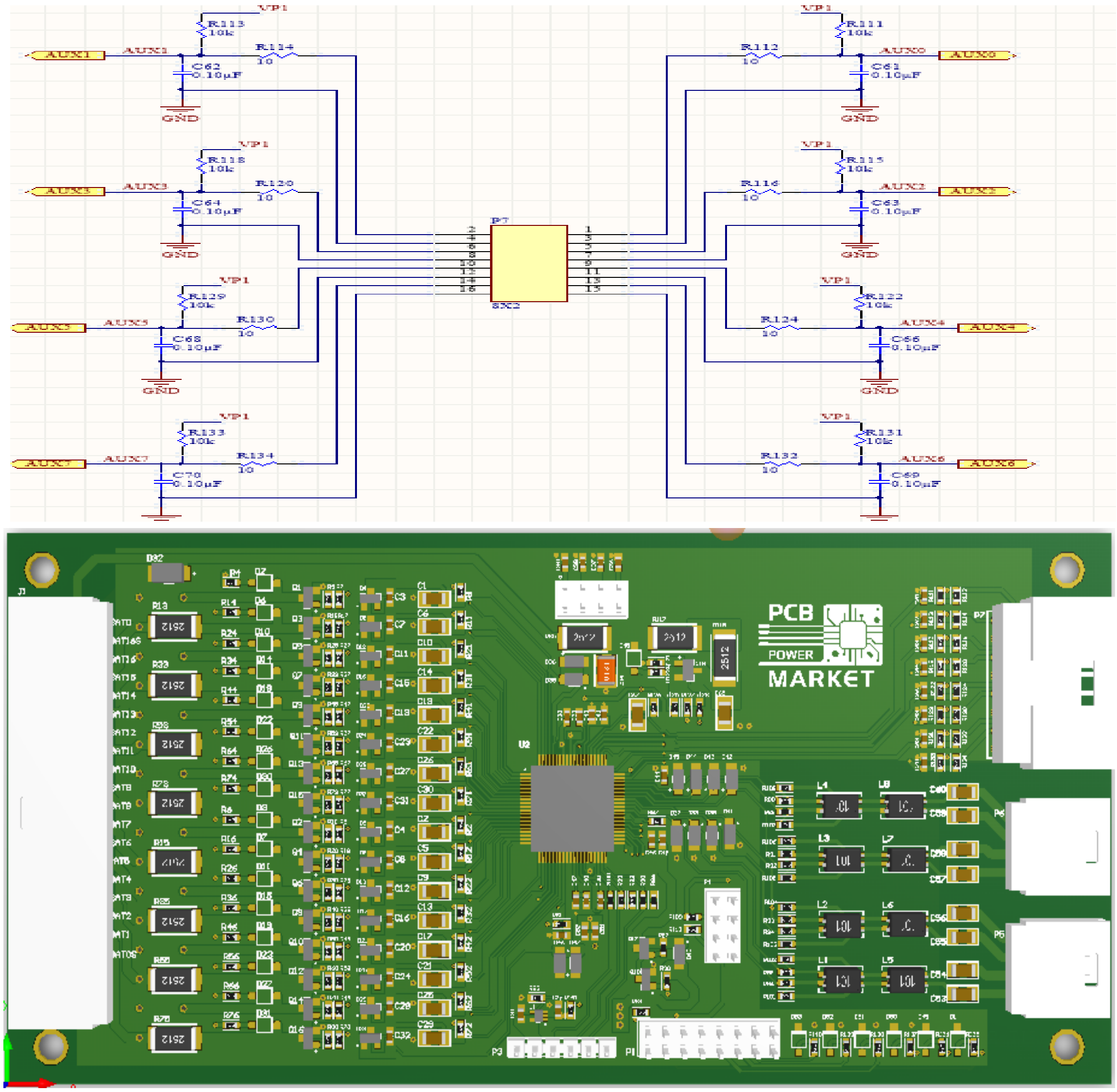

Fig 44:- BMS Single Module (CAD)

2.13.2.9 Wiring, cables, current calculations, connectors

The cells are connected using copper strips. The strips are placed between the cell rabs and bolted. The specifications of the wire used are as given in the table.

2.13.2.10 Charging / Chargers

The charging circuit will be placed outside the car to follow the rule that accumulators must be removed from the car for charging. Charger supplies 5-6A constant current with self- adjusting the voltage. The charging circuit includes IMD and BMS which will be capable to switch OFF the charger in case of any insulation failure or if any cell reaches beyond its operating range.

The TS charging wires are orange and during charging the BMS is ON. Whenever a fault is detected the charging circuit shuts down to prevent any further damage. IMD is used separately and placed inside the battery box and is ON during charging as well. A red indicator light in the cockpit labeled as "IMD" and "BMS" turns on whenever a fault is detected due to it.

As the charger is purchased from the market, a shutdown circuit is designed for fault detection. It includes a Charger Emergency Shutdown Button. It is a push rotate button which will disable charger when pushed. It also has a Reset button. If the shutdown circuit is opened due to error, it won't enable the charging system until it is manually reset.

Charger type:	General electronics charger
Maximum charging power:	0.96kW
Maximum charging voltage:	96V
Maximum charging current:	10A
Interface with accumulator	Proprietary, serial communication
Input voltage:	230 VAC
Maximum Input current:	5A

Table 3.13: General Charger data

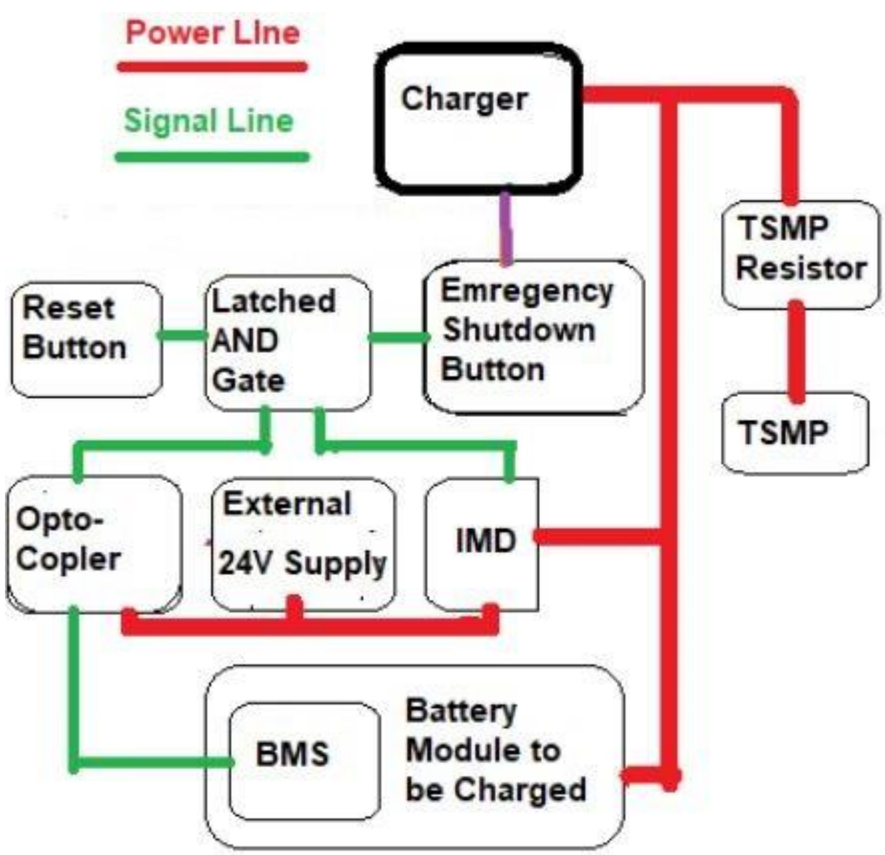

Fig 65: Shutdown Circuit Of Charger

2.13.2.11 Mechanical Configuration/materials

The 112 cells are separated into 7 segments. Each segment is enclosed in a steel case to allow heat conduction. All segments are connected in series. The top of the case is covered using a transparent sheet of Lexan. The cell terminals are bolted to copper bars. A layer of Lexan separates these terminals from AIRs. The maintenance plugs and fuse are mounted on the same sheet. The connections between them are via copper plates, bus bars, and wires. The material used for the container is mild steel 4130.

Fig 69:CAD Rendering of cells in the battery box with transparent Lexan sheet on top.

2.14 Energy meter mounting

2.14.1 Description

Voltage and Current are sensed at HV Sensing PCB through the isolated differential amplifier and the data is fed to the microcontroller. This microcontroller sends the data through CAN to Dashboard microcontroller where actual values are calculated. Energy data is calculated by the time-integrated product of V and I. The data is written to SD Card for future reference.

2.14.2 Wiring, cables, current, connectors

2.14.2.1 Current Sensing

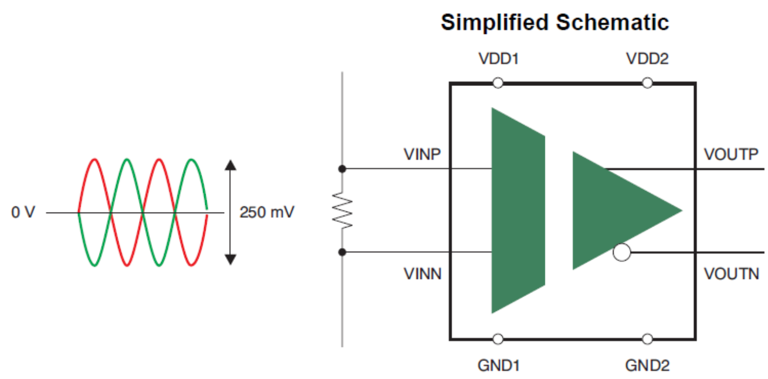

Fig 46:- Schematic of Current Sensing

The current sensing is done via an isolated differential amplifier AMC1200. The input to the isolated differential amplifier is a signal of maximum amplitude +250mV to the minimum amplitude of -250mV. The output is a 2V differential signal which is fed to a microcontroller for data logging and relaying to the DAQ.

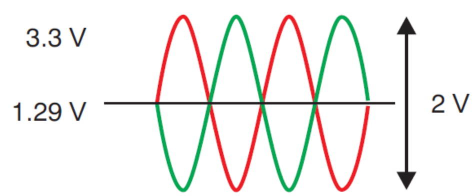

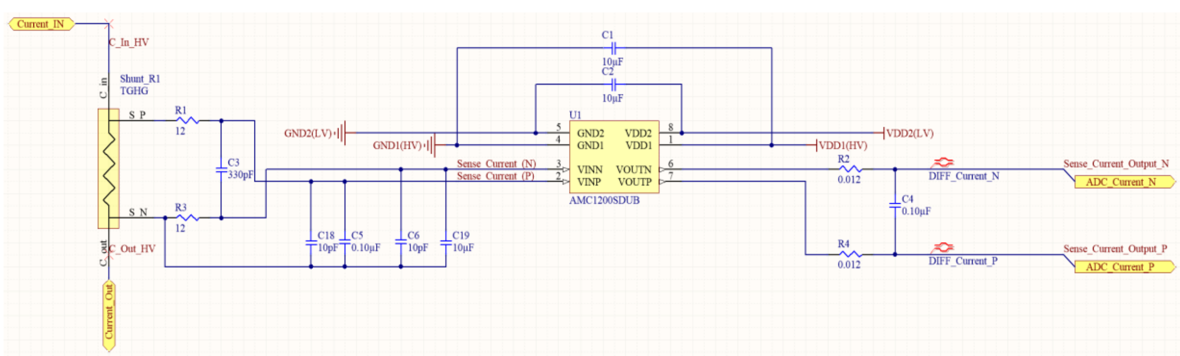

Fig 47:- Schematic of Current Sensing Circuit

The current sense circuit is based on a shunt based feed system, which generates the required ±250mV for the differential amplifier.

2.14.2.2 Voltage sensing

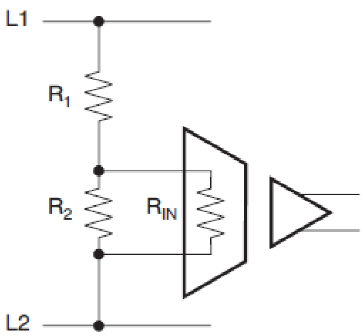

Fig 48:- Voltage Sensing

The voltage sensing is done via an isolated differential amplifier AMC1200. The input to the isolated differential amplifier is a signal of maximum amplitude +250mV to the minimum amplitude of -250mV. The output is a 2V differential signal which is fed to a microcontroller for data logging and transmitting to the DAQ. Here the required voltage is created from the HV battery using a high resistance.

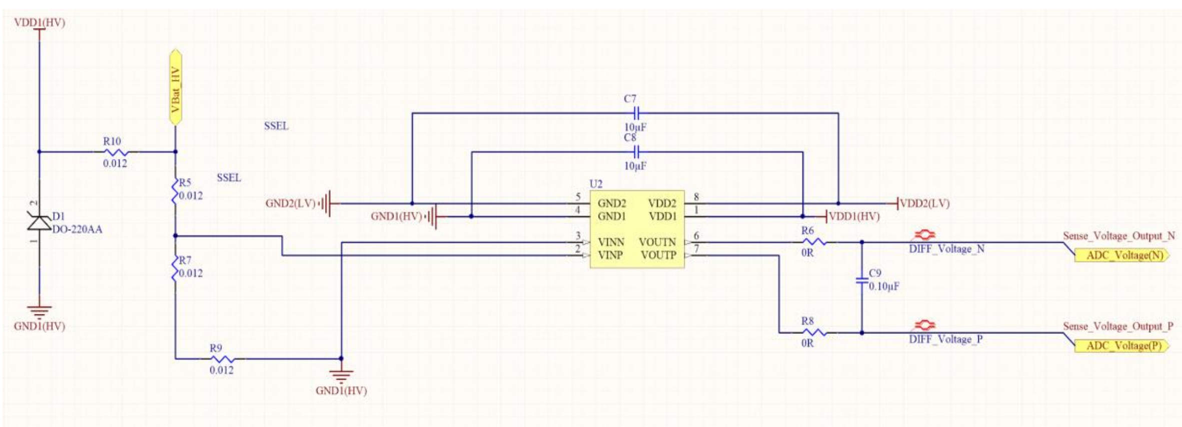

Fig 49:- Schematic of Voltage Sensing Circuit

The generalized communication mechanism of the HV sensing PCB, battery and the DAQ are as given below.

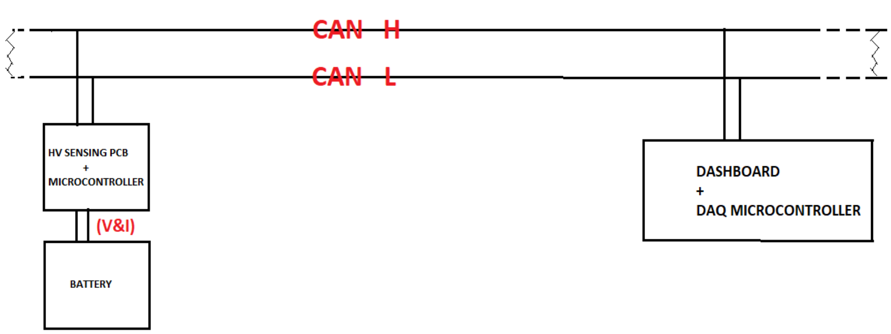

Fig.49: Energy Meter Schematic(Back to List of Figures)

2.14.2.3 Connectors

Phoenix connector cables are used in the PCB and these connectors are rated for maximum high voltage current.

2.14.3 Position in car

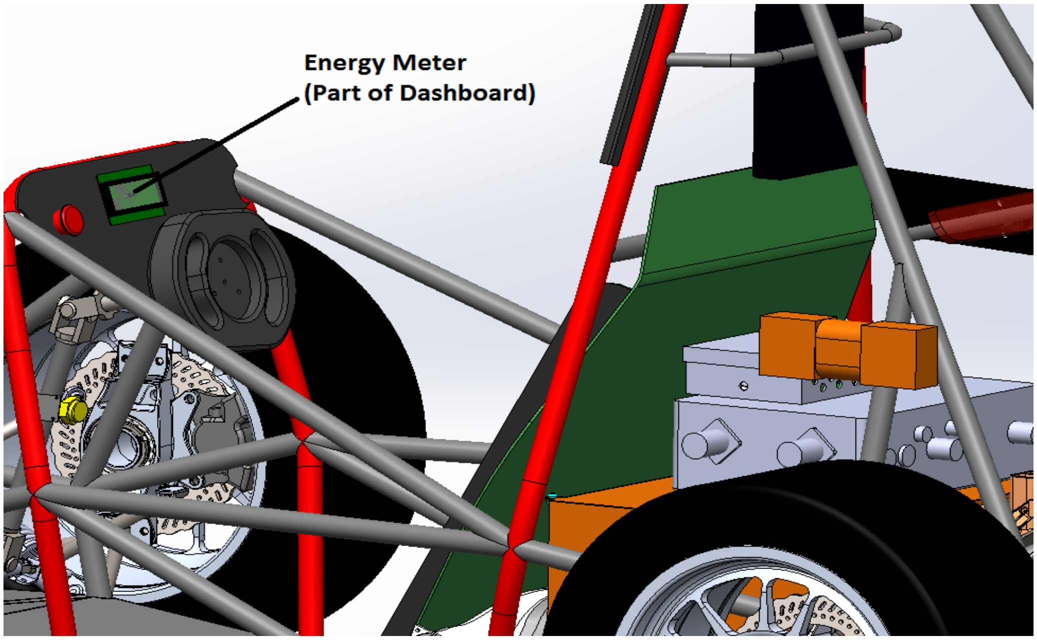

Fig 50: Energy Meter's Position

2.15 Motor controller

2.15.1 Motor controller 1

2.15.1.1 Description, type, operation parameters

The digital 3-phase current servo amplifiers BAMOCAR D3xx in combination with the motor provide a 4-quadrant drive which can be used in both rotation directions for drive operations and brake operations with energy feedback.

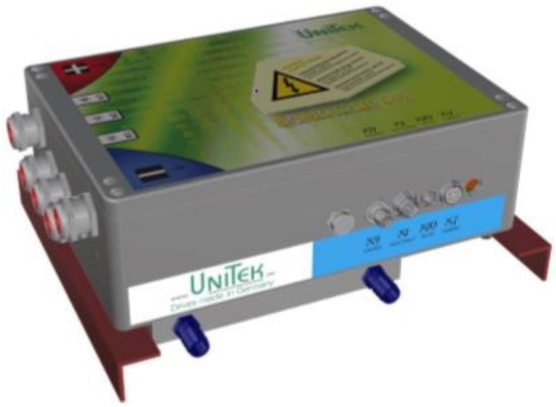

Fig 51: Motor Controller **BAMOCAR-PG-D3**

Motor controller type:	Digital three-phase Servo Amplifier BAMOCAR-PG-D3
Maximum continuous power:	140kW
Maximum peak power:	280kW
Maximum Input voltage:	700VDC
Output voltage:	3x450
Maximum continuous output current:	200A
Maximum peak current:	400A
Control method:	PWM, analog signal
Cooling method:	Liquid cooling unit max. 65°C, 12 l/min, pressure max. 1.3 bar
Auxiliary supply voltage:	24VDC

Table 5.1 General motor controller data

2.15.1.2 Wiring, cables, and connectors

Wire type	Coroplast Cables
Continuous current rating:	150A
Cross-sectional area	35mm²
Maximum operating voltage:	1000VDC
Operating Temperature range:	-40°C to 180°C
The wire connects the following components:	Motor and Motor-controller

Table 5.2: Data of wires between motor and motor-controller

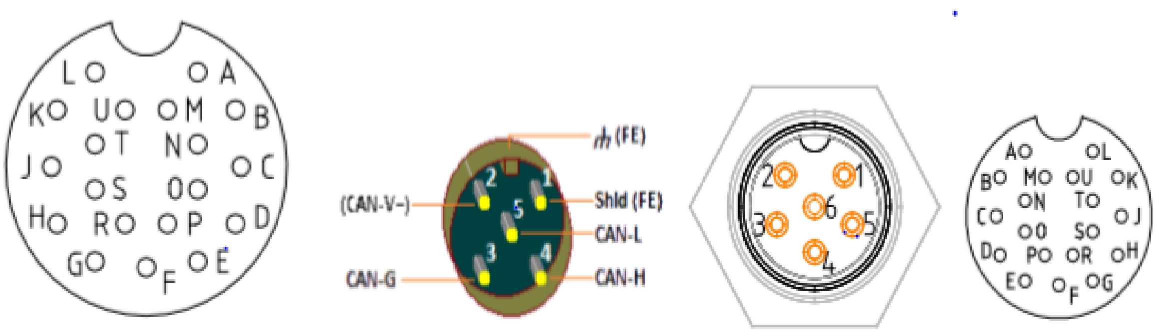

INPUT/OUTPUT Connector(Female) **CAN Connector (Female connector)** **RS232 (Female connector)** **FEEDBACK/ENCODER (Male connector)**

Fig70: Connectors of Motor controller

2.15.1.3 Position in car

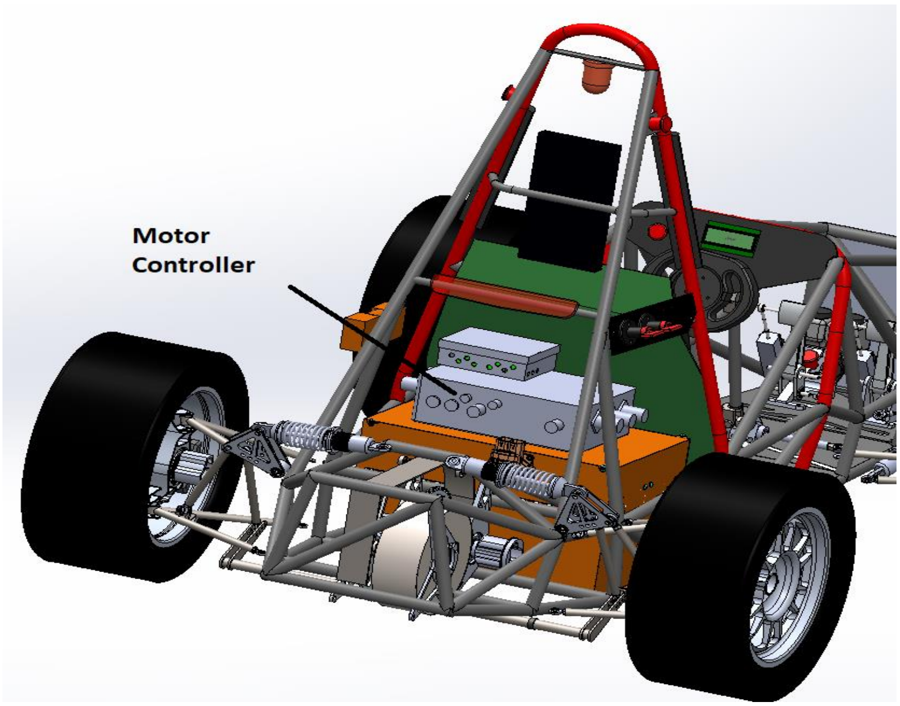

Fig 52: Motor Controller Position in Vehicle

2.15.2 Motor controller 2

In our Electric Vehicle, just one motor-controller is used.

2.16 Motors

2.16.1 Motor 1

2.16.1.1 Description, type, operating parameters

The Emrax 228 is a brushless permanent magnet synchronous motor designed to operate at 470 volts producing a peak of 100 kW (134 hp), 55 kW (74 hp) continuous, with an outrunner coil. Peak power is limited to 80kW through motor-controller. The motor has a 96% efficiency. The low working rpm of the engine means that it can turn a propeller at efficient speeds without the need for a reduction drive.

The motor is mounted on Al 6061 mounts and attached with the primary structure using AISI 1020 steel brackets of 2.5 mm thickness through M8 socket head cap screws and Nylon lock nuts (operate in ambient condition).

To protect the rotating casing of the motor from any foreign body, the scatter shield made up of 1mm thick AISI 1020 steel is used.

Fig.53: Motor (Back to List of Figures)

Motor Manufacturer and Type:	Emrax Innovative e-motors Axial flux synchronous permanent magnet motor/generator; sinusoidal three-phase
Motor principle	Synchronous, Permanently Excited
Maximum continuous power:	55kW
Peak power:	100 kW (In our vehicle it is electronically limited to 80kW)
Input voltage:	450VAC
Nominal current:	125A
Peak current:	340A
Maximum torque:	240 Nm
Nominal torque:	Up to 125 Nm
Cooling method:	Combined Cooled

Table 6.1 General motor data

Graphs valid for EMRAX 228 High Voltage Combined Cooled (CC):

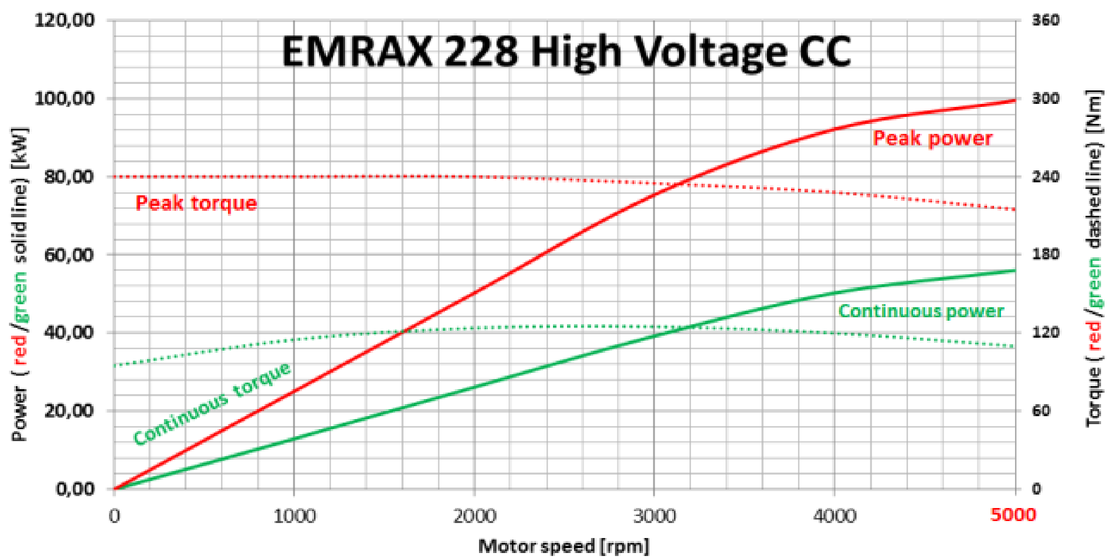

Note 1: for determening peak or continuous power (kW) you should choose motor speed and than read power from chosen power curve (in the left graph side)
Note 2: for determening peak or continuous torque (Nm) you should choose motor speed and than read torque from chosen torque curve (in the right graph side)

Fig 54:- Plot of Power vs Rpm including a line for nominal and maximum power

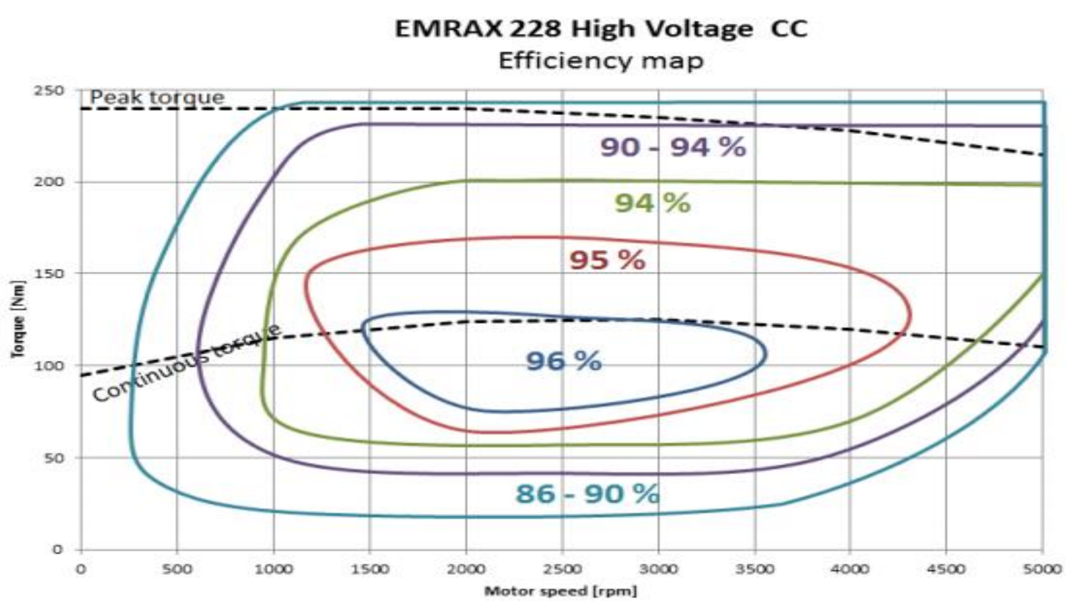

Fig 55:- Plot of torque vs rpm including a line for nominal and maximum torque

Graphs of EMRAX 228 Medium Voltage are similar to graphs of EMRAX 228 High Voltage. The only differences are the DC voltage and the motor current. These two parameters can be read from the Technical data table for the EMRAX 228 Medium Voltage motor. Medium Voltage motor needs 1.52 x higher motor current and 1/3 lower DC voltage for the same power/torque and RPM, compared to EMRAX 228 High Voltage motor.
The motor is connected to the accumulator through a motor-controller (Bamocar PG-D3).

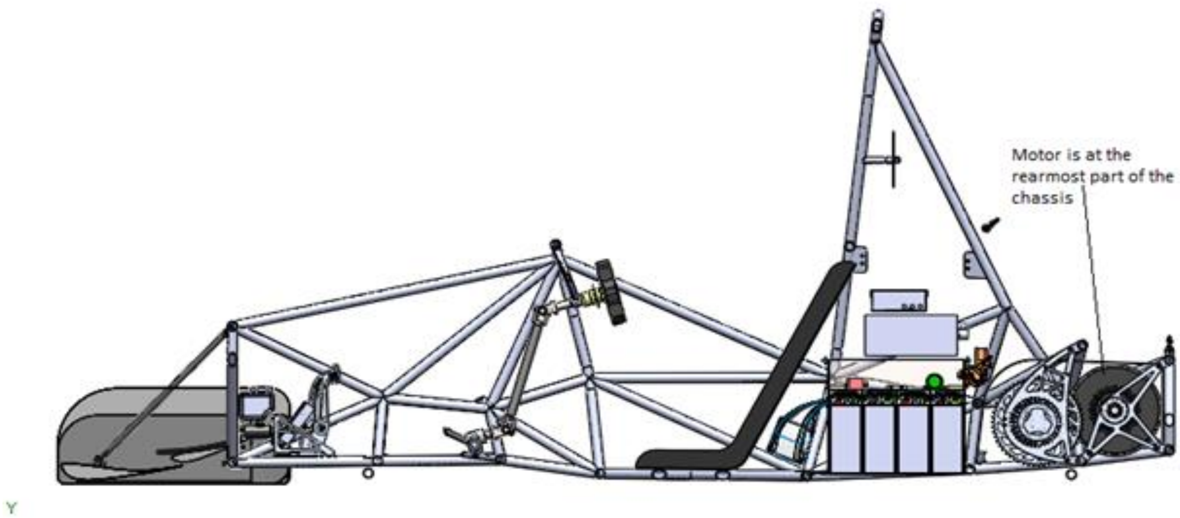

Fig.72: Motor Mounted on the rearmost part of the chassis

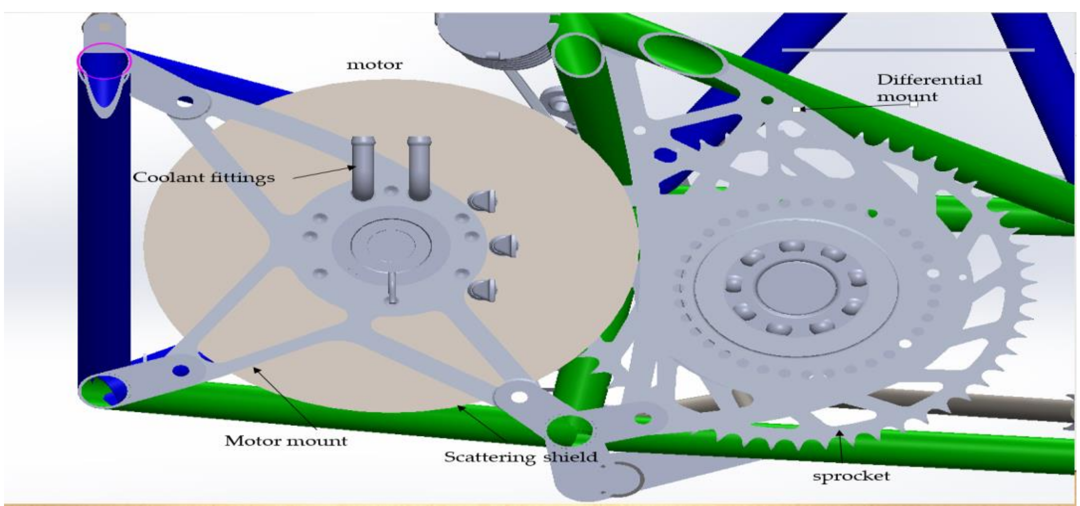

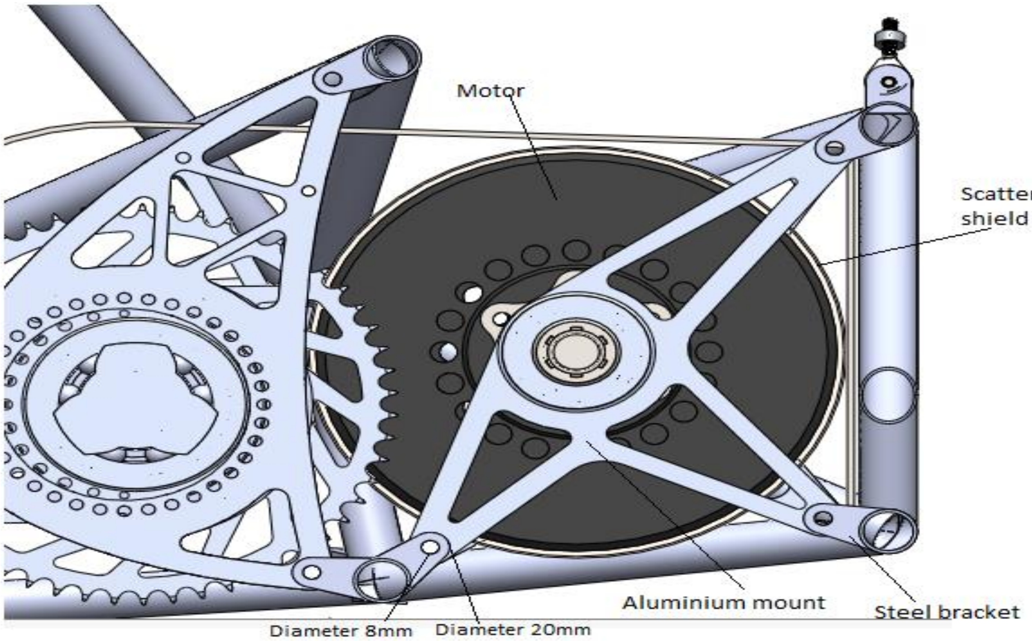

Fig.73: Detailed CAD rendering of the motor.

Motor’s Scatter shields are a 2mm thick steel casing, the diameter of the casing is 228mm. Finger guards are there in the casing to cover the motor’s spin while the vehicle is stationary with the engine running.

2.16.1.2 Wiring, cables, current calculations, connectors

2.16.1.3 Position in car

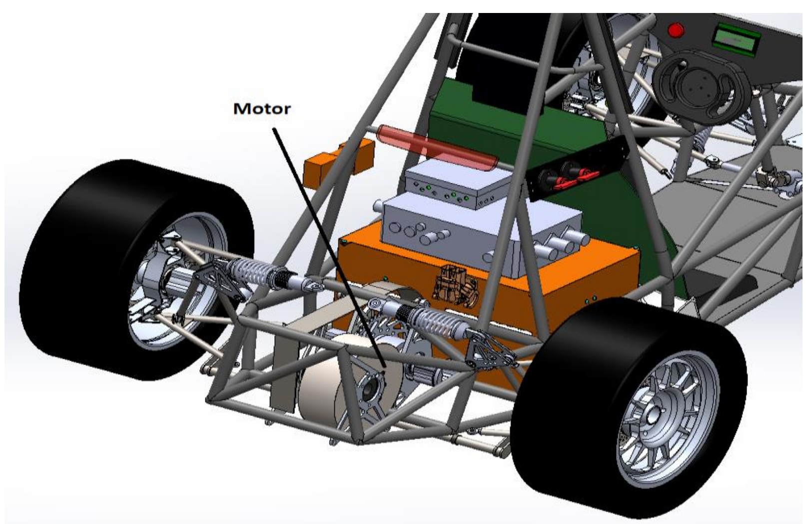

Fig 56:- Motor's Position in vehicle

2.16.2 Motor 2

In our vehicle, just one motor is used. Through differential two back end wheels are driven from a single motor.

2.17 Torque encoder

2.17.1 Description/additional circuitry

Two separate Conductive Plastic Linear Motion Potentiometer is mechanically linked to the acceleration pedal, and are electrically connected to the vehicle controller. Their output is processed by the vehicle controller and then fed to the motor controller. Both torque encoders are powered using two separate supply lines.

Torque encoder manufacturer and type:	Uni-Automation (I) Pvt Ltd MODEL UNILIN 33 Encoder
Torque encoder principle:	Linear motion potentiometer
Supply voltage:	3.3V
Maximum supply current:	10mA
Operating temperature:	-40 to +125 °C
Used output:	0-3.3V

Table 7.1 Torque encoder data

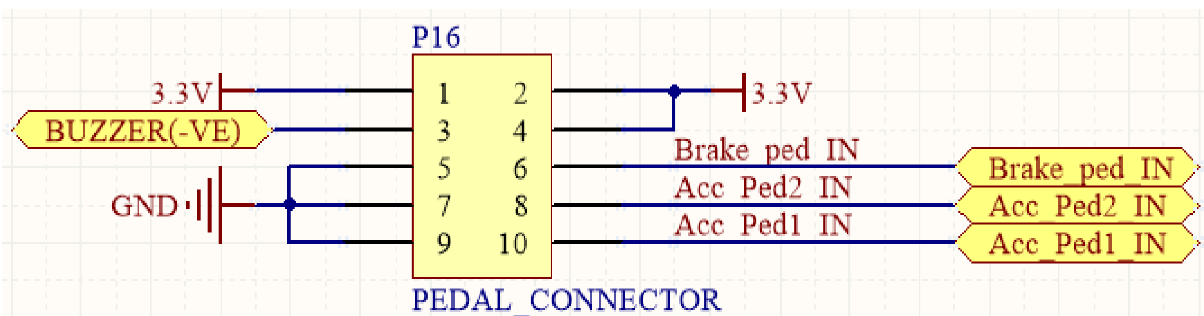

Fig71: Encoder Connector

This figure shows the Encoder Connector which can be disconnected during Technical Inspection The APPS is actuated by a foot pedal. The foot pedal can travel from 0-100%. To prevent overstressing of the encoder, it has a positive stop. Each analog sensor is separately connected with power and signal lines. Implausibility is defined as a deviation of more than 10% pedal travel between the sensors. It is checked in the vehicle controller and if the implausibility is detected, the vehicle controller will completely shut down the car. Thus, it is a system critical signal and the motor will impart 0 Nm torque if the motor encoder is fully released.

2.17.2 Wiring

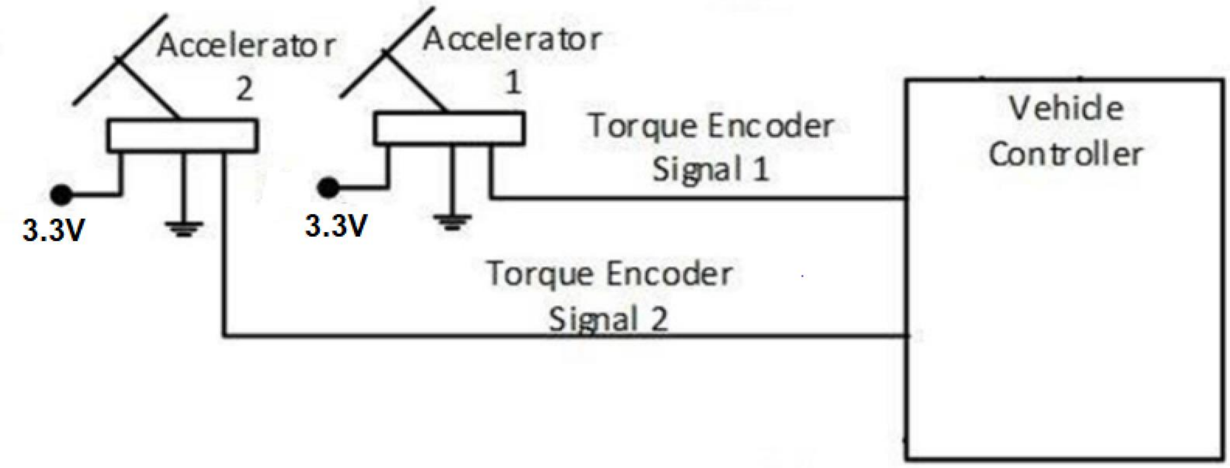

Fig.57: Torque Encoder Wiring Diagram

2.17.3 Position in car/mechanical fastening/mechanical connection

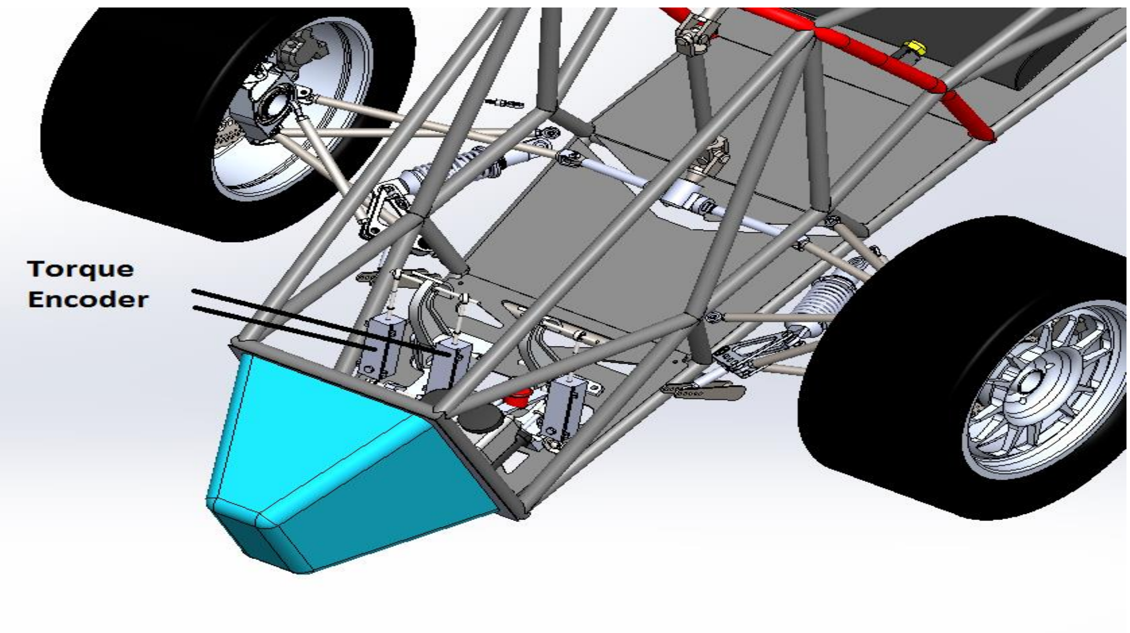

Fig 58:- Position of Torque Encoder

2.18 Additional LV-parts interfering with the tractive system

2.18.1 Isolated Current and Voltage Sensing PCB

2.18.1.1 Description

This PCB is meant to sense the bus current using a shunt resistance attached to the return path and the bus voltage using a resistor divider (R1 and R2 in Figure 48) is used to match the relatively small input voltage range of the AMC device. The isolation is introduced using the AMC1200 isolation amplifier which can provide isolation up to 800 V working voltage.

2.18.1.2 Wiring, cables, etc

Each GREEN block represents a different module (schematic sheet) in the PCB. HV +ve point is connected to the AMC device to measure the bus voltage. The current is measured using a shunt resistance attached to the return path. The outputs of both the modules are connected to the microcontroller for relaying to other nodes, analyzing and storing.

The isolated LV input from the DCDC converter is passed through a protection circuit and then connected to the GLVMS. After the GLVMS the power line is connected to an LV current sensing circuit (using ACS722KMATR-20AB-T, High Accuracy, Hall-effect Based Current Sensor IC in High Isolation SOIC16 Package) that measures the LV current and relays the output to the microcontroller. After the LV current sensing the power rail is divided into three different lines: 24V_Pump (pump and radiator fan supply), 24_VCU (VCU Supply), and 24_Sensing (HV PCB power supply).
The 24_Sensing is further converted to +12V, +5V, and 3.3V supply lines for onboard circuitry (current/voltage sensing HV and LV; CAN transceiver; BMS fault detection; etc.).

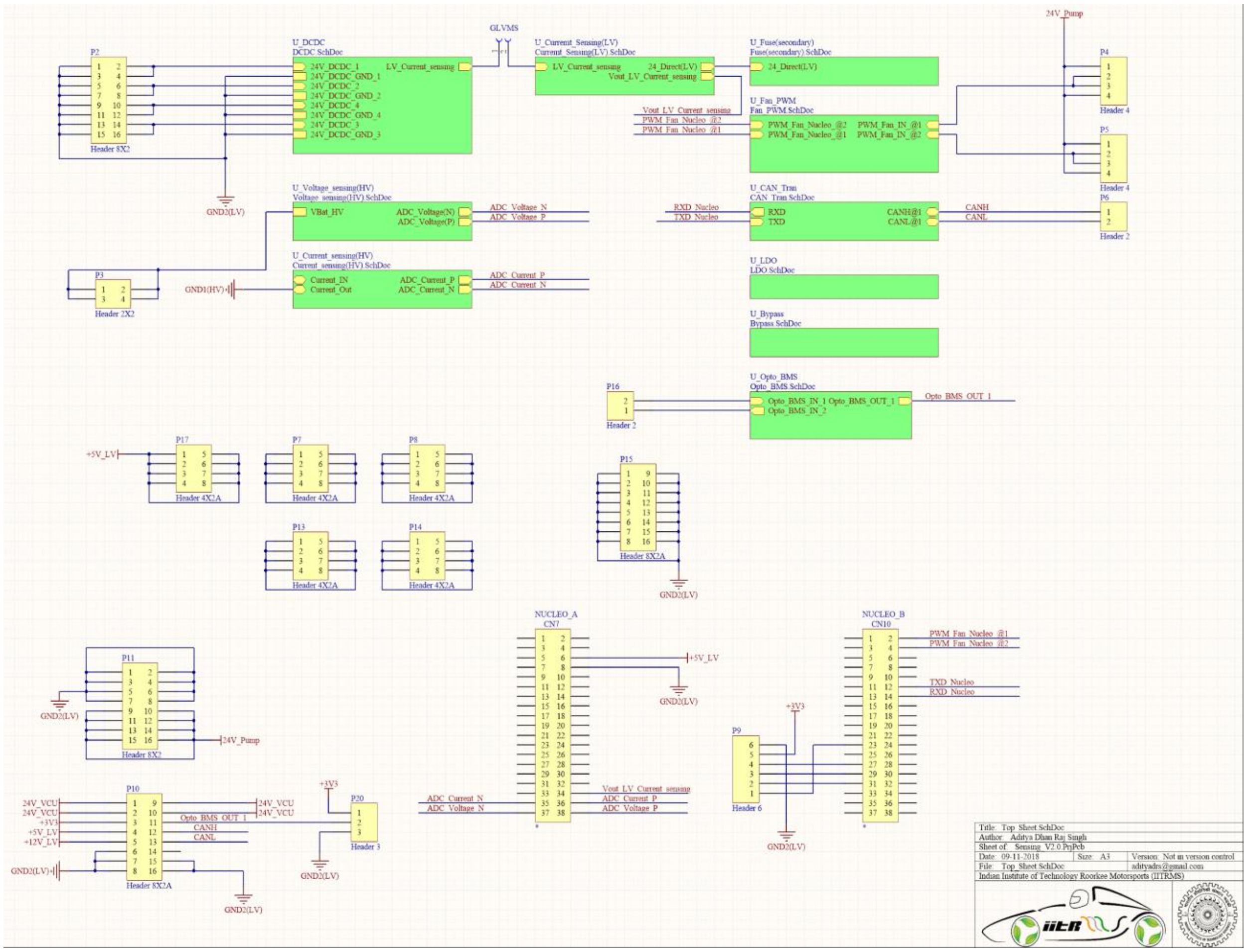

Fig 74: Connection of different modules in HV-LV Sensing PCB

2.18.1.3 Position in Car

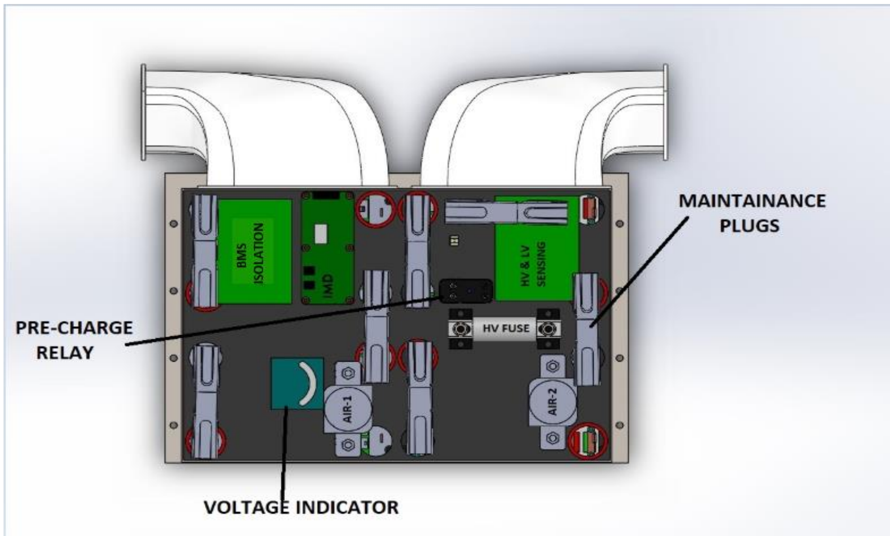

Fig 61 :- HV-LV Sensing PCB.

2.19. Overall Grounding Concept

2.19.1 Description of the Grounding Concept

All areas of the chassis within 100mm of any tractive system or GLV component ensures the resistance of less than 300m Ohm (measured with a current of 1A) to GLV system ground. All parts of the vehicle which may become electrically conductive, that are within 100 mm of any TS or GLVS component, have been ensured a resistance below 5 Ω to GLVS ground.
GLVS is grounded to chassis.
The GLVS does not use orange wiring or conduit
The rear half of the vehicle is a fully conductive steel space frame. The resistivity of chassis is 2.23*10^(-5) ohm-cm. The nuts and bolts used near the tractive system region have a resistivity of 1.1*10^(-6). All the conductive or potentially conductive parts of the frame or any parts within 100mm of any TS or GLVS component are rigidly connected to the chassis (for example through nuts) which in turn is connected to the GLVS ground to provide a resistance less than 300m Ohm.
*source for resistivity of nuts and bolts: https://steelselector.sij.si/steels/PK10.html

2.19.2 Grounding Measurements

We will measure resistance between every grounded component and GLVS ground measurement point. We will have measurement points on the outer layer of the chassis in various locations near the tractive system or areas that may become electrically conductive to measure resistance to GLVS ground.

2.20 Firewall(s)

2.20.1 Firewall 1

2.20.1.1 Description/materials

The firewall is designed to be electrically insulating, rigid, scratch-resistant and fire/heat resistant. To achieve this mix of properties, a 2-layer structure is used.

1) Aluminum substrate forming the lowermost layer facing the tractive system.

2) A coating of Lexan FR6x (electrical insulator and fire-resistant), facing the driver cockpit, which is bonded with aluminum sheet such that no metal contact of the aluminum is possible with the chassis.

The geometry of the firewall is so chosen to have its clearance fit inside the chassis structure at the rear side of the driver's cockpit. It separates all the tractive system components from the driver. It is made up of a single aluminum panel and extends in lateral and vertical directions in such a way that no component is in direct line of driver's lowest helmet point, as shown in the fig. It is rigidly attached to the chassis with four 6mm Metric grade bolts. There are no pass throughs made through the firewall panel and its extension till chassis structure eliminates the liquid leakage possibilities. The thickness, 3 mm of the firewall is so chosen to resist a force of 250 N applied by a 4 mm screwdriver. There is no conducting material between the firewall and the driver and no material is protruding across the firewall.

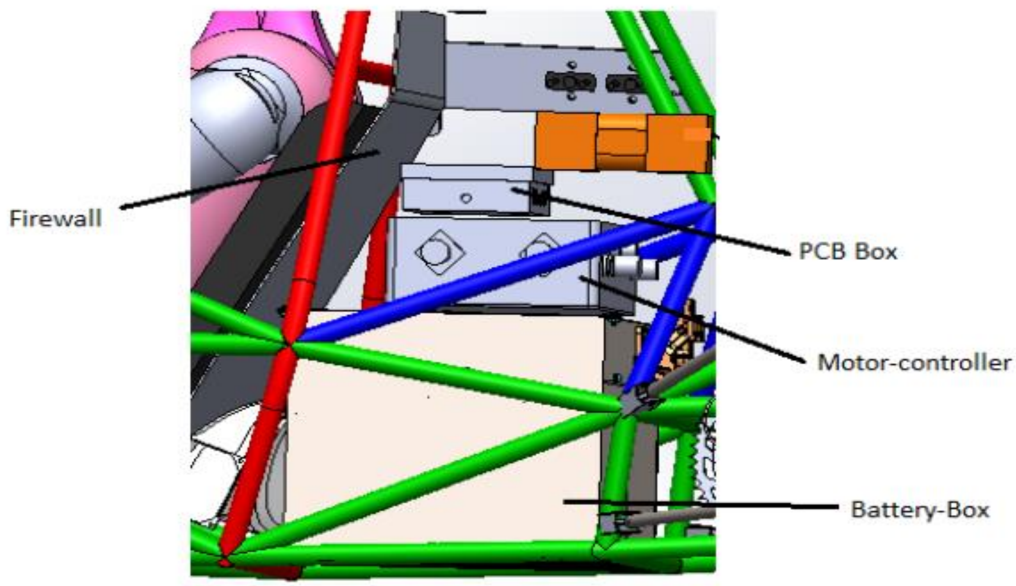

Fig. 62(a): Firewall location with respect to the Tractive system

2.20.1.2 Position in car

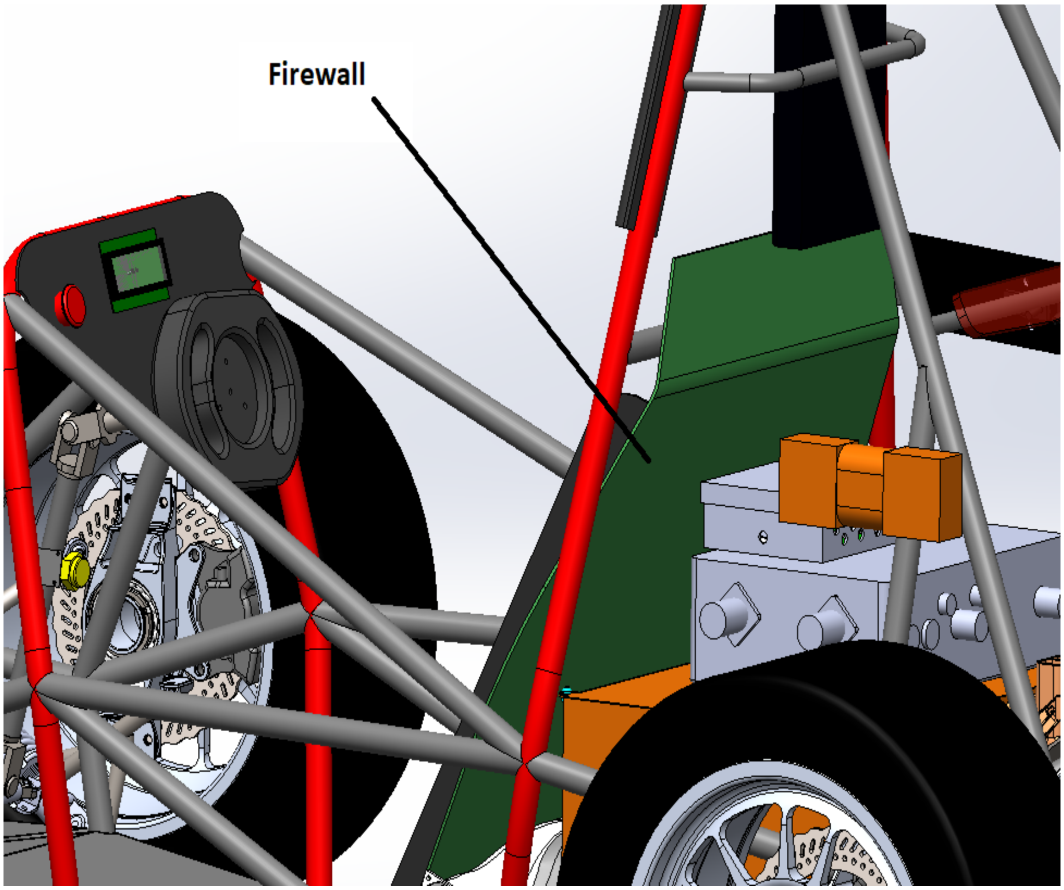

Fig.62(b): Firewall's Position

2.21 Appendix

2.21.1 Specifications of Motor (Medium Voltage)

Source: http://emrax.com/wp-content/uploads/2017/01/emrax_228_technical_data_4.5.pdf

EMRAX 228 Technical Data Table (dynamometer test data)

Type Technical data	EMRAX 228 High Voltage			EMRAX 228 Medium Voltage			EMRAX 228 Low Voltage		
Air cooled = AC Liquid cooled = LC Combined cooled = Air + Liquid cooled = CC	AC	LC	CC	AC	LC	CC	AC	LC	CC
Ingress protection	IP21	IP65	IP21	IP21	IP65	IP21	IP21	IP65	IP21
Cooling medium specification (Air Flow = AF; Inlet Water/glycol Flow = WF; Ambient Air = AA) If inlet WF temperature and/or AA temperature are lower, then continuous power is higher.	AF=20m/s ; AA=25°C	WF=8l/min at 50°C; AA=25°C	WF=8l/min at 50°C; AA=25°C	AF=20m/s ; AA=25°C	WF=8l/min at 50°C; AA=25°C	WF=8l/min at 50°C; AA=25°C	AF=20m/s ; AA=25°C	WF=8l/min at 50°C; AA=25°C	WF=8l/min at 50°C; AA=25°C
Weight [kg]	12,0	12,3	12,3	12,0	12,3	12,3	12,0	12,3	12,3
Diameter ø / width [mm]	228/86								
Maximal battery voltage [Vdc] and full load/no load RPM	670 Vdc (5300/6500 RPM)			470 Vdc (5170/6500 RPM)			130 Vdc (4400/5200 RPM)		
Peak motor power at max RPM (few min at cold start / few seconds at hot start) [kW]	100								
Continuous motor power (at 3000-5000 RPM) depends on the motor RPM [kW]	28 - 42	28 - 42	35 - 55	28 - 42	28 - 42	35 - 55	28 - 42	28 - 42	35 - 55
Maximal rotation speed [RPM]	5500 (6500 RPM peak for a few seconds)								
Maximal motor current (for 2 min if cooled as described in Manual) [Arms]	240			340			900		
Continuous motor current [Arms]	115			160			450		
Maximal motor torque (for a few seconds) [Nm]	240								
Continuous motor torque [Nm]	125								
Torque / motor current [Nm/1Aph rms]	1,1			0,75			0,27		
Maximal temperature of the copper windings in the stator and max. temperature of the magnets [°C]	120								
Motor efficiency [%]	92 – 98								
Internal phase resistance at 25 °C [mΩ]	18			8,0			1,12		
Input phase wire cross-section [mm²]	10,2			15,2			38		
Wire connection	star								
Induction in Ld/Lq [µH]	177/183			76/79			10,3/10,6		
Controller / motor signal	sine wave								
AC voltage between two phases [Vrms/1RPM]	0,0730			0,0478			0,0176		
Specific idle speed (no load RPM) [RPM/1Vdc]	9,8			14			40		
Specific load speed (depends on the controller settings) [RPM/1Vdc]	8 – 9,8			11 – 14			34 – 40		
Magnetic field weakening (for higher RPM at the same power and lower torque) [%]	up to 100								
Magnetic flux – axial [Vs]	0,0542			0,0355			0,0131		
Temperature sensor in the motor	kty 81/210								
Number of pole pairs	10								
Rotor inertia (mass dia=175mm, m=5,5kg) [kg*cm²]	421								
Bearings (front:back) - SKF/FAG	6206:6206 (for radial forces) or 6206:7206 (for axial-radial forces; for pull mode; e.g. for air propeller) or 6206:3206 (for axial-radial forces; for pull-push mode; »O« orientation, α=25°); other bearings are possible (exceptionally)								

2.21.2 Specifications of Motor Controller

For three-phase current motors

Battery voltage connection	12 V= to 700 V=
Auxiliary voltage connection	12 V= or 24 V= ±10 % / 4 A (2 A) residual ripple <10 %, regenerating fuse

Data BAMOCAR-PG- D3	Dim.	200/400	200/400
Supply voltage, rated value	V=	24 up to max. 400	24 up to max. 700
Max. output voltage, rated value	V~eff	up to 3x260	up to 3x450
Continuous current	A_{eff}	200	200
Max. peak current	A_{lo}	400	400
Max. power loss	kW	3	4
Pulse frequency	kHz	8-16	8-16
Over-voltage switching threshold	V=	440	800
Input fuse	A	250	250
Weight	kg	8.5	
Dimensions h x w x d	mm	355 x 230 x 135	
Size		2	

Source for Motor Controller's datasheet:- https://www.unitek-industrie-lektronik.de/images/pdf/BAMOCAR%20Digital/BAMOCAR-PG-D3_DE.pdf

2.21.3 Specification for Potentiometer:-

Electrical Data																						
Electrical Stroke (useful stroke 100%)	50	75	100	130	150	175	200	225	250	275	300	325	360	375	400	450	500	550	600	750	900	mm
Nominal resistance	3	3	3	5	5	5	5	7	7	7	7	10	10	10	10	10	10	15	15	15	15	kΩ
Resistance tolerance	20																					±%
Independent linearity (Typical)	0.05																					±%
Repeatability	0.01																					mm
Recommended operating wiper current	≤ 1																					mAmp
Maximum permissible wiper current (in case of system failure)	10																					mAmp
Maximum permissible applied voltage	24																					VDC
Effective temperature coefficient of the output-to-applied voltage ratio	Typical 5																					ppm/K
Insulation resistance (500 VDC)	500																					MΩ
Dielectric strength (50 Hz)	500																					Vdc
Mechanical Data																						
Body length (dimension A)	115	140	165	195	215	240	265	290	315	340	365	390	425	440	465	515	565	615	665	815	965	±3 mm
Mechanical stroke	55	80	105	135	155	180	205	230	255	280	305	330	365	380	405	455	505	555	605	755	905	±3 mm
Total weight (+/- 20 g)	133	200	230	270	300	330	360	390	400	450	480	510	550	570	600	660	720	780	850	1030	1200	g
Operating force with seal for IP 65	< 10																					N

Source for datasheet:- http://uniautomation.com/html/kcfinder/upload/files/pdf/Unilin-33%20datasheet.pdf

2.21.4 Specification of IMD:-

Technical data

Insulation coordination acc. to IEC 60664-1

Protective separation (reinforced insulation)	between (L+/L-) – (Kl. 31, Kl. 15, E, KE, M_{HS}, M_{LS}, OK_{HS})
Voltage test	AC 3500 V/1 min

Supply/IT system being monitored

Supply voltage U_S	DC 10…36 V
Max. operating current I_S	150 mA
Max. current I_k	2 A
	6 A/2 ms inrush current
HV voltage range (L+/L-) U_n	AC 0…1000 V (peak value)
	0…660 V r.m.s. (10 Hz…1 kHz)
	DC 0…1000 V
Power consumption	< 2 W

Response values

Response value hysteresis (DCP)	25 %
Response value R_{an}	100 kΩ…1 MΩ
Undervoltage detection	0…500 V

Measuring range

Measuring range	0…10 MΩ
Undervoltage detection	0…500 V default setting: 0 V (inactive)
Relative uncertainty	
SST (≤ 2 s)	good > 2* R_{an}; bad < 0.5* R_{an}
Relative uncertainty DCP	0…85 kΩ ▸ ±20 kΩ
(default setting 100 kΩ)	100 kΩ…10 MΩ ▸ ±15%
Relative uncertainty output M (fundamental frequency)	±5 % at each frequency (10 Hz; 20 Hz; 30 Hz; 40 Hz; 50 Hz)
Relative uncertainty undervoltage detection	$U_n \geq 100$ V ▸ ±10 %; at $U_n \geq 300$ V ▸ ±5 %
Relative uncertainty (SST)	"Good condition" ≥ 2* R_{an}
	"Bad condition" ≤ 0.5* R_{an}

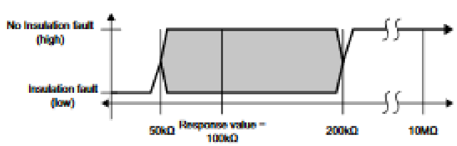

Relative uncertainty DCP	100 kΩ…10 MΩ ±15 %
	100 kΩ…1.2 MΩ ▸ ±15 % to ±7 %
	1.2 MΩ ▸ ±7 %
	1.2…10 MΩ ▸ ±7 % to ±15 %
	10 MΩ ▸ ±15 %

Time response

Response time t_{an} (OK_{HS}; SST)	$t_{an} \leq 2$ s (typ. < 1 s at U_n > 100 V)
Response time t_{an} (OK_{HS}; DCP) (when changing over from R_F = 10 MΩ to $R_{an}/2$; at C_e = 1 µF; U_n = DC 1000 V)	
	$t_{an} \leq 20$ s (at F_{ave} = 10*)
	$t_{an} \leq 17.5$ s (at F_{ave} = 9)
	$t_{an} \leq 17.5$ s (at F_{ave} = 8)
	$t_{an} \leq 15$ s (at F_{ave} = 7)
	$t_{an} \leq 12.5$ s (at F_{ave} = 6)
	$t_{an} \leq 12.5$ s (at F_{ave} = 5)
	$t_{an} \leq 10$ s (at F_{ave} = 4)
	$t_{an} \leq 7.5$ s (at F_{ave} = 3)
	$t_{an} \leq 7.5$ s (at F_{ave} = 2)
	$t_{an} \leq 5$ s (at F_{ave} = 1)
	during the self test t_{an} + 10 s
Switch-off time t_{ab} (OK_{HS}; DCP) (when changing over from $R_{an}/2$ to R_F = 10 MΩ; at C_e = 1 µF; U_n = DC 1000 V	
	$t_{ab} \leq 40$ s (at F_{ave} = 10)
	$t_{ab} \leq 40$ s (at F_{ave} = 9)
	$t_{ab} \leq 33$ s (at F_{ave} = 8)
	$t_{ab} \leq 33$ s (at F_{ave} = 7)
	$t_{ab} \leq 33$ s (at F_{ave} = 6)
	$t_{ab} \leq 26$ s (at F_{ave} = 5)
	$t_{ab} \leq 26$ s (at F_{ave} = 4)
	$t_{ab} \leq 26$ s (at F_{ave} = 3)
	$t_{ab} \leq 20$ s (at F_{ave} = 2)
	$t_{ab} \leq 20$ s (at F_{ave} = 1)
	during a self test t_{ab} + 10 s
Duration of the self test	10 s
	(every five minutes; should be added to t_{an}/t_{ab})

Measuring circuit

System leakage capacitance C_e	≤ 1 µF
Smaller measurement range and increased measuring time at C_e	> 1 µF
	(e.g. max. range 1 MΩ @ 3 µF, t_{an} = 68 s when changing over from R_F 1 MΩ to $R_{an}/2$)
Measuring voltage U_M	±40 V
Measuring current I_M at R_F = 0	±33 µA
Impedance Z_i at 50 Hz	≥ 1.2 MΩ
Internal DC resistance R_i	≥ 1.2 MΩ

* F_{ave} = 10 is recommended for electric and hybrid vehicles

Source of IMD datasheet:-
https://www.bender-in.com/fileadmin/content/Products/d/e/IR155-32xx-V004_D00115_D_XXEN.pdf

2.21.5 Specification of AIRs

Source: http://www.gigavac.com/sites/default/files/catalog/spec_sheet/gx14.pdf

PRODUCT SPECIFICATIONS

Specifications	Units	Data
Contact Arrangement		
Main	Form X	SPST-NO
Auxilary (2A, 24VDC)[4]	Form A or B	SPST-NO or SPST-NC
Mechanical Life	Cycles	1,000,000
Contact Resistance[2]		
Max	mohms	0.4
Typical	mohms	0.15 to 0.3
Operate Time[3]		
Max	ms	20
Typical	ms	13
Release Time, Max	ms	12
Insulation Resistance[4]	Mohms	100
Dielectric At Sea Level (Leakage < 1mA)	VRMS	2,200
Shock, 1/2 Sine, 11ms	G peak	20
Vibration, Sinusoidal (500-2000 Hz Peak)	G	15
Ambient Temp Range		
Operating[5]	°C	-55 to +85
Storage	°C	-70 to +150
Weight, Typical	Kg (Lb)	0.5 (1.1)
Environmental Seal	Exceeds IP67 & IP69K	
Salt Fog	MIL-STD-810	

POWER SWITCHING AND CURRENT CARRY RATINGS

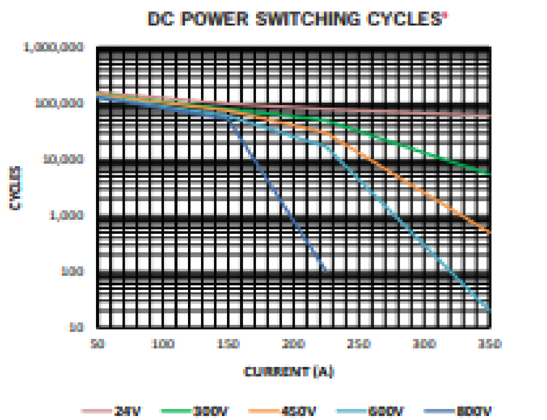

COIL RATINGS at 25°C

Coil P/N Designation	B	C	F
Coil Voltage, Nominal	12 VDC	24 VDC	48 VDC
Coil Voltage, Max	16 V	32 V	64 V
Pick-Up Voltage, Max[6,8]	8 V	16 V	40 V
Drop-Out Voltage	0.5 to 4 V	2 to 7.5 V	4 to 15 V
Pick-Up Current, Max (75 ms)[6,7]	3.9 A	1.6 A	0.97 A
Coil Current[7]	0.23 A	0.097 A	0.042 A
Coil Power[7]	2.8 W	2.3 W	2.0 W
Internal Coil Suppression			
Coil Back EMF	55 V	55 V	125 V
Transients, Max (13 ms)	±50 V	±50 V	±75 V
Reverse Polarity	16 V	32 V	64 V

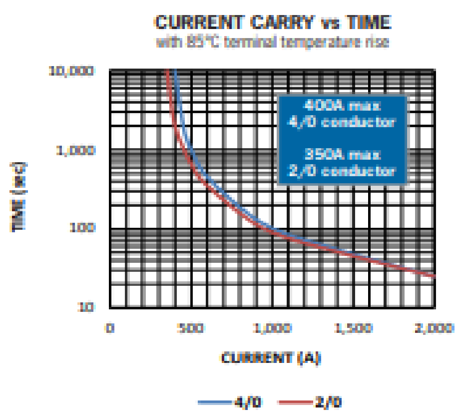

2.21.6 Specifications for Inertia Switch/Crash Sensor:-

Sensata Technologies' 360° Resettable Crash Sensors directly shut down the fuel pump or main contactor upon vehicle impact, reducing the risk of fire and electrical shock in post-crash situations. These devices are a low cost solution to vehicle safety requirements and approved for vehicle installation by major automotive manufacturers worldwide.

Sensata is an ISO and TS registered company. We provide world-class quality products error-free and on time.

Features:

- Unique magnet restrained mass inertia mechanism
- Rated at 10 Amps electrical load
- Manually resettable
- Shock calibration ranges available between 8g and 30g
- Stops fuel pump or electrical system operation
- Secondary circuit provides additional function

Benefits:

- Reduces the risk of fire following a crash
- Responsive to 360° impact
- Ability to trigger GPS distress signal
- Capable of carrying fuel-pump load
- Sensory feedback
- Customized for various installations

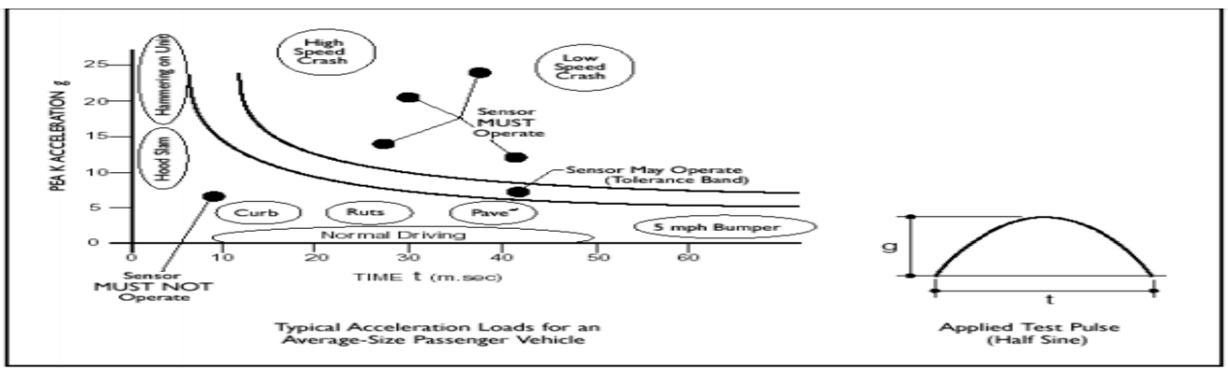

Above are the typical performance characteristics of resettable crash sensors

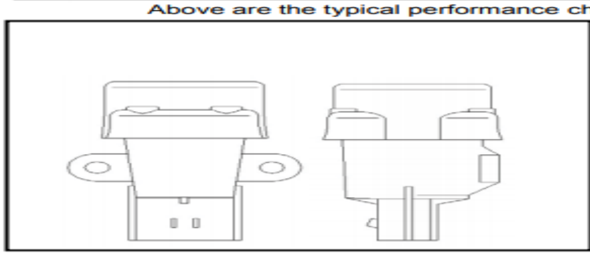

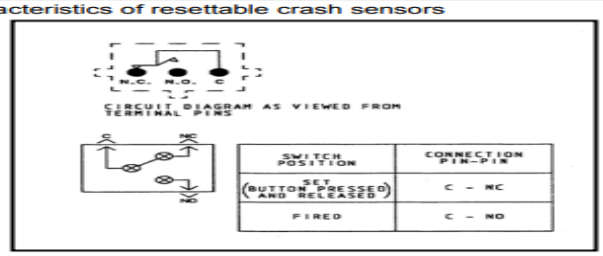

SWITCH POSITION	CONNECTION PIN-PIN
SET (BUTTON PRESSED AND RELEASED)	C – NC
FIRED	C – NO

Source for Inertia Switch:- http://sensatatechnologies.com/download/resettable-crash.pdf

2.21.7 Specification for Precharge resistor:-

TWM/TWW Series

Ceramic Housed Radial Terminal Power

RoHS Compliant

The TWM/TWW series radial terminal power resistors offer significant board space savings over axial terminal products. Generated heat is also kept away from the circuit board.
They are recommended for commercial applications requiring low cost.

FEATURES

- Economical Commercial Grade for general purpose use
- Wirewound and Metal Oxide construction
- Wide resistance range
- Flameproof inorganic construction

SERIES SPECIFICATIONS

Series	Wattage	Resistance	Voltage	Element
TWW3	3	0.01-39Ω	250	Wire
TWW5	5	0.01-47Ω	350	Wire
TWW10	10	0.04-990Ω	750	Wire
TWM3	3	43-50KΩ	250	Metal oxide
TWM5	5	51-50KΩ	350	Metal oxide
TWM10	10	1000-50KΩ	750	Metal oxide

CHARACTERISTICS

Housing	Ceramic
Core	Fiberglass
Filling	Cement based
Tolerance	5% standard
Temperature coefficient	0.01-20Ω ±400ppm/°C; >20-10Ω ±350ppm/°C
Dielectric withstanding voltage	1,000VAC
Short time overload	TWW: 10x rated power for 5 sec.; TWM: 5x rated power for 5 sec.
Operating Temperature	-55°C to 275°C
Storage Temperature	15°C-35°C, humidity: 25%-75%

Derating

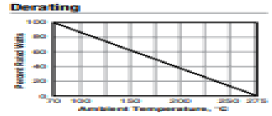

2.21.8 Specification for Discharge Resistor:-

TUM/TUW Series

Ceramic Housed Axial Terminal Power

RoHS Compliant

The TUM/TUW Series resistors are our most economical power resistors. They are recommended for commercial applications where low cost is critical.
They are available in small standard packs for standard values, or bulk packaged for even lower costs.

FEATURES

- Economical Commercial Grade for general purpose use
- Wirewound and Metal Oxide construction
- Wide resistance range
- Flameproof inorganic construction

SERIES SPECIFICATIONS

Series	Wattage	Ohms	Voltage	Element
TUW3	3	0.01-39	350	Wirewound
TUW5	5	0.01-47	350	Wirewound
TUW7	7	0.10-680	500	Wirewound
TUW10	10	0.10-990	750	Wirewound
TUW15	15	0.10-1000	1000	Wirewound
TUM3	3	180-33K	350	Metal oxide
TUM5	5	220-50K	350	Metal oxide
TUM7	7	910-50K	500	Metal oxide
TUM10	10	1000-50K	750	Metal oxide
TUM15	15	1100-150K	1000	Metal oxide

CHARACTERISTICS

Housing	Ceramic
Core	Fiberglass or metal oxide
Filling	Cement based
Tolerance	5% standard
TCR	0.01-20Ω ±400ppm/°C 20-150KΩ ±350ppm/°C
Dielectric withstanding voltage	1,000VAC
Short time overload	TUW: 10x rated power for 5 sec. TUM: 5x rated power for 5 sec.

Derating Curve

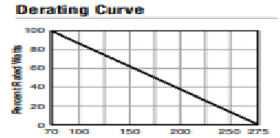

2.21.9 Specification for Measuring Point:-

MUELLER®

MODEL: BU-P2269
Double Banana Jack (Panel mount)

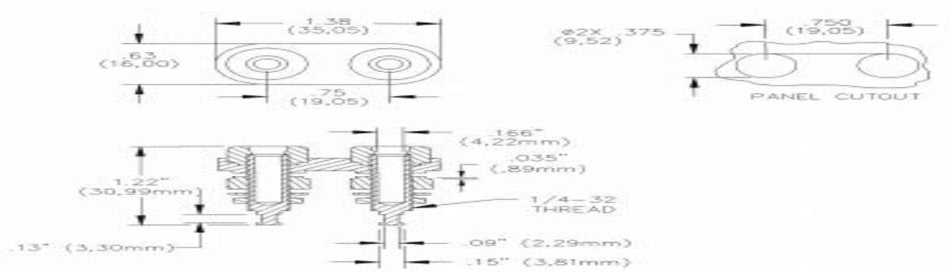

MATERIALS:
Contacts — Nickel Plated Brass
Insulators — Nylon

Solder connection

RATING:
15 Amps
Hands free testing to 1000 VDC max.
Temperature: -50°C to 120°C

2.21.10 Specification of Precharge Relay:-

PRODUCT SPECIFICATIONS

Specifications	Units	Data
Contact Arrangement	Form X	SPST-NO
Dielectric at Sea Level	Vdc	6000
Contact Voltage, Operating Max	Vdc	1200
Continuous Current Carry, Max (8 AWG)	A	30
Electrical Life (Resistive Load)		
Make and Break, 1A @ 1200Vdc	Cycles	1000
Make and Break, 5A @ 1000Vdc	Cycles	1000
Make and Break, 10A @ 800Vdc	Cycles	2000
Make and Break, 20A @ 600Vdc	Cycles	5000
Make and Break, 50A @ 300Vdc	Cycles	5000
Make and Break, 50A @ 24Vdc	Cycles	50,000
Mechanical Life	Cycles	1,000,000
Contact Voltage Drop, Max @ 50A	mV	100
Contact Resistance, Max @ 50A (after 30 sec)	mOhms	3.25
Operate Time, Max	ms	25
Release Time, Max	ms	8
Vibration, Sinusoidal (50-200Hz Peak)	G	5
Shock, Operating, 1/2 Sine, 11ms	G	20
Temperature, Operating Range 1/	°C	-40 to +65
Humidity, No Freezing or Condensing at Low Temperature	RH	5% to 85%
Weight	grams	90

CURRENT CARRY RATINGS

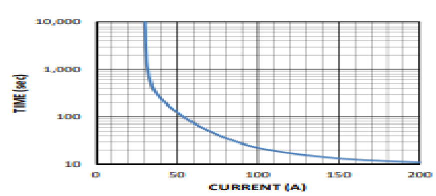

COIL RATINGS @ 25°C 2/

Coil P/N Designation	B	C	F
Coil Voltage, Nominal	12 Vdc	24 Vdc	48 Vdc
Coil Voltage, Max	16 Vdc	32 Vdc	64 Vdc
Pick-up Voltage, Max	7.5 Vdc	15 Vdc	30 Vdc
Drop Out Voltage, Max	5 Vdc	9 Vdc	18 Vdc
Drop Out Voltage, Min	0.20 Vdc	0.40 Vdc	0.80 Vdc
Coil Resistance, +/-10%	70 Ohms	280 Ohms	1092 Ohms
Coil Current at Nominal Voltage	0.170 A	0.085 A	0.045 A
Recommended External Coil Suppression	24 Vdc	48 Vdc	96 Vdc

2.21.11 Specification for Maintenance Plug:-

Electrical

Current Rating Amperes [1]	UL 1977	CSA
Singlepole (wire-wire) (3/0 AWG)	350	230
2x2 Block (wire-wire) (3/0 AWG)	350	
Singlepole (wire-busbar) (1/0 AWG)	180	
Voltage Rating AC/DC		
UL 1977	600	
Dielectric Withstanding Voltage		
Volts AC	2,200	
Avg. Mated Contact Resistance Milliohms [1]		
6" of 1/0 AWG wire	0.100	
UL Hot Plug Current Rating Amperes [4]		
250 cycles at 120V DC	75A	

Mechanical

Wire Size Range	AWG	mm²
Wire Contacts with Bushings	10 to 3/0	5.3 to 85
Max. Wire Insulation Diameter	**in.**	**mm**
	0.900	22.860
Operating Temperature [2] [*]	**°F**	**°C**
	-4° to 221°	-20° to 105°
Mating Cycles No Load by Plating	**Silver (Ag)**	
Wire and Busbar Contacts	10,000	
Avg. Mating / Unmating Force	**Lbf.**	**N**
Wire & Busbar Contacts	10	44
Min. Contact / Spring Retention Force	**Lbf.**	**N**
	120	534

Materials

Housing	
Plastic Resin	Polycarbonate
Contact Retention Spring	Stainless Steel
Housing Flammability Rating	
UL94	V-0
Glow Wire	960°C (GWFI) / 850°C (GWIT)
Contact	
Base	Copper Alloy
Plating	Silver
Contact Termination Methods	
Crimp [3]	
Hand Solder	
Wrench / Socket*	

*Busbar Contacts Only

https://www.andersonpower.com/content/dam/app/ecommerce/product-pdfs/PP180/ds-pp180.pdf

2.21.12 Specification of LEDs:-

Link to complete datasheet:-

https://www.mouser.in/datasheet/2/90/1354C4SMARGFGGFBGF-1022691.pdf

2.21.13 Specification for Firewall(Lexan FR6x):-

Lexan® FR60, FR63, FR65, FR66

Property	Test	Unit	Value+
Physical			
Specific Gravity	ISO 1183	g/cm³	1.32
Water Absorption, saturation, 23°C	ISO 62	%	0.28
Optical			
Haze	ASTM D1003	%	1.0
Light Transmission	ASTM D1003	%	85-88
Mechanical			
Tensile stress	ISO R527		
at yield		MPa	70
at break		MPa	60
Strain at break	ISO R527	%	25
Tensile Modulus	ISO R527	MPa	2200
Tear Strength			
Initiation	ASTM D1004	kN/m	298
Propagation	ASTM D1922	kN/m	6
Thermal			
Tensile Heat Distortion, 0.35 N/mm²	ASTM D1637	°C	150
DTUL, 1.82 N/mm²	ISO 75	°C	135
Electrical			
Dielectric Strength, 23°C, in oil, short term, 375 micron	IEC 243-1	kV/mm	59
Relative permittivity	IEC 250		
at 50 Hz	-		2.9
at 1 kHz	-		2.8
at 1 MHz	-		2.8
Dissipation Factor	IEC 250		
at 50 Hz	-		0.0026
at 1 kHZ	-		0.0028
at 1 MHz	-		0.0117
Volume Resisivity	IEC 93	Ohm.m	10^{14}
Flammability			
Oxygen index	ISO 4589	-	33%
UL Flammability *	UL94		V0, 0.250 mm
Flash Point	-	°C	440
Self Ignition Temperature	-	°C	605
FMVSS 302	ASTM D618	-	all pass
NFPA 258-NBS	ASTM E662	-	
Smoke Chamber Test (0.25 mm)			D(4)=6 D(max)=36

+ Typical values only.
  Variation within normal tolerances are possible for the various textures.

* These ratings are not intended to reflect hazards presented by this or any other material under actual fire conditions.

2.21.14 Datasheet of DC-DC Converter:-

Features & Benefits

- DC input range: 180 – 375V
- Isolated output
- Input surge withstand: 400V for 100ms
- DC output: 2 – 48V
- Programmable output: 10 – 110%
- Regulation: ±0.3% no load to full load
- Efficiency: Up to 89%
- Maximum operating temp: 100°C, full load
- Power density: up to 100W per cubic inch
- Height above board: 0.43in [10,9mm]
- Parallelable, with N+M fault tolerance
- Low noise ZCS/ZVS architecture
- RoHS Compliant (with F or G pin option)

Product Overview

These DC-DC converter modules use advanced power processing, control and packaging technologies to provide the performance, flexibility, reliability and cost-effectiveness of a mature power component.

High-frequency ZCS/ZVS switching provides high power density with low noise and high efficiency.

Applications

Off-line systems with auto-ranging or PFC front ends, industrial and process control, distributed power, medical, ATE, communications, defense and aerospace.

For details on proper operation please refer to the:
Design Guide & Applications Manual for Maxi, Mini, Micro Family.

Absolute Maximum Ratings

Parameter	Rating	Unit	Notes
+IN to –IN voltage	-0.5 to +410	V_{DC}	
PC to –IN voltage	-0.5 to +7.0	V_{DC}	
PR to –IN voltage	-0.5 to +7.0	V_{DC}	
SC to –OUT voltage	-0.5 to +1.5	V_{DC}	
–Sense to –OUT voltage	1.0	V_{DC}	
+OUT to –OUT, +Sense to –OUT			See Module Output Specifications
Isolation voltage			
IN to OUT	3000	V_{RMS}	Test voltage
IN to base	1500	V_{RMS}	Test voltage
OUT to base	500	V_{RMS}	Test voltage
Operating Temperature	-55 to +100	°C	M-Grade
Storage Temperature	-65 to +125	°C	M-Grade
Pin soldering temperature	500 [260]	°F [°C]	<5sec; wave solder
	750 [390]	°F [°C]	<7sec; hand solder
Mounting torque	5 [0.57]	in-lbs [N-m]	6 each

2.21.15 Datasheet of Charger:-

2.1 Electrical Performance

Specification/unit \ Model			DA3K3M17-540C
Mains Input	Rated Voltage	Vac	220
	Voltage Range	Vac	85～264 (The output from 85-176 is automatically reduced to 1.2 KW)
	FREQ RANGE	HZ	47～63
	Efficiency(max)	%	≥94
	Power Factor		≥0.99@220Vac,rated power
	Current(MAX)	A	≤16@220Vac
Mains output	Rated Output Voltage	Vdc	540
	Constant voltage output range	Vdc	400~650 (According to the customer battery final decision)
	Max Current	A	8.2 (Constant power)
	Constant power output	W	3300
	Output voltage accuracy	V	≤±1%Vo input 176Vac-264Vac，output 10%-100% load
	Line regulation	%	≤±0.2%Vo input 176Vac-264Vac，output 100% load
	Load regulation	%	≤±0.5%Vo input 220Vac，output 10%-100% load
	Ripple and noise	mV	≤±3%Vo 20M oscilloscope，Twisted-pair cable test.
Auxiliary supply	Rated output voltage	Vdc	12
	Rated output power	W	2（Activate BMS, optional power）
Property	Input over-voltage protection	Vac	≥270 CAN directive warning protection
	Input under-voltage protection	Vac	≤80 CAN directive warning protection
	Output Over-current protection	A	Io≥120% CAN directive warning protection
	Output under-voltage protection	Vdc	≤395 CAN directive warning protection
	Output over-voltage protection	Vdc	≥660 CAN directive warning protection
	Over-temperature protection	℃	85±5 CAN directive warning protection
	Output short circuit protection		yes (CPU intelligent control)
	Reverse polarity protection		yes (CPU intelligent detection)
	Dynamic response	us	≤200
	CAN		Communication interrupt, timeout of 5 seconds intelligent

2.21.16 Specifications of the cells:-

Nominal Capacity:	15Ah	**Type:**	Li-polymer
Nominal Voltage:	3.7V	**Size:**	Prismatic
Max Continuous Charge Current:	15A	**Peak Charge Current:**	30A
Max Continous Discharge Current:	150A	**Peak Discharge Current:**	225A

3.7V 15000mAh 10C (55.5Wh, 150A rate) high power high capacity LiPo battery cell

Item Specification:

Model Lithium Polymer battery SLPBA875175
Nominal Capacity: 15000mAh
Nominal Voltage: 3.7V
Cycle Life >100 times
Charge Voltage: 4.2V
Max Continuous Charge Rate: 1C (15A)
Peak Charge Rate(C): 2C (30A)
Max Continous Discharge Rate(C): 10C (150A)
Max Plus Dicharge Rate(C): 15C (225A)
AC Impedance(mOHM): <1.5
Discharging End Voltage: 2.75V
Size: 10.8 x 75.5 x 175mm
Weight Approx (g):302.5±5g
Energy Density: 180.19 Wh/kg
Power density: 1801.95W/kg

2.21.17 Specifications of Current/Voltage sensor:-

TEXAS INSTRUMENTS

AMC1200, AMC1200B

SBAS542D – APRIL 2011 – REVISED JULY 2015

AMC1200/B Fully-Differential Isolation Amplifier

1 Features

- ±250-mV Input Voltage Range Optimized for Shunt Resistors
- Very Low Nonlinearity: 0.075% Maximum at 5 V
- Low Offset Error: 1.5 mV Maximum
- Low Noise: 3.1 mV_{RMS} Typical
- Low High-Side Supply Current: 8 mA Maximum at 5 V
- Input Bandwidth: 60 kHz Minimum
- Fixed Gain: 8 (0.5% accuracy)
- High Common Mode Rejection Ratio: 108 dB
- 3.3-V Operation on Low-Side
- Certified Galvanic Isolation:
  - UL1577 and VDE V 0884-10 Approved
  - Isolation Voltage: 4250 V_{PEAK} (AMC1200B)
  - Working Voltage: 1200 V_{PEAK}
  - Transient Immunity: 10 kV/μs Minimum
- Typical 10-Year Lifespan at Rated Working Voltage (see Application Report SLLA197)
- Fully Specified Over the Extended Industrial Temperature Range

2 Applications

- Shunt Resistor Based Current Sensing in:
  - Motor Control
  - Green Energy
  - Frequency Inverters
  - Uninterruptible Power Supplies

3 Description

The AMC1200 and AMC1200B are precision isolation amplifiers with an output separated from the input circuitry by a silicon dioxide (SiO_2) barrier that is highly resistant to magnetic interference. This barrier has been certified to provide galvanic isolation of up to 4250 V_{PEAK} (AMC1200B) or 4000 V_{PEAK} (AMC1200) according to UL1577 and VDE V 0884-10. Used in conjunction with isolated power supplies, these devices prevent noise currents on a high common mode voltage line from entering the local ground and interfering with or damaging sensitive circuitry.

The input of the AMC1200 or AMC1200B is optimized for direct connection to shunt resistors or other low voltage level signal sources. The excellent performance of the device supports accurate current control resulting in system-level power saving and, especially in motor-control applications, lower torque ripple. The common mode voltage of the output signal is automatically adjusted to either the 3-V or 5-V low-side supply.

The AMC1200 and AMC1200B are fully specified over the extended industrial temperature range of –40°C to 105°C and are available in a wide-body SOIC-8 package (DWV) and a gullwing-8 package (DUB).

Device Information(1)

PART NUMBER	PACKAGE	BODY SIZE (NOM)
AMC1200, AMC1200B	SOP (8)	9.50 mm × 6.57 mm
	SOIC (8)	5.85 mm × 7.50 mm

(1) For all available packages, see the orderable addendum at the end of the data sheet.

2.21.18 Datasheet of Monostable Multivibrator:-

FUNCTIONAL TERMINAL CONNECTIONS

FUNCTION	V_{CC} TO TERMINAL NUMBER		GND TO TERMINAL NUMBER		INPUT PULSE TO TERMINAL NUMBER		OTHER CONNECTIONS	
	$MONO_1$	$MONO_2$	$MONO_1$	$MONO_2$	$MONO_1$	$MONO_2$	$MONO_1$	$MONO_2$
Leading-edge trigger/retriggerable	3, 5	11, 13			4	12		
Leading-edge trigger/nonretriggerable	3	13			4	12	5–7	11–9
Trailing-edge trigger/retriggerable	3	13	4	12	5	11		
Trailing-edge trigger/nonretriggerable	3	13			5	11	4–6	12–10

NOTES: 1. A retriggerable one-shot multivibrator has an output pulse width that is extended one full time period (T) after application of the last trigger pulse.
2. A nontriggerable one-shot multivibrator has a time period (T) referenced from the application of the first trigger pulse.

Input Pulse Train

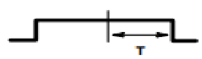

Retriggerable Mode Pulse Width (A Mode)

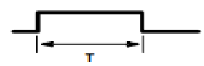

Nonretriggerable Mode Pulse Width (A Mode)

absolute maximum ratings over operating free-air temperature range (unless otherwise noted)†

Supply voltage range, V_{CC} (see Note 1) . . . . −0.5 V to 7 V
Input clamp current, I_{IK} ($V_I < -0.5$ V or $V_I > V_{CC} + 0.5$ V) . . . . ±20 mA
Output clamp current, I_{OK} ($V_O < -0.5$ V or $V_O > V_{CC} + 0.5$ V) . . . . ±20 mA
Switch current per output pin, I_O ($V_O > -0.5$ V or $V_O < V_{CC} + 0.5$ V) . . . . ±25 mA
Continuous current through V_{CC} or GND . . . . ±50 mA
Package thermal impedance, θ_{JA} (see Note 2): M package . . . . 73°C/W
PW package . . . . 108°C/W
Maximum junction temperature, T_J . . . . 150°C
Lead temperature (during soldering):
At distance 1/16 ± 1/32 inch (1,59 ± 0,79 mm) from case for 10 s max . . . . 300°C

2.21.19 HVD Datasheet:-

Table 5: Product Ratings
Tabelle 5: Produktmerkmale

Description *Beschreibung*	**Range** *Wert*
Max working voltage at 5500m above sea level *Max. Betriebsspannung bei 5500m ü. NN*	≤ 650VDC
Voltage class acc. ISO 6469-3 *Spannungsklasse nach ISO 6469-3*	**B**
Class 1 equipment acc. ISO 6469-3 *Ausrüstungsklasse nach ISO 6469-3*	**1**
Dielectric withstand voltage acc. ISO 6469-3, SAE J 1742 *Bemessungs-Stoßspannung nach ISO 6469-3, SAE J 1742*	**2700V**
Insulation resistance acc. ISO 6469-3, SAE J 1742 *Isolationswiderstand nach ISO 6469-3, SAE J 1742*	**> 200MΩ**
Isolation Group I acc. DIN EN 60664-1 *Isoliergruppe I nach DIN EN 60664-1*	**600 ≤ CTI**
Pollution degree acc. DIN EN 60664-1 *Verschmutzungsgrad nach DIN EN 60664-1*	**2**
Description *Beschreibung*	**Range** *Wert*
Ambient temperature *Umgebungstemperatur*	**-40°C to 140°C**
Degrees of protection (IP-Code) against access acc. ISO 20653 *Schutzgrade gegen Berühren gefährlicher Teile nach ISO 20653*	**IPXXB, IPXXD**
Degree of protection (IP-Code) against foreign objects and water acc. ISO 20653 *Schutzgrade gegen Eindringen fester Fremdkörper und Wasser nach ISO 20653*	**IP6K9K, IP6K7**
Color of plastic cover *Farbe der Kunststoffgehäuse*	**Orange similar RAL 2003** *Orange ähnlich RAL 2003*

2.21.20 Specifications of the 25mm^2 coroplast wires:-

Electrical properties		
Conductor resistance: (DC, 20°C)	*max. 0.743 mΩ/m* *max. 4.4 mΩ/m*	*25 mm²* *Shielding*
Test voltage:	*eff. 8.0 kVolt* *eff. 5.0 kVolt*	*(spark test)* *(5 minutes)*
Nominal voltage: (AC / DC)	*max. 600 / 1000 Volt*	
Capacitance:	*nom. 600 pF/m*	*core-screen*
Inductance:	*nom. 100 nH/m*	
Impedance:	*nom. 10 Ohm*	
Mechanical properties		
Bend radius:		
- min. 4 x cable-∅:	*static installation*	
- min. 8 x cable-∅:	*dynamic installation*	
Weight of cable:	*approx. 345 g/m*	
Thermal properties		
Operating temperature:	*-40 °C to +180 °C*	*(3000 h)*
Short term ageing	*up to +205 °C*	*(240 h)*

2.21.21 Specifications of the 35mm^2 coroplast wires:

Electrical properties		
Conductor resistance: (DC, 20°C))	*max. 0.527 mΩ/m* *max. 3.8 mΩ/m*	*35 mm²* *Shielding*
Test voltage:	*eff. 8.0 kVolt* *eff. 5.0 kVolt*	*spark test* *5 minutes*
Nominal voltage: (AC / DC)	*max. 600 / 1000 Volt*	
Capacitance:	*nom. 600 pF/m*	*core-screen*
Inductance:	*nom. 100 nH/m*	
Impedance:	*nom. 10 Ohm*	
Mechanical properties		
Bend radius:		
- min. 4 x cable-∅:	*static installation*	
- min. 8 x cable-∅:	*dynamic installation*	
Weight of cable:	*approx. 485 g/m*	
Thermal properties		
Operating temperature:	*-40 °C to +180 °C*	*(3000 h)*
Short term ageing	*up to +205 °C*	*(240 h)*

2.21.22 Specifications of Master Switch:-

Battery Master Switch

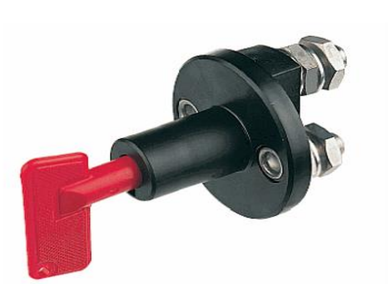

Battery Master Switch

*Note: Dimensions in Millimeters

Battery Master Switch

Features:

- For battery main lead
- Connection to either positive or negative lead
- Switch key removable in "off" position only
- Current supply interrupted when key removed
- M10 screw contacts
- 2 switch positions: 0 = off, 1 = on
- Max Load:
- 1000A at 12V (10 sec.), 500A at 24V (10 sec.).
- IP Rating: DIN 40 050 - IPX 2

Part No.:	
Battery Master Switch - 50 Amp Continuous Load	002843001
Battery Master Switch - 100 Amp Continuous Load	002843011
Replacement Key, Bulk Qty: 10	706729011

Source: http://hellahd.com/index.php/default/electrics/switches/electrics-category-12/electrics-product-11/

2.21.23 Shutdown Button datasheet:-

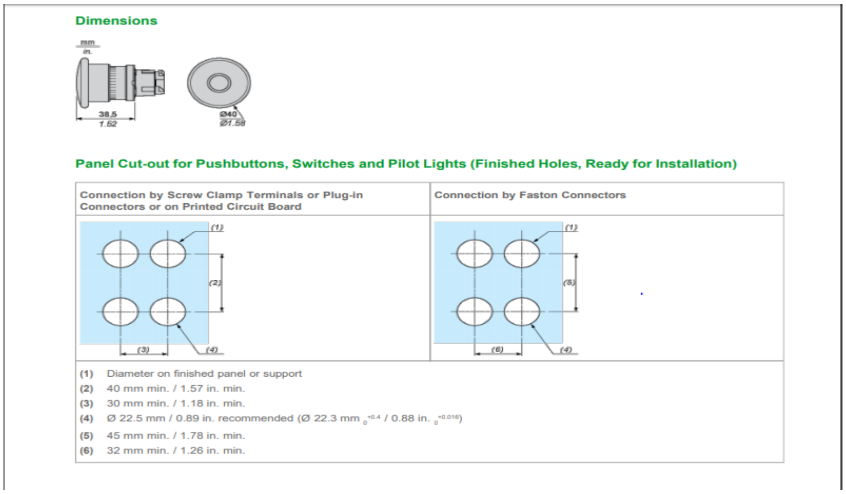
Dimensions

mm / in.

38.5 / 1.52

Ø40 / Ø1.58

Panel Cut-out for Pushbuttons, Switches and Pilot Lights (Finished Holes, Ready for Installation)

Connection by Screw Clamp Terminals or Plug-in Connectors or on Printed Circuit Board	Connection by Faston Connectors
(1) (2) (3) (4)	(1) (5) (6) (4)

(1) Diameter on finished panel or support
(2) 40 mm min. / 1.57 in. min.
(3) 30 mm min. / 1.18 in. min.
(4) Ø 22.5 mm / 0.89 in. recommended (Ø 22.3 mm $_0^{+0.4}$ / 0.88 in. $_0^{+0.016}$)
(5) 45 mm min. / 1.78 in. min.
(6) 32 mm min. / 1.26 in. min.

Source: https://docs-emea.rs-online.com/webdocs/1591/0900766b81591479.pdf

2.21.24 Datasheet of 15k ohm resistor:-

https://www.mouser.in/ProductDetail/Caddock/MP925-150K-1/?qs=3xGhc7tteJWFgUsHgFGqHw==

2.21.25 Datasheet of Nuts and Bolts:-

http://www.viewmold.com/sources/Unbrako/Metric%20Socket%20Head%20Cap%20Screws.pdf

2.21.26 Specification of HV Fuse:-

Electrical Specifications

CATALOG NUMBER	AMPERAGE RATING	VOLTAGE RATING		INTERRUPT RATING		MELTING (PRE-ARC) I^2T (A^2s)	TOTAL CLEARING I^2T (A^2s)	TOTAL CLEARING I^2T (A^2s)	WATTS LOSS AT 80 % RATED CURRENT	WATTS LOSS AT 100 % RATED CURRENT
		AC	DC	AC	DC		200 KA @ 700 V AC	50 KA @ 700 V DC	(W)	(W)
L70QS035	35	700	700	200 kA	50 kA	129	332	308	5	8
L70QS040	40	700	700	200 kA	50 kA	153*	599	416	6	9
L70QS050	50	700	700	200 kA	50 kA	196	711	588	6	12
L70QS060	60	700	700	200 kA	50 kA	269	1,233	678	9	15
L70QS070	70	700	700	200 kA	50 kA	359	1,575	1,075	10	20
L70QS080	80	700	700	200 kA	50 kA	452	2,755	1,415	12	22
L70QS090	90	700	700	200 kA	50 kA	625	3,365	1,920	13	25
L70QS100	100	700	700	200 kA	50 kA	966	3,747	2,347	15	30
L70QS125	125	700	700	200 kA	50 kA	2,208	8,795	5,570	13	24
L70QS150	150	700	700	200 kA	50 kA	3,026	13,650	8,195	17	32
L70QS175	175	700	700	200 kA	50 kA	4,219	19,550	11,650	20	38
L70QS200	200	700	700	200 kA	50 kA	5,529	22,067	16,100	22	42
L70QS225	225	700	700	200 kA	50 kA	9,226	34,900	25,400	22	40
L70QS250	250	700	700	200 kA	50 kA	10,999	43,750	31,650	27	46
L70QS300	300	700	700	200 kA	50 kA	16,296	64,400	45,500	31	57
L70QS350	350	700	700	200 kA	50 kA	24,778	91,500	65,250	35	67
L70QS400	400	700	700	200 kA	50 kA	34,225	110,667	94,666	41	79
L70QS450	450	700	700	200 kA	50 kA	38,946	145,500	113,500	45	81
L70QS500	500	700	700	200 kA	50 kA	42,747	173,000	125,500	56	112
L70QS600	600	700	700	200 kA	50 kA	67,363	220,333	179,667	67	138
L70QS700	700	700	700	200 kA	50 kA	99,387	368,000	298,000	72	138
L70QS800	800	700	700	200 kA	50 kA	156,137	466,333	415,333	76	142

Source Link: [htttp://www.littelfuse.com/~/media/electrical/datasheets/fuses/semiconductor-fuses/l70qs_high_speed_fuse_datasheet.pdf]

2.21.27 Specification of 2A fuse:-

Electrical Specifications

Catalog Number	Ampere Rating (A)	Nominal Cold Resistance (ohms)	Nominal Volt-drop @100% In (Volt)	Voltage and Interrupting Ratings	Melting I^2T @10 In (A^2 Sec)	Nominal Power Dissipation @100% In (W)	Agency Approvals
							cULus
C1S 750	750mA	0.350	0.333	See Table of Safety Approvals on Page 1 for Voltage and associated Interrupting Ratings	0.01	0.25	Y
C1S 1	1A	0.285	0.349		0.05	0.35	Y
C1S 1.25	1.25A	0.225	0.346		0.14	0.43	Y
C1S 1.5	1.5A	0.182	0.348		0.20	0.52	Y
C1S 2	2A	0.105	0.254		0.26	0.51	Y
C1S 2.5	2.5A	0.072	0.221		0.40	0.55	Y
C1S 3	3A	0.050	0.182		0.83	0.55	Y
C1S 3.5	3.5A	0.040	0.171		1.18	0.60	Y
C1S 4	4A	0.032	0.160		2.05	0.64	Y
C1S 5	5A	0.022	0.140		3.10	0.70	Y

Source link:https://www.mouser.in/datasheet/2/643/ds-CP-c1s-series-1291261.pdf

2.21.28 Specification of 4A fuse:-

MFU 0805 RATING - Very quick acting (FF)

SIZE	FUSE CHAR.	RATED CURRENT [1]	RATED VOLTAGE	PRE-ARCING [2] I^2t at 10 x I_R	VOLT. DROP [2] at 1 x I_R	COLD RESIS [2] at 0.1 x I_R	BREAKING CAPACITY DC	MARK.	APPROVAL	PART NUMBER [3][4]
0805	FF	500 mA	32 V	0.0009 A^2s	374 mV	570 mΩ	50 A at 32 V	F	UL	MFU0805FF00500P500
		630 mA	32 V	0.0014 A^2s	347 mV	420 mΩ	50 A at 32 V	CT	UL	MFU0805FF00630P500
		750 mA	32 V	0.0021 A^2s	280 mV	285 mΩ	50 A at 32 V	G	UL	MFU0805FF00750P500
		800 mA	32 V	0.0023 A^2s	262 mV	250 mΩ	50 A at 32 V	CV	UL	MFU0805FF00800P500
		1.0 A	32 V	0.0028 A^2s	243 mV	185 mΩ	50 A at 32 V	H	UL	MFU0805FF01000P500
		1.25 A	32 V	0.0040 A^2s	205 mV	125 mΩ	50 A at 32 V	J	UL	MFU0805FF01250P500
		1.5 A	32 V	0.0059 A^2s	171 mV	87 mΩ	50 A at 32 V	K	UL	MFU0805FF01500P500
		1.6 A	32 V	0.0065 A^2s	164 mV	78 mΩ	50 A at 32 V	EF	UL	MFU0805FF01600P500
		1.75 A	32 V	0.0077 A^2s	161 mV	70 mΩ	50 A at 32 V	L	UL	MFU0805FF01750P500
		2.0 A	32 V	0.0101 A^2s	176 mV	67 mΩ	50 A at 32 V	N	UL	MFU0805FF02000P500
		2.5 A	32 V	0.0157 A^2s	131 mV	40 mΩ	50 A at 32 V	O	UL	MFU0805FF02500P500
		3.0 A	32 V	0.0227 A^2s	134 mV	34 mΩ	50 A at 32 V	P	UL	MFU0805FF03000P500
		3.15 A	32 V	0.0250 A^2s	128 mV	31 mΩ	50 A at 32 V	EL	UL	MFU0805FF03150P500
		3.5 A	32 V	0.0308 A^2s	119 mV	26 mΩ	50 A at 32 V	R	UL	MFU0805FF03500P500
		4.0 A	32 V	0.0403 A^2s	105 mV	20 mΩ	50 A at 32 V	S	UL	MFU0805FF04000P500
		5.0 A	32 V	0.2275 A^2s	98 mV	15 mΩ	50 A at 32 V	T	UL	MFU0805FF05000P500

Notes

Source link: https://www.mouser.in/datasheet/2/427/mfuserie-239895.pdf

2.21.29 Specification of 10A fuse:-

Electrical Specifications

Part Number	Ampere Rating (A)	Typical Cold Resistance (ohm)	Volt-drop @100% In (Volt) max.	Voltage and Interrupting Ratings	Melting I²T <10 m Sec (A² Sec)	Melting I²T @10 In (A² Sec)	Maximum Power Dissipation (W)	Agency Approvals cULus
0679L0250-XX	250mA	0.61	0.530	See Table of Safety Approvals on Page 1 for Voltage and associated Interrupting Ratings	0.01	0.02	0.13	Y
0679L0375-XX	375mA	0.33	0.480		0.04	0.04	0.18	Y
0679L0500-XX	500mA	0.24	0.470		0.08	0.08	0.24	Y
0679L0630-XX	630mA	0.17	0.410		0.15	0.15	0.26	Y
0679L0750-XX	750mA	0.14	0.380		0.24	0.26	0.29	Y
0679L1000-XX	1A	0.09	0.280		0.51	0.54	0.28	Y
0679L1250-XX	1.25A	0.072	0.250		0.21	0.22	0.31	Y
0679L1500-XX	1.5A	0.058	0.250		0.32	0.29	0.38	Y
0679L2000-XX	2A	0.041	0.240		0.62	0.68	0.48	Y
0679L2500-XX	2.5A	0.032	0.240		0.96	1.13	0.60	Y
0679L3000-XX	3A	0.026	0.220		1.6	1.8	0.66	Y
0679L3500-XX	3.5A	0.022	0.220		2.0	2.2	0.77	Y
0679L4000-XX	4A	0.020	0.220		3.1	3.5	0.88	Y
0679L5000-XX	5A	0.014	0.200		5.3	5.5	1.00	Y
0679L6300-XX	6.3A	0.011	0.190		8.7	8.3	1.20	Y
0679L7000-XX	7A	0.010	0.175		11.1	10.8	1.23	Y
0679L8000-XX	8A	0.0089	0.170		14.8	14.1	1.36	Y
0679L9100-XX	10A	0.0066	0.150		25.7	25.7	1.50	Y
0679L9120-XX	12A	0.0056	0.140		41.0	38.9	1.68	Y
0679L9150-XX	15A	0.0038	0.130		76.7	103.5	1.95	Y
0679L9200-XX	20A	0.0030	0.130		130.5	128.0	2.60	Y

Source link: https://www.mouser.in/datasheet/2/643/ds-CP-0679l-series-1291227.pdf

2.21.30 Specification of 20A fuse:-

Electrical Characteristics

Model	Rated Current (Amps)	Fusing Time	Resistance (Ω) Typ.***	Rated Voltage	Interrupting Rating	Typical I²t (A²s) ****
SF-2410F1200W-2	12.0	Open within 20 sec. at 200 % rated current	0.0053	AC 65 V DC 65 V	AC 65 V 50 A DC 65 V 50 A DC 32 V 300 A	49.2
SF-2410F1500W-2	15.0		0.0038			102.5
SF-2410F2000W-2	20.0		0.0034		AC 65 V 50 A DC 65 V 100 A DC 32 V 300 A	126.2

Source link: https://www.mouser.in/datasheet/2/54/sf-2410fxxxw-1324390.pdf

2.21.31 Specification Of Phoenix Cables:-

Sensor/actuator cable - SAC-17P-MS/5.0-35T/FS SH SCO - 1402421

Please be informed that the data shown in this PDF Document is generated from our Online Catalog. Please find the complete data in the user's documentation. Our General Terms of Use for Downloads are valid (http://phoenixcontact.com/download)

Sensor/actuator cable, 17-pos., PUR/PVC, RAL 9005 (black), shielded, straight M12 SPEEDCON male plug (A-coded) to straight M12 SPEEDCON female plug, cable length: 5 m

Why buy this product

- Easy and safe: 100% electrically tested plug-in components
- Save time, thanks to installation with SPEEDCON fast locking system
- Save space – with high-pos. connectors
- Reliable signal transmission – 360° shielding in environments with electromagnetic interference

Key Commercial Data

Packing unit	1 pc

Source link:- https://www.phoenixcontact.com/online/portal/us?uri=pxc-oc-itemdetail:pid=1402421&library=usen&tab=1

2.21.32 Specifications of Voltmeter

Source: https://www.alibaba.com/product-detail/PCS-6C2-A-600V-Analog-DC_1694741484.html?spm=a2700.7724857.normalList.10.3f20870eKPFvDj

2.21.33 Source Of Radiator Pump Datasheet:- http://www.gripumps.com/wp-content/uploads/2018/10/GRI-Integrity-Series-Overview-1018.pdf

2.21.34 Source OF Radiator Fan Datasheet:-
https://media.digikey.com/pdf/Data%20Sheets/NMB-MAT/R200.pdf

2.21.35 Source Of Cooling Fan Datasheet:-
https://media.digikey.com/pdf/Data%20Sheets/NMB-MAT/09225VA_IP69K.pdf

2.21.36 Source of Microcontroller datasheet: https://os.mbed.com/platforms/ST-Nucleo-F103RB/

2.21.37 Source of Isolation Relay datasheet::
http://www.gigavac.com/sites/default/files/catalog/spec_sheet/gx14.pdf

2.21.38 Hall Sensor Datasheet:

PARAMETERS	VALUES	UNITS
Burden Resistance (Rb)	10000 (min.)	Ω
Voltage output @ Ipn (Vout)	± 4.0 ±2%	V
Supply Voltage (V+ / V-)	± 12 to 15	V
Current consumption @ +15V (Ic)	25.0	mA
Accuracy	± 2.0	%
Linearity	< 1.0	%
Output offset voltage @ Ip = 0 (Voff)	±25.0	mV
Temperature coefficient of Vout	± 0.1	% of rdg/k
Frequency bandwidth @ -3 dB (fbw)	DC to 20	kHz
Dielectric strength Primary to o/p terminals	3	kVrms
Operating Temperature Range	- 25 to + 85	°C
Storage Temperature	- 25 to + 85	°C
Weight	70 Typ.	g

https://www.electrohms.com/admin/image/3_HK050_500T03_Rev-03.pdf

2.21.39 Datasheet of Pressure Sensor:

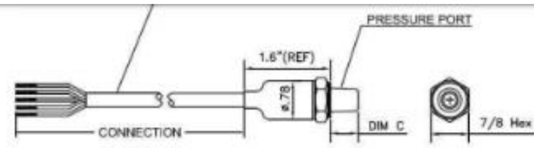

CODE	PORT	DIM C
2	1/4-19 BSPP	0.453[11.50]
4	7/16-20 UNF-A MALE SAE J514 STRAIGHT THREAD O-RING BUNA-N 70SH-904, ID8.92mm x W1.83mm	0.435[11.05]
5	1/4-18 NPT	0.596[15.14]
6	1/8-27 NPT	0.475[12.06]
E	1/4-19 BSPT	0.50[12.70]
F	1/4-19 BSPP FEMALE	0.70[17.78]
K	1/8-27 NPT FEMALE	0.70[17.78]
P	7/16-20 UNF-2A FEMALE SAE J514 STRAIGHT THREAD WITH INTEGRAL VALVE DEPRESSOR	0.689[17.50]
Q	M10 x 1.0 mm	0.42[10.67]
S	M12 x 1.5 mm	0.53[13.46]
U	G1/4 DIN 3852 FORM E GASKET DIN3869-14 NBR	0.547[13.90]
W	M20 x 1.5 mm	0.702[17.83]

CODE	CONNECTION TYPE
1	CABLE 2 FT
2	CABLE 4 FT
3	CABLE 10 FT
M	CABLE 1 M
N	CABLE 2 M
P	CABLE 5 M
R	CABLE 10 M

OUTPUT (ANALOG)

Code	Output	Supply	Ratiometricity	Red	Black	Green	White
1	0 – 50mV	5V	Yes	+Supply	-Supply	+Output	-Output
2	0 – 100mV	5V	Yes	+Supply	-Supply	+Output	-Output
3	0.5 – 4.5V	5 ± 0.25V	Yes	+Supply	Common	Cut Off	+Output
4	1 – 5V	10 – 30V	No	+Supply	Common	Cut Off	+Output
5	4 – 20mA	9 – 30V	No	+Supply	-Supply	Cut Off	Cut Off

OUTPUT (DIGITAL)

Code	Output	Supply	Red	Black	Green	White	Yellow
J	I²C	2.7 – 5.0V	+Supply	-Supply	SCL	SDA	--
S	SPI	2.7 – 5.0V	+Supply	-Supply	SCLK	MISO	SS

https://www.te.com/commerce/DocumentDelivery/DDEController?Action=showdoc&DocId=Data+Sheet%7FMSP300%7FA2%7Fpdf%7FEnglish%7FENG_DS_MSP300_A2.pdf%7FCAT-PTT0016

2.21.40 Datasheet of BMS sensing wires:

Rated voltage:600V				Experimental voltage:2000V			
temperature range:-60° C--200° C				Conductor: Tinned copper wire			
Outside diameter tolerance: 0.1mm				Insulator: Silicone			
conductor				Insulator		Electrical characterist	Maximum current
No.	Pin/Wire diameter	CSA	Diameter	Thickness	Diameter	Conductor resistance	Ampere
AWG	mm	mm2	mm	mm	mm	Ω /km	A
1	14000/0.08mm	70	11.4	2.3	16	0.45	840
2	10000/0.08mm	50	10.2	2.4	15	0.63	630
3	7000/0.08mm	35	7.7	2.6	13	0.89	500
4	5000/0.08mm	25	7.2	2.4	12	1.25	400
6	3200/0.08mm	16	5.2	1.65	8.5	1.9	300
7	2400/0.08mm	12	4.5	1.35	7.2	2.6	240
8	1650/0.08mm	8.3	3.5	1.5	6.5	3.7	190
10	1050/0.08mm	5.3	2.9	1.3	5.5	6.3	140
11	750/0.08mm	3.8	2.53	1.2	5	8.3	105
12	680/0.08mm	3.4	2.48	1	4.5	9.8	88
13	500/0.08mm	2.5	2	1	4	12.5	70
14	400/0.08mm	2	1.78	0.9	3.5	15.6	55
15	300/0.08mm	1.5	1.6	0.8	3.2	20.8	42
16	252/0.08mm	1.27	1.53	0.75	3	24.4	35
17	210/0.08mm	1	1.33	0.68	2.7	29.8	30
18	150/0.08mm	0.75	1.19	0.55	2.3	39.5	22
20	100/0.08mm	0.5	0.92	0.45	1.8	62.5	13
22	60/0.08mm	0.3	0.78	0.45	1.7	88.6	8
24	40/0.08mm	0.2	0.6	0.5	1.6	97.6	5
	[illegible]0.08mm	0.15	0.46	0.5	1.5	123	3.5

https://www.aliexpress.com/item/32820542554.html?spm=a2g0s.9042311.0.0.20c24c4dmr4ASJ

3 MECHANICAL DESIGN REPORT

3.1 System Overview

The car runs on 13 inch Oz rims with Hoosier 20inch dry and wet tires and has a total mass of 350 Kg with a 60kg driver. Double wishbone suspension geometry with unequal and non-parallel A-arms is used with a pushrod configuration in the rear and pull-rod configuration in front. Chassis is a tubular space frame made of AISI 4130 steel tubes. The Ackerman steering geometry is employed with a steering ratio of 3:1. The car is a rear-wheel-drive powered by the Emrax 228 MV Energy motor with a peak power of 100KW at 6500 rpm being transferred through a European 420 single-strand chain. The body is a glass fiber composite.

3.2 Design Goals

- Utilizing simulation software for the estimation of vehicle parameters.
- Using a higher power motor for increased performance.
- Designing components with higher load capacity due to increased acceleration.
- Incorporating adjustability of wheels and other vehicle parameters in the design.
- Use of higher specific strength material for CNC for mass reduction.
- Lightweight glass fiber body and better aerodynamic simulations for increased aero efficiency.
- Reduced wheelbase and modified vehicle parameters for a more responsive and maneuverable vehicle.
- Cooling system designing for motor and battery pack at high load conditions.
- Taking manufacturing into account during designing and provisions for manufacturing error control.

3.3 Suspension

3.3.1 Suspension Design Goals

3.3.1.1 Incorporating Adjustment for camber angle and toe angle

We wanted to include camber angle and toe angle adjustment provisions to our car this year, in order to account for manufacturing errors and optimize these parameters during testing. Clevises and shims were introduced in the upright assembly for this purpose.

3.3.1.2 Adjustable damping ratio

Since the best method to optimize the damping ratio to be used is vehicle testing, we used two-way adjustable dampers this year.

3.3.1.3 Independent roll and ride frequency

Adjustable stiffness anti-roll bars were to be introduced this year in our vehicle setup to achieve the aforementioned aim.

3.3.1.4 Using a material of higher specific strength, Al-7075 T6 in place of Al-6061 T6, for wheel assembly CNC components and lighter weight rims to compensate for increased mass due to adjustment provisions provided.

3.3.1.5 Self-designed hub lock ring that doesn't loosen due to shocks and vibrations as in our previous vehicle.

3.3.2 Vehicle weight estimation

Previous vehicle weight was as follows:

System	Components	Weight/Component	Quantity	Total Weight(g)
Suspension	Tire	6000	4	24000
	Wheel	3630	4	14520
	Hub + Upright	1500	4	6000

	Hub bearing	640	4	2560
	Bearing Retaining Ring	62.5	8	500
	Wheel lock nut	20	16	320
	Penske Dampers	480	4	1920
	Springs	160	4	640
	Bell Crank	125	4	500
	A-arms	400	8	3200
	Push Rod	150	4	600
	Rod ends	35	24	840
	Spherical Bearing	15	8	120

Braking	Brake Disc	500	4	2000
	Caliper	800	4	3200
	Balance Bar	76	1	76
	Reservoir	200	2	400
	Mounts + Base Plate	2000	1	2000
	Pedals(accelerator+brake)	1000	1	1000
	Potentiometer	500	3	1500
Structure	Chassis	36000	1	36000
Powertrain and electrical	Motor	18000	1	18000
	Motor-Mount	100	2	200
	Battery Box	90000	1	90000
	Motor Controller	4000	1	4000
	LV Batteries	4000	2	8000
	Boxes	1000	2	2000
	PCB connectors and Cables	1500	1	1500

	Driveshaft	3000	2	6000
	Sprocket	3000	1	3000
	Differential + Mount	9500	1	9500
	Chain	1500	1	1500
	Drive Shaft Lock	120	2	240
Steering	Steering Wheel	200	1	200
	Quick Release	250	1	250
	Connecting Rod	200	2	400
	Rack and Pinion	1000	1	1000
	UV Joint	200	1	200
	Rod ends	35	8	280
	Steering Rod + Tie rod	100	4	400
Driver's Equipment	Seat	2000	1	2000
	Roll Bar Padding	325	2	650
	Harness	1000	1	1000
	Head Restraint	500	1	500
	Firewall	2000	1	2000

Body	Floor	1000	1	1000
	Body Works	10000	1	10000
Impact Attenuator	Impact attenuator	500	1	500
	Intrusion plate	1000	1	1000
Miscellaneous	Flanges(bushing)	-	-	8000
	Washer			
	Mounting Plates			
	Bolts and nuts			
Driver's average mass		60000	1	60000
Weight of the car				335516

We estimated the weight for our current project as follows:

- The total increase in weight due to suspension adjustment provisions: **4 kg**
- Increase in chassis weight: **6 kg**
- Increase in body weight: **8 kg**
- Reduction in weight of motor and motor mount: **3 kg**
- Reduction in weight of sprocket and chain: **2.5 kg**
- Reduction in weight due to changing CNC material of suspension components and a rim: **2.5 kg**
- Miscellaneous increase in weight (electrical components and cooling system): **7 kg**

The weight of the new car would be around **280 kg - 300 kg** without a driver. We assumed the weight to be **290 kg** for calculation purposes.

3.3.3 Suspension geometry construction

3.3.3.1 Tyre and rim selection

As the estimated weight of our car was much higher than 250 kg. It is recommended, based on our study of tire data and some online websites and forums that we should be using **13-inch rims with 20-inch tires** that **perform better than 10-inch rim variants** available for Formula Student teams, **at that weight range**. The following curve explains our choice :(Lateral force comparison b/w 10in and 13in wheels for a **vertical load of 670N**)

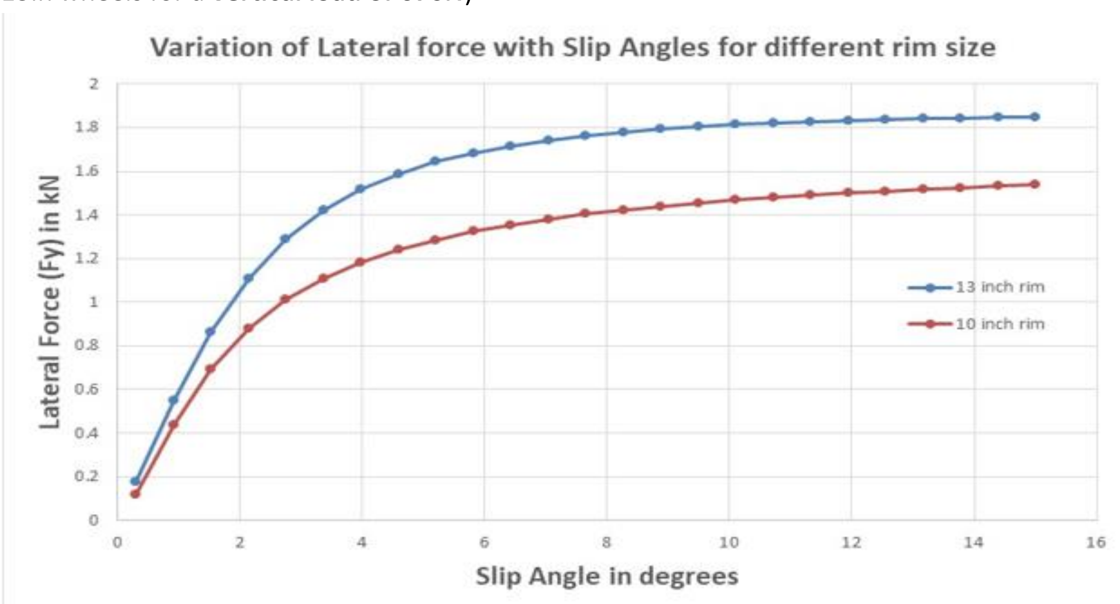

OZ cast aluminum alloy single piece four holes rims (7*13) were used because of their low weight, high strength and the premium finish that this brand offers.

Hoosier 43168 (slick) tires (20*7.5-13) were selected because their testing data was available at that time and lower cost compared to other premium makers like Goodyear and Avon, and it was decided that we will manufacture our vehicle around this tire.

Hoosier 44150 (wet) tires were selected for wet tracks despite their test data not being available to us because of their resemblance with our chosen slick tires.

3.3.3.2 Weight distribution estimation and center of gravity (CG) height

We have a rear-wheel-drive that favors more weight on the rear but for better braking, we need a weight distribution of 40:60 to 50:50 front to rear. A weight distribution lower than 45:55 front to rear is not recommended if we are using the same tires because it reduces tire life and unbalances the car.

Based on the above data and the information available, a **weight distribution of 46:54 front to rear** is selected.

CG height was assumed to be the same as the previous car, 282mm because the packing of the vehicle would remain the same.

3.3.3.3 Track width and wheelbase selection

Wheelbase should be kept as less as possible to increase the maneuverability of the vehicle but must be high enough to allow sufficient packing space without much mass overhang. From our previous vehicle, we found that packing is not a problem for us. Hence a **wheelbase of 1530mm**, 5mm more than the minimum permissible to accommodate manufacturing errors, was selected.

Track width is important for rollover stability. Following **formula was devised for rollover stability analysis:**

2*(3^.5)*CG height <= Tf*Wf/ (Wf+Wr) +Tr*Wr/ (Wr+Wf)

Where,

Tf = front track width (m)

Tr = rear track width (m)

Wf = front car weight (kg)

Wr = rear car weight (kg)

This formula gives us a **lower limit of track width (700mm - 800mm)**. **Lateral weight transfer** is improved with increasing track width, but it was **not significant for the range of track width we would be using** (upper limit of 1300mm-1350mm). Also, increasing the track width would increase the weight of the car. We chose to stick to our previous year **track widths of 1200mm front and 1175mm rear**.

3.3.3.4 Wheel parameters selection

All the parameters defined here were set according to our previous car setup and average values of these parameters for a Formula Student car. Kingpin and scrub were designed considering the packing efficiency of suspension components into account. Camber and toe angles are adjustable, so they were initially set to 0 degrees.

Static camber front (degrees)	0
Static camber rear (degrees)	0
Static toe front (degrees)	0
Static toe rear (degrees)	0
Kingpin inclination front (degrees)	6.2
Kingpin inclination rear (degrees)	9
Front castor angle (degrees)	7.04
Scrub radius front/rear (mm)	18/25.3
Front roll center height (mm)	45
Rear roll center height (mm)	50
Front ride frequency (Hz)	3.5
Rear ride frequency (Hz)	3.3

3.3.3.5 Suspension hard-point selection procedure

- Indirect actuation was to be used so that we may include ARB in the design.
- Pull rod suspension was designed at the front end of the car to reduce vehicle CG height and pushrod at the rear end because the pull rod was not possible there, owing to the presence of driveshaft.
- Outer and inner points of A-arm must give the aforementioned roll center height.
- Outer and inner points were to be kept as close to each other as possible, to reduce mass.
- As may be seen from the graph below, our camber angle must be between 0 degrees - 2 degrees, this data is used to arrive at the suspension hard-points.

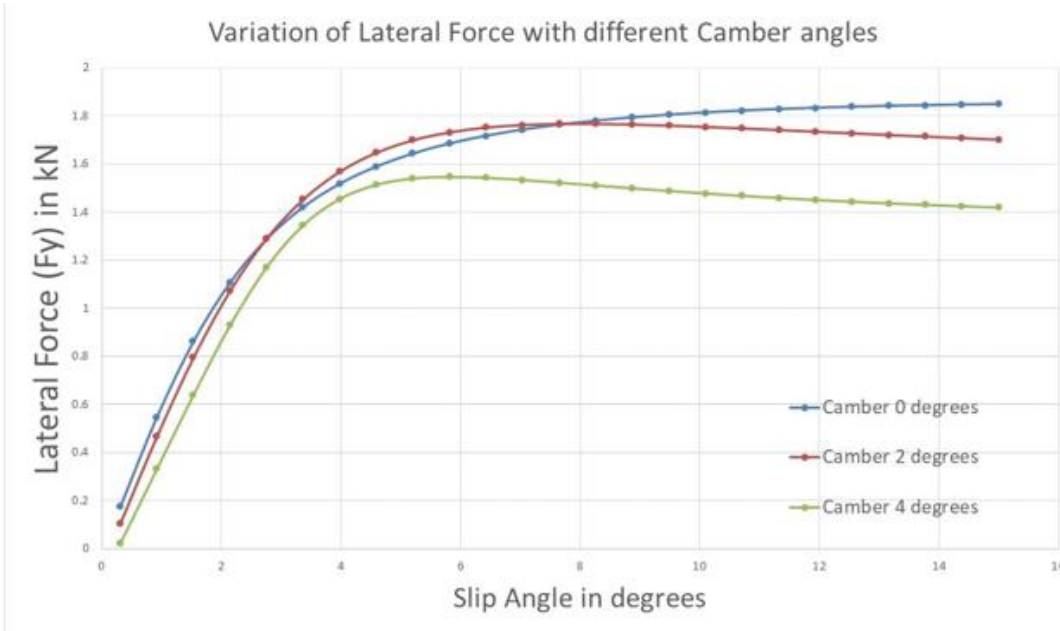

- Anti-features were included in the geometry to reduce the vehicle pitch without increasing ride stiffness.
- Pull-rod/push-rod outer point should be as close to A-arm outer points as possible and the centerline of the rod must pass through the A-arm outer point.
- Rocker, strut assembly and pull-rod/push-rod must always stay in the same plane.
- ARB drop-link must be close to perpendicular to the rocker and the ARB arm must always be perpendicular to the ARB rod.

3.3.4 Spring stiffness, damping coefficient and ARB stiffness calculations

	Front	Rear
Ride frequency, Hz (assumed)	3.5	3.3
Ride rate, N/mm (calculated using ride frequency)	26.6	27.7
Tyre stiffness, N/mm (from tyre data)	120	120
Motion ratio (from the geometry)	0.8	0.7
Spring stiffness, N/mm (calculated using motion ratio, ride rate, and	41.5	56.56

tire stiffness)		
Roll gradient, degree/g acceleration (Assuming chassis to be infinitely stiff)	0.55	
ARB stiffness, N.m/deg (calculated using roll gradient, track width data and given spring stiffness)	5.36	14.76

3.3.5 Design and selection of suspension components

Bearings used:

Bearing Location	Bearing Number	Basic Static Load Rating C_0 (kN)	Basic Dynamic Load Rating C (kN)	Life (L10)/ Factor of Safety
Hub-Upright Front	61910-2RS1	14.6	11.8	4740 hr
Hub-Upright Rear	61815-2RS1	12.5	10.8	510 hr
A-arms-Upright	GE 8 C	14.6	5.85	2.925
Tie rod outer, Pushrod-A-arms, Pull-rod-A-arms, Upper Control Arm rear inner, ARB drop-link-Rocker, ARB drop-link-ARB	POS 6 (6mm rod ends)	4.73	4.2	2.1
Lower Control Arm inner, Upper Control Arm Front inner	POS 8 (8mm rod ends)	8.64	7.01	3.5
Front ARB, Rear ARB	PHSB 6 (6mm female rod ends)	21.6	9.23	4.5
Brake Potentiometer	PHSB 8 (8mm female rod ends)	36.2	14.8	7.2
Front/rear ARB to Chassis	HK 1612	9.8	7.37	40000 hr
Rocker-Chassis	608-2Z	3.47	1.35	650 hr

Hub Bearing Formula:

$P = XF_r + YF_a$

$\frac{f_0 F_a}{C_{0r}}$	e	$\frac{F_a}{F_r} \leqq e$		$\frac{F_a}{F_r} > e$	
		X	Y	X	Y
0.172	0.19	1	0	0.56	2.30
0.345	0.22	1	0	0.56	1.99
0.689	0.26	1	0	0.56	1.71
1.03	0.28	1	0	0.56	1.55
1.38	0.30	1	0	0.56	1.45
2.07	0.34	1	0	0.56	1.31
3.45	0.38	1	0	0.56	1.15
5.17	0.42	1	0	0.56	1.04
6.89	0.44	1	0	0.56	1.00

P = XFr + YFa
P: Equivalent Load (kN)
F_r: Radial Load (kN)
F_a: Axial Load (kN)
X: Radial Load Factor
Y: Axial Load Factor

$$x_D = \frac{L_D}{L_{10}} = \frac{60\mathcal{L}_D n_D}{L_{10}}$$

$$C_{10} = a_f F_D \left[\frac{x_D}{x_0 + (\theta - x_0)(1 - R_D)^{1/b}} \right]^{1/a}$$

The Weibull parameters are $x_0 = 0.02$, $(\theta - x_0) = 4.439$, and $b = 1.483$.

Rod end load calculation:
FOS = C/F (=load on rod end)

Spherical bearing load calculation:
FOS = C/F (=load on rod end)

ARB Bearings:
Since ARB is not a rotating body but an oscillating one, special formulations should be used to calculate the life of the bearing.
Here, we have used the **Harris1 approach** to arrive at the solution.

P_{oscn}: Dynamic Corrected Load

L_{ref}: 10^6 oscillations

φ: Half angle of oscillation

$L_{10} = a_{oscn} * L_{ref} * (C/P_{osc})^p$

$P_{oscn} = (2*\varphi/\pi)^{1/p} * P$

$a_{oscn} = (\pi/2*\varphi)$

Front Rocker:
Mass: 166 gm
Material: Aluminium 7075-T6

Supports	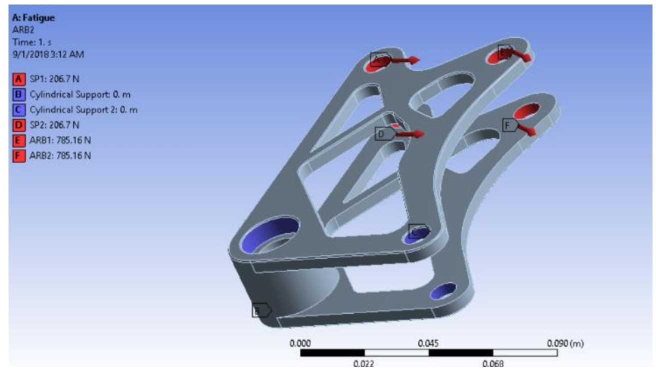
Equivalent stress	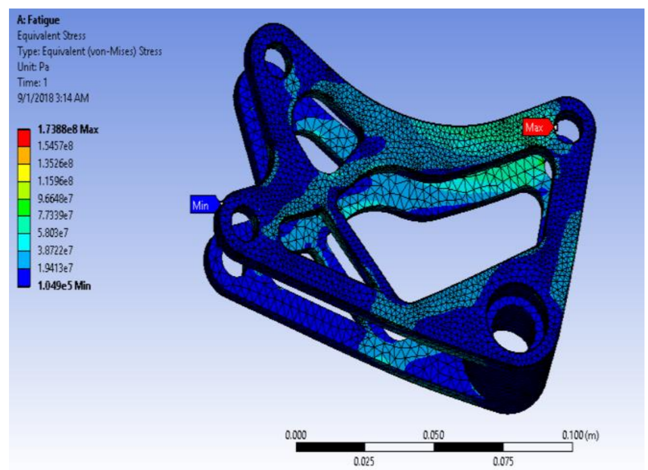

Factor of Safety	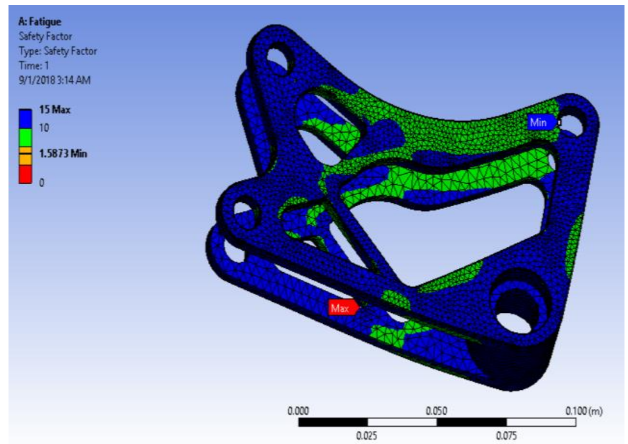
Fatigue Life	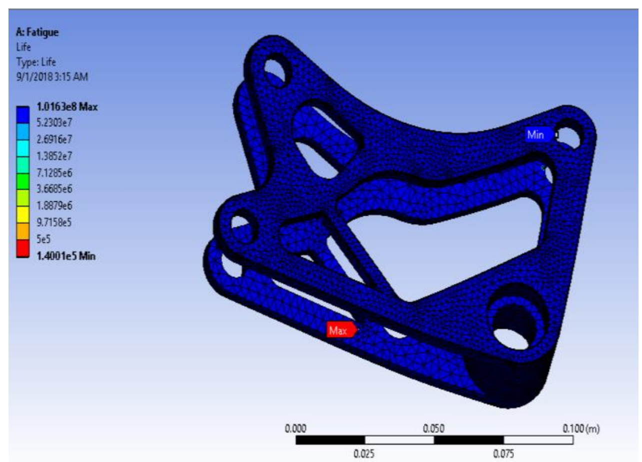

Rear Rocker:

Mass: 143 gm
Material: Aluminium 7075-T6

Supports and Force Application	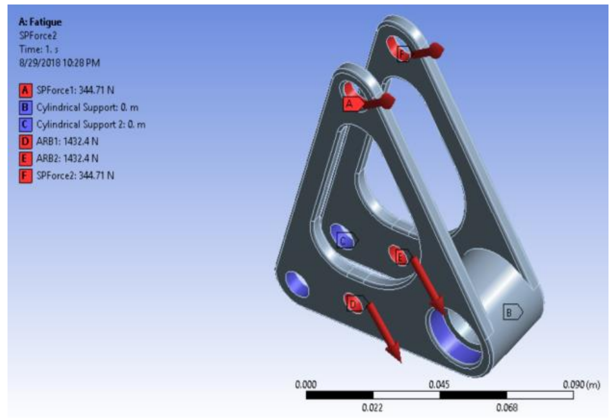
Equivalent Stress	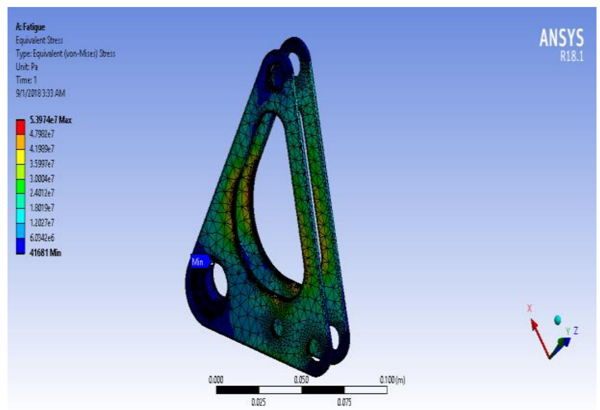

Factor of Safety	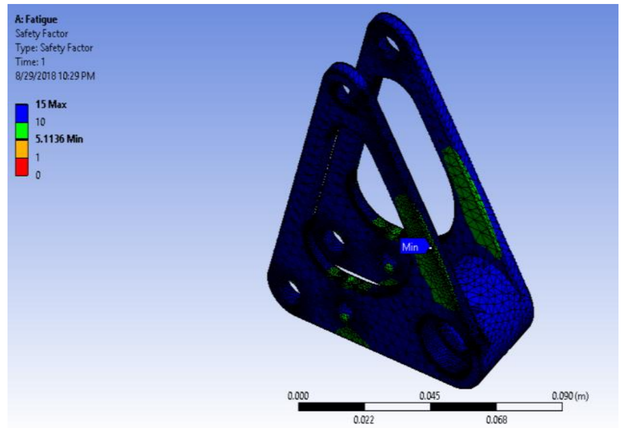
Fatigue Life	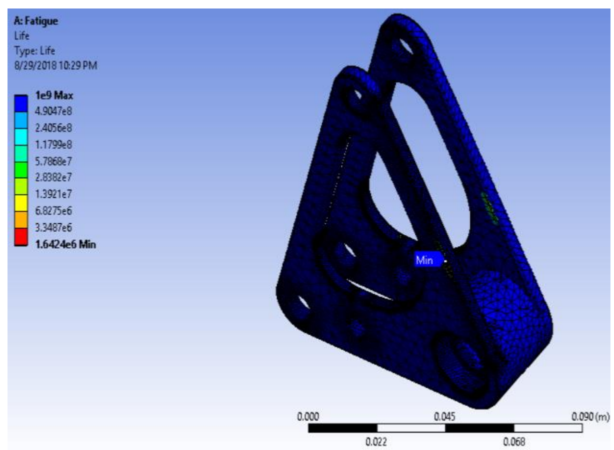

Front Hub:
Mass: 607 gm
Material: Aluminium 7075-T6

<table>
<tr>
<td>Stress</td>
<td>
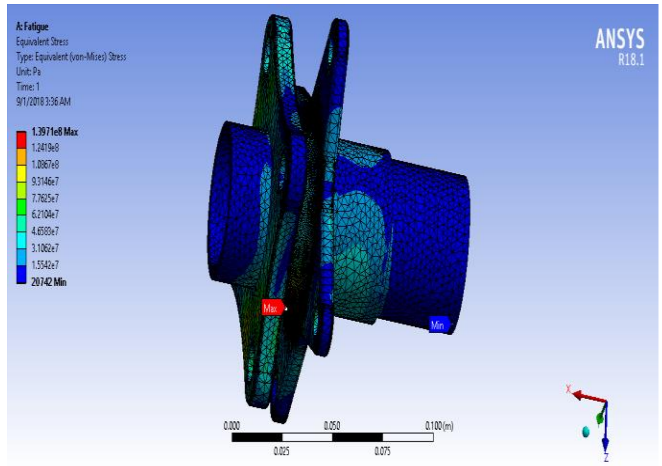

</td>
</tr>
<tr>
<td>Factor of Safety</td>
<td>
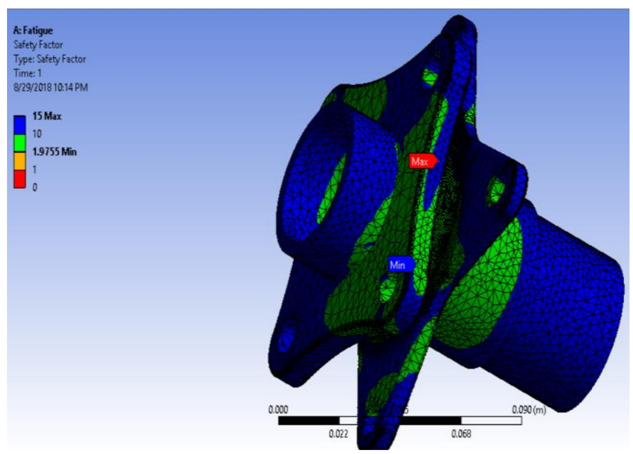

</td>
</tr>
</table>

Fatigue Life	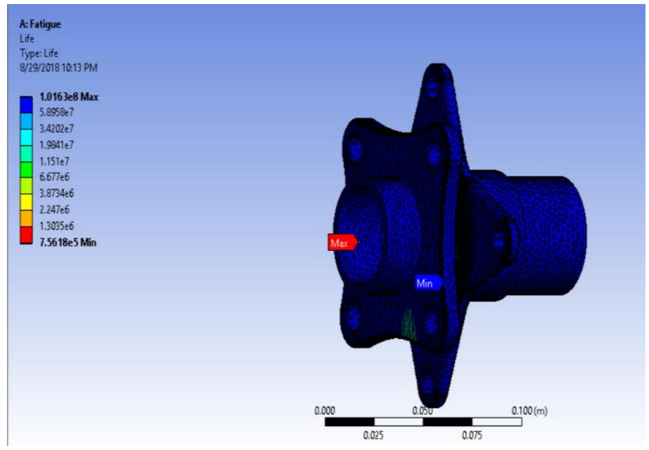

Rear Hub:
Mass: 712gm
Material: Aluminium 7075-T6

Equivalent stress	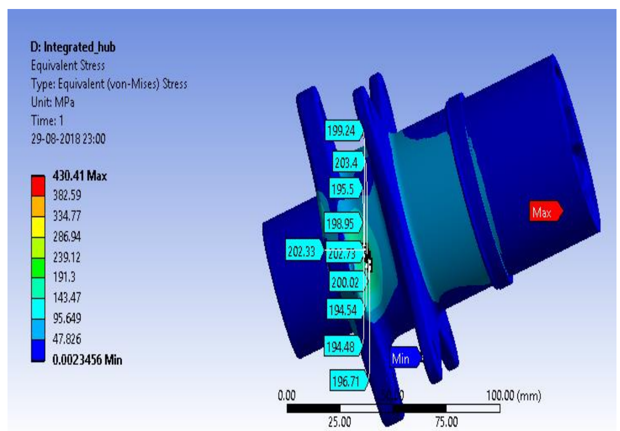

Front Upright:
Mass: 474 gm
Material: Aluminium 7075-T6

Supports and Force Application	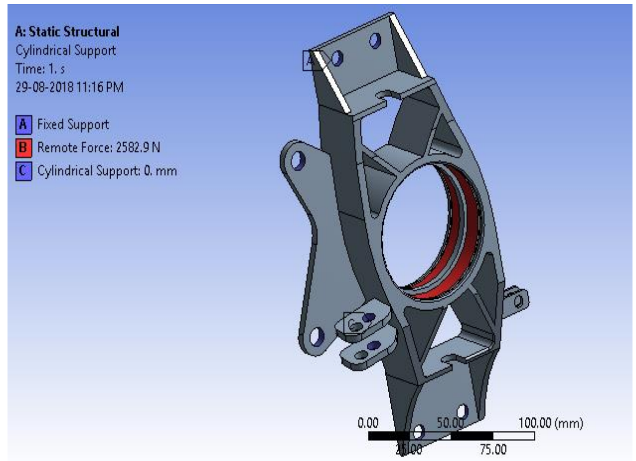
Equivalent stress	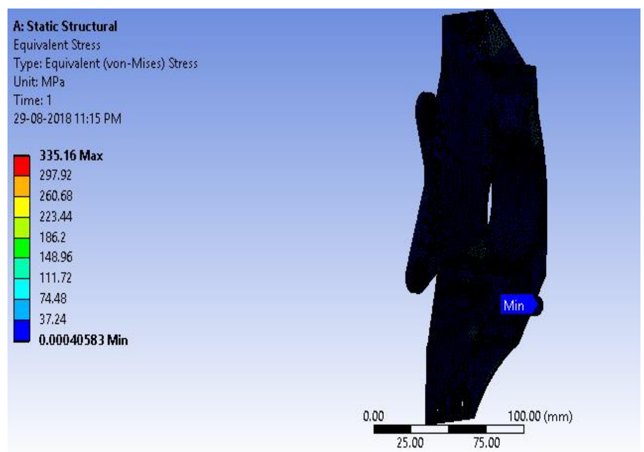

Factor of Safety	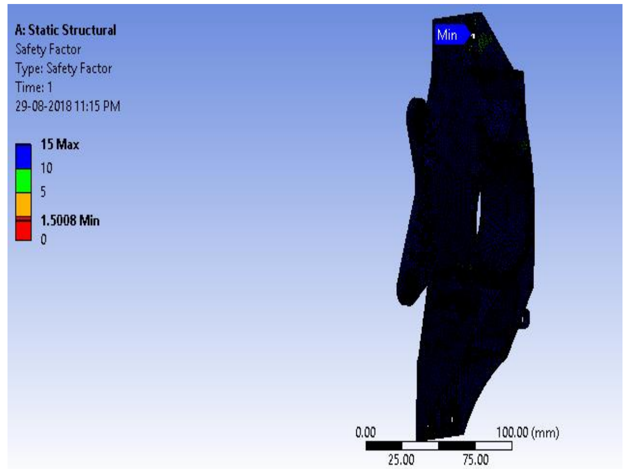

Rear Upright:
Mass: 573 gm
Material: Aluminium 7075-T6

Supports **Supports**	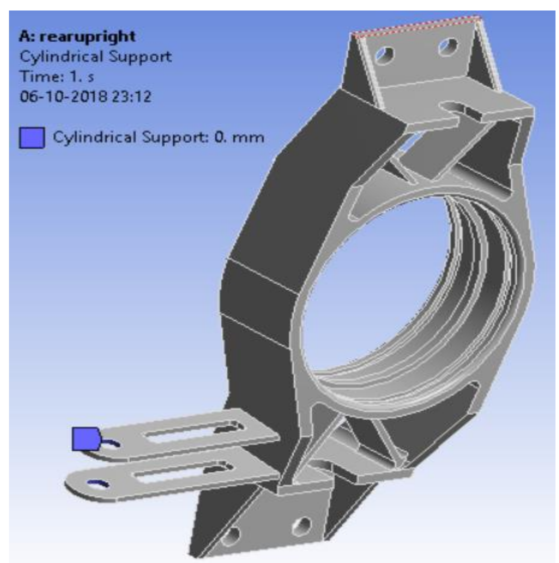

	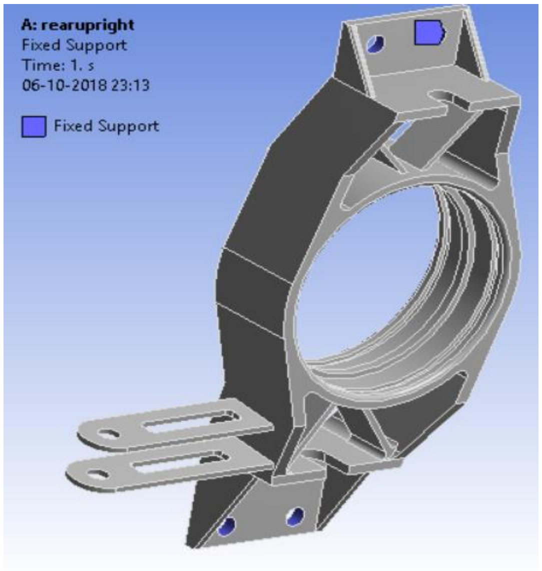
Equivalent Stress	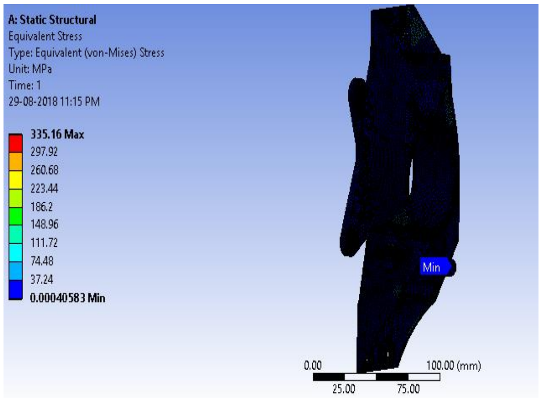

Factor of Safety	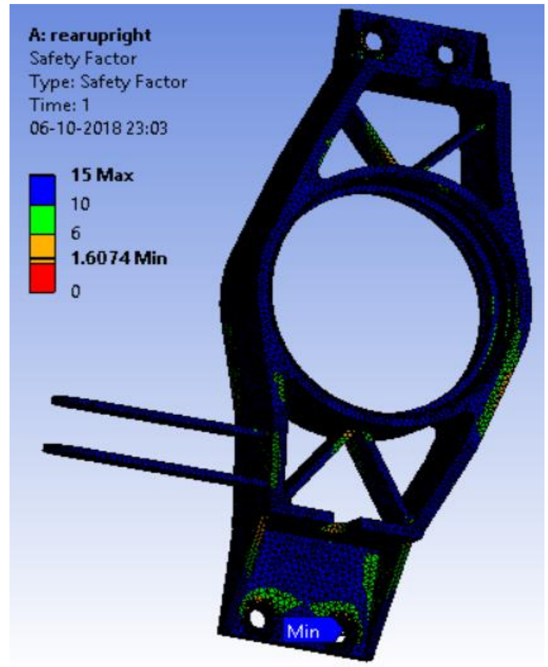

Spring designing:

These equations along with space constraints were used to arrive at the dimensions of the springs.

$$k_{spring} = \frac{G d_{wire}^4}{8(D_{coil} - d_{wire})^3 n_{active}}$$

Maximum shear stress for helical spring

$$\tau = K_s \frac{8FD}{\pi d^3}$$

The static factor of safety of spring achieved: 1
Fatigue factor of safety of spring achieved: 1.5

Hub lock ring thread:
The equation used for thread-safety calculation (failure at thread root by shear):

$$A_{TS} = \pi n L_e D_{min} \left[\frac{1}{2n} + 0.57735(D_{smin} - E_{nmax}) \right]$$

$$L_e = \frac{S_{st}(2A_S)}{S_{nt} \pi n D_{smin}[(1/2n) + 0.57735(D_{smin} - E_{nmax})]}$$

Self locking condition: (pi)*(mean dia)*(friction coeff)*(sec(half thread angle))>lead

Previous year our lock ring was loosened because of shocks and vibrations. To overcome that problem, we **increased the pitch of the threads from 1mm to 1.5mm** so as to increase the shock resistance of the threads without affecting fatigue life much.

3D Printed Shims:
Mass: 8.5gm
Material: PLA

It was decided to manufacture 3D printed shims (PLA) for mass reduction. Analysis results below justify our choice:

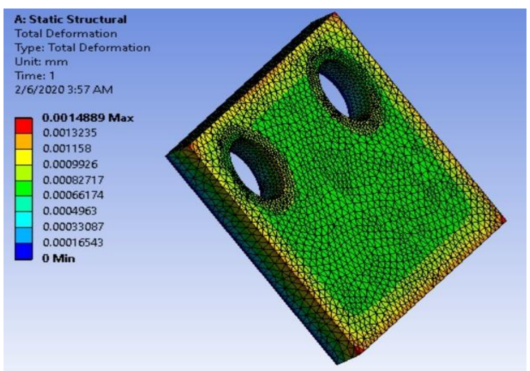

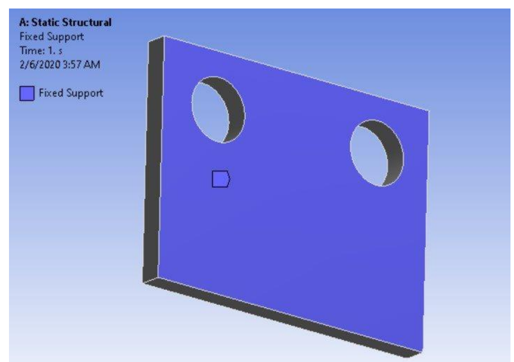

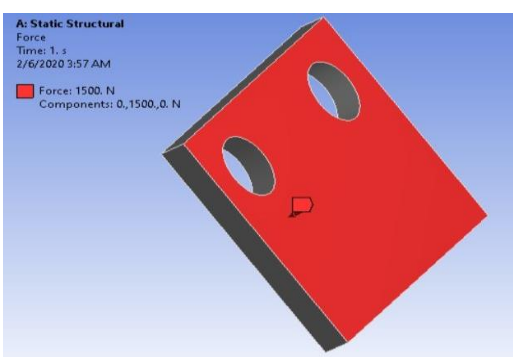

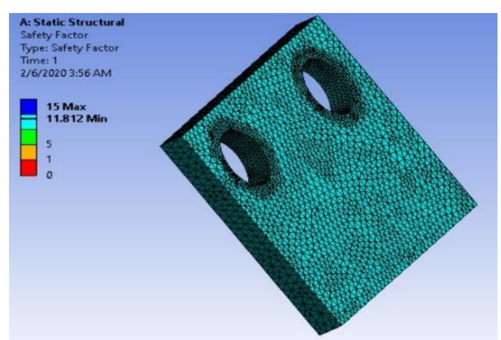

3.3.6 Simulation results of our setup (IPG)

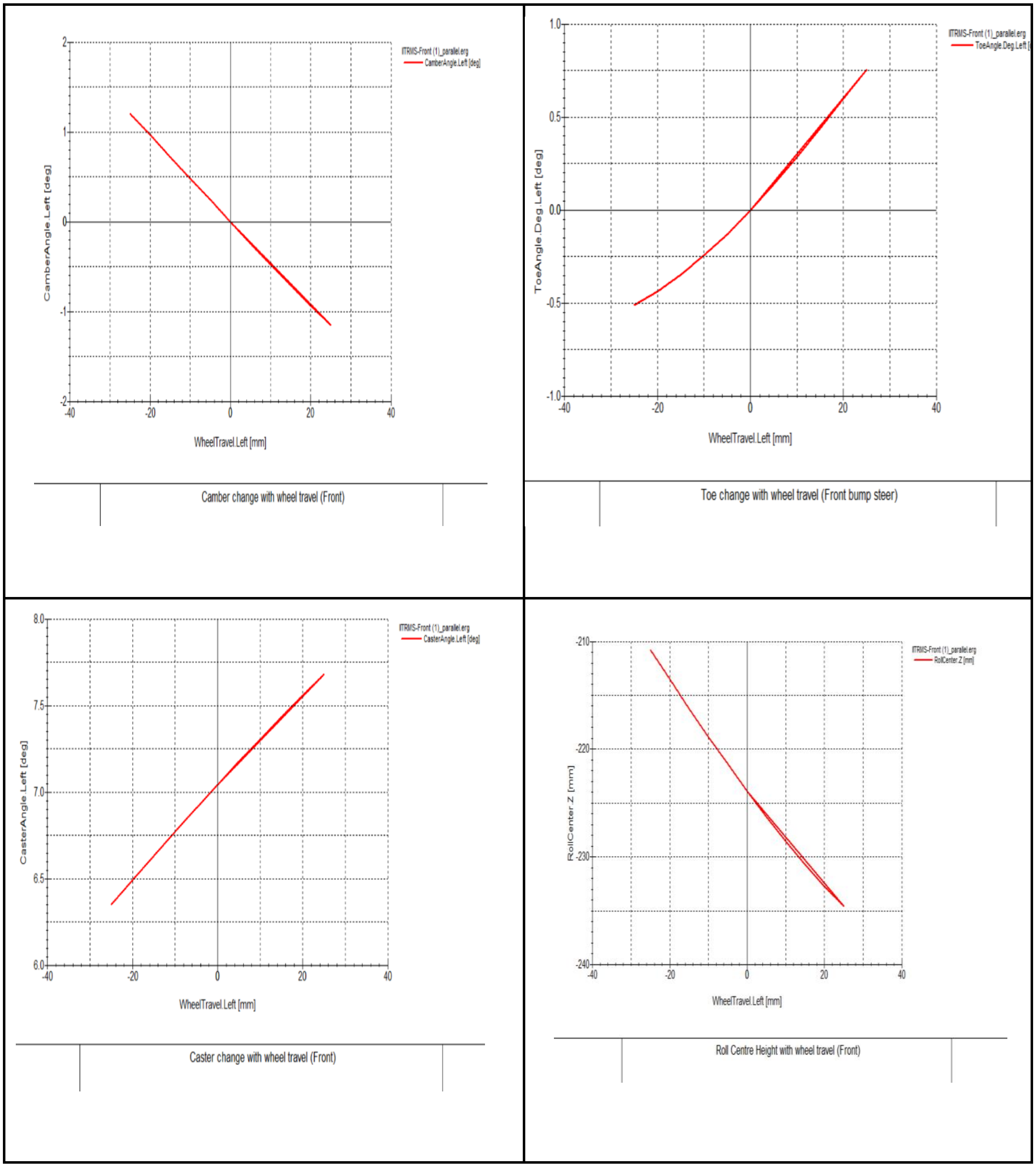

Camber change with wheel travel (Front)

Toe change with wheel travel (Front bump steer)

Caster change with wheel travel (Front)

Roll Centre Height with wheel travel (Front)

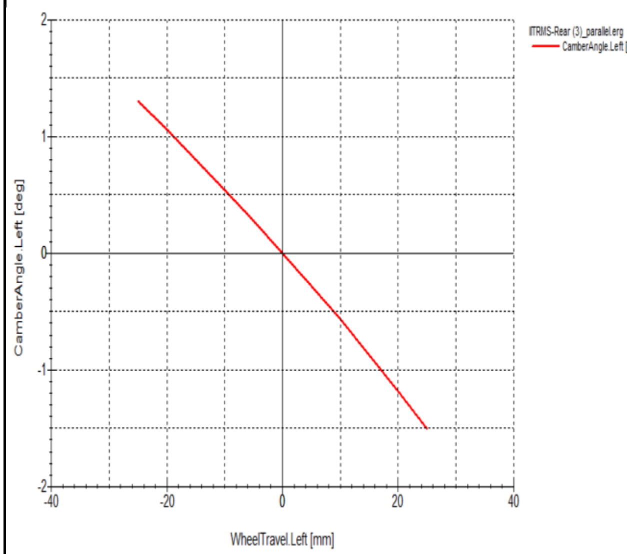

Camber change with wheel travel (Rear)

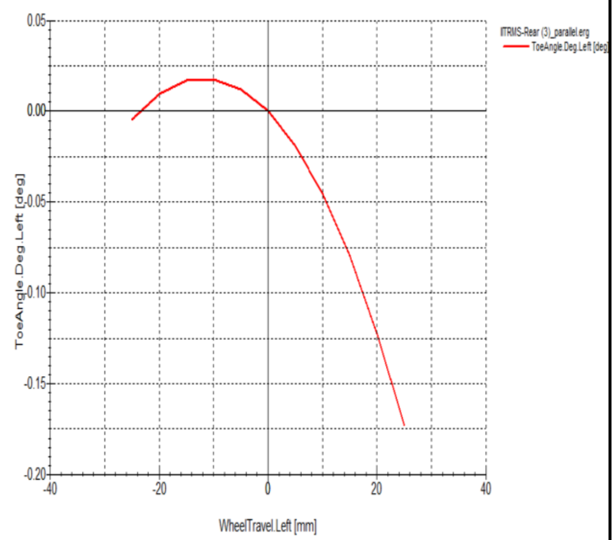

Bump steer Rear

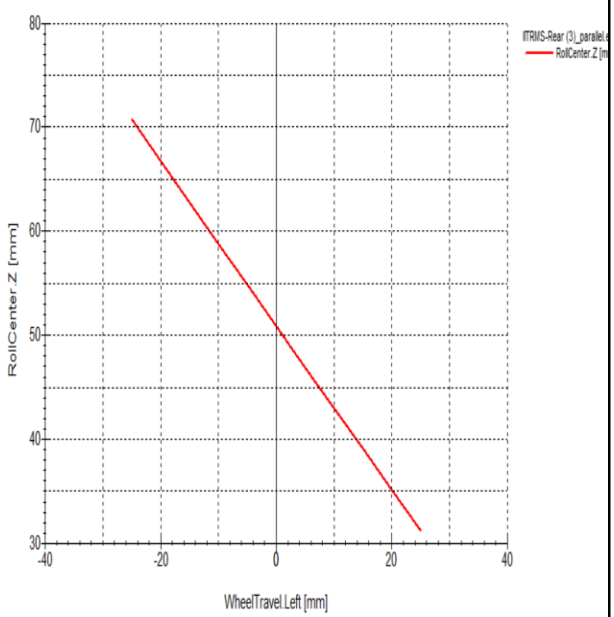

Roll Centre Height with wheel travel (Rear)

3.4 Structural Design

3.4.1 Introduction

A chassis is the load-bearing framework of a car, which structurally supports its various components. It deals with static as well as dynamic loads without undue deflection or distortions. Driver's safety, ergonomics, and sometimes aesthetics are some significant concerns in it.

3.4.1.1 Why Steel Space Frame?

Space frames have been using in the construction of racing car chassis, since the introduction of car racing in the 1940s. From Monocoque and Space-frame options, there are aesthetics and weight-related advantages in the former. Still, the latter one is logical in aspects like cost, existing facilities as well as lack of expertise in composites. It also offered ease of use in material availability, machinability, and welding.
Thus, for our project, a steel space frame is the most logical choice.

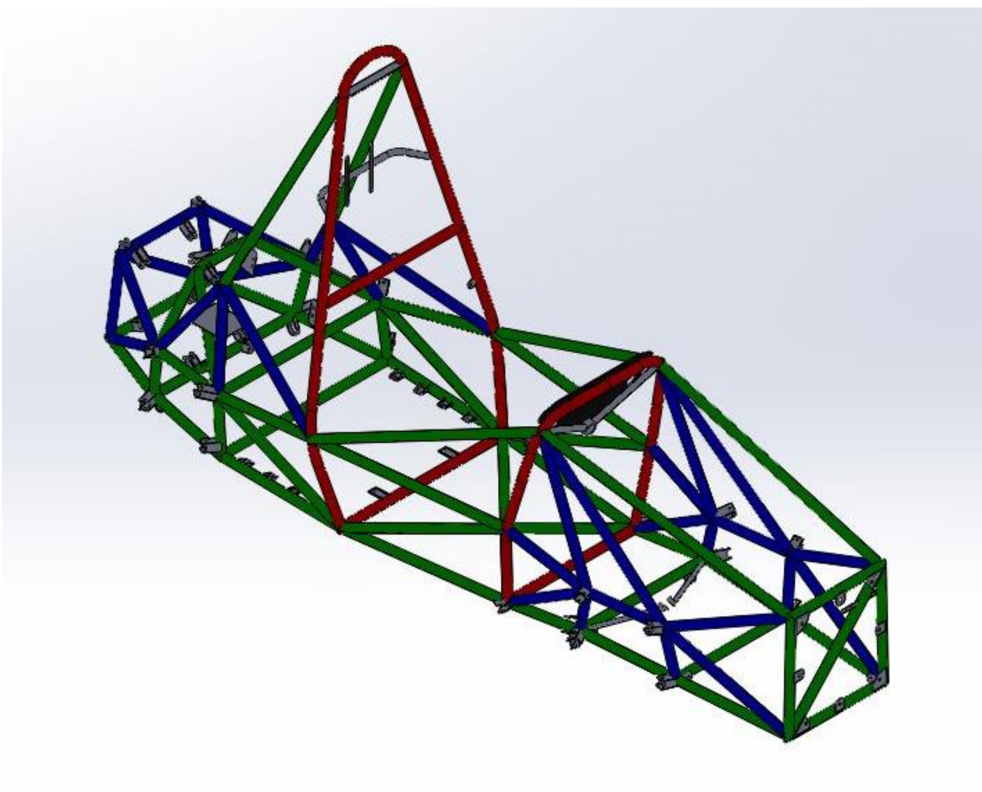

Isometric view of Chassis

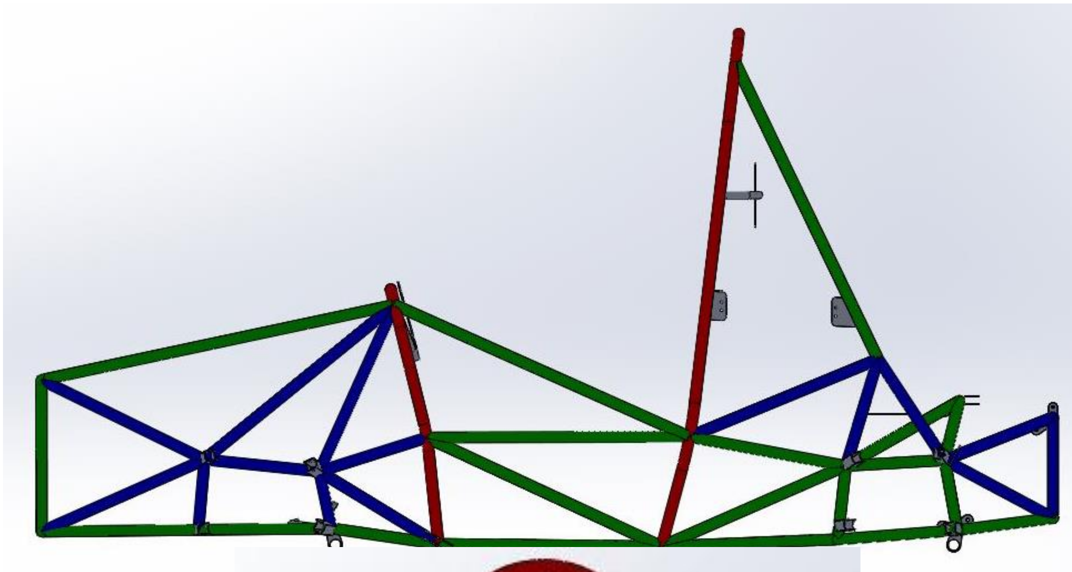

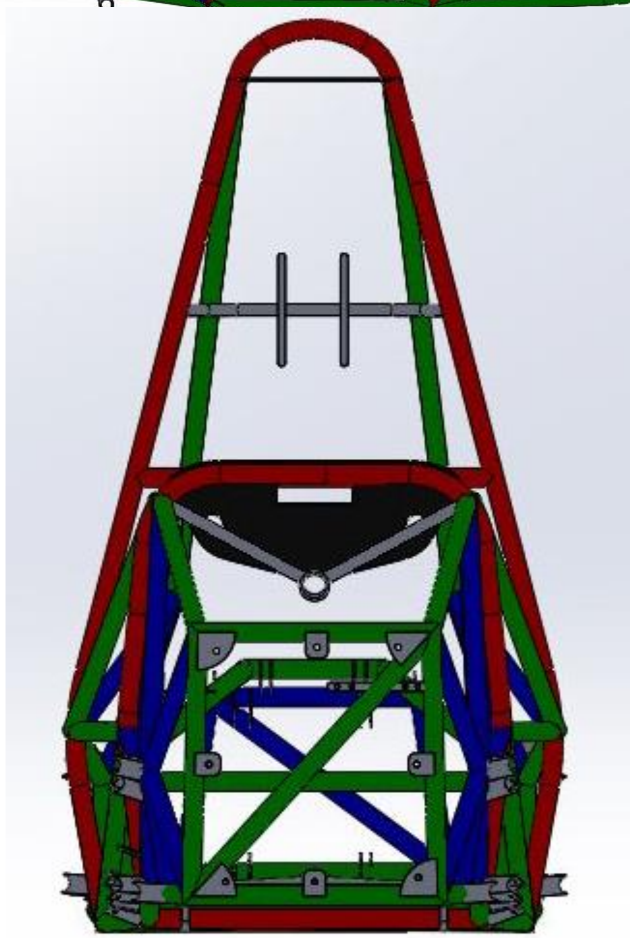

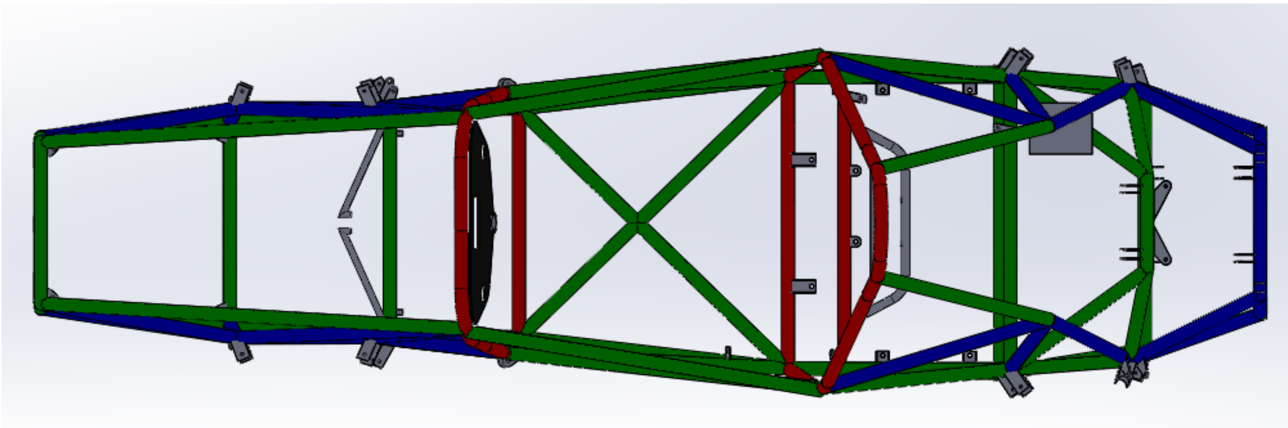

Different views of Chassis

3.4.1.2 Objectives

- Easy Manufacturing, low cost, and material availability
- Light and Strong
- Reliable
- Satisfactory Torsional Stiffness
- Easy and efficient Battery Box Packaging
- Flexibility in Powertrain Selection
- Driver Ergonomics

3.4.2 Material Selection

When selecting materials, the most common factors considered are strength, cost, and weight. In order to design a competitive vehicle, it must be light and yet strong.

The material selected for the tubes of the space frame structure is a **German Standard ST52-3** mild steel equivalent to AISI 4130. Its mechanical properties fulfill the baseline material property requirements.

Properties:
Young's Modulus (E) = 200 GPa (29,000 ksi)
Yield Strength (Sy) = 355 MPa
Ultimate Strength (Su) = 490 MPa

Bending and buckling strength requirements:
Young's Modulus (E) = 200 GPa (29,000 ksi)
Yield Strength(Sy) = 305 MPa (44.2 ksp)
Ultimate Strength(Su)= 365 Mpa (52.9 ksi)
Further, the material is lighter with a mass density of 7700 kg/m^3. We chose the material because it meets all the material strength requirements, is cheaper, easily available and manufacturable.

3.4.3 Engineering Design and Analysis

3.4.3.1 Design Process

To begin the Designing part, we first developed a rough chassis design and modified it gradually, complying with all the specified rules and minimum dimension requirements in the Rule-book.
The chassis is designed to ensure flexibility in powertrain configuration and to loosen the battery box packaging.
For a comfortable and effective design, we also had to consider Driver Ergonomics. So, we constructed a wooden model and took data of driving position, for persons of different height, size, and weight. This ensured the proper arm and steering position. This test allowed us to choose front packaging dimensions which increased driver comfort with less fatigue. Eventually, we come up with a Satisfying design. The chassis is modeled and designed using the software **SOLIDWORKS 2018**.

3.4.3.2 Finite Element Analysis

For analysis purposes, our team uses the simulation package of ANSYS.
From the initial design of chassis in Solidworks, some preprocessing requirement was there, to convert it to the wire-frame model (making it convenient for simulations). The thickness of tubes assigned as per the design and 1D meshing applied on the whole beam model for gaining advantages in time and better results too. The boundary conditions were calculated from various static and extreme dynamic loading conditions on the car and considering various deformation

modes. Post-processing and evaluations of results with improvement in design considering weight, strength, and desired stiffness was the iterative process.

3.4.4 Static Structural (FEM)Analysis

For the optimization of the Chassis Design, we simulated the various static and dynamic loading conditions on ANSYS to which the chassis will be subjected while riding the car. The main deformation modes for an automotive chassis are:

1. Longitudinal Torsion
2. Vertical Bending
3. Lateral Bending
4. Horizontal Lozenging

But out of these four, the worst deformation mode is Longitudinal torsion. So, it is considered that if the chassis withstands the Longitudinal torsion or have Satisfactory torsional stiffness then it can withstand the other loads as well.

3.4.4.1 Longitudinal Torsion:

For demonstrating the structural integrity of the chassis, a torsional load was applied on the front control arms, while the fixed area was the rear control arms mounting positions. A positive static load applied on one side of the chassis and negative on the opposite side, which translates to torsion. This analysis was found to be the most critical since it defined the reaction of every member throughout the chassis in cornering, which is vital in any racing that incorporates turning or extremely high torques on the chassis.

3.4.5 ANSYS Simulation

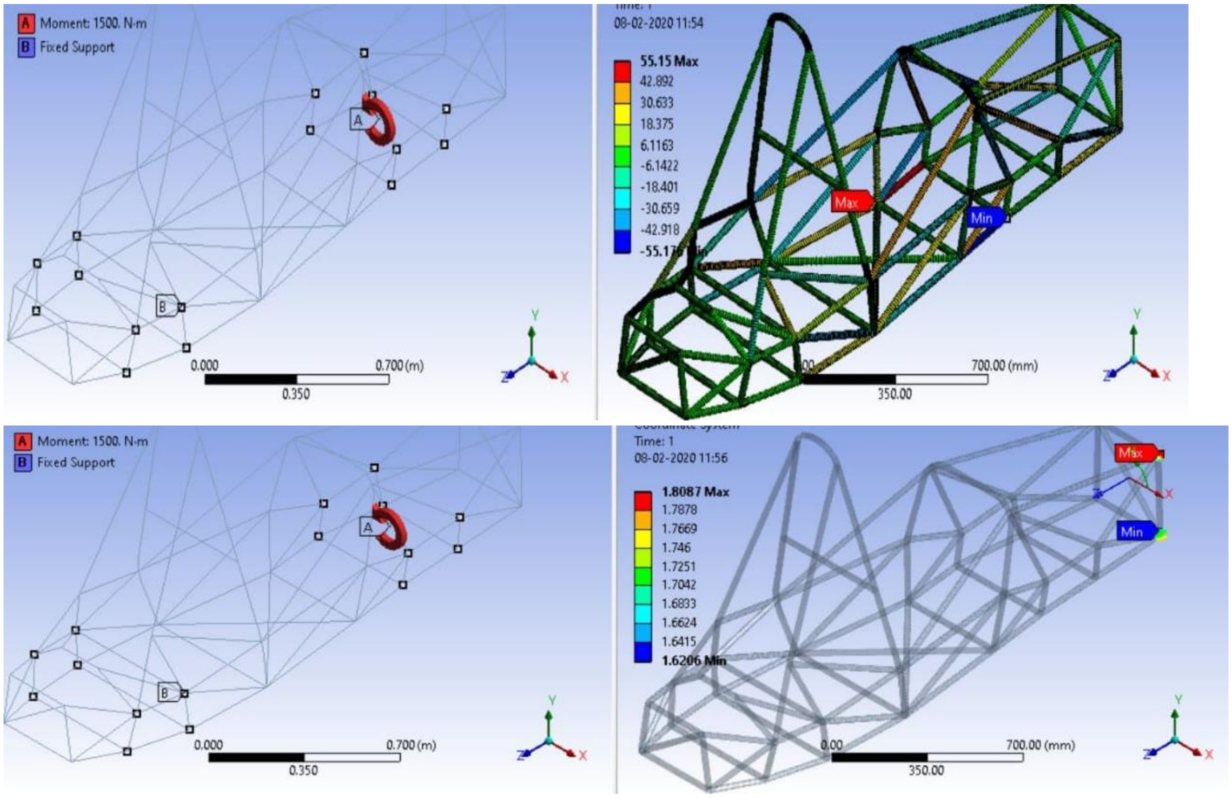

Torsion Analysis

Boundary Conditions: Fixed rotation (x, y, z) and displacement (x, y, z) at the four nodes/mounting points of control A-Arms on both the sides of rear suspension bay.

Maximum Deflection(degree): 0.65

In a similar manner, we calculated torsional stiffness using different moments on the structures i.e. we modified the boundary conditions to attain different results.

3.4.5.2 Calculations

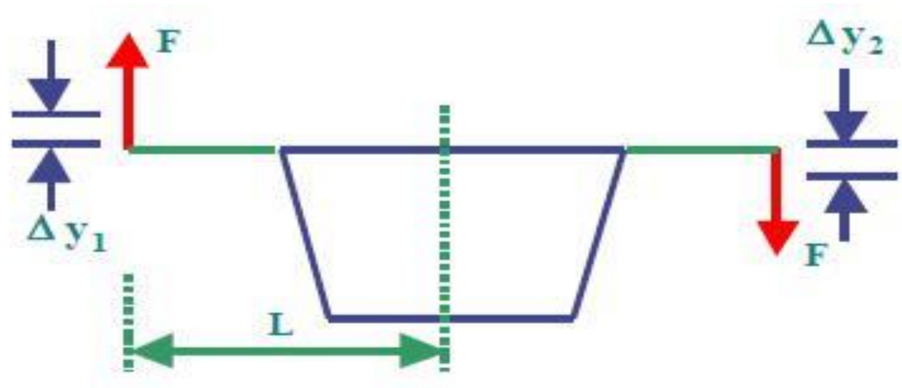

Torsional Stiffness = (F*2L)/tan^{-1}((y1+y2)/2L)
(or)
Couple Applied/ Angle of Rotation (N-m/deg.)

Calculation of Rolling Stiffness of the Chassis						
Moment Applied (N-m)	**δ1 (m)**	**δ2 (m)**	**δavg (m)**	**θavg (rad)**	**θavg (deg)**	**Stiffness (k)**
500	0.00060289	0.0006034	0.00060313	0.003780194	0.216589362	2308.515966
1000	0.0012058	0.0012067	0.00120625	0.007560326	0.433175133	2308.535104
1500	0.0018087	0.0018101	0.0018094	0.011340646	0.649771677	2308.503208
2000	0.0024115	0.0024135	0.0024125	0.015120652	0.866350265	2308.535104
2500	0.0030144	0.0030169	0.00301565	0.018900971	1.082946809	2308.515966
3000	0.0036173	0.0036202	0.00361875	0.022680978	1.299525398	2308.535104
4000	0.0048231	0.004827	0.00482505	0.030241617	1.732718486	2308.511182
5000	0.0060289	0.0060337	0.0060313	0.037801943	2.165893619	2308.515966

Final Torsional Stiffness(average) = 2308 N
Final Specific Torsional Stiffness = 2308/Wt. Of Chassis(Kg) = 2308/36.8 = 62.72 N-m/deg-kg

3.4.6 Alternative Loading Conditions

3.4.6.1 Side Impact

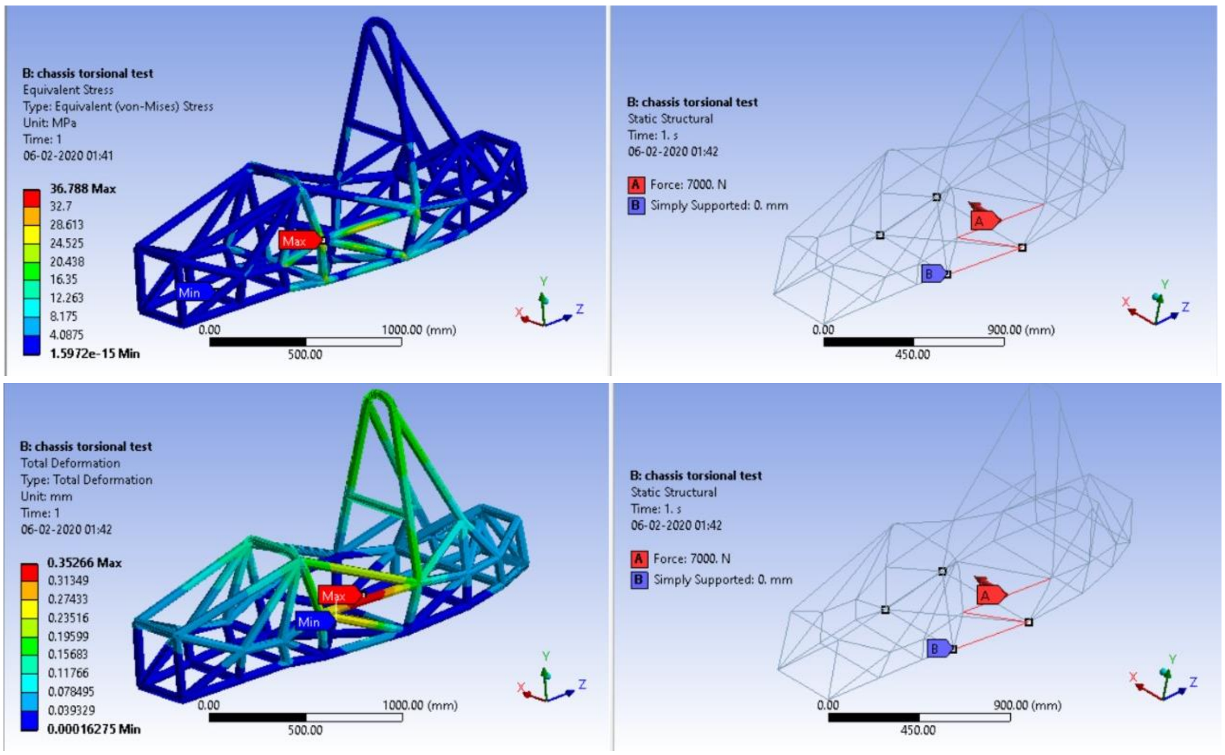

Side Impact Analysis

Load Applied: Fx= 7 kN, Fy= 0 kN, Fz=0 kN
Application point: All structural locations between front roll hoop and main roll hoop. So, the load is applied uniformly on the three tubes of the side impact structure.
Boundary Condition: Fixed displacement (x, y, z) but not the rotation of the bottom nodes of both sides of the front and main roll hoops.
Maximum Deflection:
Allowable - 25mm
By Analysis - 0.35mm

3.4.6.3 Main Roll Hoop

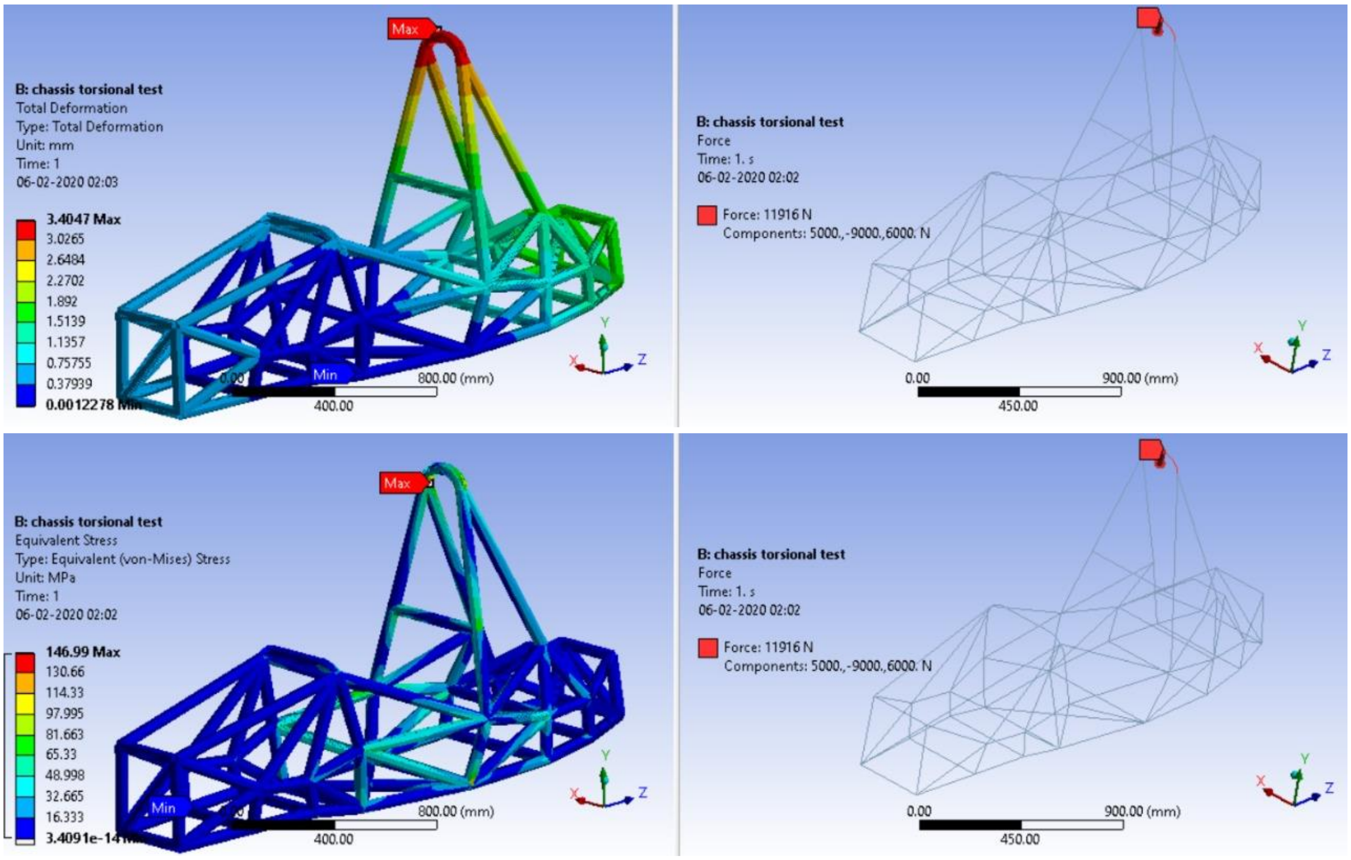

Main Hoop Analysis

Load Applied: Fx =5000 N Fy= -9000 N Fz= 6000 N
Application point: Topmost point of the main roll hoop
Boundary Condition: Fixed displacement (x, y, z) but not the rotation of the bottom nodes of both sides of the front and main roll hoops.
Maximum Deflection: Allowable--- 25mm
By Analysis ---- 3.4 mm

3.4.6.4 Front Roll Hoop

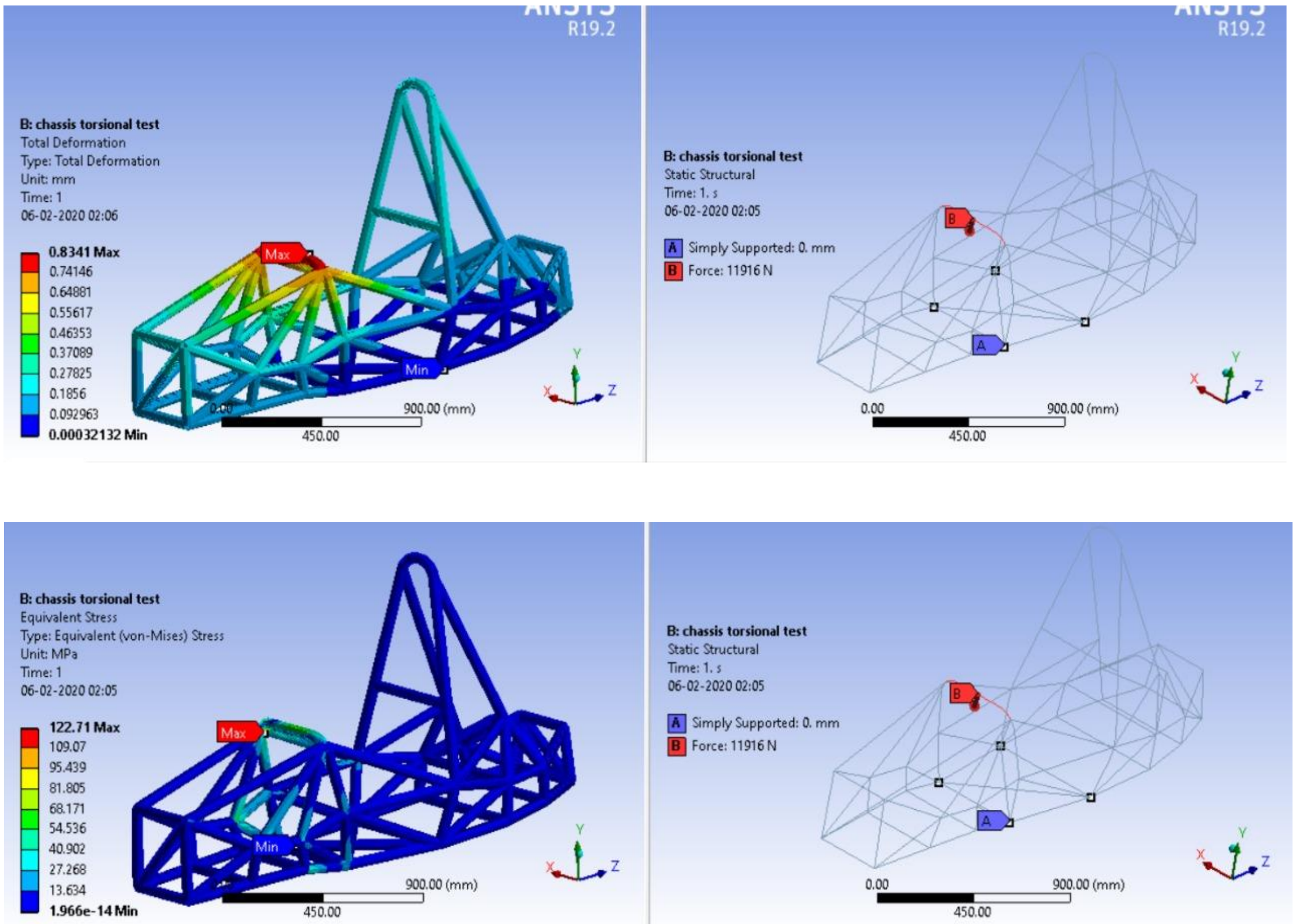

Front Roll Hoop Analysis

Load Applied: Fx =5000 N, Fy= -9000 N, Fz= 6000 N
Application point: Top of the front Roll Hoop
Boundary Condition: Fixed displacement (x, y, z) but not the rotation of the bottom nodes of both sides of the front and main roll hoops.
Maximum Deflection: Allowable--- 25mm
By Analysis ---- 0.83 mm

3.4.6.5 Front Bulkhead and Bulkhead Support:

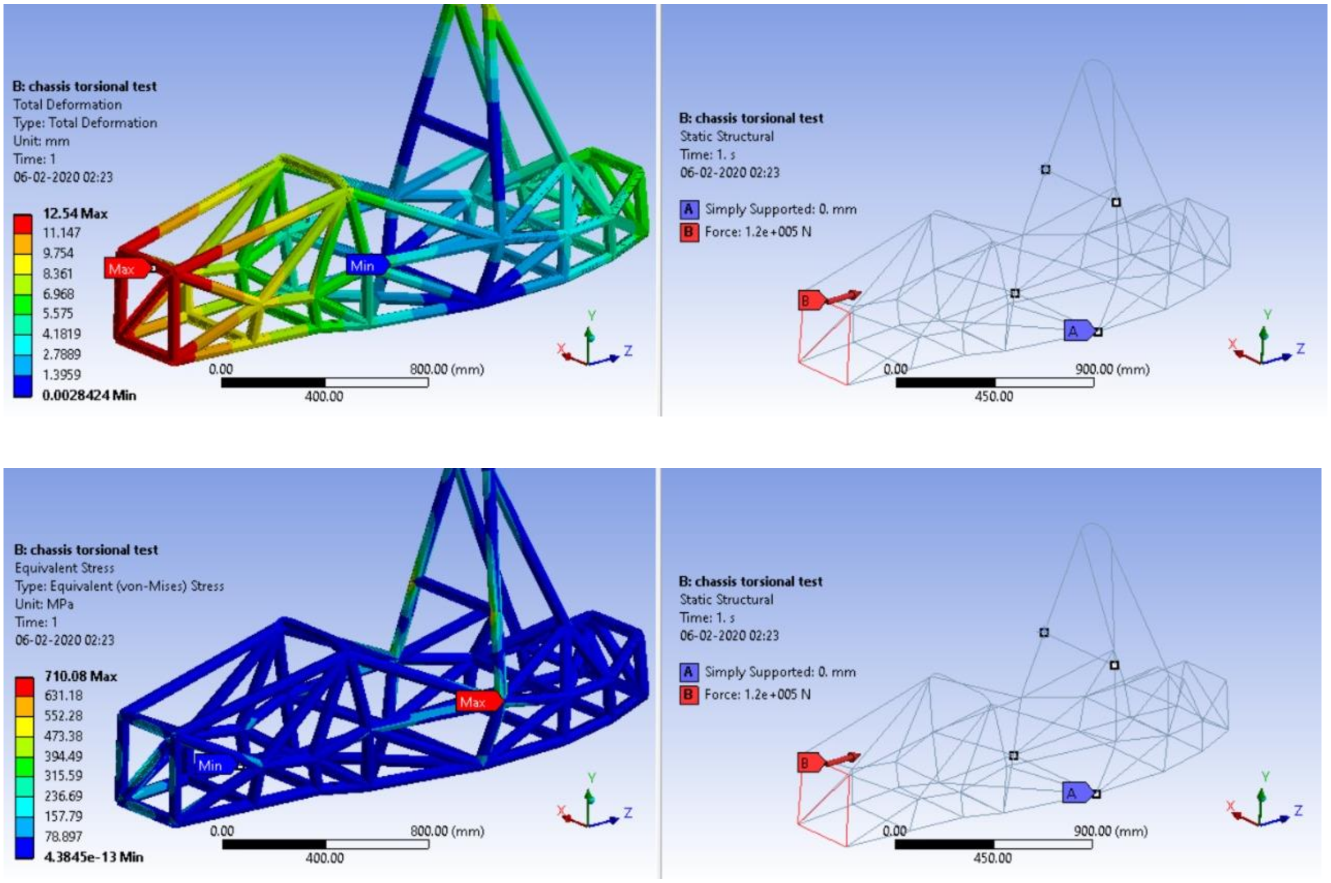

Front Bulkhead & its Support Analysis

Load Applied: Fx =0 kN Fy= 0 kN Fz=120 kN

Application point: Uniformly distributed load on the four tubes of Front Bulkhead (Attachment of Impact Attenuator to the Bulkhead)

Boundary Condition: Fixed displacement (x, y, z) but not the rotation of the bottom nodes of both sides of the main roll hoop and both locations where the main hoop and shoulder harness tube connect.

Maximum Deflection: Allowable--- 25mm

By Analysis ---- 12.54 mm

3.4.6.6 Front Bulkhead and Bulkhead support off-axis:

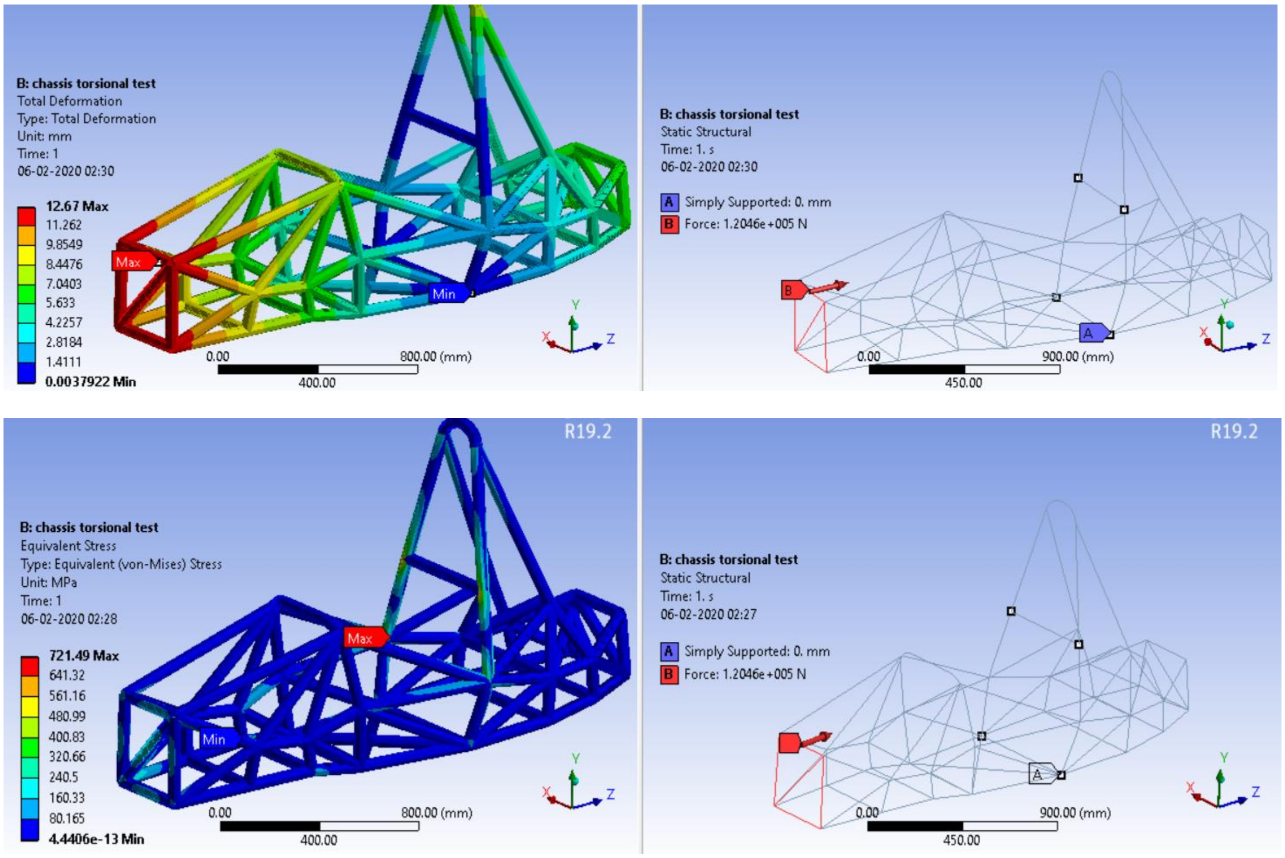

Front Bulkhead and Support Analysis

Load Applied: Fx =10.5 kN Fy= 0 kN Fz= 120 kN

Application point: Uniformly distributed load on the four tubes of Front Bulkhead (Attachment of Impact Attenuator to the Bulkhead)

Boundary Condition: Fixed displacement (x, y, z) but not the rotation of the bottom nodes of both sides of the main roll hoop and both locations where the main hoop and shoulder harness tube connect.

Maximum Deflection: Allowable--- 25mm

By Analysis ----12.67mm

3.4.6.7 Accumulator Container:

The Accumulator container is made by AISI 1020 Steel plates to form a rigid and sturdy structure that can sustain all strength constraints of the rule book. The sole reason for the material selection is availability. Further, it has 8 compartments that contain battery modules made up of ABS, supported by a glass fiber sheet and covered by a polycarbonate sheet.

It was designed on SOLIDWORKS with simulation package of ANSYS was used.
The rulebook constraints for the strengths (along with simulation reports) are:

A) 40g in the lateral left/right

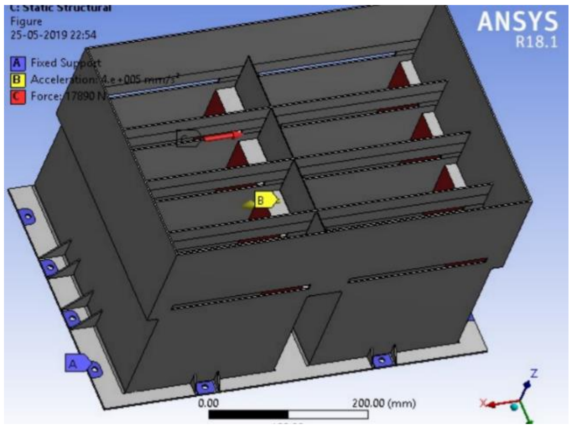

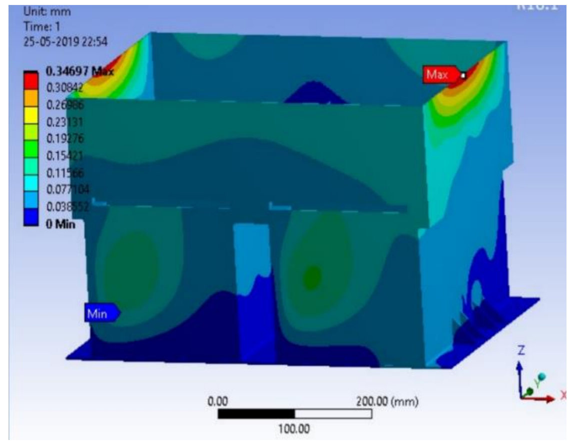

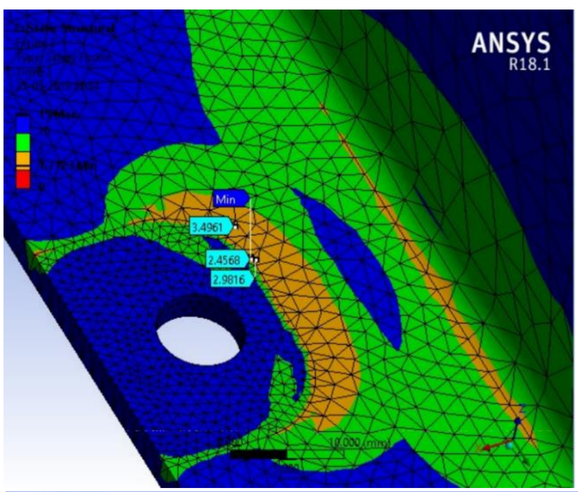

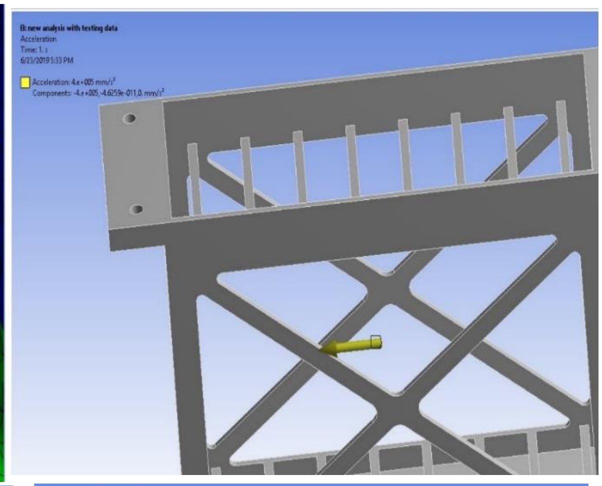

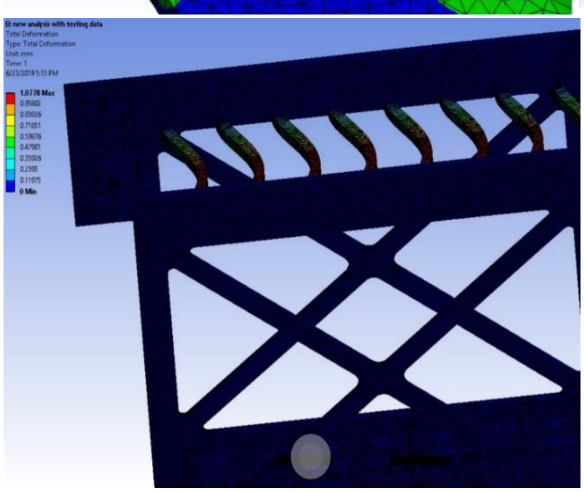

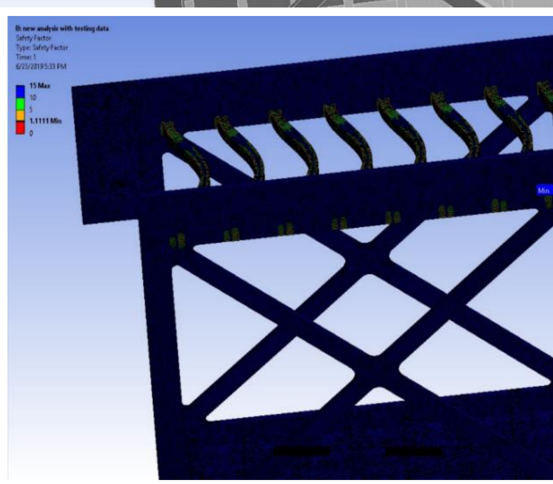

Accumulator Container and Module Analysis

Load Applied: 40g acceleration in the lateral left/right direction in total

Application Point: The surfaces which are normal to the lateral direction

Boundary Conditions: Fixed rotation (x, y, z) and displacement (x, y, z) of all the accumulator attachment/mounting points.

FOS= 1.7121 for steel container

1.1111 for ABS module

B) 40 g in the longitudinal direction(forward/rear):

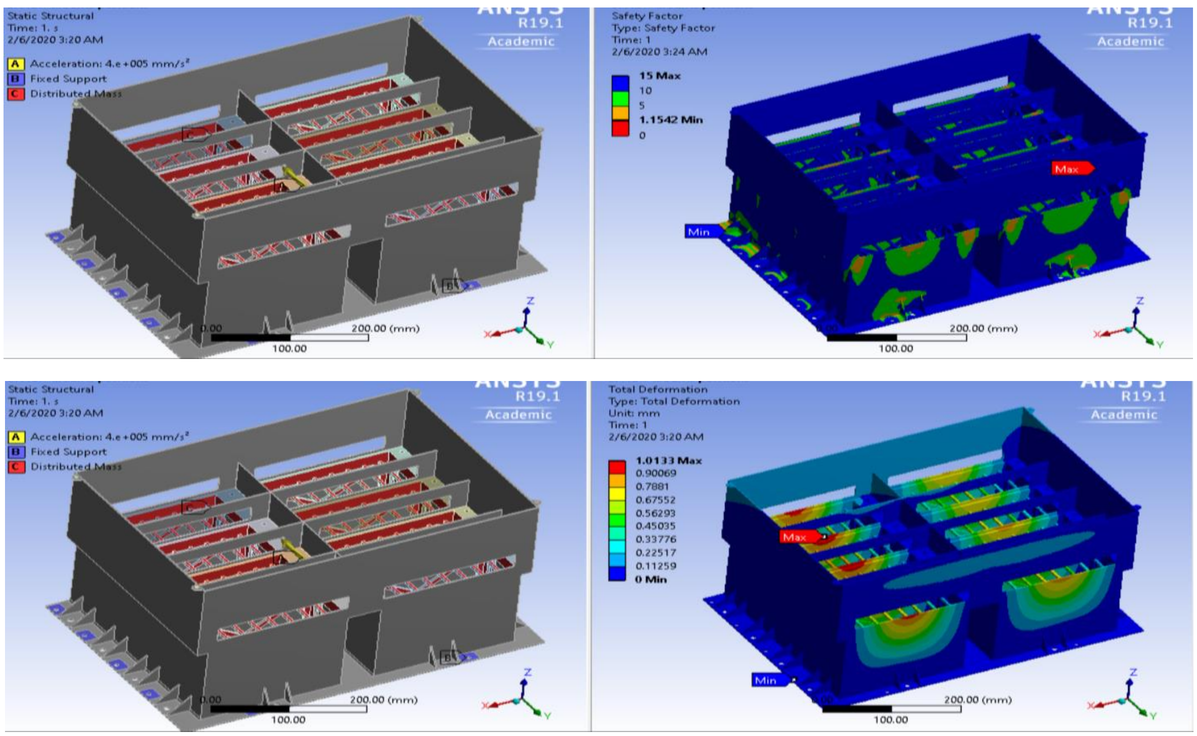

Accumulator Container and Module Analysis

Load Applied: 40g acceleration in the longitudinal backward/forward direction in total

Application Point: The surfaces which are normal to the longitudinal direction

Boundary Conditions: Fixed rotation (x, y, z) and displacement (x, y, z) of all the accumulator attachment/mounting points.

FOS= 1.1542 (overall)

3.5 Braking

3.5.1 Introduction

The braking system was designed as a hydraulic system for a one-man performance racing vehicle. Generic parameters of the vehicle that were used in the system design were a total vehicle weight, including the driver, of 350kg and a maximum velocity of 136km/h. Further details of parameters will be defined in the report corresponding to the braking system.

The three main categories/ components designed and analyzed for this system are the following: calculation and evaluation of the hydraulic system in order to select calipers and master cylinders, the design of the pedal box and the design of the rotors. For the first component, the overall functionality and free variables of the braking system will be analyzed for optimum caliper, master cylinder, and rotor size selection. The second main component of the design encompasses the pedal box design. This design includes the acceleration pedal, brake pedal, and master cylinder orientation as well as the Brake over Travel Switch (BOTS) placement and orientation. The third and final main component involves the design of the rotors. The main focus on the design of the rotors was material selection as well as the geometry of the rotors.

The constraints and limitations based on the competition rules of these components will be defined later in each of their sections. The objective of these major component designs was to minimize the weight for the lightest design possible while at the same time designing to all of the mechanical and thermal conditions that the system would be subjected to. In the pedal box and rotor design sections, the optimization processes will be discussed as well as the finite element analysis that supports the final design. In the final sections of the report, the manufacturing of the pedal box and rotors will be discussed.

3.5.2 Braking System Theory, Calculation & Design

3.5.2.1 Design Objective & Overview

The main objective of the braking system is to convert the kinetic energy of the vehicle into thermal energy, thus allowing the vehicle to decelerate. The braking system was designed as a hydraulic system with two master cylinders, one for the braking of the front two tires and one for braking of the rear two tires. Attached to each master cylinder are two fixed calipers, one located at each of the wheels for a total of four calipers for the system, as well as four rotors (brake discs). The flow of the braking system is as follows: the driver exerts a force on the brake pedal, the brake pedal channels that force to the master cylinders, thus displacing the braking fluid in the master cylinders. The displaced fluid then exerts pressure on each of the calipers allowing the caliper pistons to exert a clamping force on the rotors. Therefore, the input of the system is the driver’s applied foot force and the output is the clamping force of the calipers exerted on the rotors. Based on the competition rules and conditions the designed braking system must be able to lock all four wheels of the vehicle completely during an emergency stop braking scenario. What this translates to physically is that the moment generated from the caliper force placed on the rotor must be equal to or greater than the moment the tire exerts on the surface of the road. Therefore, for this braking hydraulic system design, the main objective is to design the system so that the driver has to place a substantial, but not excessive force on the brake pedal in order to completely lock the tires of the vehicle. The system was designed for this foot force to approximately be 2000 N.

3.5.2.2 Calculations

3.5.2.2.1 Boundary Conditions

Deceleration is the measure of how rapidly a vehicle slows down. The maximum achievable velocity of the car is limited to 136km/h. Although observed competition speeds are considerably lower, this value is taken as the worst possible condition during hard braking since energy dissipation is a function of velocity squared (E = 1⁄2mv2).

Deceleration (and acceleration) is measured in units of gravity or "G's". So, we fixed the maximum deceleration value to be 1.5G.

3.5.2.2.2 Longitudinal Weight Transfer

The center of gravity (CG) is a point on an object where all its mass is concentrated and it is completely balanced. The CG also serves as a location where the combination of all inertial forces summed into a focused single inertial force. CG is located closer to the rear wheels to the battery pack and motor, more weight of the car is distributed to the rear wheels while the car is static. Under deceleration forces due to rotational inertia tend to load the front tires and lift the rears (i.e. car rotates about the CG) as the CG is located above the ground (tire contact patch) [2]. The actual weight of the car does not change, rather the amount of load witness by the front and rear tires varies with dynamic conditions.

Longitudinal load transfer = (acceleration (g) * weight *cg height * acceleration (g)) /
(Wheelbase (m) * reference Carroll smith tune to win)

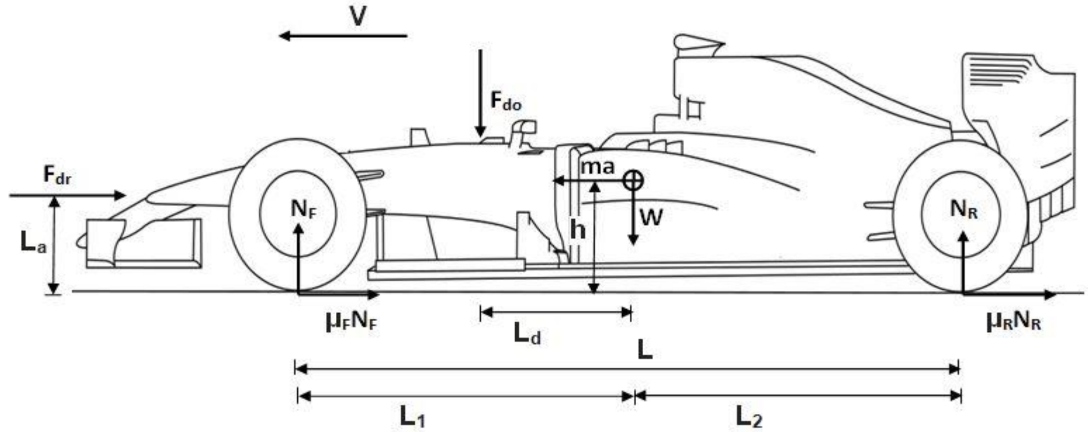

Fig. Forces acting on the car while braking

On balancing the moment of all the forces acting on the car, the following equations will be obtained.

$N_R L + \mu_F N_F h + \mu_R N_R h + F_{dr} h - F_{do}(L_1 - L_d) – F_{dr} L_a - W L_1 = 0$

$N_F L - \mu_F N_F h - \mu_R N_R h - F_{dr} h - F_{do}(L_2 + L_d) + F_{dr} L_a - W L_2 = 0$

$N_F + N_R = W + F_{do}$

Where,

W = Weight of the car

N_F = Total reaction force on front wheels

N_R= Total reaction force on rear wheels

F_{do}= Total Aerodynamic downforce acting on the car

F_{dry}= Total Aerodynamic drag force acting on the car

L = Wheelbase of the car

L_1 = Distance of front wheel from the center of mass of the car

L_2= Distance of rear wheel from the center of mass of the car

L_a = Distance between center of force of total drag force from the ground

L_d= Distance between center of force of total downforce from the center of mass

H = Height of the center of mass from the ground

μ_F, μ_R = Coefficient of friction for the front wheel and the rear wheel respectively

On solving the above equations, N_R and N_F can be obtained.

$$N_R = \frac{F_{do}\left(L_1 - L_d - \mu_F h\right) - F_{dr}\left(h - L_a\right) + W\left(L_1 - \mu_F h\right)}{\left(L + \mu_R h - \mu_F h\right)}$$

$$N_F = \frac{F_{do}\left(L_2 + L_d + \mu_R h\right) + F_{dr}\left(h - L_a\right) + W\left(L_2 + \mu_R h\right)}{\left(L + \mu_R h - \mu_F h\right)}$$

Aerodynamic downforce and drag force can be written as a function of velocity 'V' of the car as follows.

F_{do}= 0.876 V^2
F_{dr} = 0.578 V^2
L_1 = 821.45mm
L_2= 728.55mm
L_a = 534.43mm
L_d= 185.28mm
h = 250mm
μ_F= μ_R = 2

Putting all these values N_F and N_R can be obtained as a function of velocity (V).

N_F = 0.693 V^2 + 2251.613
N_R = 0.183 V^2 + 590.387

A. Solving to obtain velocity as a function of time

We know that

$$-m\frac{dV}{dt} = \mu\left(N_F + N_R\right) + F_{dr} = \mu\left(W + F_{do}\right) + F_{dr}$$

Putting all the values

$$-m\frac{dV}{dt} = 2\left(2842+0.876V^2\right)+0.578V^2$$

$$-290\frac{dV}{dt}=5684+2.33V^2$$

$$-290\int_{V_0}^{V'}\frac{1}{5684+2.33V^2}dv = \int_0^{t'}dt$$

$$\frac{124.46}{49.3913}\left[\tan^{-1}\frac{V}{49.3913}\right]_{V_0}^{V'} = t'$$

$$-2.52\left[\tan^{-1}\frac{V'}{49.3913}-\tan^{-1}\frac{V_0}{49.3913}\right]=t'$$

$$-2.52\left[\tan^{-1}0-\tan^{-1}\frac{V_0}{49.3913}\right]=t'$$

$$t' = 2.52\left[\tan^{-1}\frac{V_0}{49.3913}\right]$$

$$t' = 2.52\left[\tan^{-1}\frac{20}{49.3913}\right]$$

$$t' = 0.96956\ Seconds$$

If the initial velocity of the car is 20 m/sec then braking time can be calculated to be 0.96956 seconds.

Balancing the torque acting in the front and rear axle

$$I_{Front}\frac{d\omega}{dt} = -\left(T_{BF} - \mu N_F R_T\right)$$

$$I_{Rear}\frac{d\omega}{dt} = -\left(T_{BR} - \mu N_R R_T\right)$$

Where,

I_{Front}= Mass moment of inertia of all the rotating mass in the front axle

y_{ear}= Mass moment of inertia of all the rotating mass in the rear axle

T_{BF}= Applied braking torque on the front axle

T_{BR}= Applied braking torque on the rear axle

R_T= Rolling radius of the tire

It is better to have similar angular deceleration on front wheels and rear wheels

$$-\left(T_{BR} - \mu N_R R_T\right) I_{Front} = -\left(T_{BF} - \mu N_F R_T\right) I_{Rear}$$

For initial velocity of 20 m/sec, velocity as a function of time can be written as

$$For\ V_0 = 20\ {}^{m}/_{sec}$$

$$V' = 49.3913 \tan(0.38475 - 0.3968\, t')$$

B. Calculation of braking distance

Braking distance can be calculated by integrating velocity from t=0 to t=0.9695 sec

$$\frac{dx}{dt} = v' = 49.3913 \tan(0.38475 - 0.3968t)$$

$$x = \int_0^{0.9695} 49.3913 \tan(0.38475 - 0.3968t)\, dt$$

$$x = 9.4477\ m\ (for\ intial\ velocity\ of\ 20\ m\ and\ \mu = 2)$$

Maximum braking torque will be required at t = 0 i.e. at V = 20 m/sec

$$Required\ braking\ torque\ on\ front\ axle = ground - wheel\ frictional\ torque\ at\ t=0$$

$$T_{BF} = \frac{\mu N_{F\,(at\ V = 20\ m/sec)} R_T}{2}$$

$$T_{BF} = \frac{2 \times 2528.813 \times 0.3}{2}$$

$$T_{BF} = 758.6439\ Nm$$

C. Solving to obtain angular velocity as a function of time

Initial angular speed ωi= V0/R Where R = radius of the tire

$$I_{Front} = 0.35067\ kg \times m^2$$

$$\frac{0.35067}{2}\frac{d\omega}{dt} = 0.208V^2 - 85.2451$$

$$\frac{0.35067}{2}\frac{d\omega}{dt} = 0.208(49.3913\tan(0.38475 - 0.3968\,t))^2 - 85.2451$$

$$0.17535\,(\omega_f - \omega_i) = \left[0.208 \times 49.3913^2 \times \int_0^{t'} \left(Sec^2(0.38475 - 0.3968t) - 1\right) dt\right] - 85.2451 \int_0^{t'} dt$$

$$-1278.77\left[\tan(0.38475 - 0.3968t') - \tan(0.38475)\right] - 592.6612t' = 0.17535\,(\omega_f - \omega_i)$$

$$putting\ \omega_f = 0\ and\ \omega_i = \frac{20}{0.25} = 80\ rad/sec$$

$$-1278.77\tan(0.38475 - 0.3968t') - 592.6612t' = -531.84$$

on solving

$$t' = 0.4135\ Sec$$

This is the time period after which the wheel’s angular speed will become zero, after this time the wheels will only slip.

D. Master Cylinder

Selection of master cylinder diameter (front)

$$T_{BF} = \frac{\mu N_F R_T}{2}$$

$$F \times \frac{P_r}{2} \times \frac{1}{d_m^2} \times d_p^2 \times \mu_P \times R_F \times 2 = 2528.813 \times 0.3$$

$$F = 550\,N,\ P_r = 4,\ d_P = 1.75\ inch,\ \mu_P = 0.45,\ R_F = 0.1\ m$$

$$d_m = 0.64\ inch$$

Selection of master cylinder diameter (rear)

$$T_{BR} = \frac{\mu N_R R_T}{2}$$

$$F \times \frac{P_r}{2} \times \frac{1}{d_m^2} \times d_p^2 \times \mu_P \times R_R \times 2 = 663.587 \times 0.3$$

$$R_R = 0.1\ m$$

$$d_m = 1.25\ inch$$

Where,

F = Force applied on the pedal
Dm = Diameter of the master cylinder
D_P= Diameter of the piston of the caliper
P_r = Pedal ratio
μ_P= Coefficient of friction between brake pads and brake disc
R_F, R_R= Radius of the front and rear wheel's brake discs

$$\frac{I_{Front}}{I_{Rear}} = \frac{\left(T_{BF} - \mu N_F R_T\right)}{T_{BR} - \mu N_R R_T}$$

$$I_{Front} = 0.35067\ kg \times m^2,\ I_{Rear} = 0.37837\ kg \times m^2$$

$$0.926791 = \frac{\left(T_{BF} - \mu N_F R_T\right)}{\left(T_{BR} - \mu N_R R_T\right)}$$

$$0.926791 = \frac{85.2481 - 0.2079V^2}{21.96 - 0.0549V^2}$$

$$0.15701\ V^2 = 64.895769$$

$$V^2 = 413.322$$

$$V = 20.33\ \frac{m}{sec}$$

3.5.3 Master cylinder selection

Based on the above calculation, master cylinders with bore diameter 0.64" for front and 1.25" for rear needs to be selected. After researching on the internet and narrowing down to a handful, **Wilwood push-type** master cylinders with a 0.625" bore diameter (for front) and 1.125" bore diameter (for rear) were selected.

Wilwood Compact Remote Flange Mount Master Cylinder
FRONT: single outlet; bore diameter 0.625in; area 0.310in^2
REAR: single outlet; bore diameter 1.125in; area 0.97in^2

3.5.4 Brake Caliper selection

At this stage of the design, it was necessary to select a caliper and brake pad. The number of Pistons in the caliper and the coefficient of friction of the brake pads were the free variables for these selections. After researching the internet possible caliper choices and drafting a caliper selection matrix (see below) based on a number of pistons, weight, size, and cost, the ***Wilwood DynaPro Single***-caliper was selected.

Company/ Model Name	Piston Diameter (mm) /material	Weight	Disc thickness range(mm)	Cost $	No. of Pistons	Picture
ISR-22027	34 mm /Tufram coated aluminium alloy	0.53 kg	4.5-6 mm	234.89	2	
ISR-22028	34 mm /Tufram coated aluminium alloy	0.53 kg	4.5-6 mm	238.59	2	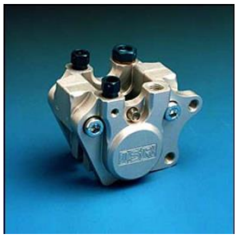
ISR-22048	25 mm /Tufram coated aluminium alloy	0.46 kg	4.6-5 mm	476.94	4	
ISR-22049	25 mm /Tufram coated aluminium alloy	0.29 kg	4.6-5 mm	262.01	2	

AP racing CP4227-2S0	25.4 mm	0.50 kg	4.0 mm	484.83	4	
AP racing CP4226-2S0	25.4 mm	0.24 kg	4.0 mm	277	2	
AP racing CP7003-2S0	25.4 mm	0.25 kg	4.0 mm	209.64	2	
Wilwood PS-1	28.5 mm /stainless steel	0.50 kg	3.8-5.0 mm	91.74	2	
Wilwood GP-200	31.78 mm /stainless steel	0.408	4.83-6.35 mm	104.93	2	
Wilwood Dynalite single	44.4 mm /stainless steel	0.816 kg	9.65 mm	115	2	

Wilwood Dynalite Single IIIA	44.4 mm /stainless steel	0.907 kg	4.57-6.35 mm	88	2	
Wilwood Dynapro single 120-9689-LP	**44.4 mm/stainless steel**	**1.04 kg**	**3.81-5.08 mm**	**107**	**2**	
Wildwood GP 320 120-8524`	31.75 mm/	0.907 kg	4.57-6.1 mm	161.99	4	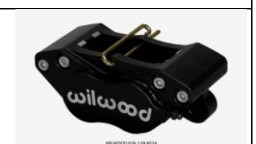
Wilwood GP 310 120-12116-BK	31.75 mm/ stainless steel	0.95 kg	4.57-6.35 mm	284.47	4	

3.5.4 Brake pad selection

After selecting a Wilwood caliper, a Wilwood brake pad was chosen that would fit the style and the size of the caliper Wilwood BP-20 brake pad was chosen for its overall high coefficient of friction. Based on the company's performance chart (see below) between temperatures of 100°F & 700°F the average coefficient of friction was approximated as 0.45.

COMPOUND: BP - 20

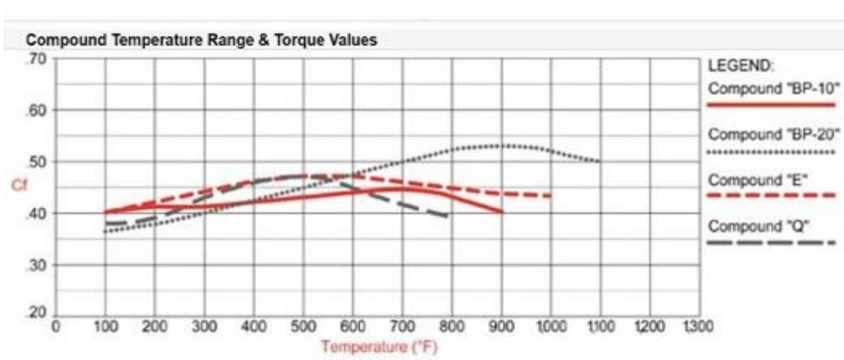

Fig. Wilwood Brake Pad Performance Graph

Temperature range and overall friction value are the primary considerations for pad selection. The pads must be capable of maintaining the proper amount of friction for stopping power within the temperatures that will be realized on the track during the event. Then, the overall wear rate must be considered. Many factors and unforeseen influences can affect brake temperatures. The best indicator for pad selection will always be on track performance. If pad fade (friction loss) due to overheating occurs, then improved cooling, a heavier rotor, or a higher temperature range pad may all become necessary.

3.5.5 Pedal box design

3.5.5.1 Design Criteria

The idea was to design a pedal box that could accommodate all of the essential components of braking, while also leaving enough clearance for the other elements of the car. After spending quite a lot of time tinkering with the stiffness, rigidity, and adjustability of the design; the team came up with the current design.

The following are the constraints of the pedal box design:

- The pedal box needed to be designed around the geometry constraints set in the results from the braking system calculations. That is the master cylinder mount height and the distance between the master cylinder pivot and the brake pedal are fixed.
- The length of both the acceleration and the brake pedal need to be approximately the length of a human foot (~ 9.5").
- The competition rules designate that the brake pedal must be able to withstand a force of 2000N.

Due to these constraints, the material selection of the brake pedal and the overall pedal box must be strong, stiff and have high toughness. The prime objective of the pedal box design was to satisfy all of the constraints mentioned above and optimize for minimal weight. The rest of the design encompassed mounting both pedals, mounting the master cylinders and mounting the Brake fluid reservoir and emergency stop switch to the pedal box. The pedal box was designed with a single base plate; that is, all of the mounts would be fixed to this single plate. The brake pedal and master cylinder mounts were designed to be symmetrical for ease of manufacturing and were short, approximately 1.5'' in height. The emergency stop mount needed to be positioned where, under the circumstance that there was a leak in the brake line and there was no longer substantial pressure in the line, the pedal would strike the switch at approximately 90% displacement of the master cylinders.

3.5.5.2 Material Selection

The material selection process of the pedal box was based around the initial constraints of the design mentioned prior, but more specifically, the component of the pedal box that would be subjected to the most stress, the brake pedal. Based on the type of loading the pedal box would be subjected to it was modeled as a beam in bending and was decided that the desired material needed to have the following mechanical properties:

- High Strength and be stiff
- Good toughness
- Machinability

From these constraints, it was decided that metals, composites and possibly some polymers would make optimal choices. Analysis of quite a few materials rendered the optimal choice was, based on the material properties that were most dependent on the functionality and taking cost into consideration; carbon steel, cast iron or an aluminum alloy. Out of the three, the aluminum alloys are the lightest, this material group was selected for the design. 6061 Aluminum was the final selection as the material choice of the pedal box and the material properties for 6061 Aluminum will be referred to in the upcoming discussions related to the pedal box design.

3.5.5.3 Initial Design

The initial design of the pedal box was drawn using the three-dimensional graphics software SolidWorks.

3.5.5.4 Optimization & Weight Reduction

Optimization of the pedal box was conducted using the finite element analysis simulations in Ansys. Each of the components was subjected to a specific force, based on application, and a minimum factor of safety of 1.0 was used as design criteria. The following is a breakdown of each component and the force that is was subjected to during simulation:

Brake Pedal: 2000 N

Accelerator Pedal: 1000 N

On all the other mounts in the pedal, assembly analysis is being done on forces transmitted by pedals. After running FEA on the individual components, sections of each component, where the least amount of stress occurred, were removed. This process resulted in many holes and skeletal cuts in most of the components. FEA was conducted again on these optimized components to verify each still passed the force criteria. This process was repeated until each component was reduced to its minimal mass and still passed the FEA simulations. The original components are shown below as well as the optimized final components:

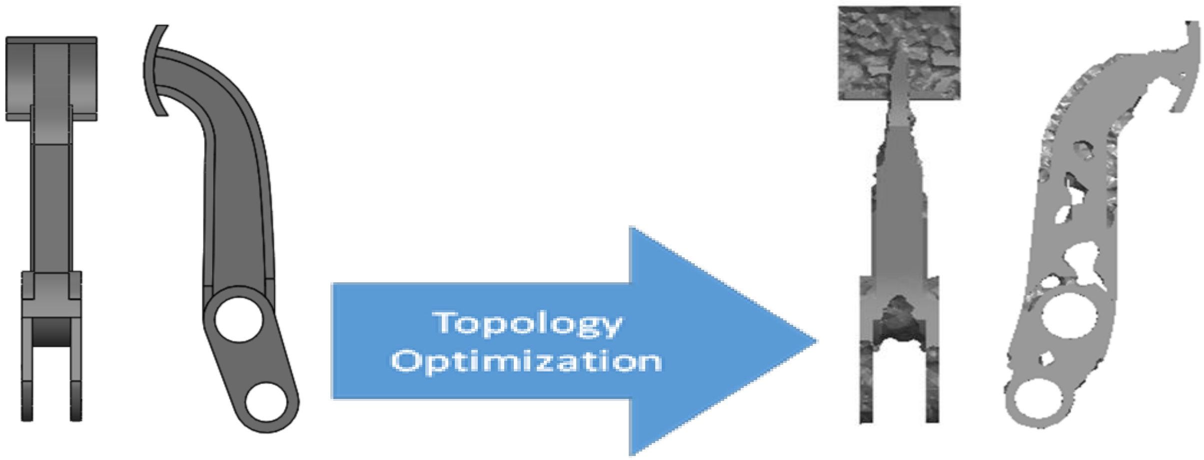

Initial Design

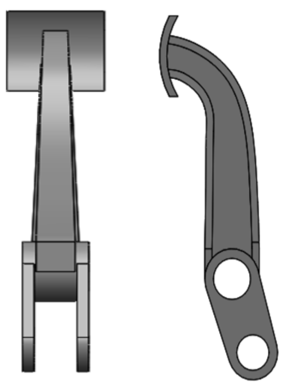

Final Design

Fig. Brake Pedal Design

3.5.5.5 FEA Analysis

3.5.5.5.1 Brake Pedal

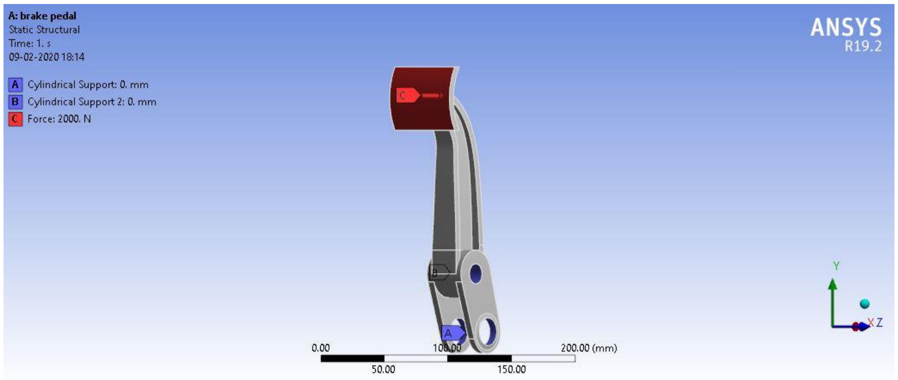

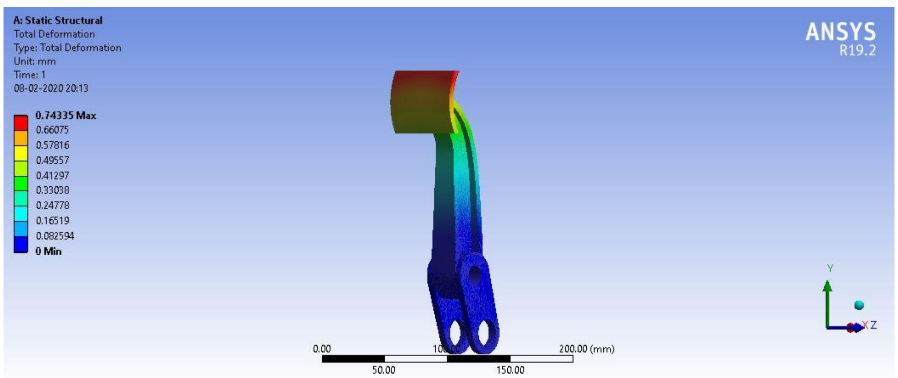

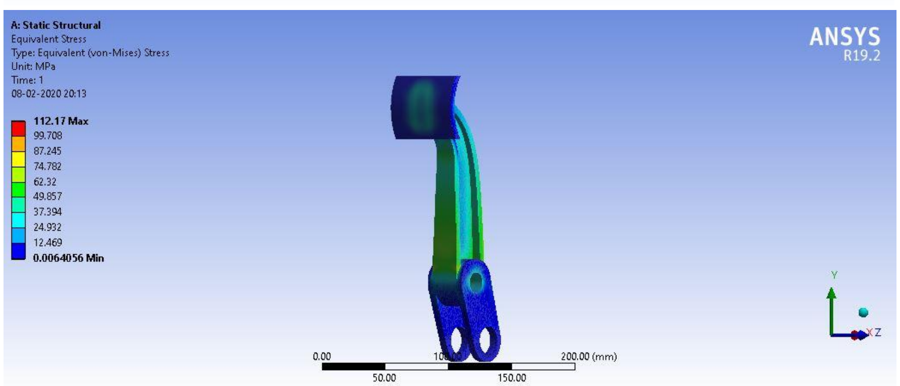

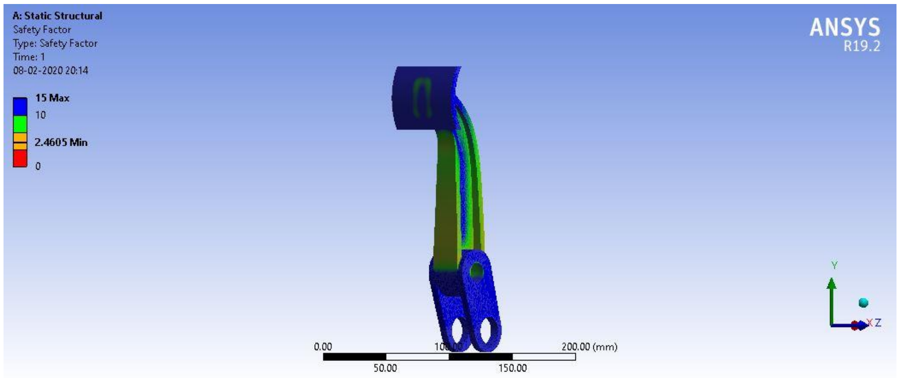

3.5.5.5.2 Accelerator Pedal

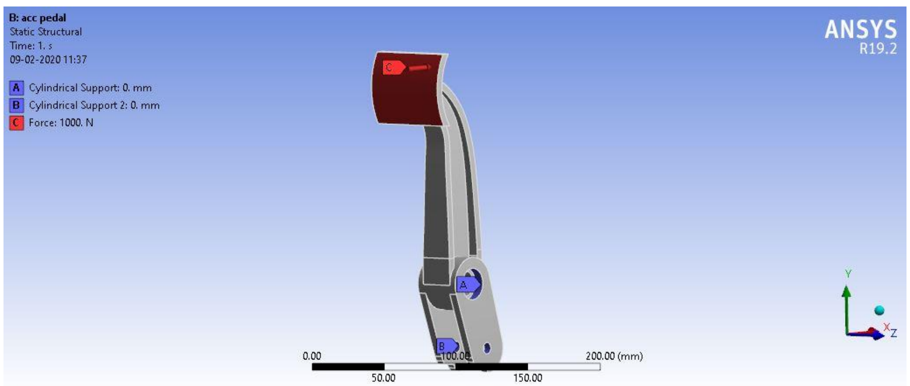

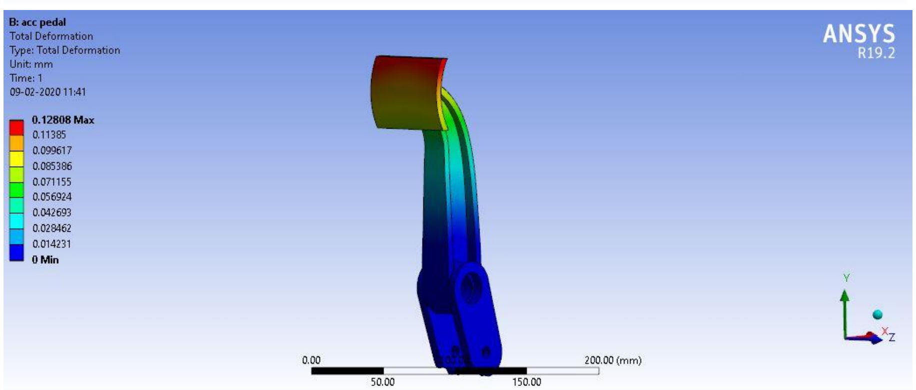

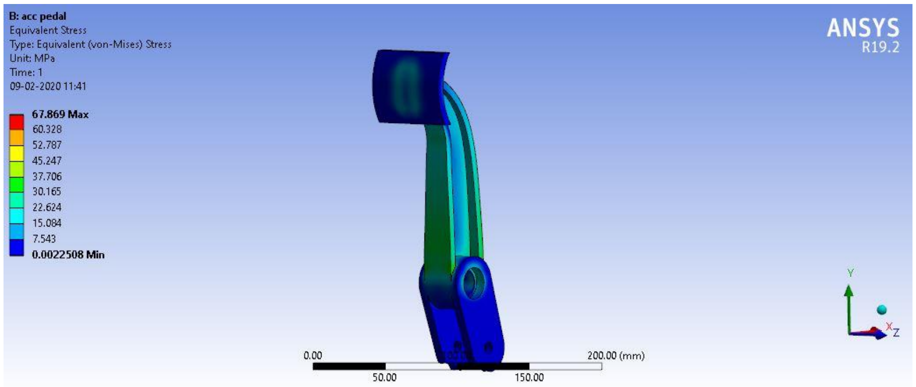

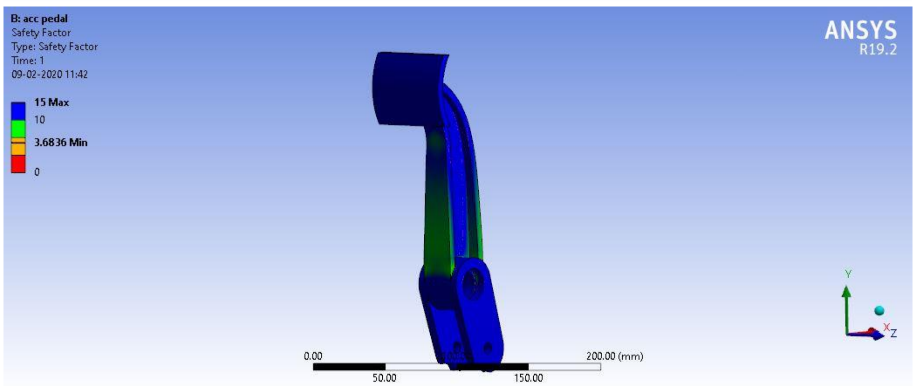

3.5.5.5.3 Brake pedal mount and base plate

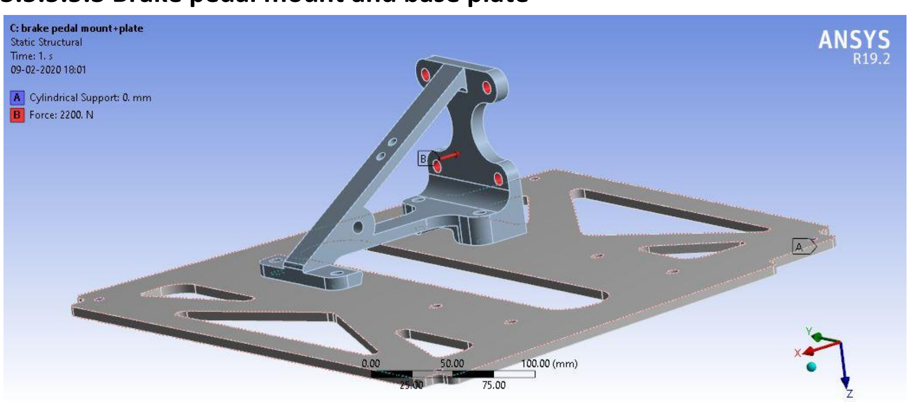

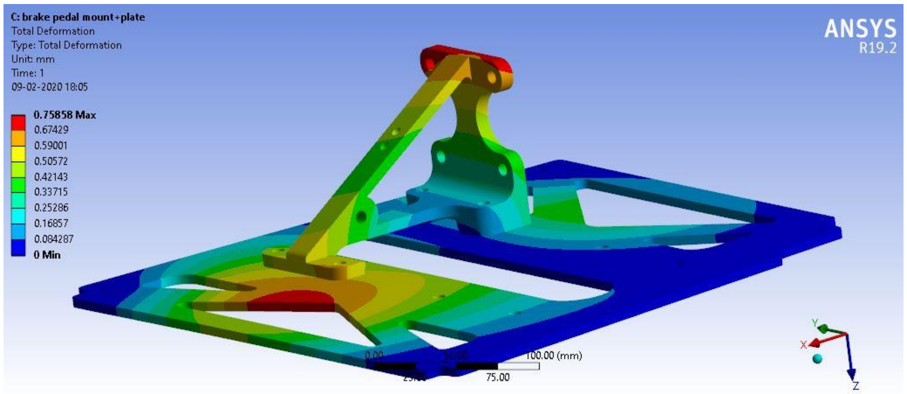

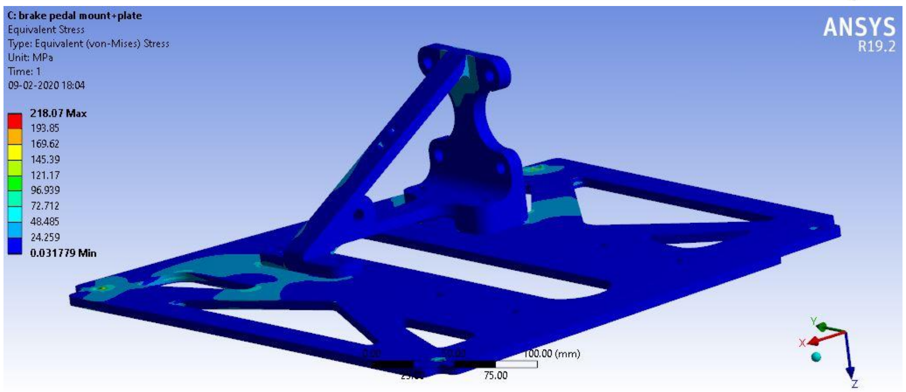

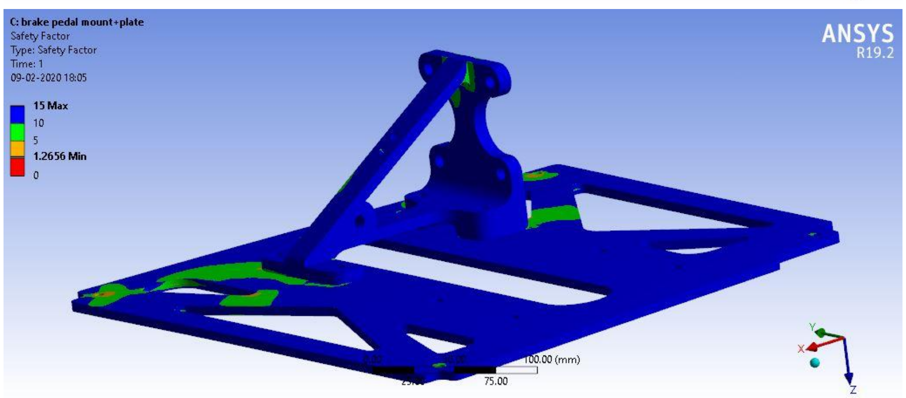

3.5.6 Rotor design

The rotors of the vehicle are the medium in which the kinetic energy from the motion of the vehicle is converted into thermal energy and then dissipated. From the braking system calculations earlier in the text the geometrical constraints of the rotors are:

-220 mm in diameter

-Thickness 3.81-5.08 mm (dependent on caliper selection)

Based on the application the other constraints that will be imposed on design are:

-Mechanical endurance at high temperatures

(Ability to dissipated or withstand high temperatures)

3.5.6.1 Material selection

The most crucial selection in the design of the rotors based on the above constraints was the material choice. Based on the application, a metal, ceramic or composite material was assumed to be optimal, however, based on the team's budget a metal was the only realistic choice
Based on some research on the metal and FEA, the optimal choices are:

- High Carbon Steel
- Nickel Steel
- Stainless Steel

We selected AISI 4130 normalized at 870°C steel. It possesses a high value of stiffness, a higher value of heat capacity and was in the team's budget.

3.5.6.2 CAD model

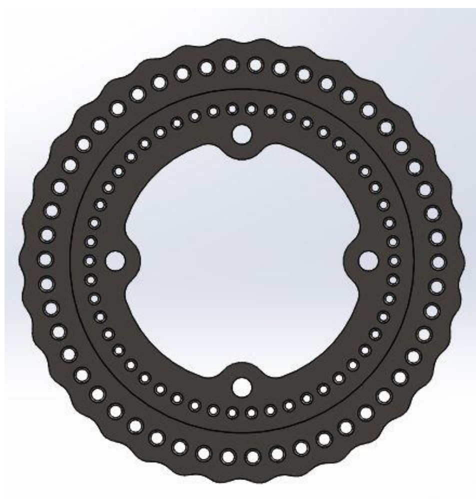

Fig. The CAD model of the brake disc

3.5.6.2 FEA analysis

We compare various models by coupling of Transient Thermal Analysis and Transient Structural analysis. The Structural Analysis included the deformations and Stresses caused by the thermal loads: both were linked in ANSYS in such a way that RESULTS from thermal were used in the MODEL of Transient structural.

1. For thermal analysis -Heat Flux was found using the following equation given in this paper

WSEAS TRANSACTIONS on APPLIED and THEORETICAL MECHANICS Ali Belhocine, Mostefa Bouchetara

Simulation of fully coupled thermomechanical analysis of disc brake rotor

ALI BELHOCINE*, MOSTEFA BOUCHETARA
Department of Mechanical Engineering
University of Sciences and the Technology of Oran
L.P 1505 El -Mnaouer, USTO 31000 Oran
ALGERIA
E-mail* : belhocine55@yahoo.fr

$$q_0 = \frac{1-\phi}{2} \cdot \frac{m\,g\,v_0\,z}{2\,A_d\,\varepsilon_p} \qquad (1)$$

$z = a/g$: Braking effectiveness
a : Deceleration of the vehicle [ms^{-2}]
ϕ : Rate distribution of the braking forces between the front and rear axle
A_d : Disc surface swept by a brake pad [m^2]
v_0 : Initial speed of the vehicle [ms^{-1}]
ε_p : Factor load distribution of the on surface of the disc.
m : Mass of the vehicle [kg]

The equation regarding heat flux uses a term Ad - the area of contact of pads, take the complete area on disk on both sides.
(1-phi)/2 - is for distribution of heat flux in two rotors (Front and rear).

In the above equation velocity was taken as variable and found by using (**v=u+at**), assuming **a=-1.5*g**, and **Vo= 72 kmph**, time in stopping comes out to be 0.97 seconds. Flux was calculated using the above equation and was used in ANSYS transient thermal analysis. Flux is applied on both faces which pad covers on the rotor. Convection with varying film coefficient and Radiation with fixed emissivity was also evaluated along with Heat flux. Final Temperature of the disc was calculated.

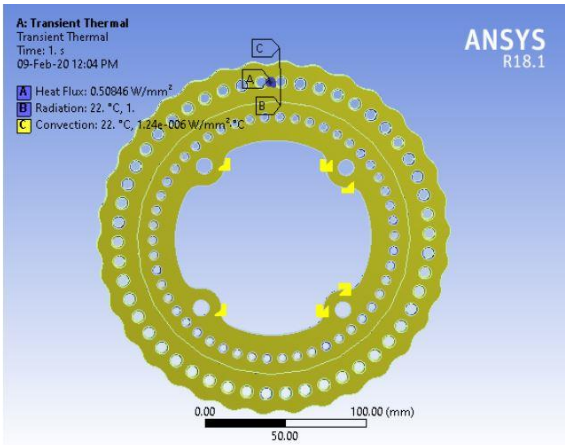

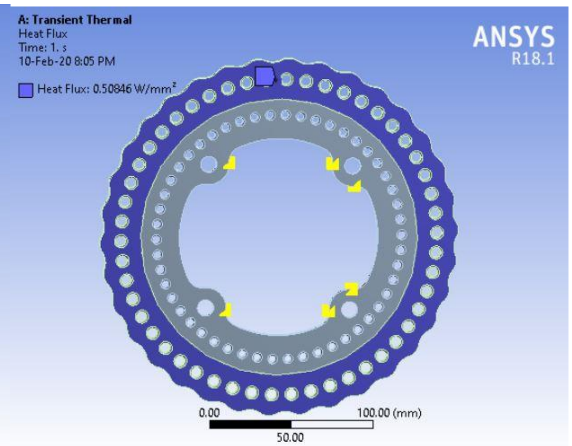

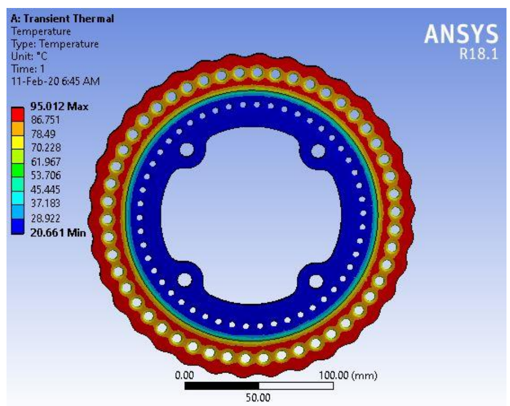

After Transient Thermal, it's the solution was taken as an input in transient structural the Disc temperature was varying with time. A time - constant moment of 759000 N.m. was applied. Equivalent stress, total deformation, and factor of safety was evaluated.

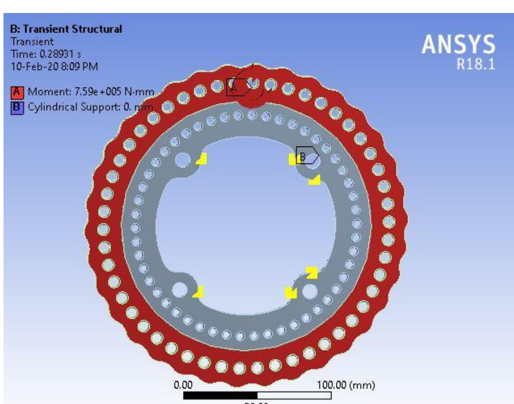

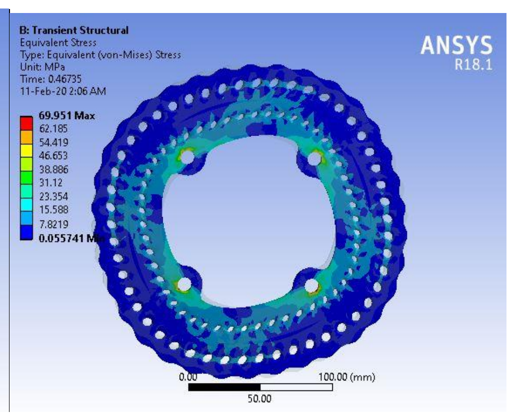

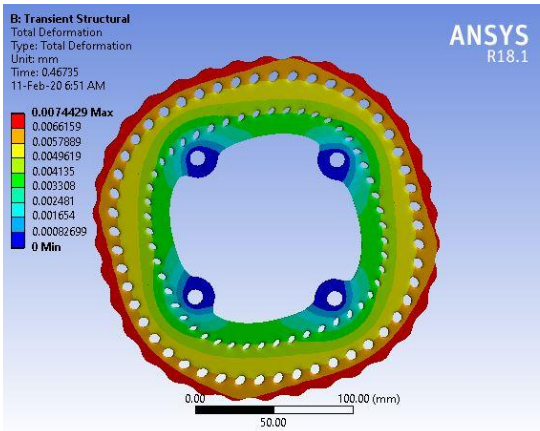

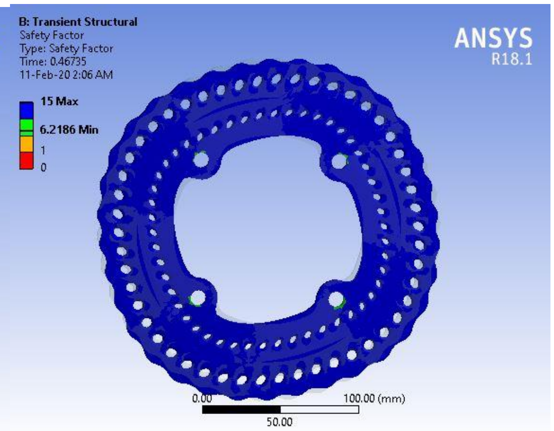

3.5.7 Brake pressure sensor

According to the rule,

T11.6.5 to detect hard braking, a brake system pressure sensor must be used. The threshold must be chosen such that there are no locked wheels and the brake pressure is ≤ 30bar. We mounted the brake pressure sensor in the front brake lines since the pressure in the front master cylinder is 3 times that of the rear master cylinder. So 30 bar pressure first reaches in the front brake line.

3.6 Bodyworks

3.6.1 Roorkee Motorsports Design 2020

Roorkee Motorsports for the 2020 competition a semi-headed up shaped nose is designed. The body is designed to decrease noticeable drag force on the overall vehicle.

The bodyworks of our current model are composed of 10 components (jointly shown in figure 1):

1. Nose-cone
2. Front side body (Left-Right)
3. Rear Side body (Left-Right)
4. Rear Body cover
5. Rear Flap
6. Lower Flap
7. Upper Flap (2 in numbers)

The material used for the fabrication of the parts is the Glass Fiber Reinforced Plastic (GFRP).

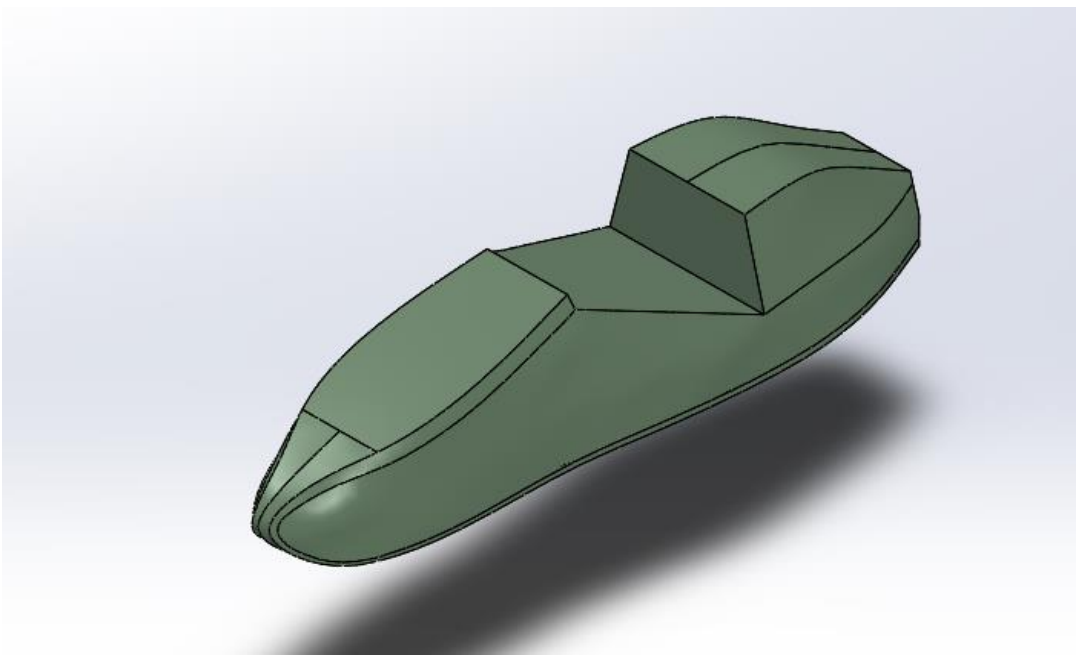

Figure 1: Isometric View of Bodyworks

3.6.2 Survey of Related Standards

As part of the literature survey, the team has reviewed specific rules and regulations mandated by Formula Green that would influence the design of the aerodynamics package for the 2020 car. Firstly, the car must be an open-wheeled “formula-style” body. FSAE defines “open-wheel” under the following criteria:

1. The top 180 degrees of the wheels/tires must be unobstructed when viewed from vertically above the wheel
2. The wheels/tires must be unobstructed when viewed from the side
3. No part of the vehicle may enter a keep-out-zone defined by two lines extending vertically from positions 75mm in front of and 75mm behind, the outer diameter of the front and rear tires in the side view elevation of the vehicle, with tires, steered straight ahead. This keeps out zone will extend laterally from the outside plane of the wheel/tire to the inboard plane of the wheel/tire. See figure 2 "Keep Out Zones" below.
4. Must also comply with the dimensions/requirements of Article 9 Aerodynamic devices.

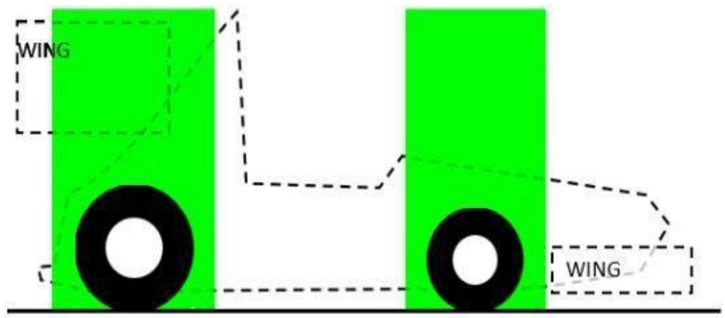

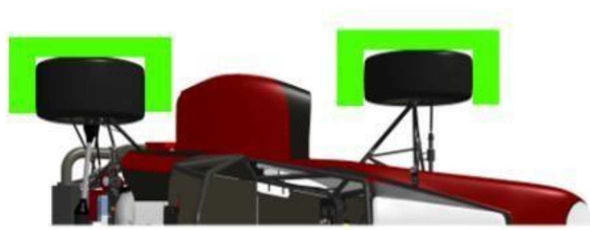

Figure 2: Keep Out Zones

3.6.3 Front Bodyworks

Sharp edges on the forward-facing bodywork or other protruding components are prohibited.
All forward-facing edges on the bodywork that could impact people, e.g. the nose, must have forward-facing radii of at least 38 mm (1.5 inches). This minimum radius must extend to at least forty-five degrees (45°) relative to the forward direction, along the top, sides, and bottom of all affected edges.

3.6.3.1 Nose Design

Nose-cone is made to be a semi head-up shaped nose with a general inclination of 14 degrees and a more downward inclination angle (about 19 degrees) in order to direct more volume of air through space beneath the car. Furthermore, the side inclination angles (23 degrees each) are decided such that enough flow is directed to increase the radiator and battery box duct cooling capacities. The minimum curvature of 38mm was also achieved in both the designing and manufacturing processes.

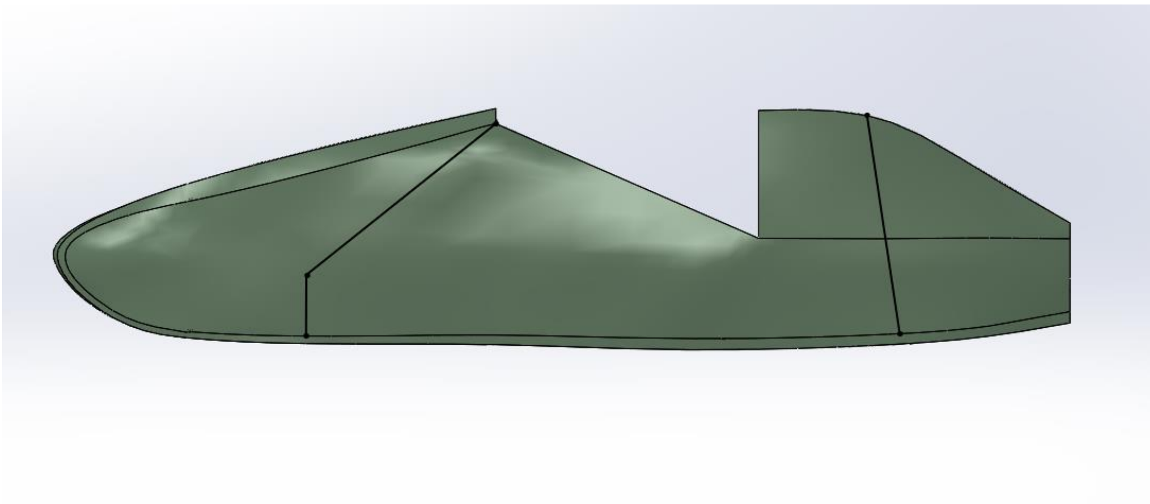

Figure 3: The nose-cone, side body and rear body bifurcations on the overall bodyworks (Side-View)

3.6.3.2 Side-pod Design

The side-body for the frame was divided into two segments the front and the rear segment. The main reason governing the discontinuity was the effective assembly of the wiring and battery box systems without hindering the front suspension assembly.

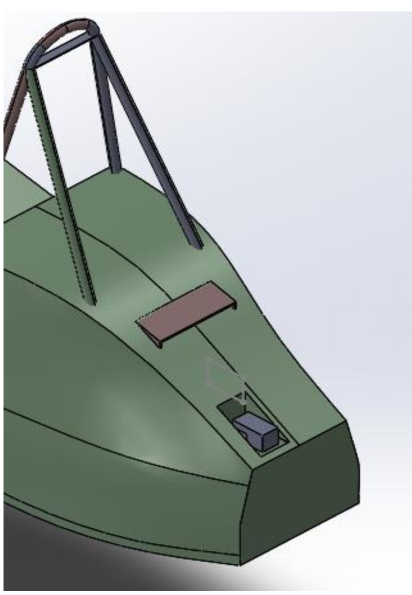

3.6.3.3 Rear Body Design

The rear body is divided into two segments, the rear cover, and the rear flap. All the segments that are created in the overall bodywork cater to the need of the electrical system assembly without any hindrance from the body. The rear body is subjected to a decent air pressure which comes from the hot air after cooling the battery box copper tabs and the air-liquid cooled motor. In order to address such a pressure, openings are created on the rear flap which ensures effective passage of the hot air. The rear cover is shaped like a diffusive structure with a diffusion angle of 10 degrees. This completes the motive of directing more air beneath the vehicle. The segment also has an opening for the HVD mounts and ensures the clear vision of the device along with enough water-proofing to protect the electric motor rule ev----.

3.6.3.4 Lower and Upper Flap Design

A lower flap was designed in addition to the rear cover and mounted with the same to ensure the protection of the electric motors from the water splashes beneath the vehicle (more prominent with rainy seasons). Finally, to complete the bodyworks an upper flap was designed to cover the overall electrical systems behind the firewall from rainwater.

3.6.3.5 Constraints and other Considerations

Since this project is ultimately meant to be entered into a competition the main constraints that the team will face will be those presented in the Formula Green Rulebook. Outlined in this aforementioned literature there are specific rules and regulations that the design must fall within in order for it to be considered valid. This will include inspections done prior to competing.

In addition to Formula Green rules, another major constraint is the fact that the chassis for the vehicle has already been previously developed. This means that the body designed for this project will have to be able to fit the existing tubular structure that makes up the chassis of the car as well as work properly with suspension components without interference.

Cost is another main constraint that the team will encounter. While there is not a specific limit to how much can be spent on the design, the team will have to adjust to the available funds allocated by funds that are provided by sponsors.

Finally, the team will be constrained by the timeline of the project. Even though the design needs to be ready for the February 2020 competition, in order for the team to successfully fulfill the Senior Design assignment, the body should be fully constructed by January 2020.

Our goal of using the least amount of material possible and keeping costs minimal, the nose was slightly redesigned to come closer to the crash attenuator reducing the overall surface area. The nose also acquired a more flattened form to reduce the body's coefficient of drag.

3.6.4 Curvature/Draft Analysis

During the design process, extreme consideration was given to curvature. Proper curvature of the model, as well as being part of the design regulations, would allow for the minimal restriction of airflow over the body as well as provide ease of manufacturing. Using the Curvature display within SolidWorks; the team was able to build these parameters into the design.

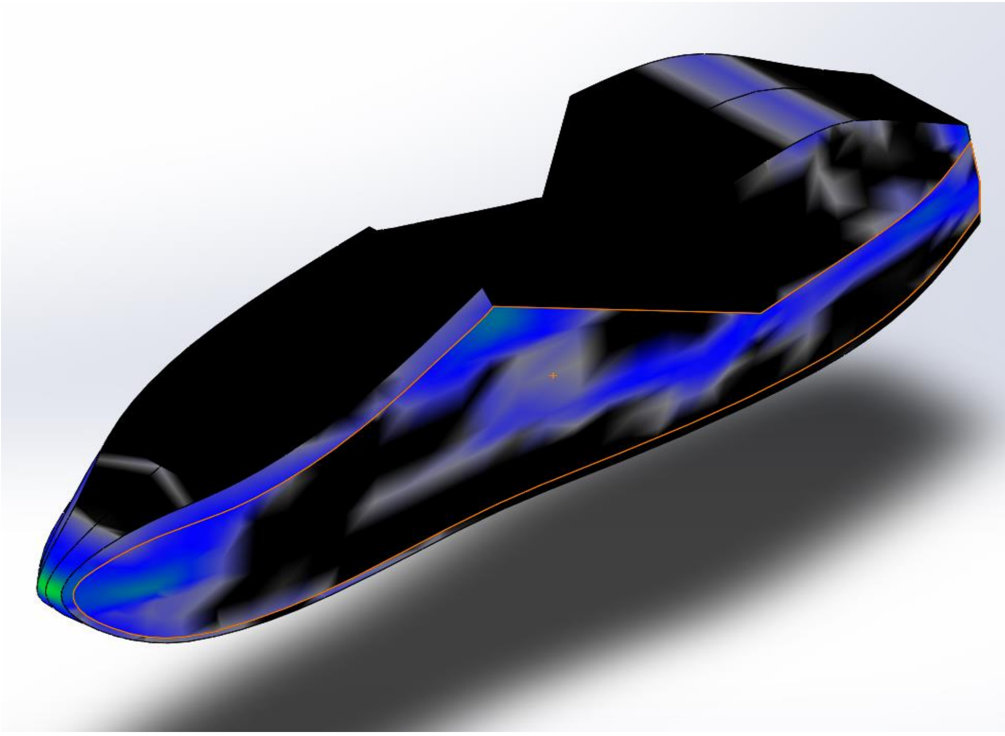

Figure 4: Curvature Analysis of Bodyworks

The **Curvature Analysis** display shows that transversally, there are dramatic changes in curvature resulting from the shape of the frame and the body being designed to fit tightly around it. Longitudinally, however, one can notice the continuity of the surface front to back.

3.6.5 CFD Analysis of Bodyworks (on ANSYS Fluent)

The bodyworks were simulated on ANSYS Fluent and analyzed for the overall drag and downforce forces. Meshing based on tetrahedral cells with appropriate aspect ratios and boundary layer characteristics was performed. The visualizations include the path lines for the velocity field (figure 5) and contours of the total pressure (figure 6).

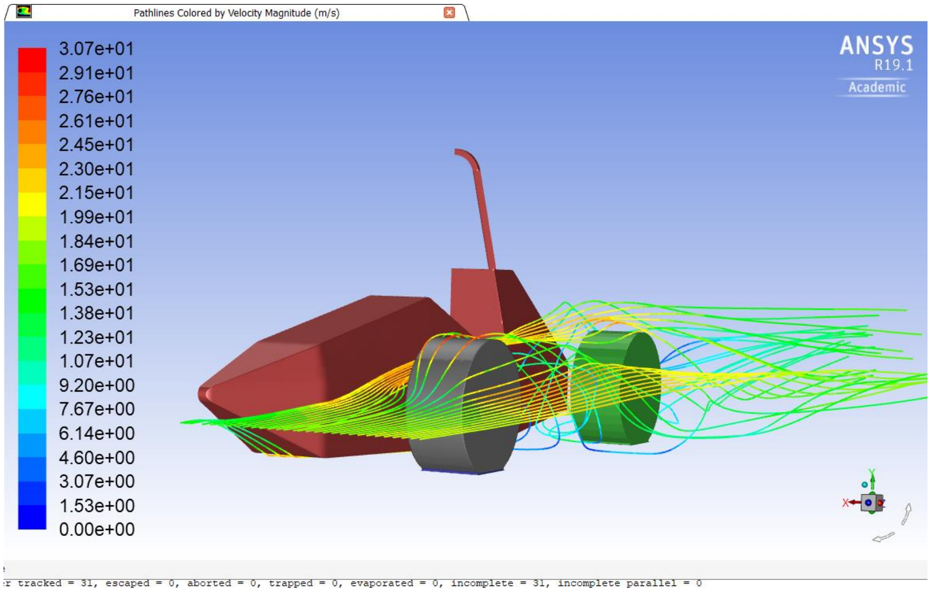

Figure 5: Path lines of the velocity field

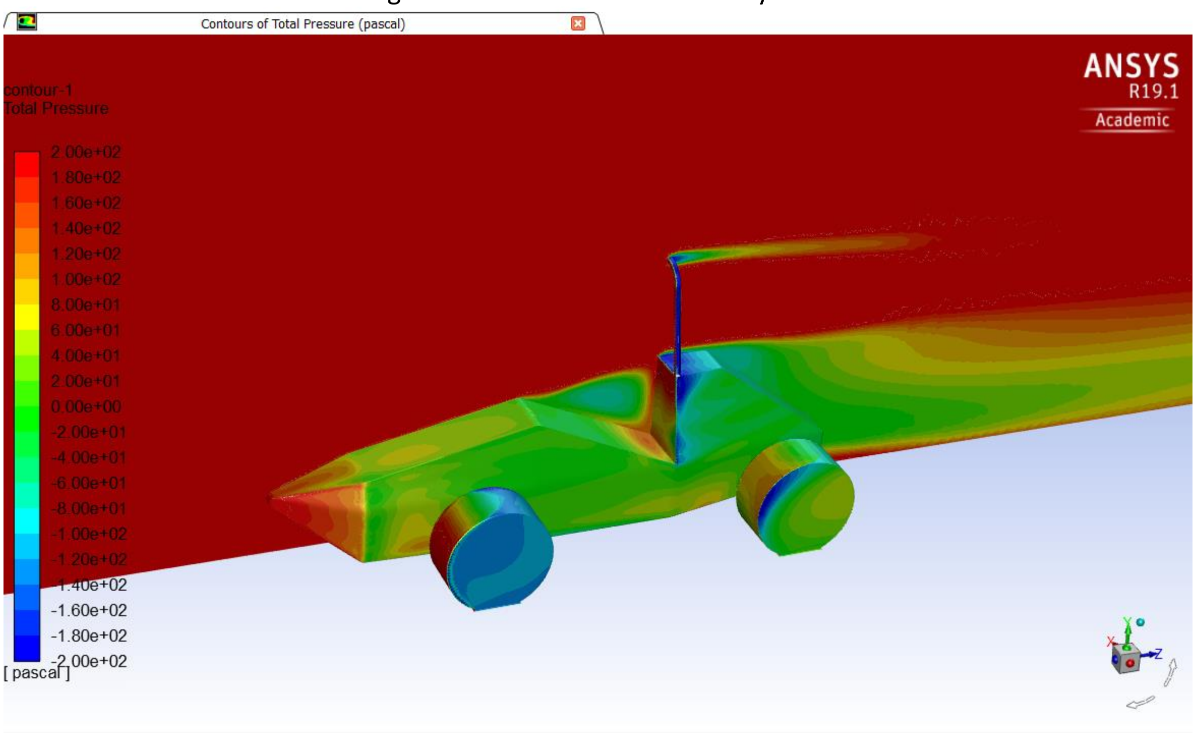

Figure 6: Total pressure distribution Map

The complete CFD analysis of the bodyworks resulted in the following visualizations for the lift and drag forces.

1. Overall Drag: 86.4 N (including all 4 tires)
2. Drag because of tires: 30 N (9.6 N on each front tire and 5.4 N on each rear tire)
3. Drag because of Bodyworks: 56.4 N
4. Lift on Bodyworks: 29.3 N
5. Frontal Area: 0.289 m^2
6. Coefficient of Drag: 0.7 (approx.)
7. Coefficient of Lift: 0.4 (approx.)
8. Aspect Ratio (C_L / C_D): 0.57 (approx.)

3.7 Powertrain

3.7.1 Design goals

1. Incorporating eccentric chain tensioner to adjust the chain.

A chain tensioning mechanism was needed to adjust tension in the chain as per requirement. We choose eccentric chain tensioner as it causes minimal wear of the chain and is suitable for high speeds.

2. Self-designed integrated hub and half-shaft.

To reduce weight and optimize the overall performance of cars this year we introduced a new modification by combining hub and tripod CV joint.

3. Robust and lightweight design.

Due to a significant increase in overall power and torque of Motor the design of drivetrain needed to be robust at the same time weight reduction needed to be focused.

3.7.2 Rules and design consideration

As mentioned above, there are a number of rules and events in the competition that guided system specifications. The limit of 80kW power output is a large constraint, with a maximum system voltage of 300V. The chain and motor need to be properly guarded with specific materials and dimensions. Certain fastener grades and sizes are required in certain locations, along with proper positive locking. Braking power regeneration is allowed, which is a performance benefit but limits the list of possible motors.

Besides specific rules, another major constraint of the design is that we must be able to manufacture components in-house or have the ability to easily source the part. Manufacturability will be a factor that drives design decisions throughout the process. Thankfully, access to some of the best machine resources on campus allows for complex parts to be machined, limiting the impact this constraint has on the design.

At the competition, the car will need to pass a "rain test" which requires the car to sit above and below sprinklers for two minutes, after which the tractive system of the car needs to function without fault. This impacts the powertrain primarily in the fact that everything will need to have a proper ingress protection rating, at least IP 65.

3.7.3 Motor-Selection

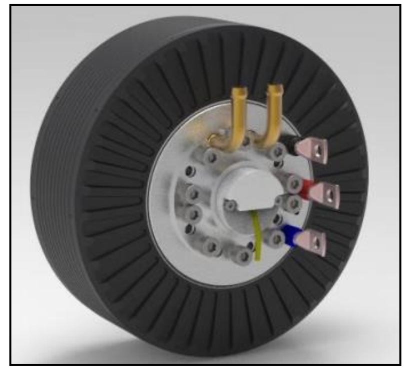

Figure2- Motor-Emrax 228

The previous year's design consisted of a single 15 kW three-phase BLDC motor along with a double-stranded chain gear reduction system. With the aim of reducing weight while increasing power, a single motor, and differential setup were preferred due to less weight and packaging constraints. Also, the differential was used from the previous car so the cost was also a factor to choose this layout.

Numerous different electric motors were examined, starting with the most used Emrax series of motors. They come in three sizes, the 208, 228 and 268 allowing for the right sizing of the motor for the specific application. Due to the voltage constraint, many high voltage motors are immediately deemed unusable. A basic metric that tire in comparing motors was the power to weight ratio of the motor, which was very good with the Emrax motors. It was found that at our voltage and power limits, the Emrax motors have the best power to weight ratios. When plugging the different motor models into the car model calculations and looking at overall packaging options, a single Emrax 228 seemed to be our best options, coming in at a power to weight ratio of 8.13kW/kg. It also had high continuous power (55kW) and required less cooling load capacity requirement at high voltages for maximum efficiency. They are also rated to IP65, which is a necessary requirement.

3.7.4 Differential selection

A differential drive was preferred to spool due to easy handling of the overall car and no slipping while taking harsh turns. Quaife Helical ATB Limited slip differential was chosen as it gives good performance automatically (mechanically) biases torque to the side with less traction. Helical ATB differentials are pure mechanical linkage and have no wear parts, allowing for longer life and faster response time. The differential was available in the market and cheap compared to Torsen differential or viscous or clutch-type differential and was meeting our packaging needs with a moderate weight of 6.35 kg.

3.7.5 Modelling and simulation

3.7.5.1 Tire data

Tire data is very important for driving the car up to its limit, thus crucial in deciding the Gear- ratio, Suspension & steering geometry and the components that will sustain the high amount of G-force leading to increasing the maneuverability and drivability of the car which eventually affects the car performance in the dynamic events.

Following are some of the useful data that were extracted from the big data cloud of Hoosier 20.54in tire provided by Tire Testing Consortium using the Pacejka model 2006 in Optimum-T software-

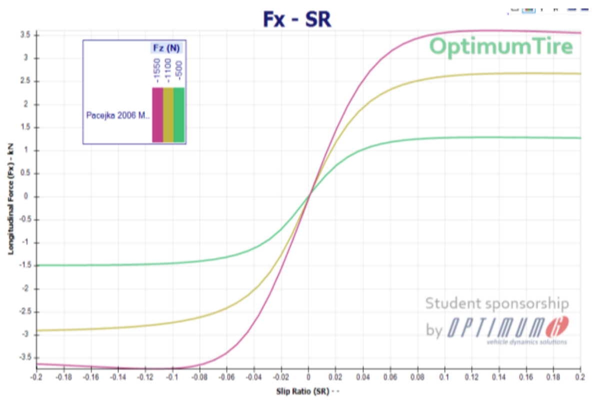

Figure 3- Fx v/s SR at different Fz

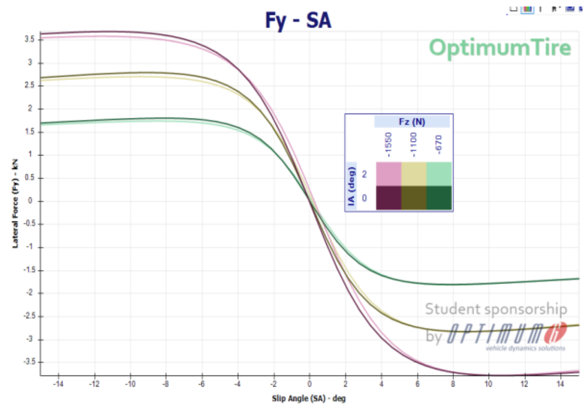

Figure 4- Fy v/s SA at different Camber and Fz

From the above graph, Longitudinal and lateral force that a tire can provide at a different configurations have been taken and the maximum value of coefficient of friction i.e. μ_x =2.65 and μ_y = 2.6 in pure longitudinal acceleration and cornering were determined at Fz=1100N respectively and for the asphalt road owing to the reports of various FS teams claiming the value an exaggerated one, they had been multiplied by 2/3.

3.7.5.2 Gear Ratio

It is important for a car to have an optimum gear ratio sets to perform well in the dynamic events (according to the track). It should be selected to provide an optimum acceleration and speed range without losing traction keeping the straightness and curvature of the tracks in mind.

On seeing the track nature – accelerative (max. straight length=65m), a 4.23 gear ratio for reaching the traction limit (i.e. maximum longitudinal load transfer) from the self-designed Gear-ratio Calculator (shown below) on Simulink was determined using the above curves of tire data for an electric vehicle. The result was simulated on Optimum lap and then on IPG for acceleration, skidpad, and endurance track, for validating the results.

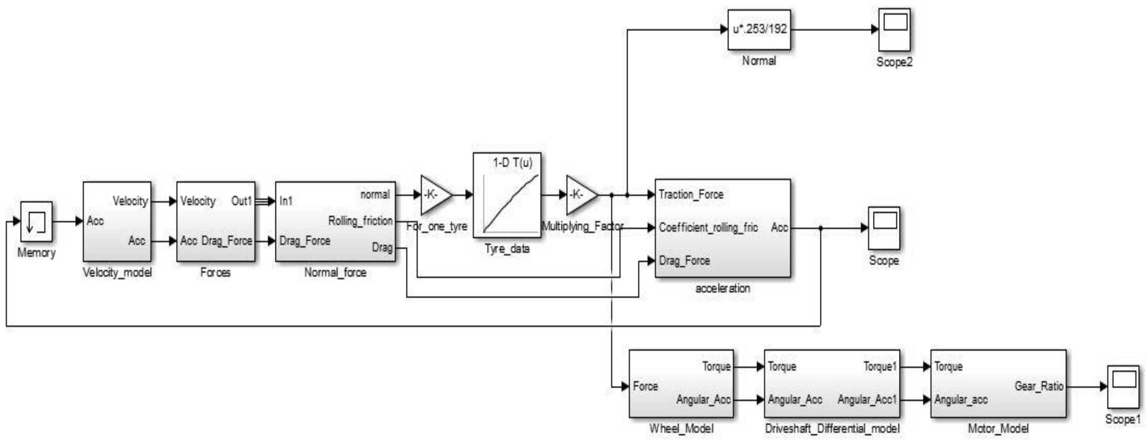

Figure 5- Gear Ratio calculator on Simulink

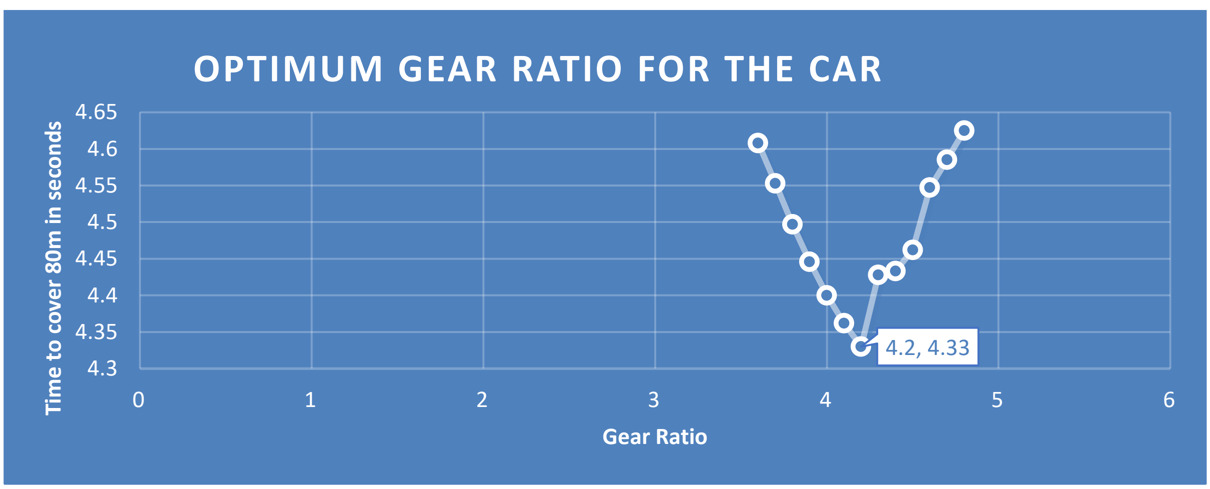

Figure 6- Optimum gear ratio as per IPG Simulation

3.7.6 Final drive-train design

The drivetrain of a motor vehicle is the group of components that deliver power to the driving wheels. The figure below shows the complete assembly of the powertrain in the car.

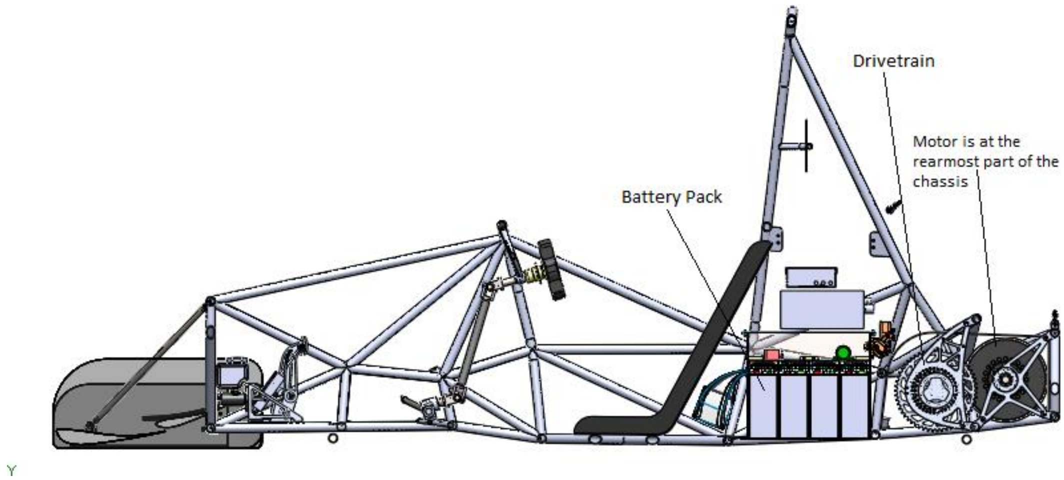

Figure 7 a) Section of the Car showing powertrain components

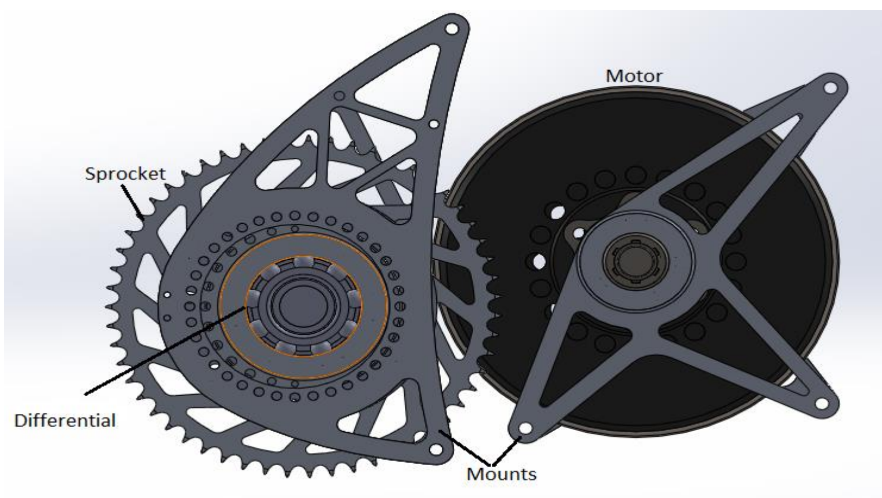

3.7.7 ANALYSIS

3.7.7.1 Integrated Hub design

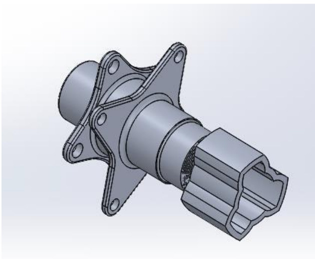

Figure 8 - Conventional Design of tripod joint and hub

The rear tripod joints integrated hubs have been used instead of a conventional tripod joint to reduce the weight from the conventional driveshafts and CV joint system. (Weight reduction of about 1.3 kg for each hub-tripod housing assembly has been achieved).
Steel inserts have been used to protect the hub inner linings from the fatigue breakdown due to the fluctuating loads acting on it by the chromium steel bearings of the spider. There is line contact between spider bearing and steel inserts so hoops stresses have been calculated for the design of inserts. The faceplate is placed in front of the face where the spider is being inserted to ensure that the spider won't come out during the wheel travel, also seeing the wheel travel, about 50 mm of hub length is provided for swooping of the spider for having smooth transmission.

Rear Hub:

Mass: 691 gm **Material**: Aluminium 6061-T6

CAD	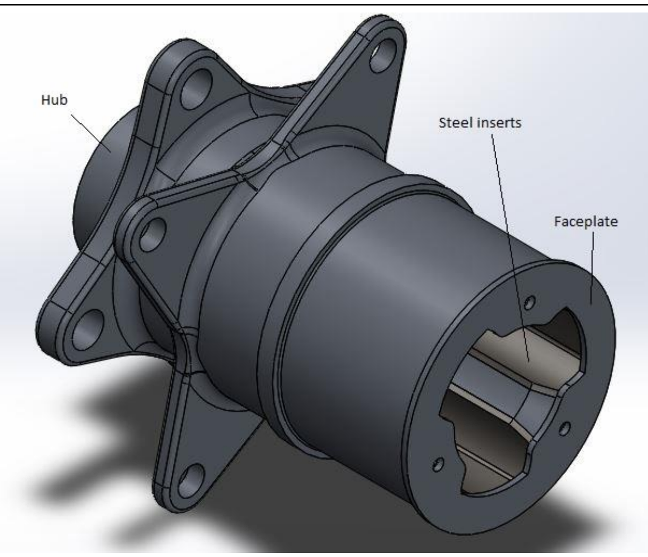

<table>
<tr>
<td>Supports</td>
<td>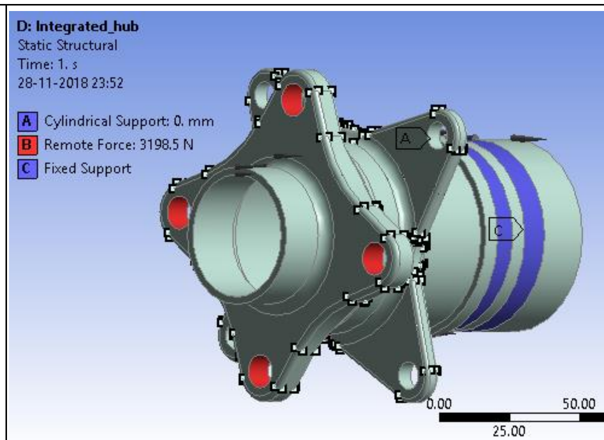
</td>
</tr>
<tr>
<td>Deformation</td>
<td>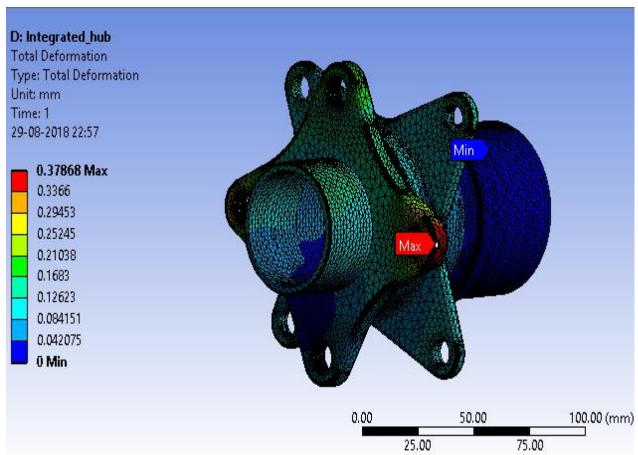
</td>
</tr>
<tr>
<td>Equivalent stress</td>
<td>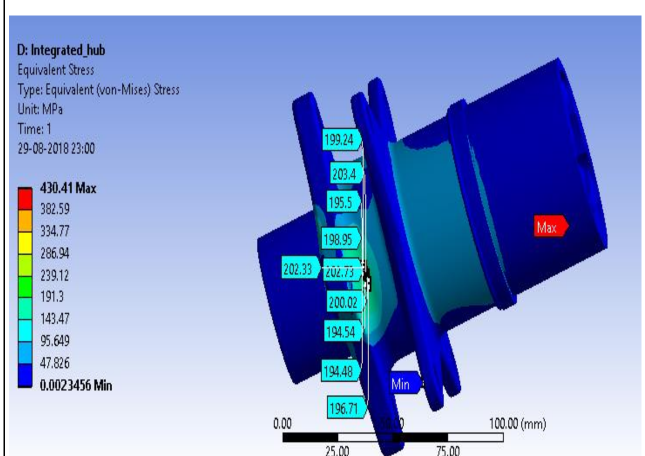
</td>
</tr>
</table>

Note:-In this case the remote forces are the forces that are coming from the contact patch of a tire.

The profile of the spider was cut by the help of the CAD model of the Swift D-Zire's spider, which had been developed by processing the data cloud generated by the Handy 3D scanner with the use of **GeoMagic design-X** software as shown below:

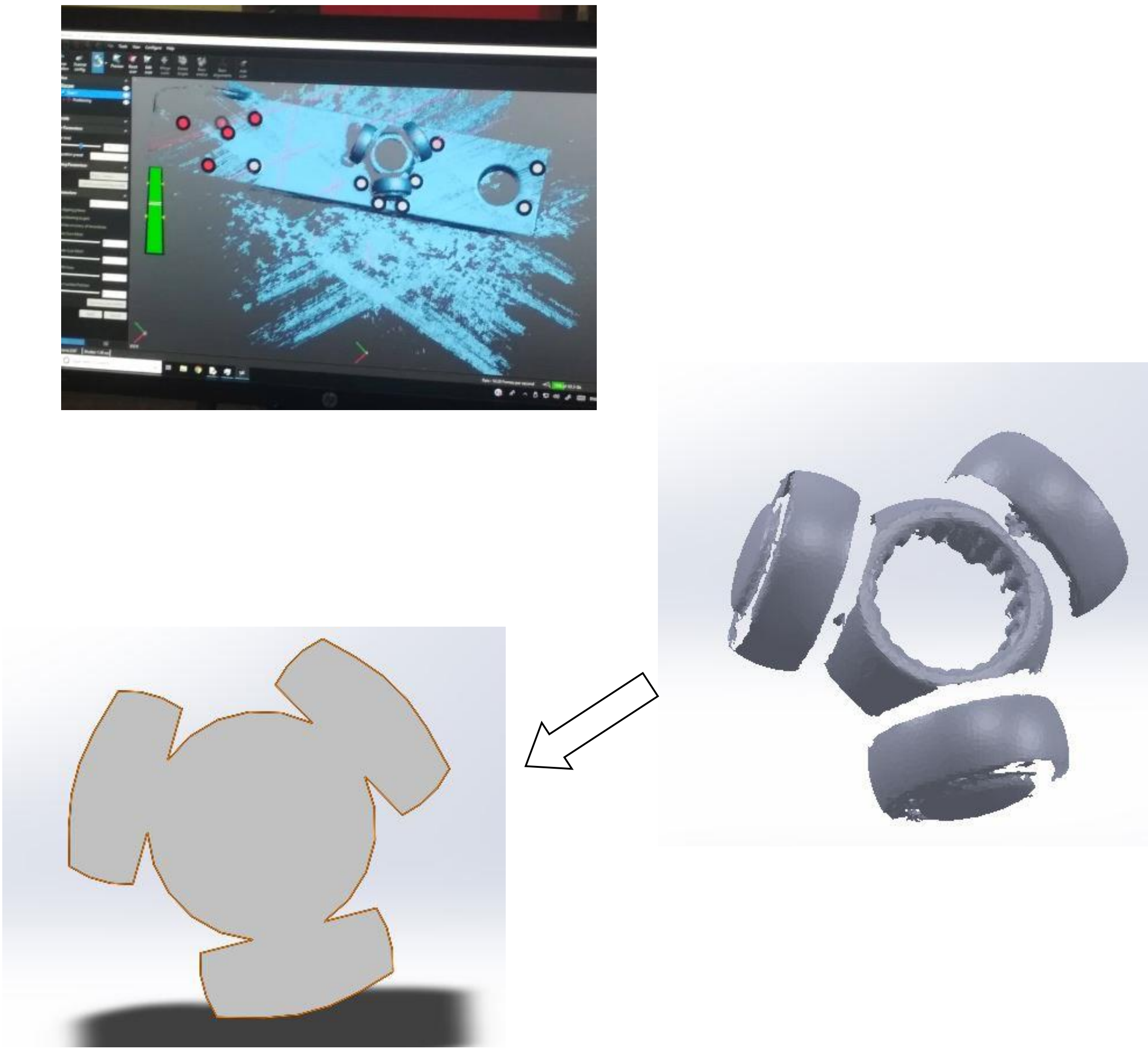

Figure 13- Flow of Reverse Engineering of spider

3.7.6.2 Sprockets

Sets of different Sprockets (used to transmit power through the chain) have been used for obtaining different gear ratios. Currently, 13-55 and 12-54 have been manufactured for obtaining the gear ratio of 4.23 and 4.5 respectively.

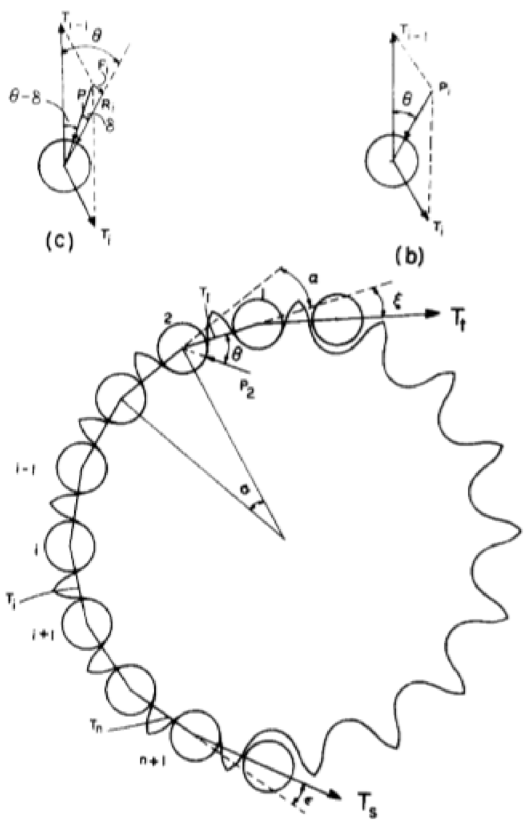

$$P_i = T_i \frac{\sin\alpha}{\sin(\theta - \delta_i)} \quad i = 1, \dots, n.$$

$$T_i = T_{i-1} \frac{\sin\theta}{\sin(\alpha + \theta)}.$$

The minimum tooth pressure angle is 17-64/N
Nominal tooth pressure angle is 35-120/N
Where N stands for number of sprocket teeth

CADs of the final sprockets for obtaining the gear ratio of 4.15 are shown below:-

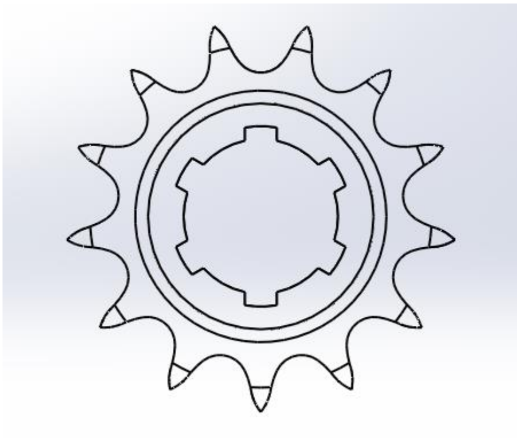

Figure 14- 13 teeth Sprocket for chain-428

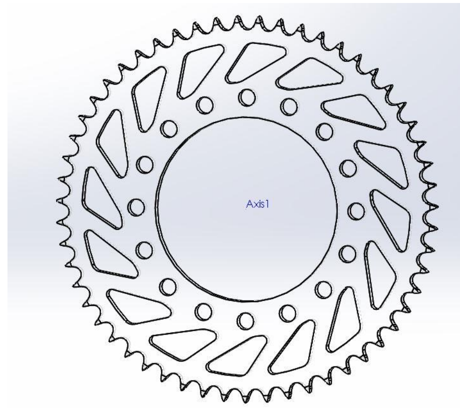

Figure 15- 54 teeth Sprocket for chain-428

Before obtaining the above CAD of 54 teeth sprocket, the following iterations with its design were performed for getting a better factor of safety to mass ratio (Keeping mass as low as possible).

Figure 16- Design1: 55 teeth Sprocket

Figure 17- Design2: 55teeth Sprocket

Analysis of Sprocket is shown below:-

55 Teeth Sprocket:

Mass: 389 gm

Material: Aluminium 7075-T6

CAD	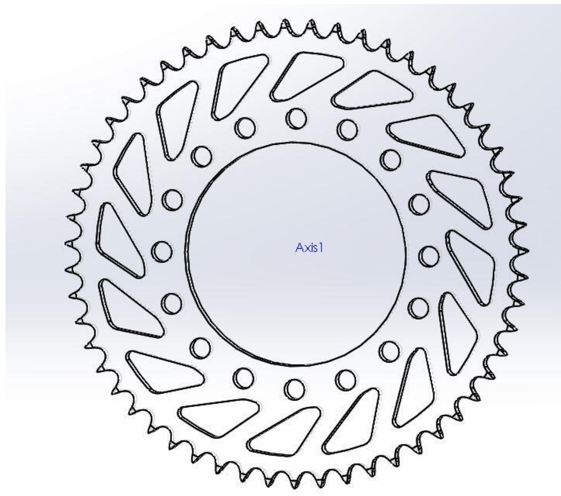
Supports	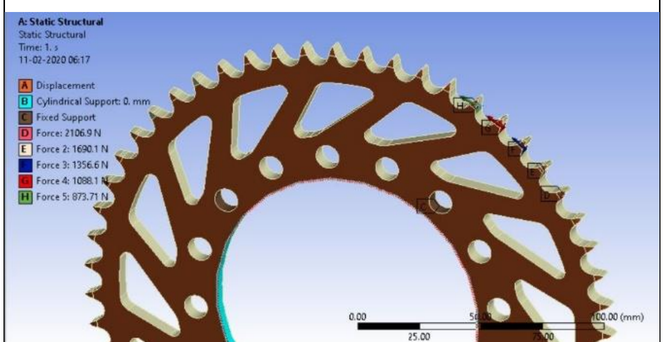
Deformation	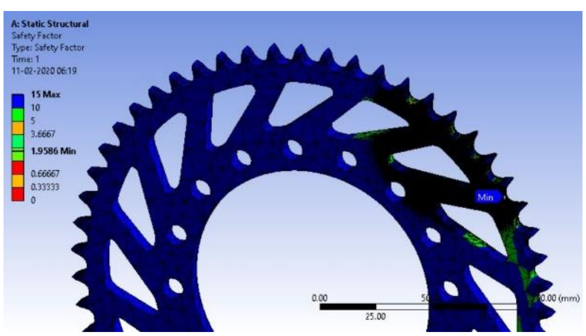

Equivalent stress	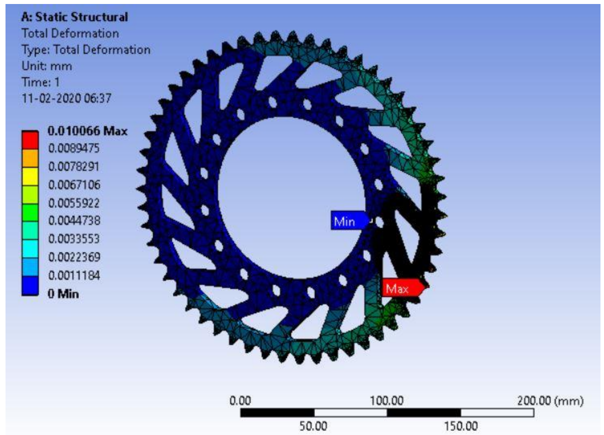

13 Teeth Sprocket:

Mass: 147 gm

Material: Aluminium 7075-T6

CAD	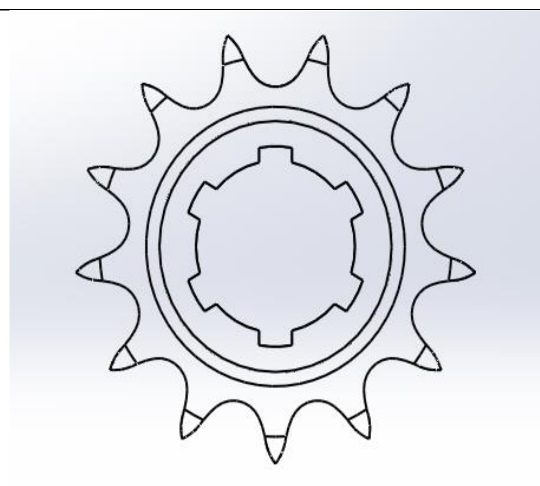

Supports	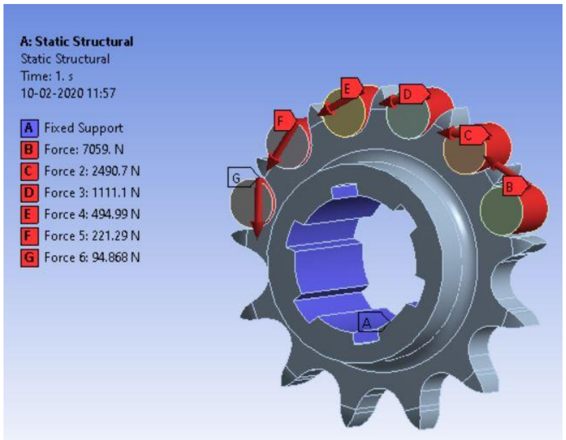
Deformation	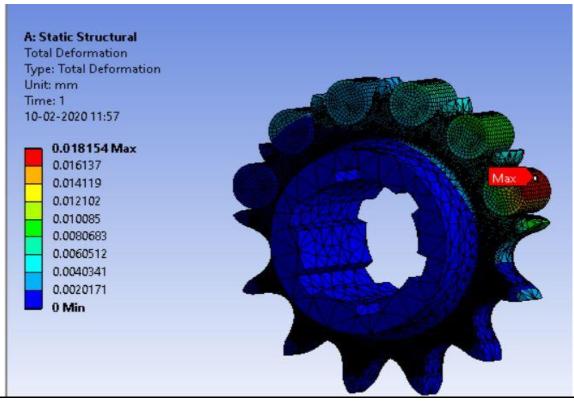
Equivalent stress	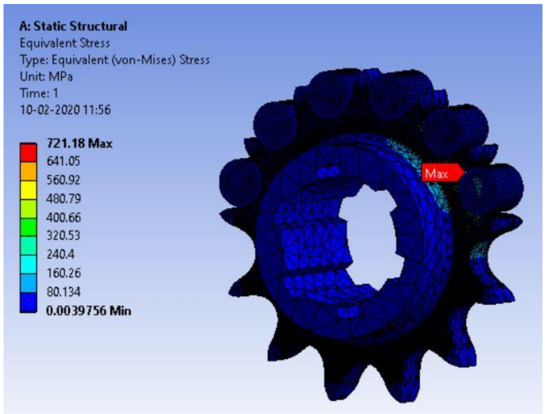

3.7.6.3 Chain selection

A TIDC 428 Chain for transmission is being selected over the 520 chains since being light weighted it can transmit the required tensile force.
The total tensile force will be coming around 7384 N in the chain. Considering moderate shock factor =1.5
Total tensile force during impact =7384*1.5=11076 N

428 Chain	520 Chain
Max. Strength =19.3kN	Max. Strength of 520= 27.5kN
Weight/m = 0.693 kg	Weight/m = 0.944 kg

3.7.6.4 Mounts Differential and motor

Eccentric mounts having 5 mm of offset are being used for mounting the differential with the primary structure since by rotating an eccentric disc, the chain gets easily tighten which helps in smoother torque transmission. With time the chain gets longer thus eccentric or turnbuckle type of chain tensioner mounts are suitable. Turnbuckle was avoided since there is a probability that one turnbuckle gets more tighten than others, leading to more force at the shortest one and eventually leads to drivetrain failure. (Thus, Single bolt should be used for mounting the turnbuckle with the chassis).

The forces that will be produced by the sprocket through the differential on mounts have been calculated by considering the differential as a prismatic beam on a pin-type supports (bearings). Thus the chain force is the cause behind the forces at mounts.

The forces(gravity, pseudo forces (during acceleration) and the chain force)acting on the mounts have been calculated by considering the motor and the shaft as a prismatic beam of the same cross-section mounted on a two-pin type supports i.e. bearings and these bearings are interfacially fit into the mounts thus all the supportive reactions will be provided by the motor mounts itself.

Bearing Reaction Forces:-

Forces Y-Z plane	Py(b) =-6.06157(Kn) Py(c)=.137(Kn) Mz(b)=0.192(Kn*m)

Diagram	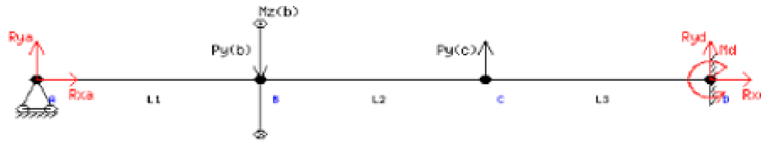
Shear force diagram	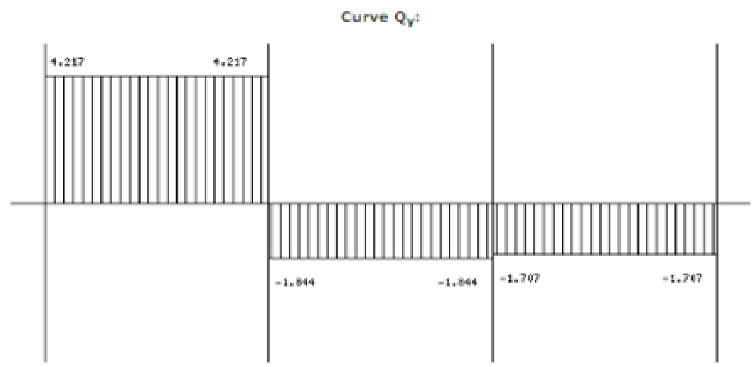
Bending moment Diagram	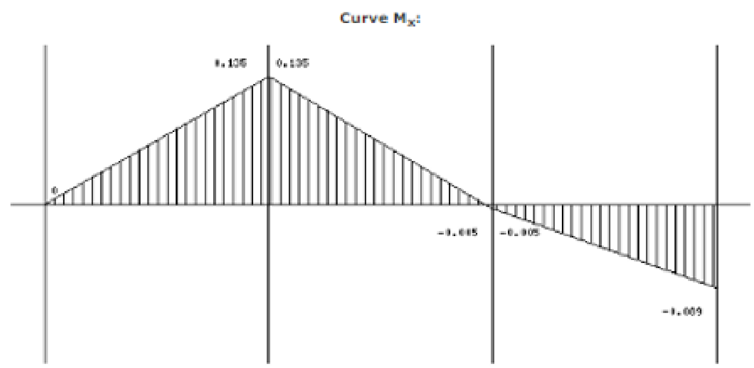
Reaction Forces	Rya=4.217(kN) Ryd=1.707 (kN) Md = -0.089 (kN)

Forces X-Z	Py(b)=-3.9683(kN) Py(c)=-0.12753(kN)

Diagram	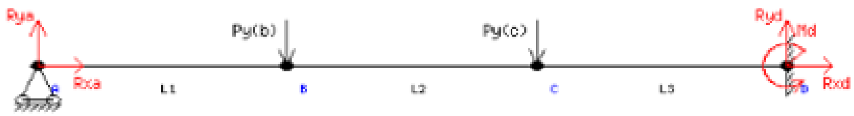
Shear force diagram Bending moment diagram	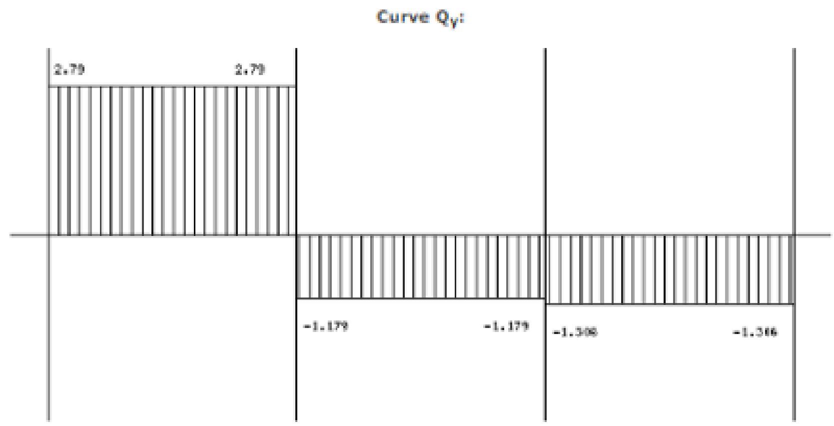 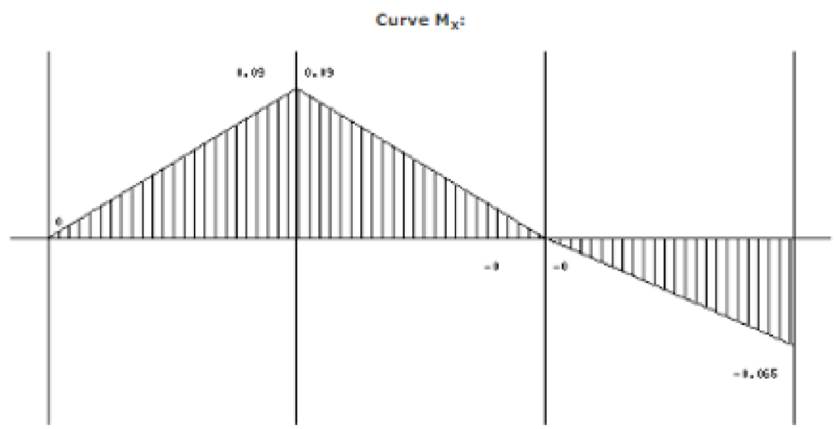
Reaction forces	Rya=2.79(kN) Ryd=1.306(kN) Md=-0.065(kN)

For differential mounts

Force in the X-Y plane	Py(b)=5.595765

Diagram Shear force Diagram Bending moment diagram	For Differential Mounts X-Y plane 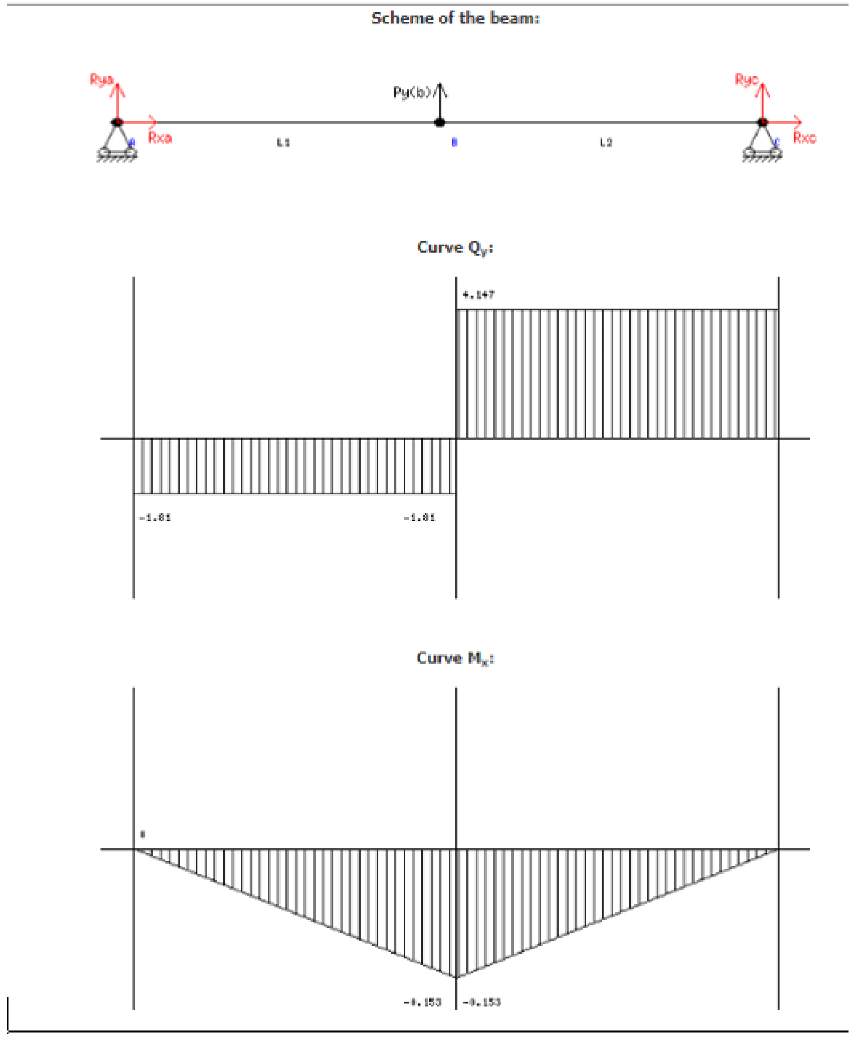
Reaction forces	Rya=-1.81(kN) Ryc=-4.147(kN)

Forces	Py(b)=-0.0506(kN) Py(c)=4.10684(kN)
Diagram Bending moment diagram	For X-Z Plane 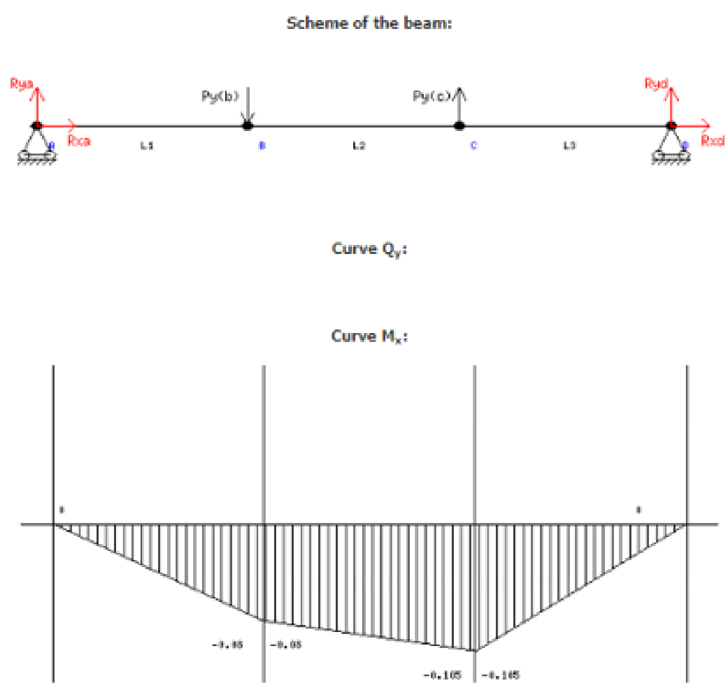
Reaction force	Rya=-1.228(kN) Ryc=-2.828(kN)

Analysis and results after applying those forces on Motor as well as differential mounts.

Eccentric Disc:

Mass: 210 gm

Material: Aluminium 6061-T6

CAD Drawing	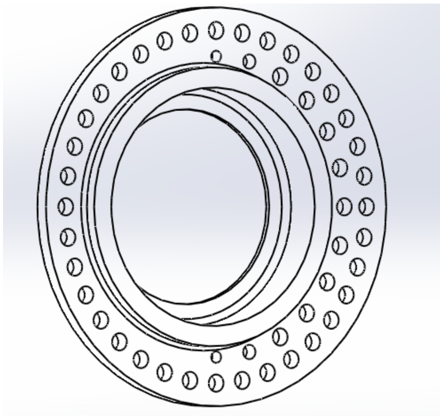
Support	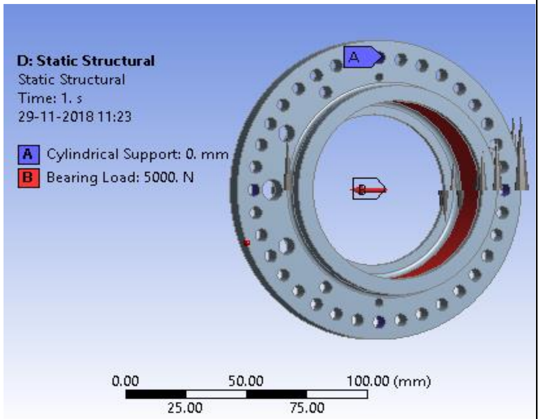

Deformation	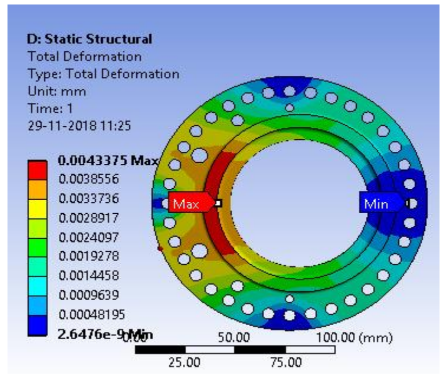
Equivalent Stress	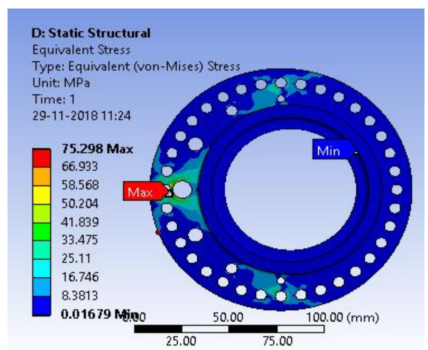

Differential mount left:

Mass: 387 gm

Material: Aluminium 6061-T6

	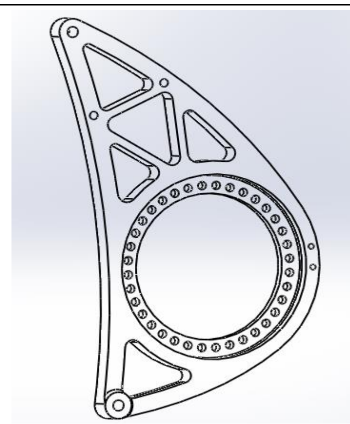
Supports	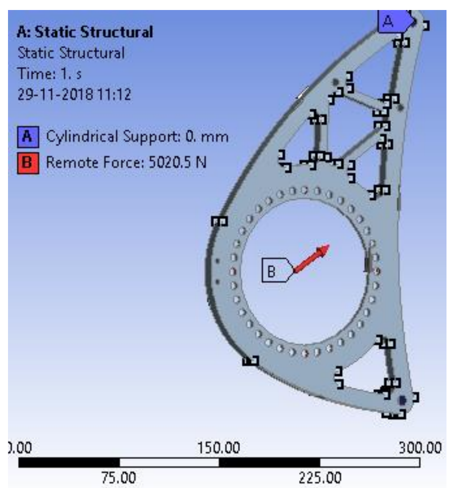

<table>
<tr>
<td>Deformation</td>
<td>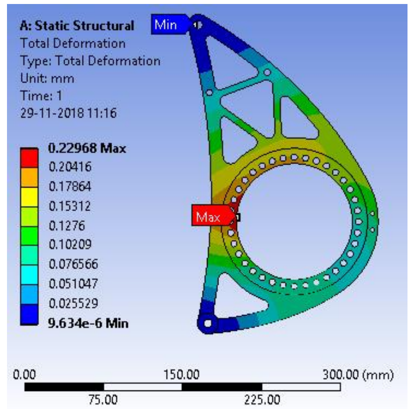
</td>
</tr>
<tr>
<td>Equivalent stress</td>
<td>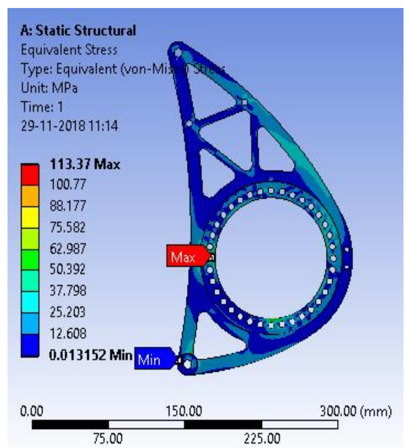
</td>
</tr>
</table>

Differential mount right :

Mass: 303 gm **Material**: Aluminium 6061-T6

CAD	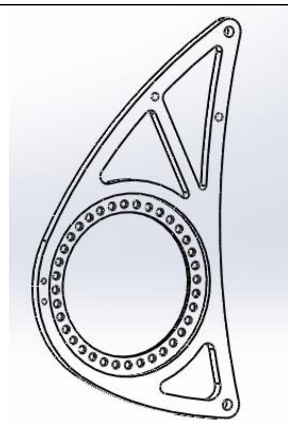
Supports	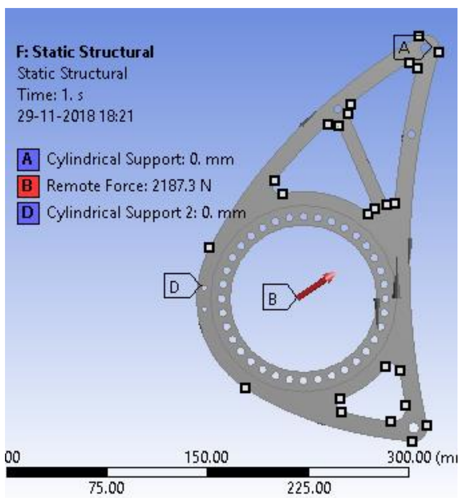

Deformation	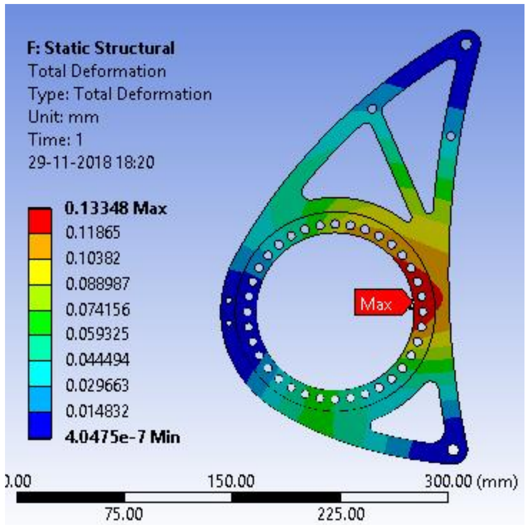
Equivalent stress	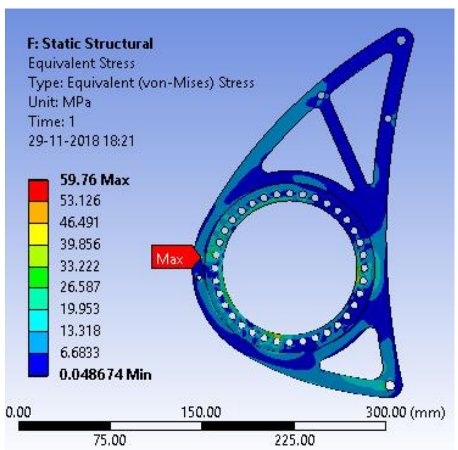

Similarly, the motor is mounted on Al 6061 mounts and attached with the primary structure using AISI 1020 steel brackets of 2.5 mm thickness. The CADs and equivalent stress of the motor mounts are shown below:

Motor mount left:

Mass: 267 gm

Material: Aluminium 6061-T6

CAD Drawing	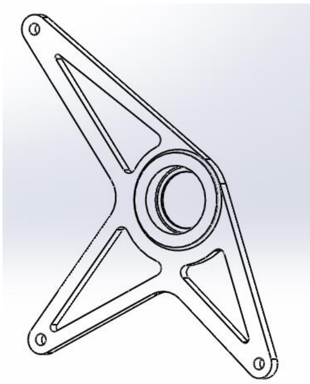
Supports	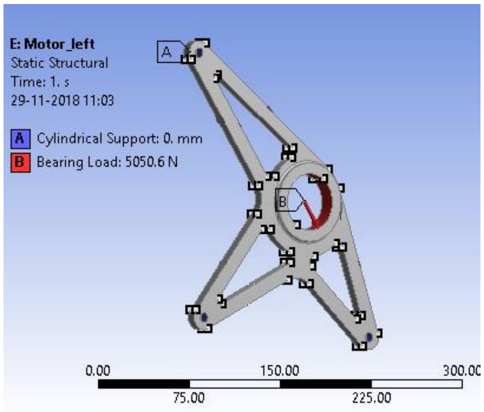
Deformation	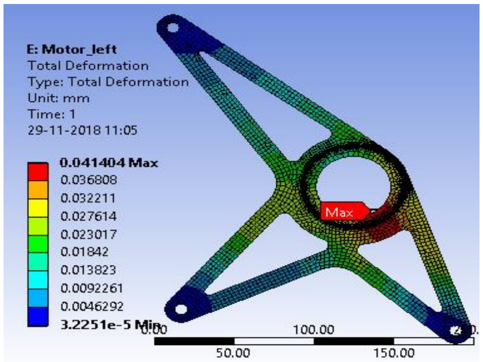

Equivalent stress	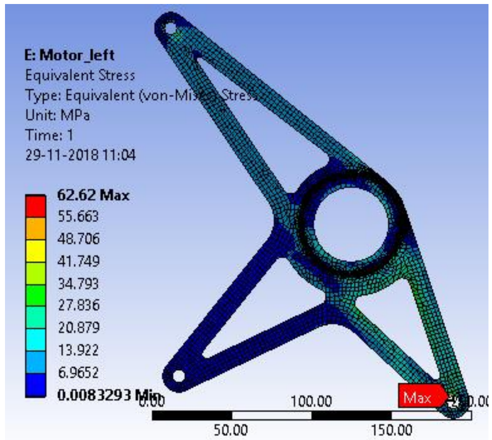

Motor mount right:

Mass: 426 gm **Material**: Aluminium 6061-T6

CAD Drawing	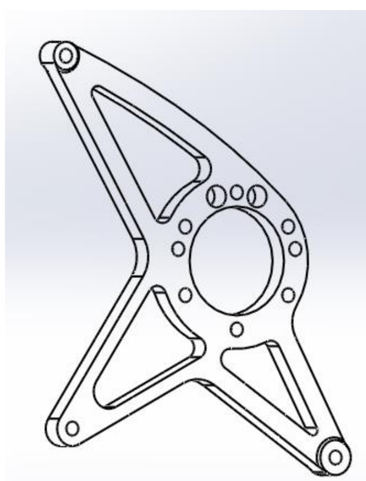

Supports	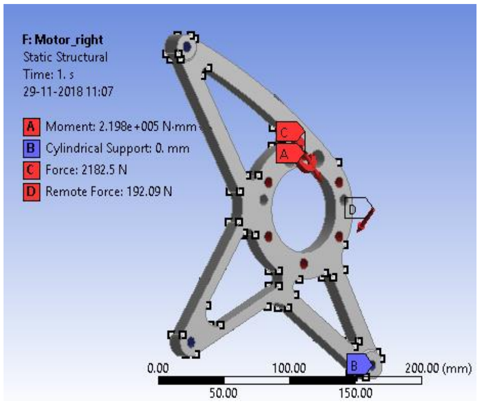
Deformation	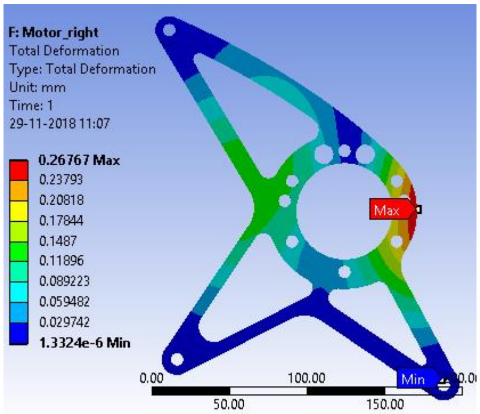
Equivalent stress	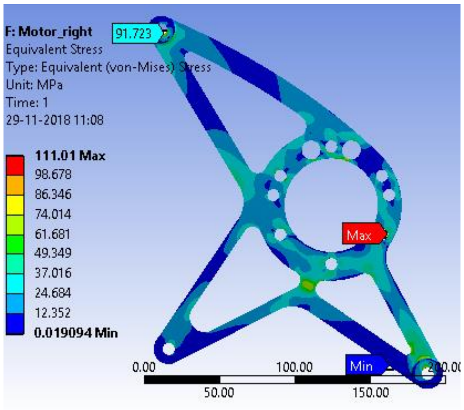

3.7.6.5 Motor Shaft

The motor shaft is attached directly with the motor and transmits the power to the differential via the chain-sprocket mechanism. Its material is AISI 4340 i.e. En 24 Z type and it has been designed by taking the insights from the drawing of the shaft for Emrax-228, given by the manufacturer. The CAD of the motor shaft along with its boundary conditions is shown below:

<table>
<tr><td>CAD Drawing</td><td>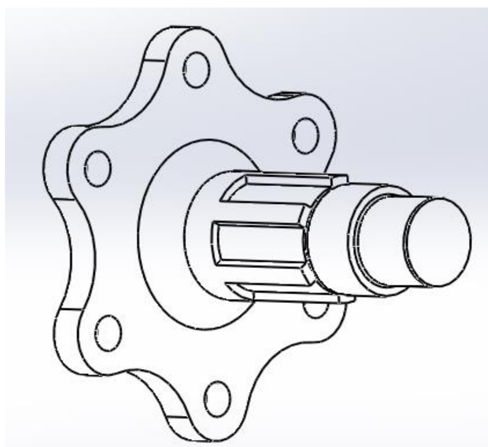</td></tr>
<tr><td>Supports</td><td>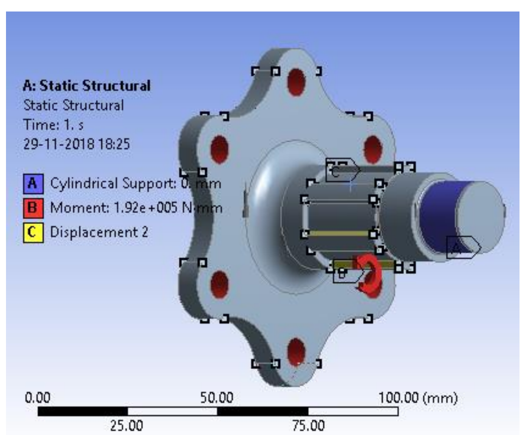
</td></tr>
</table>

Deformation	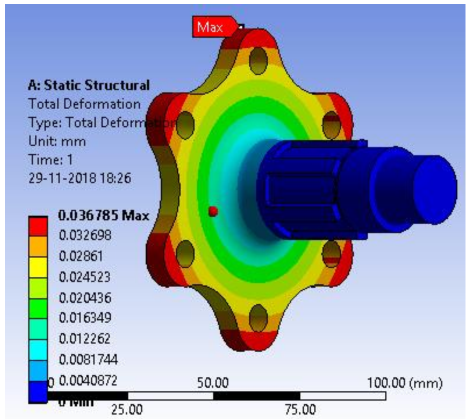
Equivalent stress	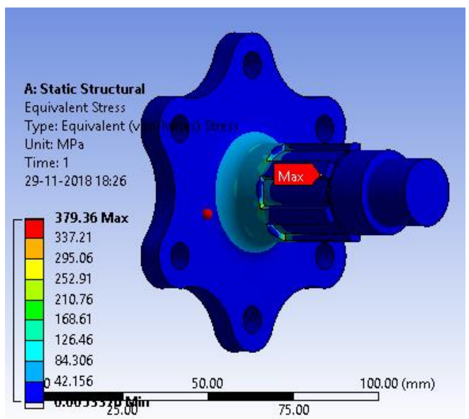

3.7.6.6 Half shafts

As the differential stands in the center of the vehicle both half shafts are of almost equal length so have equal diameter considering losses due to rotational inertia. Half shafts are made of cold-drawn EN-24 T type as it is easily available in the market and has higher fatigue life as well as good torsional rigidity. Tensile tests were conducted on three sample materials to choose the correct type of EN-24 Fatigue life of driveshaft was tested on MATLAB using torque data generated by running vehicles on a sample endurance track considering harsh acceleration and braking. Later the results were verified using ANSYS and fatigue life of driveshaft came about to be 3*10^5 cycles of harsh acceleration and braking which was enough for driving the vehicle up-to 3000 KM. The splines at the end for Spider CV joint were flame hardened which ensures hardening at the surface while retaining its toughness.

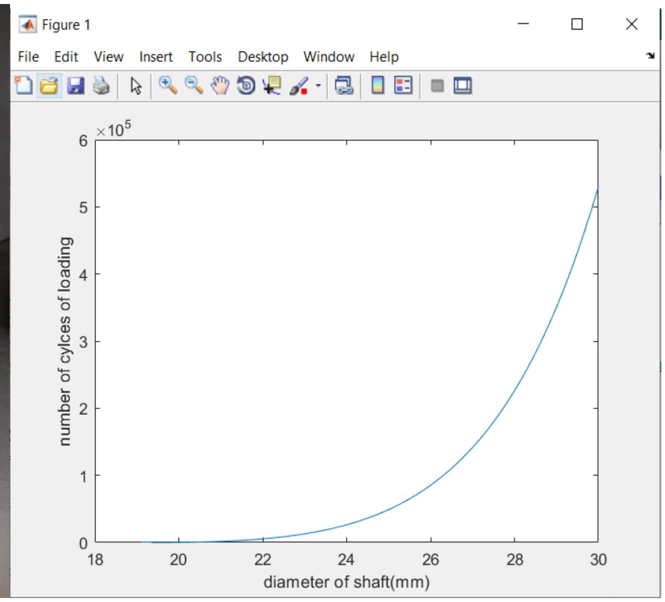

Tensile testing of material

Graph between diameters of half shaft to cycles of loading

3.7.7 Bearing calculation

Motor shaft Bearing Formula:

P = XFr + YFa

P: Equivalent Load (kN)

F_r: Radial Load (kN)

F_a: Axial Load (kN)

X: Radial Load Factor

Y: Axial Load Factor

$P = XF_r + YF_a$

$\frac{f_0 F_a}{C_{0r}}$	e	$\frac{F_a}{F_r} \leq e$		$\frac{F_a}{F_r} > e$	
		X	Y	X	Y
0.172	0.19	1	0	0.56	2.30
0.345	0.22	1	0	0.56	1.99
0.689	0.26	1	0	0.56	1.71
1.03	0.28	1	0	0.56	1.55
1.38	0.30	1	0	0.56	1.45
2.07	0.34	1	0	0.56	1.31
3.45	0.38	1	0	0.56	1.15
5.17	0.42	1	0	0.56	1.04
6.89	0.44	1	0	0.56	1.00

$$x_D = \frac{L_D}{L_{10}} = \frac{60\mathcal{L}_D n_D}{L_{10}}$$

$$C_{10} = a_f F_D \left[\frac{x_D}{x_0 + (\theta - x_0)(1 - R_D)^{1/b}} \right]^{1/a}$$

The Weibull parameters are $x_0 = 0.02$, $(\theta - x_0) = 4.439$, and $b = 1.483$.

3.8 Steering

3.8.1 Design Methodology of Steering

a) Defining the objective.
b) Selection of steering geometry.
c) Iterations for Ackerman angle geometrically (Analysis of 2D geometry)
d) Finding net steer angle geometrically (3D geometry simulation)
e) Deciding other parameters using iterations by the kinematic analysis (an overall mechanism)

3.8.2 Defining the objective

Various pillars of steering design should be considered for a good steering system design like steering effort, the sensitivity of the steering system, feedback to the driver, boundary conditions to prevent kinematic chain inversion, etc. Sensitivity and feedback are very critical parts in this case as both have an inverse relationship with each other.

As the main objective of the project is to design a steering system for an open-wheel race car for the formula student competition, the race track characteristics should be kept in mind.

The steering system is designed for the *hairpin turn,* tightest turn with a turning radius of 3.0 m, at a speed of 40 kmph keeping the appropriate balance between sensitivity of the steering system and the feedback to the driver through the steering.

Steering system elements:

- Steering wheel
- Quick disconnect mechanism
- Steering column
- Universal joint
- Rack housing (rack-pinion)
- Tie rods
- Steering arms
-C connector

3.8.3 Steering geometry selection

3.8.4 3D Geometry:

Once we have our 2D geometry, the next step is to generate 3D geometry.

3D geometry focuses on minimizing bump steer in the vehicle. Ideally, zero bump steer is achieved when tying rod extended meets the front view instantaneous center of suspension geometry, but since this case is not practically possible due to geometric constraints (to exactly meet that point, rack would be needed to shifts below the base plate of chassis which practically not possible to use), we try to keep the tie rod extended point as close as possible to the IC, to minimize bump steer.

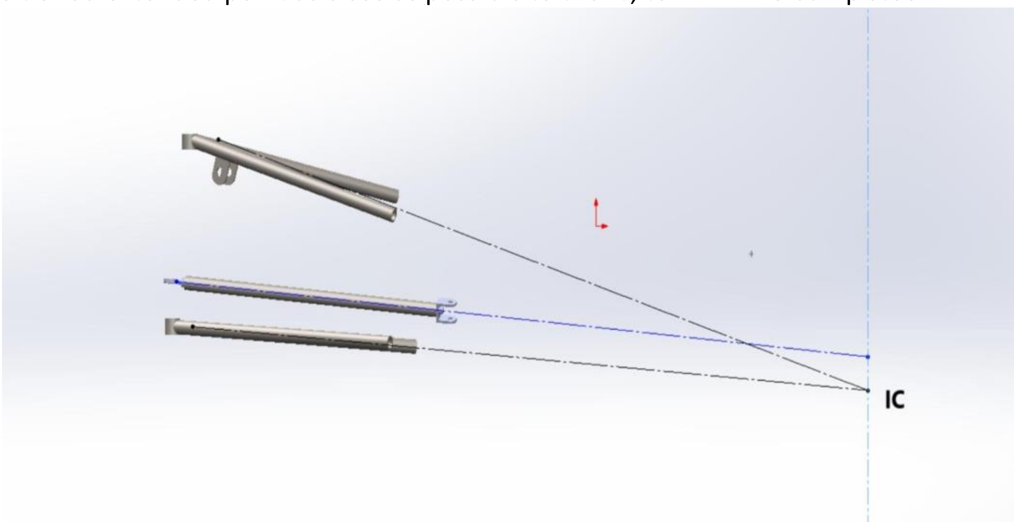

Fig 3.8.4 3D geometry of The Rod

Optimize:

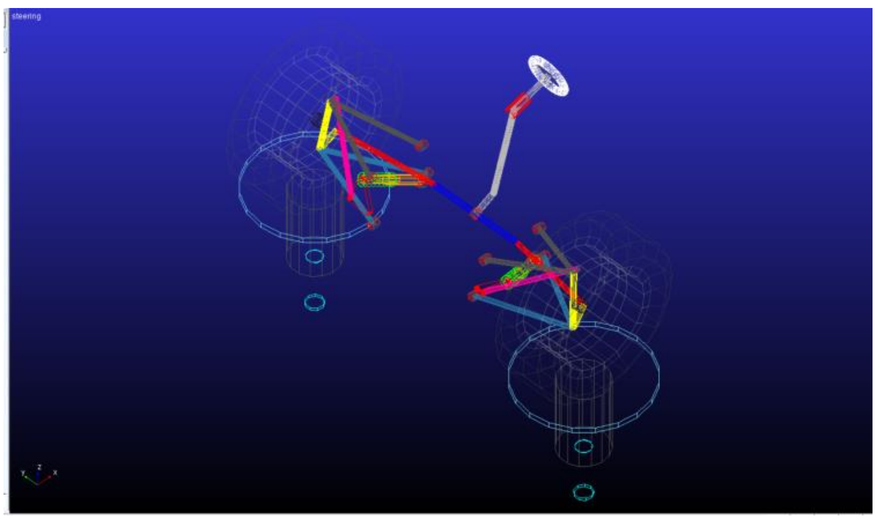

Fig 3.8.4 Simulation Results

After obtaining a 3D geometry, the next step is to run dynamic simulations and be able to optimize the 3D geometry. For this we followed an iterative process, by changing the position of an out-board point of the tie rod and studying various characteristics like change in camber with steering angle and time, a variation of the toe when the encountered bump of 25mm using ADAMS software. Adams was used because it has a predefined subsystem and algorithm to generate the behavior of entities like toe angle change or camber angle change during conditions such as bumping or rolling.

The following are the results:

The following is the final characteristic of camber with steer angle on encountering bump of 25mm-

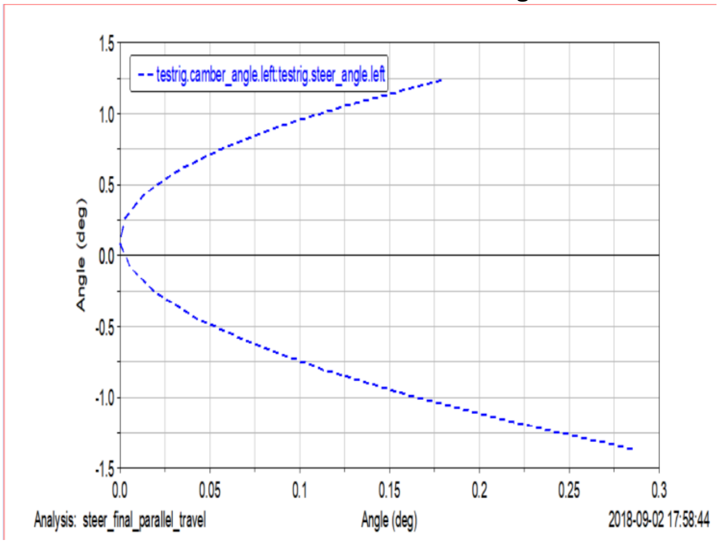

The following shows the iterations done with the position of outer tie rod hard point to optimize toe angle change with time while in bump-

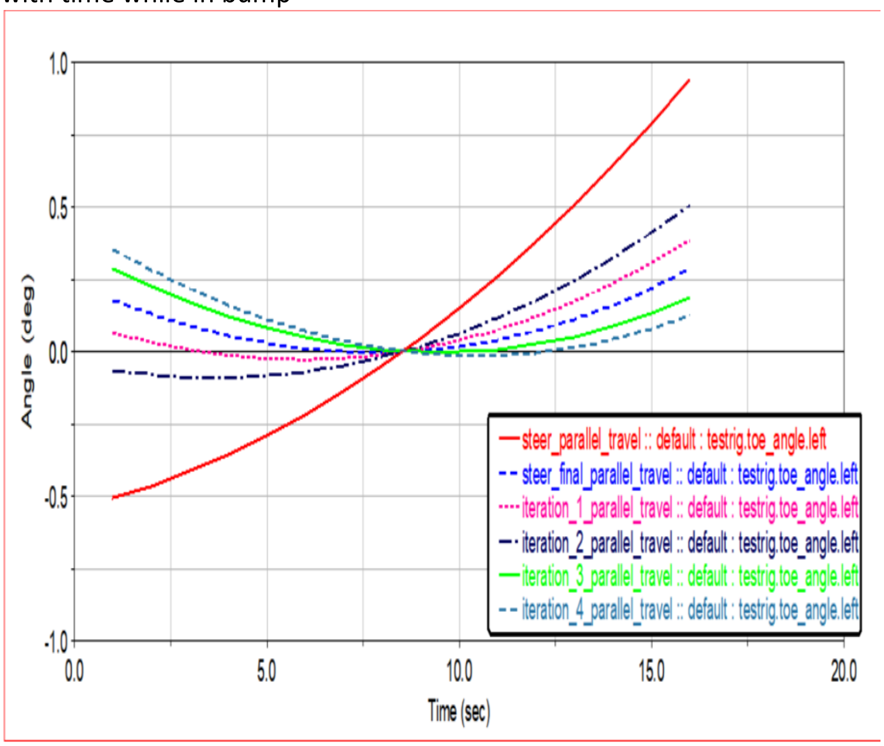

(Green line is final design)

The various iterations obtained by changing tie rod mounting point vertically(a point is varied vertically only as any horizontal variation would change 2D Geometry)

The final curve of the toe angle in bump is shown:

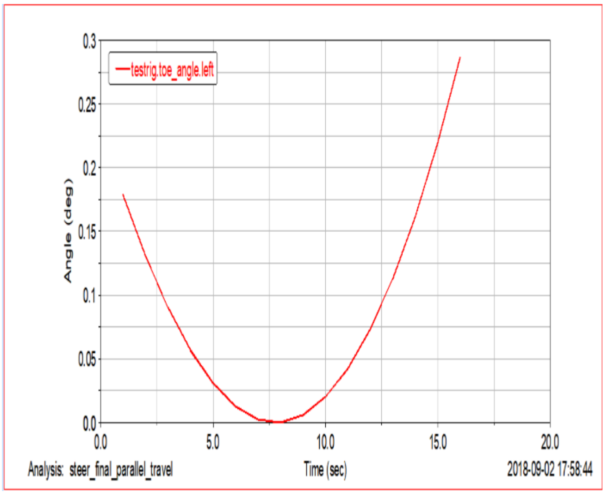

The next step in optimizing is to optimize the shape/thickness of shaft ensuring fail-safe nature as minimum thickness will add to the reduced weight of our subsystem.

For this, we conducted the torsion analysis of our shafts at maximum possible shear force.

We saw a variation of various factors like maximum stress achieved, max. deformation, the factor of safety, fatigue factor of safety

Calculations are done for torsion of 10Nm. (But max value encountered dynamically is 7N-m)

So, a shaft of **outer diameter 20mm** is employed of **thickness 1.5mm**.

3.8.5 Components

Components of Steering System Design:

3.8.5.1 Rack and Pinion System:

The rack and pinion system was custom made. It was wholly designed according to the above-mentioned C- Factor and for optimum size. The final design had a rack length of 360mm and pinion

had a pitch circle diameter of 26mm. The housing was made with Aluminium of 6061 grade and the rack and pinion were made from Mild Steel. The locking of the rack is done by welding metal plates at appropriate positions.

Fig 3.8.5 Rack and Pinion Housing

3.8.5.2 Universal Joint:

Two Universal joints incorporated in the design so as to reduce the angle between the joints for optimum performance. The angle between the shafts is 60 degrees. The position of the universal joints is near the fixed positions so that the unnecessary sway is reduced

Fig 3.8.6 Universal Joint

3.8.5.3 Steering Arm:

The steering arm is incorporated in the uprights and the respective lengths of the steering arm are 60mm each according to the iterations shown above.

The steering wheel is designed to an optimum size and to protect the steering wheel from vibrations. The construction of the steering wheel was done using carbon fiber to get greater strength and reduce the effect of vibration.

Fig 3.8.7 Steering Wheel

3.8.5.5 Tie Rod:

The length of the tie rod has been finalized by finding out the length of the projection of the tie rod from the bump steer calculations. For minimum bump steer the calculated tie rod projection is 416.38mm.

3.8.5.6 Quick Release mechanism:

The function of the Quick release mechanism is to disconnect the steering wheel from the steering column at the driver's consent.

Fig 3.8.8 Quick Release

3.8.5.7 C-connector:

The function of the C-connector is to connect the pinion with a tie rod for completing the transfer of motion from the steering wheel to tire.

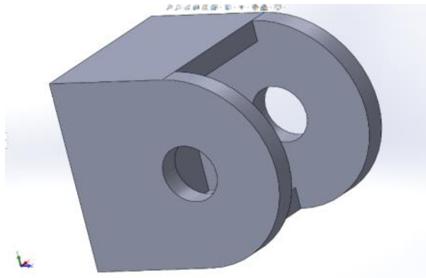

Fig 3.8.9 C-connector

C-connector is analyzed by putting the force of 3550 N (F.r=Torque on the steering wheel) which gives us the factor of safety 1.1094.

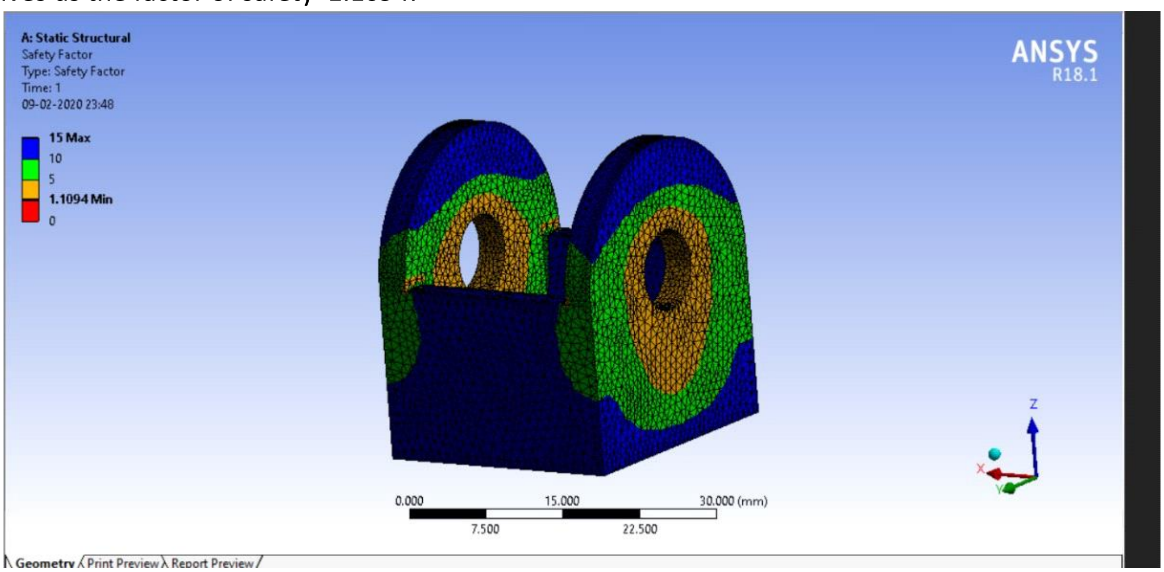

Fig 3.8.10 Analysis showing the factor of safety of c-connector

3.8.5.8 Steering Column :

The automotive steering column is a device intended primarily for connecting the steering wheel to the steering mechanism. The dimension of the steering column (For analysis: length- 320mm and thickness - 1mm)

Fig 3.8.11 Steering Column shaft

The shaft is analyzed by applying a torque of 10Nm on it and it gives the factor of safety of 14.282 and fatigue factor of safety of about 11.181

Factor of Safety

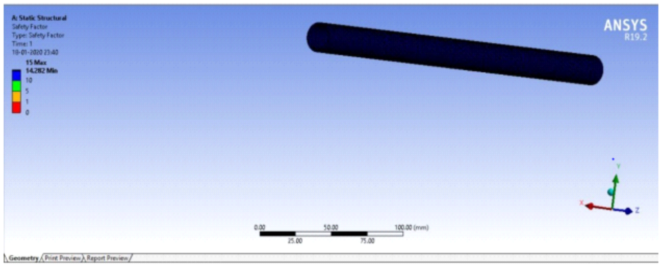

Fig 3.8.12 Analysis result of the steering column (Factor of safety)

Fatigue Factor of Safety

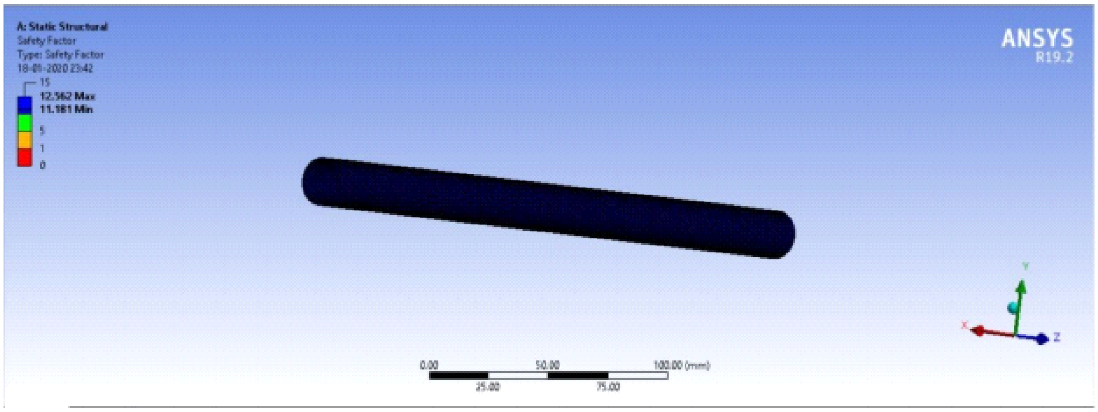

Fig 3.8.13 Fatigue factor of safety of steering column

3.9 Cooling

3.9.1 Selection of pump (Pressure drop analysis of entire cooling system)

The purpose of this project was to design and implement an effective cooling system for our Formula SAE Vehicle. Our aim was to participate in Formula Green 2020. The main components of the drivetrain of the electric vehicle are the motor and the motor controller. The cooling system was designed to cool the motor and motor controller to ensure that they operate in an optimal temperature range thus increasing drivetrain efficiency and ultimately improving vehicle performance.

From the specifications provided by the manufacturer of the motor controller, the maximum flow rate of cooling water was 12 Litre/minute. In order to maximize the cooling of the system, this maximum value of the flow rate was selected. Hence the corresponding mass flow rate was 0.2 kg/s (m=rho*V). The pressure drop across the motor and the motor controller for different flow rates of the cooling water were already specified by the respective manufacturers. However, the pressure drop across the radiator had to be determined for the given flow rate.

While selecting a pump, the important parameters to look out for were:

a. Total Head – The pump must provide enough head so as to ensure fluid motion throughout the system i.e. it should be higher than the head loss in the system. Cavitation should also be considered in determining the total head required.

b. Flow Rate- The pump should be able to provide the required head at the specified flow rate.

c. Weight of Pump- Pump should not be very heavy.

d. Power Required – The specification of the pump (12V/24V) is determined by the electrical team. The power required by the pump should not be higher than that which can be provided by the DC-DC converter, which again will be specified by the electrical team.

The total head loss in the system was determined to be close to 42 feet for the flow rate of 7 LPM. Thus a pump was selected which could produce a maximum head of 50 feet for 7 LPM flow keeping in mind unaccounted losses and cavitation.

From reviews of other FSAE teams, the GRI (Gorman-Rupp Industries) pump series was deemed to be trustworthy and from their manuals, the INT-G3 572 pump model seemed to serve our purpose effectively, taking into consideration all above parameters. GRI pumps agreed to donate us 2 pumps.

3.9.2 Selection of Radiator

We chose a radiator provided by Bajaj Auto, which is used in the Bajaj Pulsar 220 NS range of motorcycles. Note that the radiator used as a single pass radiator (water flows once only across the radiator). On analyzing the radiator, we observed that there would be pressure drops in the following regions:

- 90 degrees bend into the inlet of the radiator
- Sudden expansion from the inlet
- The entry of fluid into the tubes
- Pressure drop during flow through tubes
- Exit of tubes
- Sudden contraction to the outlet
- 60 degrees outlet bend

The measurements of the relevant dimensions of the radiator were manually taken by visiting the Bajaj showroom.
Flow rate: Q = 12 LPM = 2 e-4 m^3/s; rho = 1000 kg/m^3

a) Area of inlet (calculated) = 1.59 e-4 m^2
Velocity of water in inlet = V = 1.25786 m/s
Loss coefficient for 90 degrees inlet bend = k =0.3
Hence loss in bend = k*rho*V^2/2 = **237.33 Pa**

b) Area of cross section of inlet reservoir = 46.45 e-4 m^2
Area of inlet = 1.59 e-4 m^2
Velocity of water in inlet = V = 1.25786 m/s
Loss coefficient for sudden expansion from inlet to reservoir = K = 0.95
Hence loss due to sudden expansion = K*rho*V^2/2 = **751.551 Pa**

c) No. of tubes in radiator = 21
Velocity of water in tubes = v = 0.2886 m/s
Loss coefficient for entry of fluid into tubes = k = 0.8
Hence loss due to entrance of fluid into tubes = k*rho*v^2/2 = **33.32 Pa**

d) For pressure drop for flow through tubes
Velocity of water in tubes = v = 0.2886 m/s
Length of tube = 10 inch = l = 254 mm
Hydraulic diameter of rectangular tubes = D_h= 2.3 mm (See Cengel book for formula)
Temp. of water in tubes = 40 degrees Celsius
Hence, dynamic viscosity of water at this temp = mu = 6.354 e-4 kg/m-s
Reynold's number of flow = rho*v*D_h/mu = 1044.66
Hence, Darcy friction factor = f = 0.062 (from Moody chart)
Hence pressure drop in tubes = f*l*rho*v^2/ (2*D_h) = **285 Pa**

e) For exit of water from tubes into outlet reservoir
Loss coefficient = k = 1.0
Pressure drop at exit = k*rho*v^2/2 = **41.64 Pa**

f) For the sudden contraction of water into outlet
Loss coefficient = k = 0.5
Velocity of water in outlet = V = 1.25786 m/s
Pressure drop due to sudden contraction = k*rho*V^2/2 = **395.55 Pa**

g) Outlet bend of 60 degrees
Velocity of water in outlet = V = 1.25786 m/s
Loss coefficient = k = 0.4
Pressure drop due to outlet bend = k*rho*v^2/2 = **316.44 Pa**

Hence total pressure drop across the radiator = 237.33 + 751.55 + 33.32 + 285 + 41.64 + 395.55 + 316.44 = **2060.83 Pa = 2.06 kPa = 0.02 bar**

After final considerations and going through the pump models available, for a lower cost pump, a flow rate of 7 LPM was decided. From the Simulink model, it was deemed that this flow rate was capable of dissipating the heat effectively.
Though the above pressure drop has been calculated for 12 LPM flow, the pressure drops for different flow rates across the radiator can also be determined with negligible error. Let the LPM for which pressure drop across the radiator is to be calculated by Q. Then:
Pressure drop = $(Q/12)^2$ * 2060.83 Pa
Hence, for 7 LPM flow, the pressure drop = $(7/12)^2$ * 2060.83 = **701.25 Pa**

3.9.3 Items to be cooled

Bamocar-PG-D3 700-400 Motor Controller:

Der Kühlkanal hat einen Druckverlust bei einem Volumenstrom = 10l/min von $\Delta p_{v,ges} = 0{,}274\ bar$

R_German__CONFIDENTIAL__.pdf

Volumenstrom V [l/min]	Druckverlust in bar
4	0,050
6	0,106
8	0,181
10	0,274
12	0,389

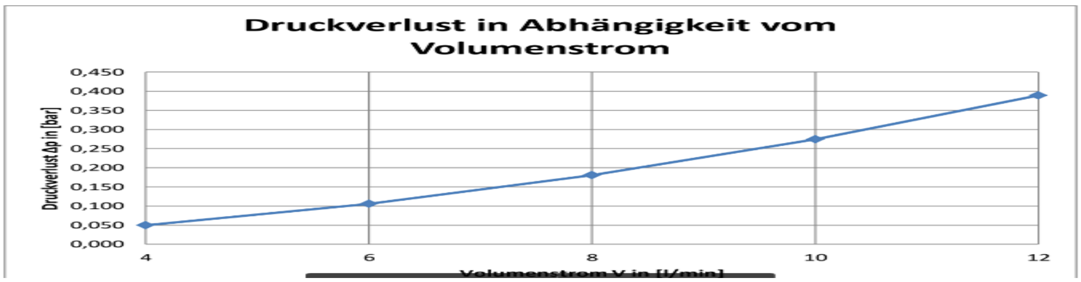

The motor-controller specifications sheet was obtained from the manufacturer. From the graph, we see that for 7 LPM, the pressure drop across the motor controller is **0.145 bar**.

Emrax 228 Motor:

According to the user manual of EMRAX 228, the pressure drop across the motor for 7 LPM flow is approximately **0.9 bar**.

Motor size	Water/glycol flow pressure (pressure drop)	Water/glycol flow rate
188	0,5 bar	7 l/min
208	0,6 bar	7 l/min
228	0,9 bar	7 l/min
268	1,0 bar	6 l/min
348	1,0 bar	6 l/min

3.9.4 Coolant Lines

The head loss in a pipe is inversely proportional to the cube of the diameter of the pipe (for constant flow rate). Hence, in order to decrease head loss, lines with a bigger diameter need to be selected. The coolant lines would be selected from the local market. We have selected a 3/4” diameter hose of length 4m to be used for cooling calculations. The pressure drop was found to be **0.0141 bar.**

3.9.5 Selection of Fans:

The fan's purpose is to pull air through the radiator and ensure efficient cooling occurs in the system. The primary function of the fan comes into play when the car is stationary and there is no natural circulation of air through the radiator. The fan is selected after modeling the air’s pressure drop across the side pod.

Due to varying cross-section and skin friction, the air stalls in the side pod and requires external forced circulation to pass through. Modeling of the pressure drop across the radiator was done through experiments at different flow rates. The system characteristics curve was obtained and was compared with various fans operating curves to find the resulting operating points.

The MINIBEA R200A4 fan was selected primarily because of an operating point lying within the suggested region and costs.

Specifications of fan: R200A4-051-D0550

Voltage (V)	Current (A)	Power (W)	Speed (RPM)	Max Air Flow(CFM)	Max Static Pressure (Pa)	Noise (dB)	Mass (kg)
24	2.8	67	5000	590	828	67	1.2

Heat Calculation:

For beginning with the heat transfer calculation, one should have the prerequisite knowledge on the design of heat exchangers, conduction and internal flow convection (reference of formulas is given in the attached file).

Assumptions:

- All the heat exchange will take place only through the core of a radiator.
- The coolant pipe is insulated in nature.
- The coolant will exit at a 2˚C higher temperature than exit air from the radiator.
- The heat will be dissipating at its average rate through the radiator thus the system has been studied in static equilibrium condition.
- Battery current and the current flowing into the motor controller are the same.

Thus following is the block diagram depicting the coolant flow exchanging heat with the motor, motor controller and the radiators-

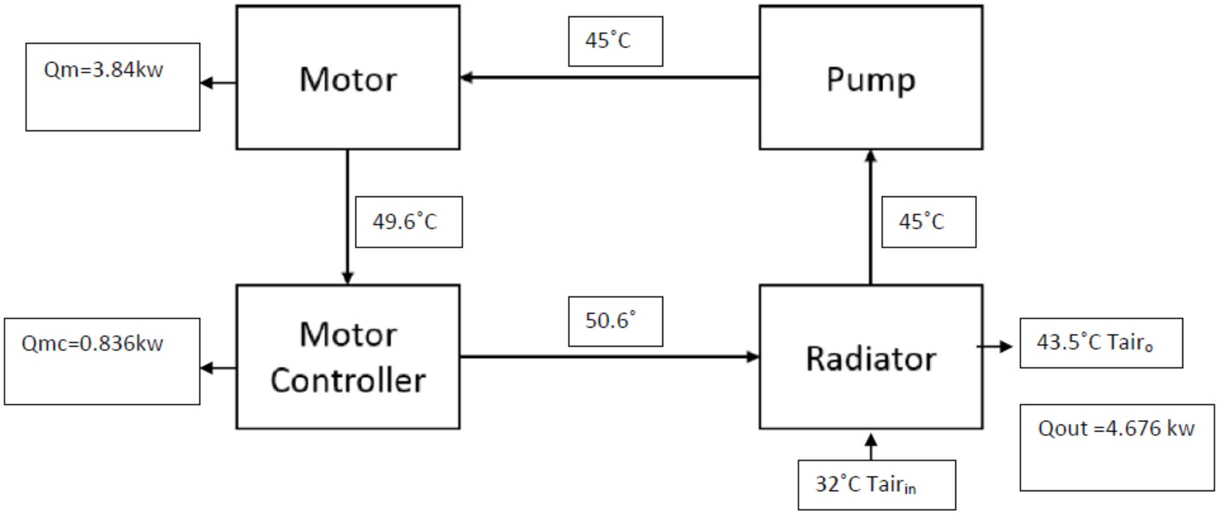

There are two heat sources- Motor and motor Controller and a heat sink i.e. 2 Radiators in the system. Owing to the major pressure losses in parallel flow and a constraint to the pump capacity, flow in a series has been decided for the coolant through two radiators. (Since there is more pressure drop in parallel flow due to the involvement of T connector in fittings)

It was assumed that all the losses of the motor would convert into heat, so interpolating the efficiency of the motor at various torque and RPM we can anticipate heat dissipation by the motor at that instant. Using the optimum lap software, we can calculate the heat that would be dissipating from the motor at an instant using the efficiency lookup table in the given excel, thus we can get the average value of heat produced during an endurance event.

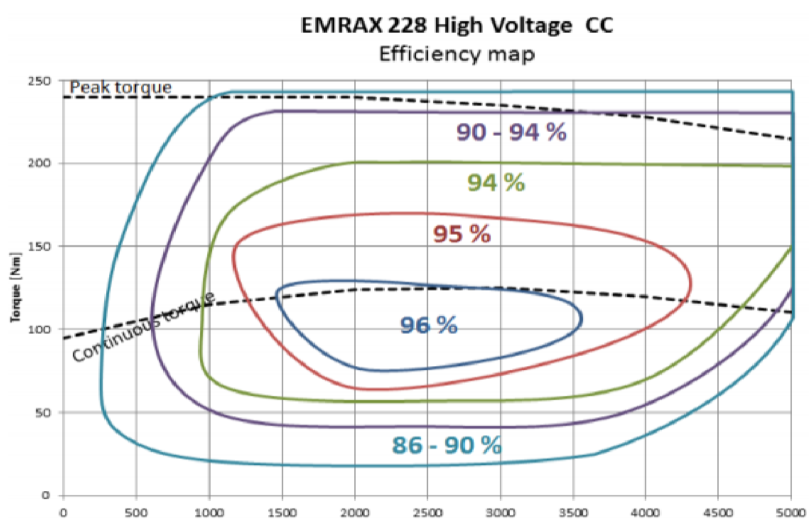

Similarly, the same procedure can be followed for the motor controller but in a slightly different manner, since the company Unitek, has provided us with the data sheets along with heat v/s current curves, let us calculate the heat dissipation at an instantaneous flow of current through the motor controller.

The current can be calculated by balancing the power of the accumulator pack with the heat loss and the power consumed by the motor, thus-
Considering the voltage of battery remains constant during the endurance event = 470V

Battery power = Heat loss at motor controller + Power consumed by the motor
(470-I*R)*I = 4*v*I + (Heat loss + Mechanical power)
R – Battery internal resistance= 128*0.1mΩ=0.0128Ω
v – Seeing the motor controller heat curve linear, it can be assumed that it only varies with a current having the same voltage v = 1.8275V across the IGBT module and there are 4 IGBT modules that will be working in a motor controller.

Calculations of motor and controller heat losses have been done in the attached excel sheet –Cooling Nebraska (1).

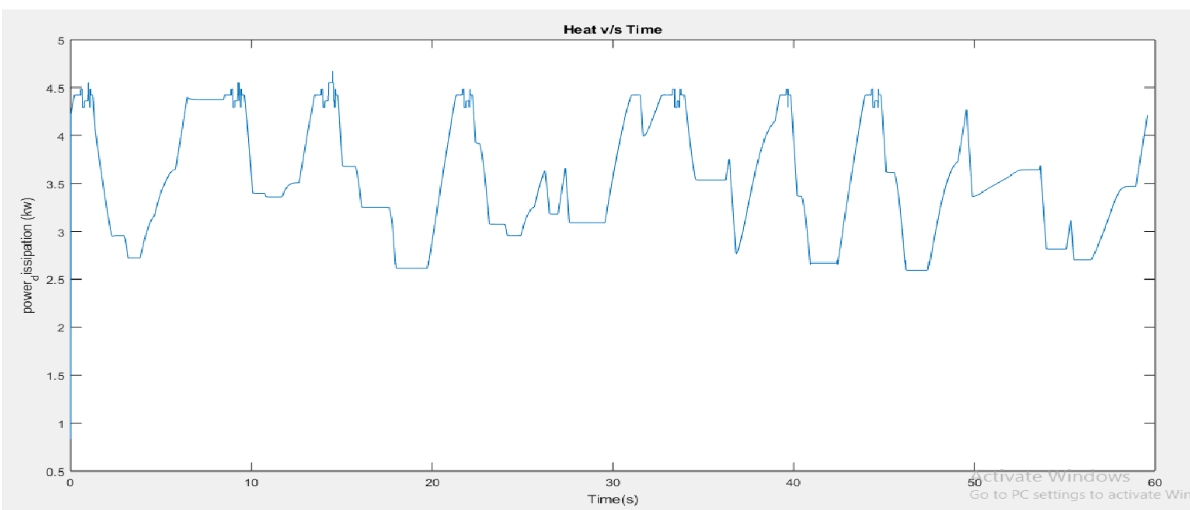

Graph showing the heat dissipation of the motor and motor controller for one lap of Nebraska Track

The average heats dissipated by the motor and motor controller were calculated as 2.9kW and 1kW respectively that sums up 3.9kW.

A radiator of Bajaj Pulsar 220 NS motorbike was selected using the heat transfer Simulink based model and validating it in the lab in the normal operating conditions. However, 2 radiators were required for the dissipation of the total load. A single big radiator was not possible to implement due to packaging constraints.

3.9.6 Testing at the lab:

Testing at the lab was done by making a small wind tunnel from the plywood covering its inner side with a plastic cover for getting a smoother inner side for airflow.

The air pressure has been provided by using the table fan at one mouth of the wind tunnel. The fan is placed in such a way that it should be sucking the air from another mouth since this way of pulling air will replicate the actual conditions of the placed radiator in the sidepod of the car where the fan is placed just behind the radiator. The speed of air flowing through the tunnel was measured using the Anemometer.

The coolant was made to flow across the radiators and the fittings using the controlled flow provided by a pump and a valve and measured using a flow-meter placed in the mid of the coolant pipes.

Temperatures only at the entrance and exit of the radiator were measured with the help of a T-type thermocouple setup. Thus, at varying flow conditions of coolant and air, the dissipated heat could be calculated using $m*C_p*\Delta T$.

We can validate the results easily with a Simulink based heat transfer model and can use this model further for selecting the other radiators without any lab testing.

After calculating the final amount of heat dissipation from the system, heat dissipated at an individual heat sinker- radiator can be calculated by using the NTU method. In this method, we know the core dimensions of the radiator and effectiveness for unmixed cross flow–

z=1-exp (1/Cr)*NTU^0.22*(exp (-Cr*(NTU) ^0.78)-1));

And considering the ambiance conditions at 36˚C (avg. temp. of entering and exiting air), properties of air were selected. Similarly, anticipating the average coolant temperature at 40˚C, the water properties were selected accordingly.

Thus by getting values of all the parameters, the nusselt number through the radiator tubes and through for the fins were calculated using Mills relation for laminar flow across a tube.

NU=3.66+.065*Rea*Pr*Dha*Cd/(1+.04*((Rea*Pr*Dha/(Cd))^(2/3)));

And succeeding the nusselt number calculations, the overall heat transfer coefficient can be calculated, and after that, the calculated area required of a radiator from the calculations can be compared with the selected radiator for a cross-check.

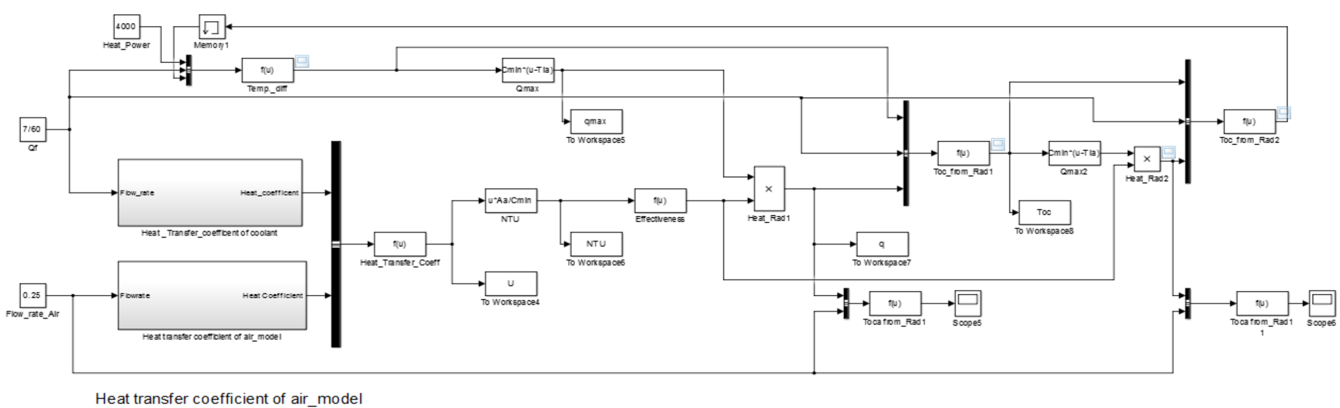

Figure 33- **Radiator Heat Transfer Simulink model**

3.10 Materials Used

AISI 4130 Steel (Chromoloy)	7.85 g/cc	460 MPa	228
IS 3074 Steel	7.79 g/cc	420 MPa	228
Aluminium 6061-T6	2.73 g/cc	276 MPa	107
Aluminium 7075-T6	2.81 g/cc	503 MPa	175
1020 Steel	7.87 g/cc	294 MPa	115
Glass Fibre reinforced structure/ epoxy	2.55 g/cc	1700 - 3000 MPa (tensile)	-
Carbon fibre/ epoxy (standard, for bending)	1.55 g/cc	2068 MPa (tensile)	-
EN24 T TYPE	7.85 g/cc	654-680	248-302**(Brinell)**
EN24 Z TYPE	7.85 g/cc	1235	444**(Brinell)**